UNIVERSITY OF HAWAII
LIBRARY
FEB 10 '61

Geochimica et Cosmochimica Acta

JOURNAL OF THE GEOCHEMICAL SOCIETY

Executive Editors: C. W. CORRENS, *Göttingen.* E. INGERSON, *Austin, Texas.* L. R. WAGER, *Oxford.*

Editors: L. H. AHRENS, *Capetown.* S. R. NOCKOLDS, *Cambridge.* H. C. UREY, *La Jolla, Calif.* JOHN VERHOOGEN, *Berkeley, Calif.* A. P. VINOGRADOV, *Moscow.* W. A. WAHL, *Helsingfors.*

CONTENTS VOLUME 21, NOS. 1/2 DECEMBER 1960

J. D. JONES and J. R. VALLENTYNE: Biogeochemistry of organic matter —I. Polypeptides and amino acids in fossils and sediments in relation to geothermometry 1

WERNER RICKE: Ein Beitrag zur Geochemie des Schwefels . . . 35

N. HERZ and C. V. DUTRA: Minor element abundance in a part of the Brazilian shield 81

R. M. CARR and W. S. FYFE: Synthesis fields of some aluminium silicates 99

R. PARK and S. EPSTEIN: Carbon isotope fractionation during photosynthesis 110

K. R. DAWSON, J. A. MAXWELL and D. E. PARSONS: A description of the meteorite which fell near Abee, Alberta, Canada 127

T. HARA and E. B. SANDELL: Meteoritic abundance of ruthenium . 145

Geochemical Note:

BARTHOLOMEW NAGY, PAULETTE HAMWAY, G. C. GAGNON and M. CEFOLA: Separation of n-octadecane-1-C^{14} from asphaltic mixtures by elution chromatography 151

Letter to the Editor:

J. P. SHEDLOVSKY: Cosmic-ray produced manganese-53 in iron meteorites 156

PERGAMON PRESS OXFORD • LONDON • NEW YORK • PARIS

GEOCHIMICA ET COSMOCHIMICA ACTA

EXECUTIVE EDITORS

PROF. C. W. CORRENS (1959) *Sedimentpetrographisches Institut der Universität, Lotzestr.* 13, *Göttingen, Germany*
PROF. E. INGERSON (1959–1960) *Department of Geology, University of Texas, Austin* 12, *Texas, U.S.A.*
PROF. L. R. WAGER, F.R.S. (1959–1961) *Department of Geology and Mineralogy, The University Museum, Oxford, England*

EDITORS

PROF. L. H. AHRENS (1959–1960) *Department of Chemistry, University of Capetown, Rondebosch, Cape Province, South Africa*
DR. S. R. NOCKOLDS *Department of Mineralogy and Petrology, The University, Cambridge, England*
PROF. H. C. UREY, For. Mem. R. S. (1959) *University of California, La Jolla, California, U.S.A.*
DR. JOHN VERHOOGEN (1959–1961) *Department of Geology, University of California, Berkeley, California, U.S.A.*
PROF. A. P. VINOGRADOV (1959–1961) *Vernadsky Institute, Moscow, U.S.S.R.*
PROF. W. A. WAHL (1959–1961) *Observatoriegaten* 8, *Helsingfors, Finland*

EDITORIAL ADVISORY BOARD

EUROPE

T. F. W. BARTH, *Oslo*
L. CAPDECOMME, *Toulouse*
E. J. CONWAY, *Dublin*
P. ESKOLA, *Helsinki*
P. GALLITELLI, *Modena*
A. HADDING, *Lund*
O. HAHN, *Göttingen*
H. W. HARVEY, *Plymouth*
F. HEIDE, *Jena*
A. HOLMES, *Edinburgh*
W. Q. KENNEDY, *Leeds*
PH. H. KUENEN, *Gröningen*
S. LANDERGREN, *Stockholm*
F. MASHATSCHKI, *Vienna*
A. MUIR, *Harpenden*
J. ORCEL, *Paris*
E. RAGUIN, *Paris*
E. REINHARD, *Basle*
TH. G. SAHAMA, *Helsinki*
C. E. TILLEY, *Cambridge*
T. VOGT, *Trondheim*

AMERICAN CONTINENT

A. F. BUDDINGTON, *Princeton*
D. GUIMARAES, *Belo Horizonte*
G. E. HUTCHINSON, *New Haven*
B. H. MASON, *New York*
F. WHIPPLE, *Cambridge*
R. WILDT, *New Haven*
H. S. YODER, *Washington*

FAR EAST

T. WATANABE, *Tokyo*

Publishing Offices: Pergamon Press Ltd., Headington Hill Hall, Oxford

Four issues per volume, three volumes per year

Subscription *per annum* (including postage) (A) £21 (U.S.A. $60.00); (B) For individual subscribers who write directly to the publisher certifying that the Journal is for their private use, £7. 7s. (U.S.A. $21.50). Members of the Geochemical Society, or non-members who occasionally publish papers in the Journal, £3. 11s. 6d. (U.S.A. $10.00) *per annum*.

Back numbers, £10 (U.S.A. $28.00) per volume

Single issues, £2. 10s. (U.S.A. $7.00) each

Copyright © 1960 Pergamon Press Ltd.

PERGAMON PRESS LTD.

HEADINGTON HILL HALL, OXFORD 122 EAST 55TH STREET, NEW YORK 22, N.Y.

PRINTED IN NORTHERN IRELAND AT THE UNIVERSITIES PRESS, BELFAST

INTERNATIONAL SERIES OF MONOGRAPHS ON

EARTH SCIENCES

General Editor: Professor **EARL INGERSON**

Volume 1

CONTRIBUTIONS IN GEOPHYSICS

IN HONOUR OF BENO GUTENBERG

Edited by **Hugo Benioff, Maurice Ewing, Benjamin F. Howell, Jr.,** *and* **Frank Press**

The diverse nature of the topics chosen by the contributors is a measure of the breadth of Dr. Gutenberg's interests; and the wide geographic distribution of the contributors' homes indicates the range of his influence.

60s. net (\$9.00)

Volume 2

CLAYS AND CLAY MINERALS

PROCEEDINGS OF THE SIXTH NATIONAL CONFERENCE ON CLAYS AND CLAY MINERALS

Edited by **Ada Swineford**

The papers in this volume stress crystal structure of clay minerals, alteration of feldspars, clay mineralogy of soils, morphology of clay particles, water vapour sorption and diageneses.

60s. net (\$8.50)

Volume 3

PRINCIPLES OF GEOCHEMICAL PROSPECTING

TECHNIQUES OF PROSPECTING FOR NON-FERROUS ORES AND RARE METALS

by **I. I. Ginzburg**

Constitutes the first effort to cover the entire subject of geochemical prospecting comprehensively, including hydrochemical, biogeochemical and geobotanical methods.

70s. net (\$11.50)

Volume 4

OVERVOLTAGE RESEARCH AND GEOPHYSICAL APPLICATIONS

Edited by **James R. Wait**

Contains the results of the first concerted effort to apply the overvoltage phenomenon to geophysical prospecting, made by the geophysical laboratories of the Newmont Mining Co.

55s. net (\$9.00)

Volume 5

CLAYS AND CLAY MINERALS

PROCEEDINGS OF THE SEVENTH NATIONAL CONFERENCE ON CLAYS AND CLAY MINERALS

Edited by **Ada Swineford**

Volume 5 in this series covers a wide variety of topics. The papers stress regional clay mineralogy, the effect of saline water on clay minerals, genesis and identification of soil clays, and viscosity of clay suspensions.

60s. net (\$8.50)

Please send for further details of this series

PERGAMON PRESS

OXFORD LONDON NEW YORK PARIS

Headington Hill Hall, Oxford 4 & 5 Fitzroy Square, London W.1

122 East 55th Street, New York 22, N.Y.

Two important new titles

CLAYS AND CLAY MINERALS

PROCEEDINGS OF THE EIGHTH NATIONAL CONFERENCE

Edited by **ADA SWINEFORD**

This latest volume in the very successful annual series on Earth Sciences is again sponsored by the Committee on Clay Minerals of the National Academy of Sciences—National Research Council. It contains reports of some of the latest developments in clay research in the United States, and it includes research papers involving many aspects of clay technology and clay mineralogy. It stresses clay-water systems and clay mineral-geochemical prospecting.

Because of the central role clays play in the origin and migration of gas, petroleum and other fluids, in the earth, the petroleum engineer and geologist are taking an increasing interest in these materials discussed in this volume. Clays are important constituents in many catalysts so that chemists in the refining industry will wish to consult this authoritative book to keep abreast of this fast-moving field.

63s. net ($9.50)

SOIL ORGANIC MATTER

by **M. M. KONONOVA**

This important book is the first comprehensive review of work on soil organic matter for several decades. This first English translation edition has been thoroughly revised by the author and brought completely up to date to 1960.

The book opens with a historical survey of work on soil humus, leading to a discussion of present-day ideas on the composition of soil humus. A very detailed account of the biochemistry of humus formation is given. The role of organic matter in soil formation and its influence on soil fertility are thoroughly discussed. This authoritative and invaluable volume will be indispensable for anyone working on soil organic matter.

There is an extensive bibliography containing over 900 references.

In production *Approx.* **80s. net ($15.00)**

Please write for further details

PERGAMON PRESS

OXFORD LONDON NEW YORK PARIS

Headington Hill Hall, Oxford 4 & 5 Fitzroy Square, London W.1

122 East 55th Street, New York 22, N.Y.

Geochimica et Cosmochimica Acta, 1960, Vol. 21, pp. 1 to 34. Pergamon Press Ltd. Printed in Northern Ireland

5856-27

Biogeochemistry of organic matter—I

Polypeptides and amino acids in fossils and sediments in relation to geothermometry

J. D. Jones* and J. R. Vallentyne†
Department of Biology, Queen's University, Kingston, Ontario, Canada

(*Received* 21 *January* 1960, *revised* 4 *June* 1960)

Abstract—Quantitative data are presented on ninhydrin-reacting substances in hydrolysates and extracts of Recent sediments, sedimentary rocks, and fossils, as determined by column chromatography. The recovery of amino acids added in small amounts to a concentrated calcium chloride solution was found to be 94–96 per cent, after precipitation of the calcium as calcium sulphate and removal of the HCl by vacuum distillation. Seventeen amino acids and three unknowns were detected in hydrolysates of surface and subsurface sediment samples, from Lake Opinicon, Ontario, with amino acids and other ninhydrin-reacting organic compounds accounting for nearly two-thirds of the soluble-N in the hydrolysate, and ammonia for most of the remaining third. Only five amino acids (aspartic acid, glutamic acid alanine, leucine(s) and γ-aminobutyric acid) and one unidentified ninhydrin-reacting organic compound were present in a hydrolysate of shale from the Green River formation (Eocene). Amino acids accounted for only 0·014 per cent of the total-N in the shale. It was calculated from the alanine content that the maximum temperature that the Green River shale could have been *continuously* subjected to during its history was 74°C. Amino acids were not detected in hydrolysates of two pre-Cambrian sedimentary rocks, nor in a hydrolysate of a Miocene lignite. An acid extract of carnosaur "teeth" from the Upper Cretaceous contained leucine(s), ammonia, ethanolamine, and one unidentified ninhydrin-reacting substance that chromatographed similarly to an unknown found in a hydrolysate of laboratory heated *Mercenaria* shells.

Of the total-N in a shell of the univalve mollusc *Cassis Madagascarensis*, 50 per cent was extractable with cold HCl, this fraction consisting of amino acids, ammonia and unidentified compounds, some of which reacted with ninhydrin. Only 57 per cent of the nitrogen in a hydrolysate of the conchiolin-fraction of the shell was recovered in the form of amino acids and ammonia. Fifteen amino acids and two unknowns were detected in the hydrolysate of the conchiolin-fraction. The periostracum of a Pleistocene *Mercenaria mercenaria* shell liberated sixteen amino acids and three unidentified ninhydrin-reacting substances on acid hydrolysis. The periostracum-free fossil shell had approximately the same amino acid composition as reported elsewhere for shells of living *Mercenaria*. Quantitative data on amino acids and other ninhydrin-reacting compounds were reported for samples of Pleistocene *Mercenaria* shells pyrolysed in the laboratory at 213 and 219°C. In the shell, alanine decomposed at a faster rate, and phenylalanine at an equal or slower rate, than the rates characteristic of the same amino acids in dilute aqueous solution. The nitrogen liberated from amino acids during pyrolysis could mostly be accounted for in the hydrolysates as acid-insoluble-N, ammonia, and soluble nitrogenous compounds, some of which reacted with ninhydrin. Amines were detected only in samples pyrolysed in sealed tubes.

Introduction

This is the first of a proposed series of papers dealing with the application of biochemical techniques to ecological and geological problems. Our purpose is to trace the fate of certain biochemical compounds in the sedimentary column. Although it has been known for 35 years that some biochemical compounds can resist complete destruction over geologically long periods of time, it was only 6 years ago that the concept of biochemical fossilization began to be widely known in scientific circles. It was then that Keilin (1953) first reviewed data on the stability of a variety of biological substances, and Abelson (1954) reported that amino acids were present in hydrolysates of a number of fossil shells and bones.

* Present address: Agricultural Research Council, Ditton Laboratory, Larkfield, N. Maidstone, Kent, England.
† Present address: Dept. of Zoology, Cornell University, Ithaca, New York, U.S.A.

Prior to 15 years ago it was generally believed, without adequate basis, that compounds such as proteins, amino acids, carbohydrates, etc., could not be preserved in sedimentary deposits. It was assumed that sedimentary bacteria would rapidly and quantitatively decompose any nutritionally important organic compounds released by decomposition processes. Although there is extensive bacterial degradation of organic matter in recent sediments, the process is by no means complete (see VALLENTYNE (1957a) for a review of the literature). The current viewpoint is that many biological compounds may have appreciable stabilities in the geological sense. It is now commonplace to assume that almost any type of biological compound can be preserved in fossil material. The important questions are: To what extent? For how long? Under what conditions? As has been the case in so many other scientific revolutions, the position has changed from a qualitative negation to the beginning of a quantitative understanding.

Notable among the early contributions to "paleobiochemistry" were the following discoveries: cellulose in early Tertiary lignites (GOTHAN, 1922; KOMATSU and UEDA, 1923; LUFT, 1930; STAUDINGER and JURISCH, 1939; and others); chitin in Eocene remains of beetle wings (ABERHALDEN and HEYNS, 1933); porphyrins in shale, coal and petroleum (TREIBS, 1934a, b, 1935a, b, 1936); ABO blood group substances in Egyptian mummies (BOYD and BOYD, 1934, 1937); and carotenoids and chlorophyll-like substances in cores of marine sediments (FOX *et al.*, 1944). A complete historical review of the developments in paleobiochemistry will not be attempted here inasmuch as the subject is being treated elsewhere (BREGER, 1960).

A full recognition of the biochemical aspects of organic geochemistry necessarily had to await the development of sensitive analytical techniques. The problem was one of separating single organic compounds from large amounts of extraneous matter, for example, a single hydrocarbon or hydrocarbon fraction from a Recent sediment, or a series of amino acids from a carbonate deposit. This methodological need was largely overcome by the development of paper chromatography (CONSDEN *et al.*, 1944). Extensive studies have since been made on chromatographic, electrophoretic and ion-exchange separations of many organic compounds. In spite of the ready availability of these methods, relatively few attempts have been made to apply them to geologic materials.

To obtain a proper perspective of the present state of organic geochemistry (a field much wider in scope than the biochemical aspects referred to above) one might consider the chaos that geology would be in if all minerals were invisible. The analogy is appropriate for it is the molecule in organic geochemistry that assumes the deductive role of the mineral in inorganic geochemistry. The geologic meaning that resides within a fossil organic molecule is like that within a mineral in that both tell something of the conditions of origin and subsequent history of a particular deposit. The essential differences are only in dimensions and units. Molecular composition must be the basis for differentiating among similar samples of organic matter, just as mineralogical composition lies at the basis of rock classification. The problem of elucidating the complete molecular structure of fossil organic matter will doubtless be as difficult in the future as it has been in the past due to the complexity of the macromolecular units involved. We believe,

however, that many important data can be gathered, and conclusions reached, from a study of the small molecules released by extractive or hydrolytic procedures. It is in this manner that we have approached the problem. The present study is restricted to a group of biochemicals that forms only a very minor fraction of the totality of organic matter in sedimentary deposits.

In selecting a group of biological compounds for a "type" geochemical investigation, we were attracted to amino acids for the following reasons: (a) polypeptides and amino acids form one of the main classes of biological compounds; (b) the zwitter-ion structure and high melting points of amino acids indicated a relatively great thermal stability; (c) sensitive methods of amino acid analysis had already been developed; and (d) amino acids, both free and peptide-bound, had been isolated from a variety of soils and sediments. ABELSON's (1954) discovery of fossil amino acids corroborated our original suspicions, and his study of the kinetics of the thermal decomposition of alanine provided a concrete basis for further experimental investigation.

Previous geochemical studies of polypeptides and amino acids in soils, Recent sediments, plankton and natural waters have been briefly summarized by VALLENTYNE (1957a). Later studies, dealing with aquatic systems and fossil materials, are outlined below. Amino acids, both free and peptide-bound, have been isolated from mummy tissues (SCHMIDT, 1908; ABERHALDEN and BRAHM, 1909; ABERHALDEN and WEIL, 1911; KERNBACH, 1924) and from fossil human bones (THIEME *et al.*, 1956; EZRA and COOK, 1957). Histamine has been detected in mummy skin (GRAF, 1949). SINEX and FARIS (1959) isolated gelatin from 12,000-year-old deer antlers. The isolated gelatin had a moleular weight of 41,000 (in the same range as gelatin from fresh bone) and had the same hydroxyproline content as modern gelatin. STEPPUHN and LJUBOWZOWA (1930) found active proteolytic enzymes in frozen mammoth flesh and in Egyptian mummy flesh. YAMADA (1934) reported that active lipase was present in Peruvian mummy tissues. These enzymic studies showed that the active centres of enzymes had remained without denaturation for several thousand years. KRAUSE (1959) has recently assayed freshwater zooplankters for free and peptide-bound amino acids. Amino acids in hydrolysates of freshwater sediments have been quantitatively measured by KLEEREKOPER (1957), POVOLEDO (1959) and SWAIN *et al.* (1959). ABELSON (1954, 1955, 1957) was the first to demonstrate the presence of amino acids in hydrolysates of pre-Pleistocene fossils. SHABAROVA (1955) and ERDMAN *et al.* (1956) later isolated amino acids from hydrolysates of Miocene and Eocene sedimentary rocks, respectively.

It is possible that some of the nitrogenous compounds that HALL and MILLER (1908) extracted from Paleozoic and Mesozoic shales and clays may have been amino acids, but direct evidence was not presented. Their results could possibly be attributed to nitrogen fixation by the soil micro-organisms used in the study, rather than to extraction of organic nitrogenous compounds from the sedimentary rocks. The early report of amino acids in hydrolysates of lignites, bituminous coals and anthracite coals (SHACKLOCK and DRAKELEY, 1927) similarly needs verification since the analyses were based on indirect methods rather than direct isolation and identification.

General Methods

Only the methods of analysis used repeatedly throughout the study will be referred to here. Details on specific treatments of samples are given under the heading of results.

In analysing fossils and sedimentary rocks with low concentrations of amino compounds care must be taken to avoid three major sources of contamination: (a) from root fragments or micro-organisms on the surface of the specimen used for analysis; (b) inclusion of post-depositional materials that have been added in pores, cracks or bedding planes; and (c) laboratory contamination from hands, dust, reagents, etc. Surface contamination can be removed either by solution of the outer layers (HCl for carbonate-containing specimens; HF for siliceous materials) or by cutting. Acid treatment was used on the specimens analysed in this investigation. In order to avoid contamination from younger materials deposited in cracks and bedding planes, each specimen was first coarsely broken, and the pieces then scrubbed with a wire brush in the presence of 4% HCl or 50% HF to remove the outermost few millimetres. Sweat is known to contain amino acids (Korting and Nitz-litzow, 1952; Pankov, 1953). If the absolute amounts of amino acids in the sample are particularly low, excessive handling of the sample and glassware may result in significant contamination. One of the more serious sources of contamination in our locality is from pine pollen during the late spring. Pollen may visibly coat a clean surface within a few hours when pollen liberation is at a maximum.

After initial cleaning, all samples were ground to pass through a 100-mesh sieve, using an electric hammer-type pulverizing mill. The mill was first thoroughly cleaned and then prechilled to −15°C in order to reduce frictional heat during use. The moisture content of each specimen was determined as the weight loss on drying at 110°C for 48 hr. Ash content was measured by heating a dry pulverized sample in an electric muffle furnace for 6 hr at 250°C, followed by 24 hr at 450°C. Longer heating at the latter temperature failed to produce appreciable weight changes; however, heating for an additional 24 hrs at 550°C usually resulted in a 2% weight loss.

Total-N was determined after digestion by microdistillation and titration of ammonia, according to the method of Conway (1957, p. 98). Samples of high ash content were digested in a mixture of equal amounts of concentrated H_2SO_4 and $KHSO_4$ using 0·2% (w/v) of Na_2SeO_4 as a catalyst. Samples of low ash content were digested in small Pyrex test tubes using alternate treatments with heat (aluminium block) and 30% H_2O_2. After the digest had cleared it was refluxed in the same tube with concentrated H_2SO_4 for 1 hr. All nitrogen analyses were performed in duplicate with the appropriate reagent blanks.

The ion-exchange column chromatographic method of Moore and Stein (1954a, b) was used for separation and estimation of amino acids. This method, though more laborious than paper chromatography, was preferred to the latter for the following reasons: (a) moderate concentrations of inorganic ions do not seriously interfere with the ion-exchange separations, whereas they cause distortion of spots on paper chromatograms; (b) the separation of amino acids is more efficient on ion-exchange columns than on paper, particularly when the relative

amino acid concentrations vary within wide limits; (c) weighable amounts of amino acids are readily obtained from column eluates after desalting; and (d) the position of an unknown in the column eluate is to some extent indicative of chemical structure.

The MOORE and STEIN (1954a, b) procedure was closely followed with a few exceptions. A drop-counting fraction collector was used to collect samples of eluate from the column. In order to reduce the length of time spent on each analysis we resorted to collecting 3·5–7·0 ml (39–68 drop) fractions, and simply accepted the poorer separation of peaks that resulted. There was a slight diminution in drop volume during each analysis, but this was reproducible and could be corrected for in calculating the results. Fraction numbers are listed for all tabulated data on amino acid concentrations since these serve to characterize the amino acid (or unknown) in question. The column was packed using a different procedure from that described by MOORE and STEIN (1954a). The Dowex 50 × 4 resin was first wet sieved through a 100-mesh screen, then mixed with 0·2 N pH 5·0 buffer. The resin and buffer were slurried into a column half-filled with the same buffer solution. The resin was allowed to settle by gravity, but before it had completely compacted the clear supernatant solution was suctioned off from the top. Additional slurries were added in a like manner until the column had been packed to a height of 150 cm. Each slurry was added before the previous one had completely settled. The resulting column had a flow rate of about 12 ml/hr. A control flow rate of about 8 ml/hr was obtained by varying the height of the buffer reservoir.

The optical densities of amino acid solutions (after reaction with ninhydrin) were measured with a Beckman DK-2 recording spectrophotometer provided with a specially designed cell holder for optically matched test tubes. Relative ninhydrin colour yields at a wavelength of 570 mμ were determined for a number of amino acids, and the results found to be in good agreement with those listed by MOORE and STEIN (1954b). During normal chromatographic separations the eluate fractions constituting a peak were bulked and desalted according to the method of DRÈZE, *et al.* (1954). The desalted solutions were evaporated to small volume in a rotary evaporator under reduced pressure. The concentrates were then transferred to small test tubes and taken to dryness in a vacuum desiccator. Each concentrate was subjected to one-dimensional paper chromatography, usually in two different solvent systems: 20% water–80% phenol (v/v); and the butanol–acetic acid–water system (4 : 1 : 5, vvv) of PARTRIDGE (1948). Standard amino acids were chromatographed beside the samples. The location of amino acid spots on paper chromatograms was routinely determined with a ninhydrin spray. More specific spray reagents were used in some cases: the Sakaguchi reagent for arginine (BLOCK *et al.*, 1952); Pauly's reagent for histidine and tyrosine (BLOCK *et al.*, 1952); isatin reagent for proline (ACHER *et al.*, 1950); Nessler's solution saturated with sodium periodate for serine and threonine (BLOCK and BOLLING 1951); and ethanolic bromophenol blue for acidic amino acids (COCHRANE, 1955).

In the results presented below, total-N refers to that measured (after digestion of samples) by CONWAY's (1957) procedure; amino-N to the N present in amino groups, measured here as "leucine-equivalent" ninhydrin reaction products; amino acid-N to the N present in the form of amino acids; and ammonia-N to the

base volatilized under the conditions of microdistillation described by Conway (1957). In calculating the amounts of nitrogen present in unknowns it was assumed that the extinction coefficients of the ninhydrin reaction products were equivalent to that of leucine, and that each unknown contained one nitrogen atom per molecule.

Tests of Methods

Recovery of amino acids added to Dowex 50 × 4 columns

A solution containing eight amino acids (10 μmoles each of aspartic acid, glutamic acid, glycine, valine, leucine and tyrosine; and 20 μmoles each of lysine and arginine) was chromatographed on a Dowex 50 × 4 column according to the Moore and Stein (1954a) procedure. The recoveries were 100–102 per cent for glutamic acid, leucine, tyrosine and arginine; and 105–109 per cent for aspartic acid, glycine, valine and lysine. The high recovery values for the last four amino acids are unexplained.

Recovery of amino acids from concentrated solutions of calcium chloride

After dissolving and hydrolysing carbonate-rich specimens in HCl some method has to be adopted to separate amino acids from the resulting $CaCl_2$ solution. Abelson (1954) separated amino acids from calcium ions by selective elution of amino acids from a Dowex 50 column using 5 N NH_4OH as an eluant. Ammonia was then removed by repeated evaporation of the eluate. Our procedure has been to precipitate calcium as the insoluble sulphate by step-wise addition of H_2SO_4; then to remove the HCl by vacuum distillation. The bulk of the calcium was first precipitated by nearly quantitative addition of H_2SO_4. Both this precipitate and those formed subsequently during vacuum distillation were thoroughly washed with distilled water at 90–100°C. The filtrates and washings were concentrated by further vacuum distillation. Usually three to five filterings were required and some additional H_2SO_4 to make the final concentrate essentially calcium-free.

In order to determine whether the recovery of amino acids was quantitative under these conditions, small amounts of standard amino acid solutions were added to 200 ml samples of a 50% (w/v) solution of $CaCl_2$ (U.S.P., Merck). The $CaCl_2$ was removed by the procedure outlined above. The final calcium-free concentrates were brought back to original volume with distilled water and the concentrations of amino compounds determined photometrically with ninhydrin (Moore and Stein, 1954b). A $CaCl_2$ solution without any added amino acids was used as a blank. This solution contained small amounts of ninhydrin-reacting material. The recoveries of added amino acids (after subtraction of the $CaCl_2$ blank) were calculated as percentages of distilled water controls. The results are reported in Table 1. A recovery of 94–96 per cent was observed in each case, with no evidence of fractionation among the amino acids tested. Tarte (1945) reported that aspartic acid was the only amino acid of many tested that was strongly held by aged activated $BaSO_4$ granules. It is possible that some losses of aspartic acid may have occurred in our analyses, however, these were certainly not complete losses, as evidenced by the presence of aspartic acid in shell hydrolysates (see below). In any case, the results for the other amino acids appear to be reliable.

Contamination level

For accurate amino acid analysis the contamination level must remain low in relation to the absolute amount of amino acids in the sample. Errors arising from contamination are most serious for those amino acids present in the lowest concentrations. In order to determine our usual contamination level the following experiment was performed. A 200 g sample of HCl-washed quartz sand was pulverized to pass through a 100-mesh screen. The sample was then treated in the

Table 1. Recovery of amino acids from 200 ml of a 50% (w/v) solution of $CaCl_2$* after precipitation of calcium with H_2SO_4 and removal of HCl by vacuum distillation
(Recovery is expressed as a percentage of that recovered from a distilled water control.)

Amino acid	Weight added (mg)	Recovery (%)
Casamino acids (Difco)†	1·2	96
Arginine	13·0 (75 μmoles)	94
Glycine	5·6 (75 μmoles)	96
Glutamic acid	11·0 (75 μmoles)	95

* The $CaCl_2$ (U.S.P., Merck) contained small amounts of ninhydrin-reacting substances that remained in solution after precipitation of the calcium. All percentage recovery values were corrected for this background level of ninhydrin-reacting substances. It was also found that quantitative determinations of amino acids using the photometric ninhydrin method could not be made in the presence of appreciable amounts of $CaCl_2$ due to changes in the position of the absorption maximum and in the value of the extinction coefficient.

† A casein hydrolysate.

same way as a sample of Green River shale (see below) with the exception that only one period of hydrolysis was used for the quartz sand. The hydrolysate of the sand contained 2·47 mg of total-N. Of this amount, 1·67 mg of N was accounted for as ammonia-N on the basis of microdistillation of ammonia. Direct tests showed that all the ninhydrin-reacting material in the hydrolysate could be accounted for as ammonia. The non-ammonia-N was evidently not in a form capable of reacting with ninhydrin. Less than 0·7 per cent of the total-N in the hydrolysate could have occurred in the form of amino acids. Under the usual conditions of analysis this amount of contamination (<10 μg of amino acid-N per 100 g of sample) is insignificant.

Results and Discussion

Recent lake sediments

Two sediment samples were collected from Lake Opinicon, a small eutrophic lake of 10 m maximum depth, located in the Rideau watershed about 30 miles NW of Kingston, Ontario. The samples were collected with a modified Livingstone piston sampler (Vallentyne, 1956a) at a point with the co-ordinates 11.5 and 23.0 on the map of Lake Opinicon published by Curran *et al.* (1947). The depth of water at the sampling site was 7 m. One sample was taken from the sediment surface and the other at a depth of 3 m directly below. The age of the buried

sample is not accurately known, but is estimated to be 1000–3000 years on the basis of unpublished pollen diagrams constructed by John Potzger shortly before his death.

Table 2. Chemical data for surface and subsurface sediment samples from Lake Opinicon, Ontario, and for a sample of Green River shale (Eocene) collected near Rifle, Colorado

Datum	Lake Opinicon		Green River shale
	Surface sediment	Subsurface sediment	
Water content (% of fresh wt.)	96·6	93·3	—
Ash (% of dry weight)	46·3	30·0	46·4
Total N (% of dry wt.)	2·51*	2·49*	1·03
Total N (% of dry ignitable matter)	4·68*	3·56*	1·92
N soluble in cold 1 N HCl (% of total N in oven-dried sediment):			
(a) in the form of ammonia	2·6	5·3	—
(b) other forms of N†	5·4	5·7	—
(c) sum of (a) and (b)	8·0	11·0	—
N soluble in hot 1 N HCl (after extraction with cold 1 N HCl) (% of total N in oven-dried sediment):			
(a) in the form of ammonia	0·0†	1·0	—
(b) other forms of N†	3·5†	5·2	—
(c) sum of (a) and (b)	3·5†	6·2	—
N in 6N HCl hydrolysate (% of total N in dry sediment):			
(a) insoluble in 6 N HCl	—	—	89·5
(b) in the form of ammonia	(34·6)‡	(29·8)†	§
(c) in the form of amino acids	(64·8)‡	(69·4)†	0·014
(d) other forms of N†	(0·0)‡	(0·8)‡	—
(e) sum of (a) to (d)	100·0	100·0	

* These values were determined on oven-dried samples. Subsequent work has shown that lake sediments lose an appreciable fraction of Kjeldahl nitrogen on drying. In the case of a surface mud sample from Lake Opinicon about 11 per cent of the original nitrogen was lost in this manner, so the given values are low by approximately this percentage.

† Measured by difference.

‡ The percentages given here refer to the nitrogen in each fraction as a percentage of the total-soluble-N in the hydrolysate, and not as a percentage of the total-N in the sediment. The data cannot accurately be expressed as a percentage of the total-N in the sediment because the total-N values were low due to loss of N on drying (see footnote*).

§ Excess ammonia was added to the shale hydrolysate to precipitate iron and aluminium. Thus the percentage of ammonia-N in the shale could not be ascertained.

Separate aliquots of a homogenized wet surface sample were extracted with cold (5°C) 1 N HCl and hot (90–100°C) 1 N HCl. Both extractions were performed step-wise and terminated only when successive extracts were found to contain negligible amounts of ninhydrin-reacting substances. A separate aliquot of the surface sample was hydrolysed with 6 N HCl for 26 hr. The excess HCl was removed from the extracts prior to chromatography by repeated evaporation

under reduced pressure at temperatures not exceeding 45°C. Some breakdown of labile nitrogenous substances in the cold acid extract doubtless occurred during concentration. The subsurface sample was treated in the same way as the surface

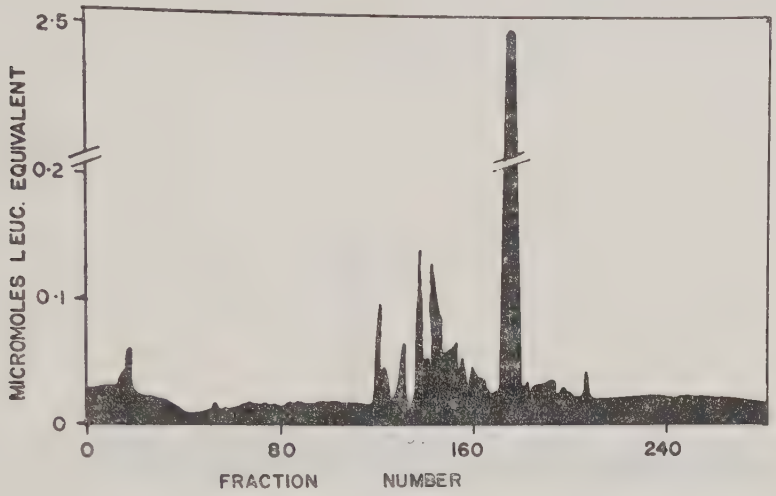

Fig. 1. Histogram of ninhydrin-reacting compounds in a cold 1 N HCl extract of 30·4 g wet weight (1·04 g dry weight) of surface sediment from Lake Opinicon, Ontario. The highest peak was due to ammonia.

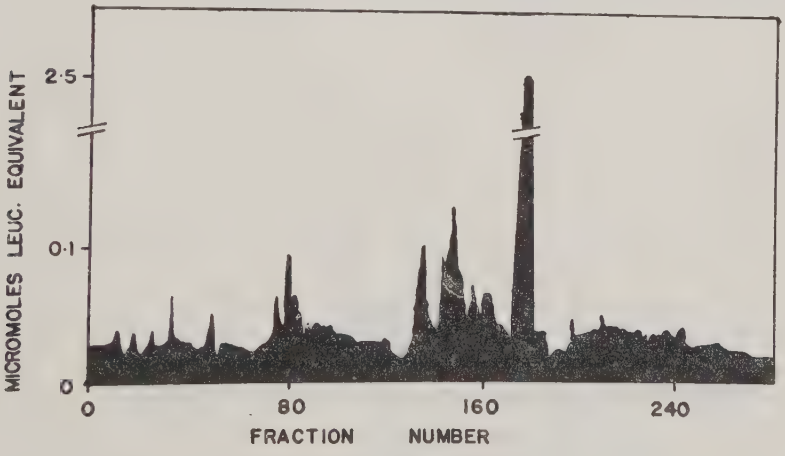

Fig. 2. Histogram of ninhydrin-reacting compounds in a hot 1 N HCl extract of 30·0 g wet weight (1·03 g dry weight) of surface sediment from Lake Opinicon, Ontario. The highest peak was due to ammonia.

sample, with this exception: that a single aliquot was successively extracted with cold, then hot 1 N HCl. The concentrates from all extracts were chromatographed directly on Moore and Stein (1954a) columns, i.e. without hydrolysis. A separate aliquot of the subsurface sample was hydrolysed with 6 N HCl for 26 hr.

The results of column chromatography of the acid extracts are shown graphically in Fig. 1–4. Quantitative data on the forms of nitrogen in the extracts and in the hydrolysates are listed in Table 2. It is notable that only a small percentage

(8 per cent and 11 per cent, respectively for the surface and subsurface sediment samples) of the total-N expressed as a percentage of the total-N in the dried sediment was extracted with cold acid, and little more with hot acid. These values are lower than those found for other Ontario lake sediments by Kleerekoper (1957). The low values cannot be explained by losses of volatile-N on drying

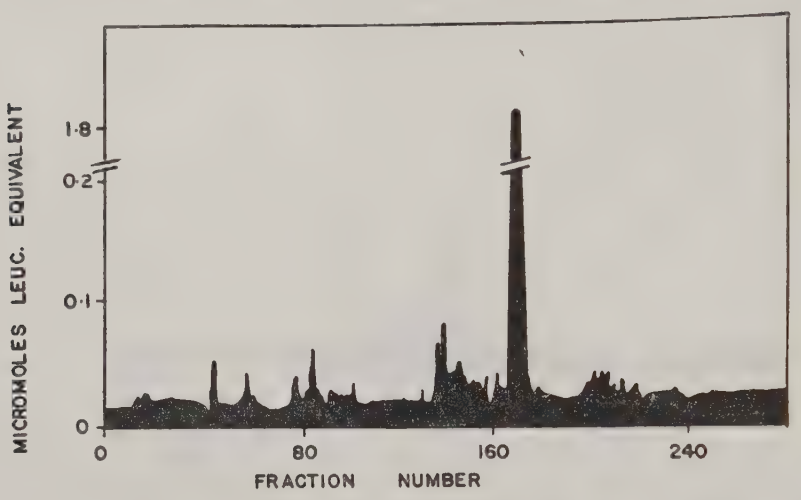

Fig. 3. Histogram of ninhydrin-reacting compounds in a cold 1 N HCl extract of 20·0 g wet weight (1·34 g dry weight) of subsurface sediment from Lake Opinicon, Ontario. The highest peak was due to ammonia.

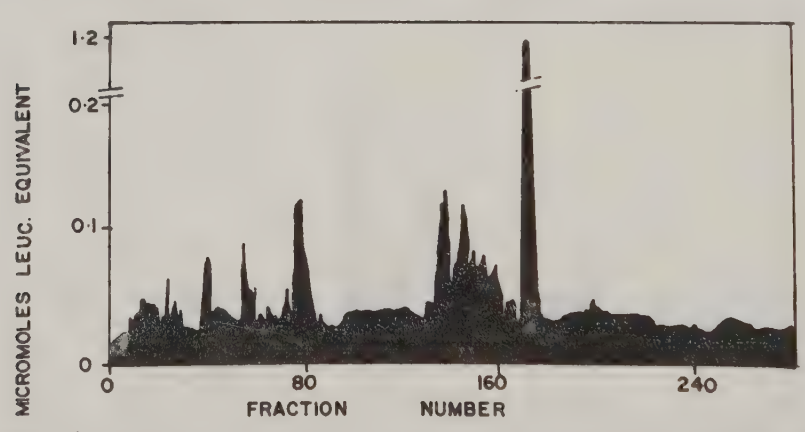

Fig. 4. Histogram of ninhydrin-reacting compounds in a hot 1 N HCl extract of the cold 1 N HCl-insoluble residue from 20·0 g wet weight (1·34 g dry weight) of subsurface sediment from Lake Opinicon, Ontario. The highest peak was due to ammonia.

since the samples used for extraction were not dried. The amount of ammonia in the cold acid extract of the subsurface sample was approximately double that of the surface sample. Although the data on hand do not permit a conclusive statement, it seems reasonable to suppose that the excess ammonia in the buried sample represents ammonia derived from the *in situ* breakdown of organic nitrogen compounds during the period of burial. Most of the inferred breakdown was probably biological rather than chemical.

Although no attempt was made to identify the ninhydrin-reacting materials in the acid extracts by paper chromatography, an examination of Figs. 1–4 shows that more peaks were present than could reasonably be accounted for as free amino acids. Knowing the amount of total-N placed on the columns, and the moles of ninhydrin-reacting substances (calculated as leucine equivalents) recovered in the eluate, one can calculate the amounts of nitrogen in the extracts that were not in a form capable of reacting with ninhydrin. If it is assumed that all the non-ninhydrin-reacting nitrogen was in the form of peptide bonds, then it is possible to calculate the average chain lengths of the peptides in the extracts.

Table 3. Calculation of the average number of amino acid units per peptide in cold 1N HCl extracts of surface and subsurface sediments from Lake Opinicon, Ontario
(The nitrogen values are given as mg of N per 100 mg of N placed on the Dowex 50 × 4 column.)

Sample	NH_3-N (mg)	Amino—N* (mg)	N unaccounted for (mg)	Average number of amino acid units per peptide
surface	32·3	10·7	57·0	6
subsurface	48·8	1·4	49·8	36

* The quantity of ninhydrin-reacting substances other than ammonia, calculated as leucine equivalents.

The pertinent data are presented in Table 3. The presence of higher molecular weight peptides in the subsurface sample may possibly have resulted from a hydrolysis of acid-insoluble sedimentary polypeptides to large acid-soluble peptides during the period of burial.

Quantitative data on the amino acids present in the hydrolysates of the surface and subsurface samples are given in Table 4. In the case of the surface sample 11·0 per cent of the total-N in the *undried* sediment was insoluble after hydrolysis. The corresponding value of the subsurface sample is unknown, but it is known that 2·47 mg of total-N was solubilized after hydrolysis of an amount of wet subsurface sediment corresponding to 100 mg dry weight. One of the difficulties in quantitative nitrogen analyses of sediments is that on a dry weight basis, dried sediments have a lower Kjeldahl-N content than do the same fresh (wet) sediments.

Virtually all the soluble-N in the hydrolysates was accounted for as ammonia-N and amino acid-N, with the latter comprising roughly two-thirds of the total soluble-N. Approximately 85 per cent of the ammonia present in the hydrolysates must have arisen during hydrolysis, for neither the hot nor the cold acid extracts contained such a large quantity of ammonia. It is also apparent that all the excess ammonia in the hydrolysates (as compared to the acid extracts) could not have originated by hydrolytic deamination of any asparagine or glutamine that might have been present in the sediment. The quantities of aspartic and glutamic acids in the hydrolysates were insufficient to account for all the excess ammonia. A small amount of the ammonia may have originated by deamination of some amino acids during hydrolysis.

The subsurface sample contained noticeably lower mole percentages of proline, valine, histidine and lysine, and higher mole percentages of alanine and unknowns

(nos. 2–4) than did the surface sample. These differences could either be due to selective breakdown and/or formation during the period of burial, or to differences in the types of polypeptide originally deposited. There is no way of determining which was the case. Peak no. 1 probably represents cysteic acid, an oxidation product of cystine produced during hydrolysis. The R_f values of the unknowns on paper chromatography with butanol–acetic acid–water (b) and aqueous phenol (p) were as follows: no. 2: 0·42(b), 0·05(p); no. 3: 0·39(b), 0·79(p); no. 4: 0·36(b), 0·78(p). The positions of no. 3, and no. 4 in the eluates lie close to that expected for glucosamine, but the R_f values on paper chromatography are too high for either glocosamine or galactosamine.

From the data given in Table 4 the amounts of sulphur present in the form of sulphur-containing amino acids were calculated to be 0·12 and 0·06 per cent of the dry weights of the surface and subsurface samples, respectively. The total-S contents of the samples were not determined.

Green River shale

An organic-rich sample of shale from the Green River formation (collected near Rifle, Colorado) was selected as a fossil counter-part of modern lake sediments. The sediments of the Green River formation were originally deposited in a relatively shallow inland body of water, Lake Uinta, during the middle part of the Eocene epoch. The paleobiology and paleolimnology of Lake Uinta have been discussed by Bradley (1931). The sample used for analysis contained 46·4% ash and 1·03% N on a dry matter basis, values corresponding closely to those of the Recent sediments from Lake Opinicon. Our purpose was to make a quantitative comparison of the forms of nitrogen in the Eocene and modern sediments, in order to assess the results of diagenetic processes.

A 200 g sample of the powdered shale (passed through a 200-mesh sieve) was refluxed with 400 ml of 6 N HCl for 50 hr. The residue was repeatedly refluxed with additional acid until aliquots of the supernatant yielded only a slight precipitate with excess NH_4OH. The insoluble material remaining after hydrolysis was centrifuged, washed well with hot distilled water, and analysed for total-N. The HCl-soluble fractions were combined and evaporated to about 100 ml under reduced pressure. An aliquot was removed for determination of total-N and the remainder was repeatedly evaporated under reduced pressure with occasional additions of water to remove excess HCl. The final evaporate was thoroughly mixed with 500 ml of hot distilled water. Excess ammonia was added to precipitate iron and aluminium hydroxides. The precipitate was thoroughly washed with several portions of hot distilled water, and the water washings were added to the filtrate. The precipitate was dried and analysed for total-N in order to determine whether any nitrogenous materials had been co-precipitated. Negative results were obtained. It was calculated that less than 0·1 per cent of the total-N in the hydrolysate had been lost to the precipitate.

The clear solution that remained after the iron and aluminium had been precipitated contained high concentrations of ammonium chloride. This solution was diluted to 1 l. with distilled water and then percolated through a column of Dowex-50 (H-form). The column was washed with distilled water and then

developed with 5 N NH_4OH. Three fractions of the eluate were collected separately: (a) the percolated solution plus water washings; (b) the eluate that emerged from the column just before the eluant (5 N NH_4OH); and (c) some of the alkaline eluate. Each fraction was taken to dryness under reduced pressure and separately

Table 4. Quantitative data on the forms of nitrogen in 6 N HCl hydrolysates of surface (A) and subsurface (B) sediments from Lake Opinicon, Ontario, and of a sample of Green River shale (C) from Rifle, Colorado

(The amino compounds are listed in order of elution from the column. Concentrations of unknowns are expressed as leucine equivalents. The volumes of the fractions for (A) and (B) varied from 3·9 ml at the start to 3·4 ml at the end of the run; those for (C) varied from 7·0 ml at the start to 6·0 ml at the end of the run. The mole % column refers to the number of amino acid units per 100 total amino acid units.)

Amino acid	Fraction numbers			mg N/g ignitable matter			Mole% of total amino acid		
	(A)	(B)	(C)	(A)	(B)	(C)	(A)	(B)	(C)
No. 1	—	6–9	—	0·00	0·09	0	0·0	0·3	0
No. 2	—	23–27	—	0·00	0·19	0	0·0	0·9	0
Aspartic acid	45–54	42–48	23–27	2·73	2·61	4×10^{-4}	10·6	11·8	14
Threonine	54–60	48–51	—	4·04	0·90	0	15·5	4·1	0
Serine		51–54	—		1·34	0		6·1	0
Proline	64–66	59–63	—	1·31	0·22	0	5·0	1·0	0
Glutamic acid	68–72	62–73	33–39	1·94	2·07	17×10^{-4}	7·4	9·4	63
Glycine	74–78	73–81	—	4·17	3·86	0	15·9	17·5	0
Alanine	78–80	81–87	43–48	2·40	2·96	1×10^{-4}	9·2	13·4	2
Valine	84–94	95–104	—	3·25	1·65	0	12·4	7·5	0
Methionine	134–141	144–153	—	1·03	0·62	0	3·9	2·8	0
Leucine(s)	144–148	153–160	61–66	1·39	0·93	1×10^{-4}	5·3	4·2	4
No. 3	—	161–168	—	0·21	1·64	0	0·8	7·4	0
No. 3A*	—	—	69–72	0·00	0·00	2×10^{-4}	0·0	0·0	9
No. 4	152–153	170–175	—	0·00	0·34	0	0·0	1·6	0
Tyrosine and phenylalanine	159–164	177–185	—	1·36	1·72	0	5·2	7·8	0
γ-Aminobutyric acid	—	186–188	76–80	0·00	0·11	2×10^{-4}	0·0	0·5	8
Ammonia	169–185	193–208	81–91	16·17	10·37	—		—	—
Lysine	192–202	215–230	—	2·68	0·41	0	5·1	0·9	0
Histidine	202–209	231–235	—	0·94	0·39	0	1·2	0·6	0
Arginine	238–243	262–269	—	2·82	1·95	0	2·7	2·2	0
Unaccounted for†				1·76	0·29	—	—	—	—
Total				48·20	34·66	27×10^{-4}	100	100	100

* Unknown no. 3A could be identical to no. 3 or no. 4. Insufficient material was on hand for determination of R_f values by paper chromatography.

† By difference. These values refer to nitrogen placed on the column that was not accounted for as nitrogen in ninhydrin-reacting compounds.

analysed for ammonia-N and total-N. Only fractions (b) and (c) contained nitrogen that could not quantitatively be accounted for as ammonia-N. These fractions were accordingly bulked and dissolved in 5 ml of distilled water. A 4 ml aliquot was removed for separation of amino acids on a Moore and Stein (1954a) column.

Quantitative data on amino acids in the hydrolysate are presented in Tables 2 and 4. The data for the shale contrast sharply with those for Lake Opinicon, both in regard to the percentage of the total-N that occurred in the form of

amino compounds (0·014 per cent as compared to approximately 60 per cent) and in regard to the number of amino acids identified (five as compared to seventeen). It is not unreasonable to suppose that the sediments deposited in Lake Uinta about 45 million years ago originally had about the same quantitative distribution of nitrogenous compounds as the sediments from Lake Opinicon. If one accepts this assumption, then it is clear that the bulk of the polypeptides and amino acids originally present in the Lake Uinta deposits was transformed into other types of nitrogenous compounds. Most of these transformation products are insoluble in HCl and form part of the "kerogen" of the rock. Of course, we do not know how much nitrogenous material may have been added to, or removed from, the sediments by post-depositional processes.

The percentage molar composition of the amino acids recovered from the shale hydrolysate is given in Table 4. Glutamic acid was present in the highest concentration, with lesser amounts of aspartic acid, γ-aminobutyric acid, leucine(s), alanine, and unknown no. 3A. These were the only amino acids left of a presumed total of about seventeen amino acids originally present. Not only had there been an overall destruction of amino acids; there was a selective decomposition as well. The results are shown graphically in Fig. 5. The pattern is thus similar to that found for recent and fossil *Mercenaria* shells (Abelson, 1956) and Recent and fossil sediments of marine origin (Erdman *et al.*, 1956). Of the amino acids found in the shale hydrolysate, only aspartic acid is among those listed as thermally unstable in aqueous solution by Abelson (1956). It is well known (Hurd, 1929) that γ-aminobutyric acid is a decomposition product of glutamic acid when the latter is thermally degraded. Some of the γ-aminobutyric acid in the shale could have originated in this way, but it is also possible that this compound was originally present in the Lake Uinta sediment. Povoledo (1959) has found γ-aminobutyric acid in lake sediments.

Pre-Cambrian-sedimentary rocks

Hydrolysates of two pre-Cambrian sedimentary rocks were examined for amino acids. The first was a sample of chert from the Gunflint formation, from the locality described by Tyler and Barghoorn (1954). Analyses of glauconites collected from beds within the Gunflint formation for A^{40}/K^{40} ratios yielded an average date of $1{\cdot}6 \times 10^9$ years (personal communication from P. Hurley to E. S. Barghoorn). Tyler and Barghoorn (1954) found microfossils resembling blue-green algae and fungi in the Gunflint chert. In view of the rarity of well-preserved pre-Cambrian fossils, and the significance of the Gunflint discovery, we considered it important to analyse the chert for amino acids. The second sample analysed was an excavated sample of coal-like material from the Michigamme formation in northern Michigan (Tyler *et al.*, 1957). The age of the deposit is somewhat uncertain, but probably of the order of $1{\cdot}1$–$1{\cdot}3 \times 10^9$ years old (personal communication from Barghoorn). The sample was of interest because of its high organic matter content (75·7 per cent ignitable matter) and its nitrogen content (0·91% N on a dry matter basis).

In neither case was a positive result obtained from 6 N HCl hydrolysates of thoroughly cleaned samples. A positive result was obtained for the first sample of

the Gunflint chert that was analysed, but this was later shown to be due to inadequate cleaning of the rock before analysis. The limits of detection were 0·1 and 0·02 μmoles of amino acid per g of rock for the chert and "coal," respectively. Of

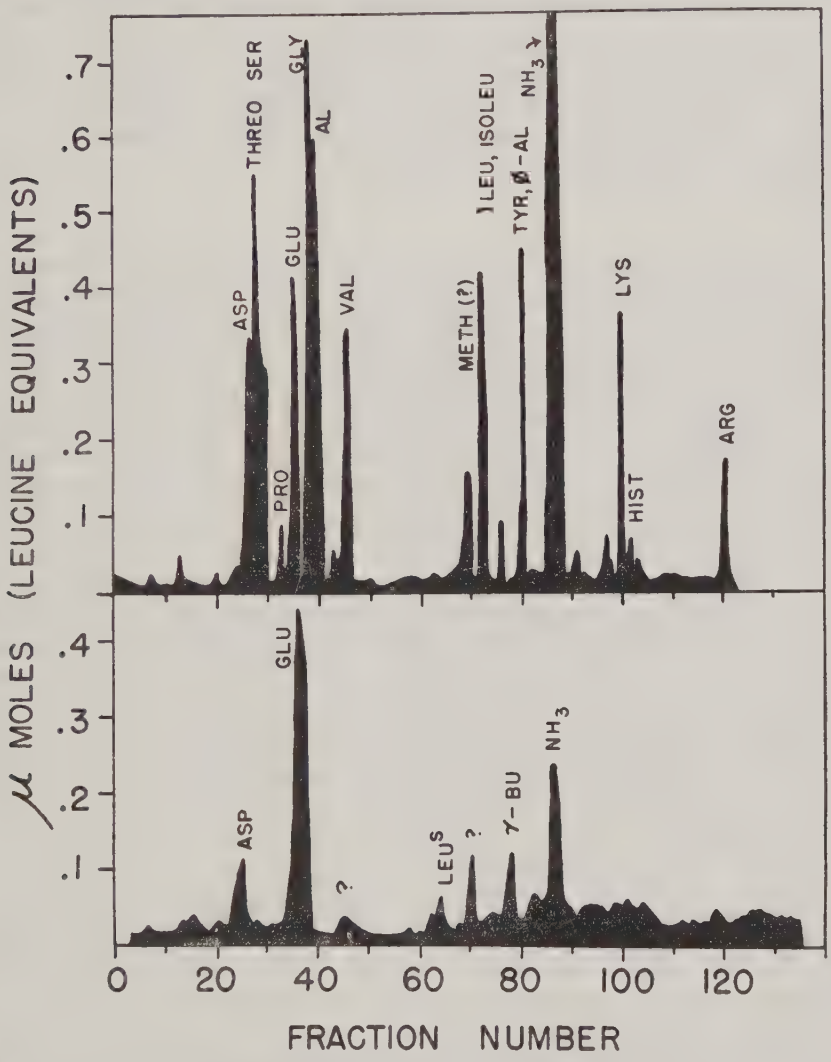

Fig. 5. A. Upper. Histogram of ninhydrin-reacting compounds in a 6 N HCl hydrolysate of 0·106 g dry weight of subsurface sediment from Lake Opinicon, Ontario. B. Lower. Histogram of ninhydrin-reacting compounds in a 6 N HCl hydrolysate of 160 g dry weight of shale from the Green River formation, collected near Rifle, Colorado.

the total-N in the "coal," only 1·2 per cent was solubilized by hydrolysis with 6 N HCl, and of this amount 96 per cent was in the form of ammonia. Nitrogen in the form of amino acids could therefore not account for more than 0·04 per cent of the total-N in the "coal." Comparable data for the chert were not obtained.

The absence of amino acids in the hydrolysate of the pre-Cambrian "coal" agrees with the findings of Tyler *et al.* (1957) on another sample from the same

formation, but we were unable to corroborate Barghoorn's (1957) report from Abelson that amino acids were present in the Gunflint chert to the extent of 2·0 μmoles/g. It is possible that local differences may exist in the chert. In any case, the absence of amino acids in a hydrolysate of a rock does not necessarily mean that amino acids are not, or were never, present in the rock. The amino acids could have been present originally, but degraded after burial, or perhaps partly during hydrolysis. It is worthwhile noting that no relevant tests have thus far been made on the breakdown of amino compounds during the hydrolysis of rocks and fossils.

Miocene lignite

A hydrolysate of a Miocene coniferous lignite from the Liblar Mine, near Cologne, Germany, was analysed for amino acids. The lignite contained 4·8% ash and 0·26% N on a dry matter basis. A 30 g sample of the powdered lignite was hydrolysed with 2 N H_2SO_4 for 8 hr under reflux. The residue was further hydrolysed with the same concentration of acid for 1 hr in an autoclave at 15 lb pressure. The combined acid-insoluble residues from hydrolysis contained 89·8 per cent of the original nitrogen of the lignite. The combined residues were exhaustively extracted with 2 N NaOH. This treatment bought 59 per cent of the acid-insoluble-N into solution. On making the alkaline extract slightly acid with HCl, 82 per cent of the nitrogen in the alkaline extract precipitated out.

The filtrate of the hydrolysate and the acid-soluble and acid-insoluble parts of the 2 N NaOH extract of the residue left after acid hydrolysis were separately analysed for amino acids using a test tube ninhydrin reaction (Moore and Stein, 1954b). In no case was a positive result obtained. The data showed that less than 0·07 per cent of the total-N of the lignite could have been in the form of amino-N. It is interesting to note that although amino acids were not detected in this sample, Brasch and Jones (1959) did recover 3·2 per cent of the dry weight of the lignite as holocellulose. The holocellulose liberated glucose and mannose on hydrolysis in a ratio of about 14 : 1.

Carnosaur "teeth"

A sample of carnosaur "teeth" (unidentified as to species) from the Edmonton formation (Upper Cretaceous) was used for analysis. The "teeth" had been partly cemented together from broken fragments with "Duco" cement. The cement was removed by immersing the sample in acetone for a week, followed by rinsing in clean acetone. Surface contamination was removed by brief immersion in 1 N HCl with brushing.

A 100 g sample of the dry powdered material, containing 0·032% N on a dry matter basis, was extracted over a 3-month period with successive portions of 1 N HCl at a temperature of 4°C. The extracts were combined and the HCl removed by repeated evaporation under reduced pressure. On suspending the undistillable residue in distilled water a white powder, presumably $Ca_3(PO_4)_2$, remained insoluble. This powder was filtered off and washed with hot distilled water. The washings were added to the filtrate. Calcium was removed from the filtrate by controlled addition of H_2SO_4 as described under the heading of General

Methods. The final low-calcium concentrate was dissolved in a standard volume of distilled water. Aliquots were removed for determination of total-N and for column chromatography of amino acids.

The fraction of the powdered "teeth" that failed to dissolve in cold 1 N HCl was refluxed with 6 N HCl for 24 hr. The insoluble residue left after hydrolysis was centrifuged down and washed with hot distilled water. The solution and washings were combined and repeatedly evaporated under reduced pressure to remove excess HCl. The final concentrate was made to standard volume with distilled water. Total-N content was determined on an aliquot of the hydrolysate, but column chromatography was not attempted due to the small amount of material available.

Extraction with cold 1 N HCl removed 29·1 per cent of the nitrogen present in the powdered "teeth". Hydrolysis of the cold acid-insoluble residue only brought an additional 9·8 per cent of the original nitrogen into solution. A total of 38·9 per cent of the original nitrogen was thus brought into solution by the two acid treatments. The results from column chromatography of the cold extract are shown in Fig. 6. The series of unseparated peaks in the region of fraction numbers 60–70 represents a mixture of at least two ninhydrin-reacting substances, one of which was definitely identified as leucine(s), and the other not identified. The other main peak (fractions 82–90) was mostly composed of ammonia, but it also contained ethanolamine ($R_f = 0{\cdot}34$ on paper chromatography with butanol–acetic acid–water). A ninhydrin-positive spot was not detected on a chromatogram developed with aqueous phenol, possibly due to volatilization of the ethanolamine in phenol. Assuming leucine-equivalent colour yields for the unknown(s), the recovery of the nitrogen placed on the column was only 13·6 per cent.

It is shown below that hydrolysates of heated shells of the clam *Mercenaria mercenaria* contained ninhydrin-reacting compounds similar to those listed above. These compounds (the "leucine-companion" and the ethanolamine) were only found in samples heated in sealed tubes; not in unheated shells, nor in shells heated in an open vessel under nitrogen. It has not been proved that the "leucine-companion" in the carnosaur "teeth" extract is identical to that in the heated shell, but the chromatographic data are suggestive of such a relation. Ethanolamine was identified both in the carnosaur "teeth" and heated shells.

The shell of Cassis Madagascarensis

A shell of the univalve, *Cassis Madagascarensis*, collected in the Carribean region in 1910, and stored for 45 years in the Queen's University museum, was analysed for amino acids. After removal of the surface layers by brushing in 1 N HCl, the shell was ground to pass through a 100-mesh sieve. The powder contained 0·0108% N on a dry matter basis. A 1 kg sample of the powdered shell was exhaustively extracted with separate portions of 1 N HCl at 4°C over a period of several weeks. The insoluble residue from the cold acid treatment was successively washed with water, ethanol, and finally with dry diethylether, yielding a dark brown powder (conchiolin) weighing 437 mg and containing 13·15% N on a dry matter basis.

An aliquot of the cold acid extract was concentrated by vacuum distillation at

temperatures under 45°C to remove the excess HCl. The concentrate was decalcified with H_2SO_4 as described under General Methods and finally brought to standard volume with distilled water. Total-N was determined on one aliquot, and another aliquot was removed for column chromatography. Quantitative data on the forms

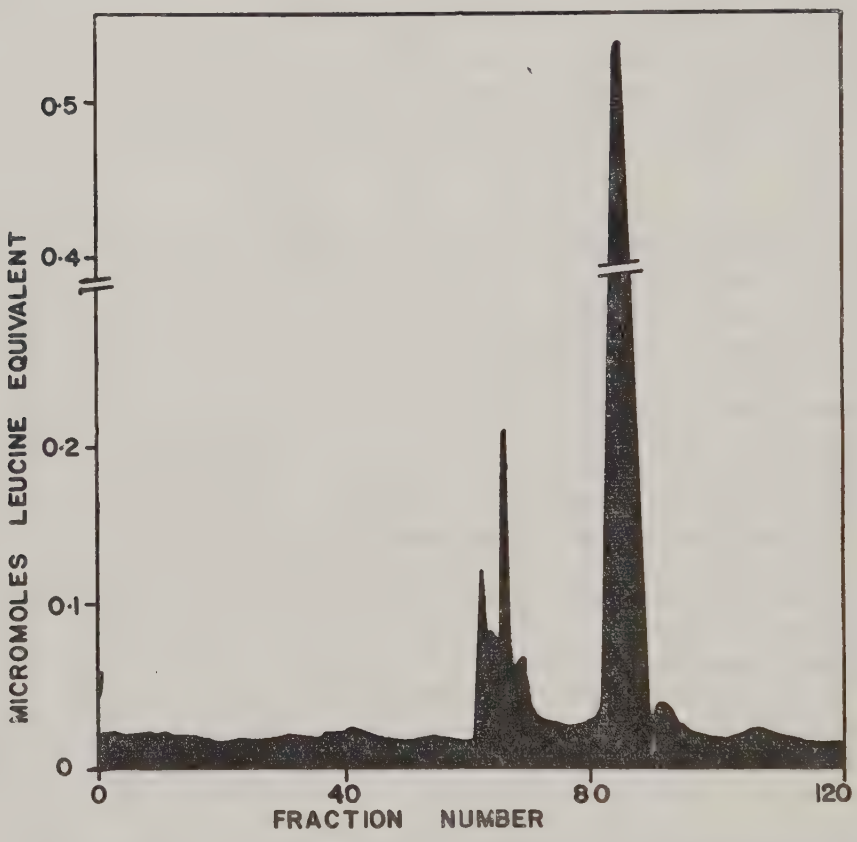

Fig. 6. Histogram of ninhydrin-reacting compounds in a cold 1 N HCl extract of 25 g dry weight of carnosaur "teeth" from the Edmonton formation (upper Cretaceous). Unidentified compounds were present in the peaks near leucine, and ethanolamine appeared in the ammonia peak.

of nitrogen present in the cold acid extract are listed in Table 5, and on the amino acids and other ninhydrin-reacting substances obtained from column chromatography in Table 6.

A 100 mg portion of the "conchiolin" (the residue left after successive extraction with cold acid, ethanol and ether) was hydrolysed for 24 hr in 6 N HCl. The excess HCl was removed by repeated evaporation under reduced pressure and the final residue made to standard volume with distilled water. One aliquot was removed for determination of total-N and another for column chromatography. The quantitative data for the hydrolysate are listed in Tables 5 and 6.

As shown in Table 5, approximately 50 per cent of the total-N in the shell was soluble in cold 1 N HCl. Such a high value was unexpected. If one assumes that

all the nitrogen unaccounted for as ninhydrin-reacting substances occurred in the form of peptide bonds, then the average chain length of the peptides in the acid extract can be estimated. The calculated value was 2·7 amino acid units per peptide on the assumption that all the peptides present appeared as ninhydrin-reacting peaks in the column eluate. This value is minimal, and doubtless mainly a function of the chain length of no. 7, the unknown that comprised the bulk of ninhydrin-reacting material in the unidentified peaks. The R_f values of unknowns

Table 5. Quantitative data on the forms of nitrogen in a cold 1 N HCl extract of the shell of *Cassis Madagascarensis*, and in a 6 N HCl hydrolysate of the cold acid-insoluble material (conchiolin) of the shell

Fraction	mg N per 100 g of dry shell	N as % of total N in the shell*
Entire shell	10·8	100
N soluble in 1 N HCl at 4°C:		
(a) in the form of ammonia	1·25	10·9
(b) in the form of identified amino acids	0·56	4·9
(c) in the form of unidentified amino compounds	1·45	12·6
(d) unaccounted for	2·50†	21·7†
(e) sum of (a) to (d)	5·76	50·1
N in hydrolysate of conchiolin:		
(a) in the form of ammonia	0·61	5·3
(b) in the form of amino acids	2·67	23·2
(c) unaccounted for	2·46†	21·4†
(d) sum of (a) to (c)	5·74	49·9

* These values were calculated on the basis of 100 per cent recovery. Actual recovery from the columns amounted to 106 per cent of the N placed on the columns.
† Calculated by difference.

no. 4A and no. 7 on paper chromatography with butanol–acetic acid–water were 0·06 and 0·11, respectively; and 0·01 and 0·12, respectively, with aqueous phenol. It is not known if no. 7 is identical to the "leucine companion" in the extract of carnosaur "teeth".

The most startling fact regarding the "conchiolin" was that 43 per cent of its nitrogen was not recovered in the form of amino acids and ammonia. There were evidently other nitrogen-containing compounds in the "conchiolin" fraction in addition to scleroproteins. The "conchiolin" contained relatively large amounts of aspartic acid, glutamic acid and glycine. Of the unidentified peaks, no. 1 was probably cysteic acid, an oxidation product of cystine; no. 4, probably methionine sulphoxide, an oxidation product of methionine; and no. 5, probably cystine. The amounts of material available from these peaks were too small to permit verification of identity by paper chromatography. The paper chromatographic R_f values of no. 2 and no. 3 were not determined.

Table 6. Quantitative data on ninhydrin-reacting compounds in a cold 1 N HCl extract of the shell of *Cassis Madagascarensis*, and in a 6 N HCl hydrolysate of the cold 1 N HCl-insoluble matter (conchiolin) of the shell

(The concentrations and nitrogen contents of unknowns were calculated as leucine equivalents. The volumes of the fractions collected varied from 7·0 ml at the start to 6·0 ml at the end of the run for the cold acid extract, and from 3·9 ml to 3·4 ml for the hydrolysate of the conchiolin).

Amino compound	Cold 1 N HCl extract			Conchiolin hydrolysate		
	Fraction numbers	mg N per 100 g shell	Mole % of total amino acid	Fraction numbers	mg N per 100 g shell	Mole % of total amino acid
No. 1	—	0·000	0·0	7–9	0·023	1·0
No. 2	—	0·000	0·0	9–11	0·029	1·3
No. 3	—	0·000	0·0	12–13	0·212	9·6
No. 4	13–15	0·085	4·6	14–16	0·008	0·4
Aspartic acid	—	0·000	0·0	41–45	0·299	13·5
Threonine	19–23	0·193	10·4	45–49	0·108	4·9
Serine				49–51	0·131	5·9
Proline	—	0·000	0·0	57–60	0·149	6·7
Glutamic acid	—	0·000	0·0	62–66	0·197	8·9
Glycine	—	0·000	0·0	67–72	0·182	8·2
Alanine	—	0·000	0·0	72–77	0·148	6·7
No. 4A	45–54	0·133	7·1	—	0·000	0·0
Valine	55–58	0·035	1·9	80–88	0·123	5·6
No. 5	—	0·000	0·0	120–122	0·014	0·6
Methionine	—	0·000	0·0	132–141	0·079	3·6
No. 6	63–64	0·002	0·1	—	0·000	0·0
No. 7	74–78	1·231	66·2	—	0·000	0·0
Leucine(s)	—	0·000	0·0	147–152	0·154	6·9
Tyrosine and phenylalanine	78–80	0·048 (t = p)	2·6	163–169	0·121(p > t)	5·5
Ammonia	81–93	1·251		177–187	0·615	
No. 8*	93–98	0·138	3·7	—	0·000	0·0
Lysine	98–103	0·106	2·8	201–219	0·266	6·0
Arginine	117–120	0·044	0·6	246–252	0·418	4·7
Unaccounted for		2·494†	—		2·464†	—
Total		5·760	100·0		5·740	100·0

* No. 8 was assumed to contain two nitrogen atoms per molecule.
† Calculated by difference.

Mid-Pleistocene shells of Mercenaria mercenaria

Fossil shells of the clam, *Mercenaria mercenaria*, were collected from just above the blue-clay layer in Wailes Bluff, Virginia, a marine deposit of somewhat uncertain stratigraphic position in the Pleistocene. The stratigraphy and paleontology of the deposit have been discussed by Blake (1953). The sediment around the shells was removed by washing with tap water. On brushing the sediment-free shells with 1 N HCl to remove surface contamination, some fibrous remains of the periostracum were observed along the growing edges of the shells. These fibres were collected in a beaker of water, washed with 1 N HCl, rinsed in distilled water, and finally air dried. Approximately 0·3 g of periostracum was collected in this manner from 3 kg of shell material. The fibres contained 55·4% ash, 19·2% C, 2·7% H and 5·3% N on a dry matter basis. These values correspond to 43·0% C, 6·05% H and 11·9% N on an ash-free, dry basis. Since the nitrogen value is low for an arginine-rich polypeptide (see below), the data suggest than non-nitrogenous organic compounds may be present in addition.

A 100 mg sample of the periostracum was hydrolysed with 6 N HCl for 24 hr. The HCl was removed by evaporation under reduced pressure, and the final evaporate made to standard volume with distilled water. The insoluble matter was centrifuged off. Aliquots of the supernatant were removed for determination of total-N and for column chromatography. The total-N determination showed that 71·6 per cent of the original nitrogen was brought into solution by hydrolysis; 28·4 per cent remained in an insoluble form. Quantitative data on the forms of nitrogen in the hydrolysate of the periostracum are given in Tables 7 and 8.

Table 7. Quantitative data on the forms of nitrogen in the periostracum and periostracum-free shell of the clam, *Mercenaria mercenaria*, collected from the Wailes Bluff formation (mid-Pleistocene), Virginia

Fraction	mg N per 100 g shell	N as % of total N in hydrolysate
6 N HCl hydrolysate of periostracum:		
(a) insoluble in 6 N HCl	—	28·8
(b) in the form of ammonia	—	10·4
(c) in the form of amino acids	—	58·5
(d) unaccounted for	—	2·3*
(e) sum of (a) to (d)	0·6†	100·0
6 N HCl hydrolysate of periostracum-free shell:		
(a) insoluble in 6 N HCl	0·0*	0·0*
(b) in the form of ammonia	3·6	20·5
(c) in the form of amino acids	15·0	85·3
(d) sum of (a) to (c)	18·6	105·8

* Calculated by difference.
† Approximate value only.

After removing the surface layers and periostracum, the shells were ground to pass through a 100-mesh sieve. The total-N content of the powdered, periostracum-free shell was 0.018 per cent of the dry weight. Of the total-N in the original shells, only about 3% occurred in the form of periostracum around the growing edge. A 150 g sample of the powdered, periostracum-free shell was refluxed with 500 ml of 6 N HCl for 48 hr. After the excess HCl had been removed by repeated evaporation under reduced pressure the concentrate was decalcified as described under General Methods. After the removal of excess HCl from the decalcified solution the residue was dissolved in a standard volume of distilled water. Aliquots were removed for determination of total-N and for column chromatography. Quantitative data on the forms of nitrogen in the hydrolysate of the periostracum-free shell are listed in Tables 7 and 8.

The data in Table 7 show that nearly all of the nitrogen of the periostracum that was solubilized by hydrolysis could be accounted for as amino compounds and ammonia. The dominant amino acids in the hydrolysate of the periostracum, in decreasing order of concentration, were: arginine, proline, aspartic acid,

Table 8. Quantitative data on ninhydrin-reacting compounds in hydrolysates of the periostracum and the periostracum-free shell of a mid-Pleistocene shell of the clam, *Mercenaria mercenaria*, collected from the Wailes Bluff formation, Virginia

(Concentrations of unknowns were calculated as leucine equivalents. The volumes of the fractions varied from 7·0 ml at the start to 6·0 ml at the end of the run in both cases. A = fraction numbers; B = concentration of amino compounds in mg N per g periostracum or in mg N per 100 g of periostracum-free shell; C = amino acids as mole % of total amino acid.)

Amino compound	Periostracum			Periostracum-free shell		
	A	B	C	A	B	C
No. 1	3–10	0·14	0·7	—	0·00	0·0
No. 2	11–12	0·04	0·2	—	0·00	0·0
No. 3	22	0·03	0·2	—	0·00	0·0
Aspartic acid	27–31	1·42	7·6			
Threonine	31–33	0·51	2·7	23–31	3·35	25·0
Serine	33–38	0·83	4·5			
Proline	36–41	1·85	9·9	32–36	3·17	23·7
Glutamic acid	38–41	0·31	1·7	33–40	1·53	11·4
Glycine	41–46	1·09	5·8			
Alanine	47–49	0·15	0·8	41–49	1·49	11·2
Valine	50–53	1·15	6·1	50–53	0·63	4·7
Cystine(?)	53–57	0·81	4·4	—	0·00	0·0
Leucine(s)	67–76	2·76	14·8	66–72	0·93	7·0
Tyrosine and phenylalanine	76–82	2·70	14·4 (t = p)	78–79	0·66	4·9 (t > p)
Ammonia	82–96	5·51		84–93	3·61	
Lysine	97–102	1·72	4·6	93–104	3·24	12·1
Histidine	102–109	2·04	3·6	—	0·00	0·0
Arginine	119–124	13·48	18·0	—	0·00	0·0
Unaccounted for	—	1·24*		—	0·00*	
Totals		37·78	100·0		18·61	100·0

* Calculated by difference.

leucine(s), tyrosine, phenylalanine, valine, and glycine (see Table 8). It is of interest to note that the fossil periostracum contained a variety of amino acids, even though it had been in intimate contact with the sediment and any percolating solutions for perhaps 100,000 years. Three of the amino acids (cystine, arginine and histidine) that were present in the hydrolysate of the periostracum, were not found in the periostracum-free shell. These results indicate that the scleroprotein of the fossil periostracum has a different amino acid composition from that of the interlayered scleroprotein of the fossil shell. The periostracum evidently contained only a small fraction of the total shell-N. The identification of cystine in the hydrolysate of the periostracum was probably correct; however, there was insufficient material left after desalting for determination of R_f values on paper chromatograms. Cystine, like the other sulphur-containing amino acids, is a rather unstable compound in the presence of oxygen, and might not be expected to occur even in a deposit as young as Wailes Bluff. Of the unknowns, no. 1 and no. 2 moved only slightly from the origin on paper chromatography with butanol–acetic acid–water;

and no. 3 was not present in sufficient amount for detection on paper chromatograms.

The nitrogen compounds in the periostracum-free shell were not separated into cold acid-soluble and cold acid-insoluble fractions as was done in the case of the *Cassis* shell. The entire periostracum-free shell was hydrolysed. In comparing our results to those given by Abelson (1954, 1956) for recent and Miocene shells of *M. mercenaria*, the Pleistocene specimen is seen to resemble the recent shell more closely than the Miocene shell in its amino acid composition. This is as would be expected from the relative ages of the three specimens. The missing amino acids in the Miocene shell (serine, threonine, lysine, tyrosine and phenylalanine) that are known to occur in recent shells (Abelson, 1954, 1956) were also found in the Pleistocene *Mercenaria* shell.

Pyrolysis of powdered Mercenaria *shells from Wailes Bluff*

Abelson (1956, 1957) suggested that there is a parallel between the thermal stabilities of amino acids, as determined by high-temperature experiments on dilute aqueous solutions in the laboratory, and the geologic stabilities as evidenced by preservation of amino acids in old fossils. As yet, no experiments have been undertaken to test the effect of the medium on the decomposition rates of amino acids. We suspected that both the relative and absolute decomposition rates of amino acids would be influenced by the nature of the medium in which decomposition occurred. In order to test this hypothesis, samples of powdered *M. mercenaria* shells from Wailes Bluff were pyrolysed under different conditions. Both the unheated sample (see above) and the pyrolysed samples were drawn from a 3 kg quantity of well mixed, powdered shell. The amino acids used in the experiments were thus the natural shell amino acids in a fossilized state. The powdered shell was pyrolysed in two different ways: (a) by heating in a round bottom Pyrex flask continuously flushed with pure N_2 at 212–213°C; and (b) by heating in sealed evacuated Pyrex tubes at 218–220°C. The samples heated in the open vessel could lose volatile constituents such as water, ammonia, amines, etc., whereas this was not the case for the sealed tubes during the period of thermal treatment.

For the sealed tube experiments, evacuation had to be conducted slowly in order to avoid loss of the powder. The tubes were alternately subjected to evacuation and flushing with N_2 until the pressure had dropped to 20 mm of Hg, at which time the tubes were sealed off. The tubes were cooled in an ice bath during evacuation so as to retain the water naturally present in the powdered shell. One of the tubes was opened after it had been sealed. The water content was found to be 0·28 per cent. The tubes were heated for periods of $8\frac{1}{2}$ and 45 hr in a sand bath in a constant-temperature oven.

The open vessel experiments were conducted by placing the samples in a glass-stoppered, round-bottom flask provided with capillary inlet and outlet tubes, and a side-well into which a thermocouple could be inserted for measurement of temperature. The entire apparatus was fitted inside a constant-temperature oven with the inlet tube protruding through a small hole in the roof of the oven. Nitrogen was flushed through the inlet tube during the experiments at a rate slow enough to permit the N_2 to attain the temperature of the oven before reaching the sample, but

fast enough to ensure exclusion of air from the sample. The last traces of oxygen were removed from the N_2 by passage of the gas through a tube of steel wool at 750°C. Samples were heated for 4, 19, 100 and 263 hr.

Temperatures were determined occasionally during the experiments with a chromel–alumel thermocouple. The temperatures of the samples rose quickly during the first $\frac{1}{2}$ hr after the samples had been placed in the oven (previously brought to temperature), but the desired temperature was not reached until about

Table 9. Concentrations of soluble nitrogenous compounds in hydrolysates of powdered shells of the clam, *Mercenaria mercenaria*, before and after different thermal treatments

Heat treatment	Total N in solution after hydrolysis with 6 N HCl	
	mg N per 100 g shell	N as % of N in unheated shell
None	17·6	100
N_2 atmosphere at 212–213°C:		
4 hr	14·8	84
19 hr	13·5	77
100 hr	13·8	78
263 hr	12·3	70
Sealed evacuated tubes at 218–220°C:		
$8\frac{1}{2}$ hr	16·9	96
45 hr	12·0	68

50 min after insertion. The experiments were considered to have started when the temperatures of the samples had risen to within 3°C of the predetermined value.

After pyrolysis, the powdered shell samples were hydrolysed in 6 N HCl for 48 hr under reflux. The treatment of the hydrolysates was identical to that of the unheated powdered shell (see above). The amounts of soluble-N in the hydrolysates decreased as the duration of heat treatment under a given set of conditions increased, as shown by the data in Table 9. In the open flask experiments the decreases of soluble-N in the hydrolysates could be accounted for in one (or more) of three ways: (a) volatilization of nitrogenous compounds during pyrolysis; (b) transformation of soluble nitrogenous compounds into an insoluble state during pyrolysis; and (c) pyrolytic transformation of soluble nitrogenous compounds into other soluble compounds that were subsequently rendered insoluble during hydrolysis. The losses of acid soluble-N in the sealed tubes must have been mostly by (b) and (c), however, the sealed tubes did have a pungent smell when first opened, suggesting possible losses by volatilization.

The data obtained by column chromatography of the hydrolysates of the pyrolysed samples are given in Table 10. The fraction collector jammed during the chromatography of sample B, and some of the serine and threonine fractions were lost. The value listed for these two amino acids is therefore minimal. In none of the chromatographic runs were glycine and alanine completely enough separated to

permit the estimation of individual concentrations; however, paper chromatography showed that both amino acids were present.

The results for samples A and B provide the most interesting comparative data. These samples were heated in an open vessel under N_2 for 19 and 263 hr, respectively. Temporarily leaving aside the anomalous datum for the "leucine" fraction of sample B, the most stable amino acids found were phenylalanine, lysine and aspartic acid, since they survived the 263-hr pyrolysis. These were followed (in

Table 10. Concentrations of amino compounds in hydrolysates of unheated and heated powdered shells of the clam, *Mercenaria mercenaria*, collected from the Wailes Bluff formation (mid-Pleistocene), Virginia

(Samples A and B were heated for 19 and 263 hr, respectively, at 212–213°C in an open flask under a N_2 atmosphere. Samples C and D were heated for $8\frac{1}{2}$ and 45 hr, respectively, 218–219°C in sealed evacuated tubes. Concentrations are given as micromoles per 100 g of shell, with unknowns calculated as leucine equivalents.)

Amino compound	Unheated	A	B	C	D
Aspartic acid	239	75	7	0	0
Threonine		10*	0	0	0
Serine			0	0	0
Proline	227	70	0	0	0
Glutamic acid	109	30	0	0	0
Glycine	107	117	0	0	0
Alanine					
Valine	45	20	0	0	0
Leucine(s)	67	37	372	258	180
Tyrosine and phenylalanine	47 (t > p)	27 (p > t)	27(p)	20(p)	18(p)
Ammonia	258	313	282	647†	486†
Lysine	116	39	46	0	0
No. 1	0	0	0	9	9
No. 2	0	0	0	14	15
No. 3	0	0	0	8	6
No. 4	0	0	0	3	6
No. 5	0	0	0	0	2
% N recovered from column‡	106	81	91	80	84
Amino acid N as % of original	100	43	11§	2§	2§

* This value is minimal. Some of the serine and threonine fractions were lost.

† These ammonia peaks also contained ethanolamine.

‡ Recoveries calculated on the basis of amino acid-N in the column eluates plus the N (leucine equivalents) in the unknowns.

§ These calculations exclude the anomalous values for the leucine peaks.

decreasing order of stability) by glycine and alanine, valine, glutamic acid, proline and tyrosine. The positions of serine and threonine in this series cannot be assessed accurately, though they would appear to fit somewhere in the group of lesser stability. The disturbing fact about these results is that the amino acids most stable to pyrolysis (phenylalanine, lysine and aspartic acid) are among the least stable during natural fossilization (Abelson, 1954, 1956). One or both of two conclusions is possible: (a) the laboratory experiments did not mimic the effects of low geologic temperatures over long periods of time; (b) the relative geologic stabilities of amino acids in *Mercenaria* shells are determined by some factor other

than temperature. We do not know which of these possibilities is the more nearly correct.

Quantitative measurements have been made of the thermal decomposition rates of alanine (Abelson, 1956, 1957) and phenylalanine (Vallentyne, 1957b) in dilute aqueous solution. Under these conditions alanine decomposes by decarboxylation with a specific reaction rate constant $(k) = 3 \times 10^{13}\ e^{-44,000/RT}$. The decomposition products of phenylalanine under the same conditions are not known, but the decomposition appears to involve a reaction with water, with a specific reaction rate constant $(k) = 1{\cdot}7 \times 10^{8}\ e^{-30,800/RT}$. At all temperatures below 270°C phenylalanine decomposed more rapidly in aqueous solution than did alanine. The times required for 63·2 per cent decomposition of alanine in dilute aqueous solution at 212°C and 219°C are 698 and 442 hr, respectively, as determined from Abelson's (1957) measurements. For phenylalanine under the same conditions the corresponding times are 139 and 88 hr, respectively (Vallentyne, 1957b).

An examination of the data in Table 10 shows that alanine was more rapidly decomposed in the carbonate shell powder than would have been the case in aqueous solution. If the decomposition kinetics had been the same in the shell powder as in aqueous solution, then alanine should have been found in all four of the heated tubes listed in Table 10. Phenylalanine, on the other hand, appears to have decomposed in the heated shells at a rate equal to, or less than, that characteristic of phenylalanine in aqueous solution. The decomposition rates for other amino acids in aqueous solution have not been determined accurately enough to permit comparisons with the data obtained by shell pyrolysis.

There are five obvious differences between the pyrolytic experiments carried out with amino acids in the powdered shell and those with amino acids in dilute aqueous solution: (a) pH relations; (b) concentration of water; (c) the possibility of reactions between amino acids and other compounds; (d) the form of the amino acids used as experimental material; and (e) solid surfaces. As regards pH, one would expect hot water in contact with $CaCO_3$ (as in the sealed-tube experiments) to have a slightly alkaline pH. Under these conditions the neutral and acidic amino acids would not occur in an isoelectric state, and a decreased stability of these compounds might be expected. This factor might account for the stability of lysine, a basic amino acid, but not of aspartic acid and phenylalanine. It is well known that some amino acids do decompose during hydrolysis with strong acids and bases at temperatures near 100°C, but how this is related to pH is not known. With the exceptions of serine, threonine and tryptophan, most amino acids are remarkably stable under conditions of hydrolysis. In regard to (b), the shell powder in the sealed tubes contained only 0·28% water, and the powdered shell samples heated in the open vessel under N_2 lost water during pyrolysis. If phenylalanine decomposed in the heated-shell experiments by interaction with water, as has been suggested (without adequate proof) to be the case for phenylalanine in aqueous solution (Vallentyne, 1957b), then one would expect to find that phenylalanine was more stable in the heated shells than in aqueous solution for a given set of thermal conditions. We can only say that the data for the heated-shell experiments are not in marked disagreement with this expectation. The effect of decreasing concentrations of water on the decomposition

rates of other amino acids is not known. Regarding (c) it is pertinent to point out that a given amino acid in a carbonate shell exists in conjunction with a number of other amino acids, and perhaps some other organic compounds as well, whereas the decomposition experiments on amino acids in aqueous solution have all been conducted on single amino acids, in pure solution. In connexion with (d) it is pertinent to note that the amino acids in Wailes Bluff *Mercenaria* shells occur mostly in the form of peptides and polypeptides (Abelson, 1955). No one has as yet determined whether a given amino acid in a protein is decomposed in aqueous solution at the same rate as the same amino acid by itself. It is known that amino acids will partly polymerize to polypeptides when they are heated in a dry state at 200°C for a few hours (Fox and Middlebrook, 1954), and that the amino and carboxyl groups of amino acids are usually the groups most affected by thermal and radiation treatment (Hurd, 1929; Collinson and Swallow, 1956). One might therefore expect that an internal amino acid in a protein might be more stable to decomposition processes than the same free amino acid. Finally (e) it is possible that solid surface reactions may have accelerated the decomposition of amino acids in the powdered shell.

In comparing the results for the open-vessel and sealed-tube experiments only part of the increased decomposition of amino acids in the latter can be attributed to the increased temperature. In other words, if the decomposition rates of the amino acids in the two sets of experiments had been identical, one would have expected to find some amino acids remaining in the sealed tubes heated for $8\frac{1}{2}$ hr at 218–220°C. Evidently the reaction rates differ under the two sets of conditions for all amino acids with the possible exception of phenylalanine.

The problematic increased concentrations of ninhydrin-reacting materials in the leucine region for samples B, C, and D as compared to the unheated control require special comment. At least two ninhydrin-reacting compounds were present in the leucine region of the column eluates, one of which was identified as leucine(s) on the basis of paper chromatography. The unknown(s) did not move far from the origin on paper chromatography, and showed considerable streaking in addition. The relative amounts of leucine(s) and the unknown(s) were not determined. It is rather unlikely that a synthesis of leucine or *iso*leucine could have occurred under the conditions of the experiments, so we are probably justified in assuming that leucine(s) formed a minor fraction of the total ninhydrin-reacting matter in the "leucine" peaks of samples B, C and D. It is also of interest to note that the ammonia fractions of samples C and D (heated in sealed tubes) contained an unknown, subsequently identified as ethanolamine on the basis of paper chromatography. The R_f values were 0·34 in butanol–acetic acid–water and 0·65 (faint) in aqueous phenol, in good agreement with those of ethanolamine. The similarity of the compounds accompanying the leucine and ammonia peaks to those in an acid extract of fossil carnosaur "teeth" has already been noted (see the section on carnosaur "teeth"). The occurrence of ethanolamine in pyrolysed clam shells and in fossil carnosaur "teeth" suggests that pyrolytic studies in the laboratory may at least to some degree mimic diagenetic processes in nature.

Unknowns nos. 1–5 were found only in hydrolysates of powdered shell that had been heated in sealed tubes. Each of these peaks doubtless represented an

amine. This is evidenced by the position in the eluate, i.e. after the ammonia peak. The R_f values of the unknowns on paper chromatograms developed with the butanol–acetic acid–water solvent were as follows: no. 1, 0·10; no. 2, 0·10; no. 3, 0·14; no. 4, 0·49. The R_f value of no. 4 resembles that of ethylamine, a known decomposition product of alanine when the latter is heated in aqueous solution (Abelson, 1954, 1956). Insufficient material was available for the detection of

Table 11. Quantitative data on the increases of nitrogen (due to amino acid decomposition) in different fractions of the hydrolysates of heated, powdered *Mercenaria* shells relative to unheated powdered shells

(Samples A and B were heated for 19 and 263 hr, respectively, at 212–213°C in an open flask under a N_2 atmosphere. Samples C and D were heated for $8\frac{1}{2}$ and 45 hr, respectively, at 218–219°C in sealed evacuated tubes. The values in parentheses refer to the percentages of the decomposed amino acid N that appeared in each category.)

Nitrogen fraction	Increased amount of N relative to unheated control (mg N per 100 g shell)			
	A	B	C	D
Insoluble in 6 N HCl	2·8(33)	5·3(40)	0·7(5)	5·6(38)
Soluble in 6 N HCl				
(a) ninhydrin-reacting organic decomposition products	0·0(0)	5·2*(39)	4·1*(28)	3·0*(20)
(b) ammonia	0·8(9)	0·3(2)	5·5†(37)	3·2†(22)
(c) decomposition products that did not react with ninhydrin	2·8(33)	1·0(8)	3·4(23)	1·9(13)
Unaccounted for	2·1‡(25)	1·5‡(11)	1·0(7)	1·1(7)
Totals§	8·5	13·3	14·7	14·8

* These values do not include data for the ethanolamine that appeared with ammonia in the eluate, but they do include data for all the of "leucine" peak.

† These values include data for the ethanolamine that appeared with ammonia in the eluate.

‡ Some of the nitrogen losses unaccounted for in samples A and B may have occurred by volatilization of nitrogen compounds during the heat treatment.

§ The totals are numerically equal to the total amounts of amino acid N decomposed in each sample.

no. 5 on paper chromatograms. Although amines are visible on paper chromatograms developed with aqueous phenol, none of the unknowns yielded ninhydrin-reacting spots on such paper chromatograms. Since the amounts were small, significant losses through vaporization may have occurred.

The final question to be raised concerns the fate of the nitrogen released from amino acids by pyrolysis. The total-N in the hydrolysates of the heated samples was partitioned into four categories: (a) nitrogen insoluble in 6 N HCl (and that volatilized during the heating of samples A and B); (b) soluble organic compounds that reacted with ninhydrin; (c) ammonia; and (d) soluble organic nitrogenous compounds that did not react with ninhydrin. The excess amounts of nitrogen in each category (over and above the amounts present in the hydrolysate of the unheated control) were calculated, with the results shown in Table 11. It is apparent from Table 11 that amino acids did not simply decompose by deamination during pyrolysis. The amounts of ammonia in the hydrolysates do not tally with

the amounts of nitrogen liberated by amino acid decomposition, even in the cases of samples C and D where the ammonia values listed are known to be high (due to inclusion of data for the ethanolamine that accompanied the ammonia fraction on chromatography). In samples A and B about one-third of the liberated nitrogen appeared to have passed directly into an insoluble state in the hydrolysate. On the other hand, the insoluble-N of the hydrolysate of sample D must have arisen from soluble organic compounds produced as decomposition intermediates (see data for sample C).

The conclusions reached above must be tempered with a word of caution. The comparisons made were between hydrolysates of heated and unheated powdered shell, and not between the samples of powdered shell themselves. It is quite possible that some of the changes attributed to pyrolysis were only induced by the pyrolysis, and brought to the final result by subsequent transformation during the period of hydrolysis.

General Discussion and Conclusions

The data assembled here are meagre in relation to those required for even a cursory understanding of all phases of the geochemistry of polypeptides and amino acids. At best, we can only hope that the data presented above will serve to orient future investigations along profitable pathways.

With regard to amino acids present in the hydrolysates of the two samples of lake sediment studied, our data are in general agreement with those of Kleerekoper (1957) and Swain *et al.* (1959), with two exceptions. The Lake Opinicon sediments contained smaller percentages of cold acid-/extractable nitrogen (8 per cent for the surface sample; 11 per cent for the subsurface sample) than the mean value (24·7 per cent) of acid-extractable nitrogen for the series of Ontario lake sediments studied by Kleerekoper (1957). Secondly, the Lake Opinicon sediments contained a much higher proportion of the total-N in the form of amino acids, peptides and polypeptides than has been found by other workers (Kleerekoper 1957; Swain *et al.*, 1959). These two facts are doubtless related since the relationships are expressed as percentages. Kleerekoper (1957) reported an inverse relation between the total-N content of lake sediments and the fraction of that nitrogen occurring in the form of amino acids after hydrolysis. The data for the sediments from Lake Opinicon form a noteworthy exception to this relationship. No major differences were found in the amino acid compositions of hydrolysates of the surface and subsurface samples, indicating that there had been no marked selective degradation of amino acids during the period of burial of the subsurface sample. Krause (1959) has shown that there is no obvious preferential decomposition of polypeptide-bound amino acids during the biological decomposition (both aerobic and anaerobic) of freshwater zooplankters over a period of 6 days in the laboratory. Our own findings, in conjunction with Krause's, indicate that the selective decomposition of amino acids during fossilization is probably non-biological.

The low content of amino acids in the hydrolysate of the Green River shale shows that most of the polypeptides and amino acids originally present had been destroyed diagenetically. Assuming the age of the Green River shale to be approximately

45 million years it is possible to calculate the *maximum* temperature that the deposit could have been subjected to *continuously* throughout its history.* Three assumptions are required for the calculation: (a) that the original concentration of alanine per g ignitable matter in the Lake Uinta sediment was the same as for Recent sediments from Lake Opinicon; (b) that the decomposition of alanine in the shale proceeded at a rate equal to or greater than that of alanine in dilute aqueous solution in the laboratory (Abelson, 1954, 1956); and (c) that significant amounts of alanine were not added to or formed in the deposit. It is unlikely that alanine would have decomposed more slowly in the shale than in pure aqueous solution, hence the estimated temperature on the basis of assumption (b) must be *maximal*. If the assumptions are correct, alanine must have passed through ten 0·37 lives† in the shale. On the basis of Abelson's data for analine in the laboratory the *maximal* temperature that the Green River shale could have been *continuously* subjected to was calculated to have been 74°C. Obviously, a variety of time–temperature combinations would all lead theoretically to the same result. An equally good *chemical* interpretation would, for example, be a continuous temperature of less than 30°C except for shorter periods at higher temperatures, namely: 98°C for 1,000,000 years; 129°C for 10,000 years; or 167°C for 100 years. We have chosen to express the result in terms of a maximal continuous temperature merely because of the simplicity of the expression. We do not attribute any precise geological meaning to this method of expression, but do believe that it may have some comparative value at least, and that it represents a true upper limit for the continuous temperature equivalent of prevailing geological temperatures. The reader should not confuse this term with maximal temperature, for the latter is an entirely different concept.

If accurate data were on hand for the thermal decomposition rates of other amino acids, it would be possible to cross-check the assumptions; but such data do not yet exist. The temperature of the Green River shale at this site probably has never reached anything like 74°C for such a long period of time. The maximum depth of burial could hardly exceed a few thousand feet at most (personal communication from W. H. Bradley).

It has already been noted that the absence of amino acids in hydrolysates of pre-Cambrian rocks should not be used as evidence that amino acids did not exist in the original deposits. Although our original purpose in carrying out this series of investigations was to attempt to use amino acids as indicators of life in the pre-Cambrian, it now seems to us that they are not sufficiently stable to persist

* It might appear to the reader that such a calculation would be erroneous and misleading in view of the many factors other than temperature that are doubtless involved in the decomposition of amino compounds in shales. We do not believe this to be necessarily so. Most of these accessory factors would probably act to increase the rate of disappearance of alanine in the shale. Their action would only cause the calculated maximal continuous temperature to be higher than it would be in the absence of such accessory factors.

† A half-life ($t_{1/2}$) is the time required for the decomposition of 50 per cent of the initial quantity of a given compound. A 0·37 life ($t_{1/e}$) is the time required for the decomposition of 63·2 per cent of the initial quantity of a given compound. The constant e is the base of the Napierian logarithms, with a numerical value of 2·718; hence $1/e$ is approximately 0·37. The value of $t_{1/e}$ for a given temperature is the reciprocal of the specific reaction rate constant (k) for the same temperature. When a compound has passed through four 0·37 lives the concentration has been reduced to 2 per cent of the original. The concepts of 0·5 and 0·37 lives are applicable only to reactions obeying first-order reaction kinetics.

over such a length of time. The best approach to understanding pre-Cambrian life will probably come from a search for optically active substances in pre-Cambrian sediments.

At the start of this investigation we adopted the working rule that two general conditions were required for an organic compound to be stable geologically: thermal stability and insolubility in water. The thermal stability rule is probably still generally valid, but has to be modified to take into account the influence of the fossil matrix on the stability relations. The water-insolubility rule was based primarily on results obtained from Recent sediments, where water-insoluble substances such as carotenoids and chlorophyll degradation products (Fox *et al.*, 1944; Vallentyne 1955, 1956b) have been found to be well preserved. In the one case where water-soluble substances (free sugars) were found in surface sediments, it was later shown that they existed there in a water-insoluble state (Whittaker and Vallentyne, 1957). A second reason for using water-insolubility as a criterion of stability is that water-soluble substances are generally more easily attacked biologically than are insoluble substances. Such biological effects are likely to be most pronounced at the conceptual interface between living and dead organisms. The third reason is that water-soluble substances should be preferentially removed from porous sediments and fossils by percolating waters. Such losses, through dissemination by solution processes, would have the same result as *in situ* decomposition: namely, a lowered concentration of the soluble compound in the remaining rock or fossil. In speaking of water-insolubility we are, of course, referring to the compound in its sedimentary or fossil state (not necessarily the pure compound) and to the percolating solution (rather than pure water). The two most obvious examples of the thermal stability and water-insolubility rules in the geologic column are provided by deposits of coal and petroleum, the latter being complicated by a temporary migration phase.

Although these two rules have useful predictive values, it does not necessarily follow that they can be applied in a quantitative sense either to geologic processes or to laboratory models that attempt to mimic geologic processes. A variety of other factors may come into play, such as oxidation–reduction reactions, effects of ionizing radiations, catalysts, and so on. Abelson (1957) found that oxygen accelerated the chemical decomposition of amino acids more at low temperatures than at high temperatures. Our own data on the temperature stability of amino acids in Pleistocene shells showed little agreement with the results of fossil shell analyses. If the laboratory and geologic treatments had been truly comparable we should have been able to duplicate the amino acid composition of a Miocene shell by pyrolysing a Pleistocene shell. The fact that we did not achieve this result provides a working basis for further experimentation.

Acknowledgements—This work was supported by a grant from the Carnegie Corporation of New York. A grant from the National Research Council of Canada permitted us to employ a summer assistant during the closing stages of the work. The junior writer was privileged to hold a fellowship at the Geophysical Laboratory, Carnegie Institution of Washington, during the latter part of the study. The sample of shale from the Green River formation was provided by W. H. Bradley of the U.S. Geological Survey through G. E. Hutchinson of Yale University. Dr. E. S. Barghoorn of Harvard University generously provided the sample of chert from the Gunflint formation. The Miocene lignite was obtained from J. K. N. Jones, F.R.S., of Queen's

University, and the carnosaur "teeth" from Dr. R. R. Langford of the National Museum of Canada. The sample of Michigamme coal was donated by the M. A. Hanna Company. The ion-exchange resins used in the study were the gift of the Dow Chemical Company. We are particularly indebted to Dr. P. H. Abelson for constructive criticism during the course of the work and for reading the manuscript; and to Dr. R. O. Earl of Queen's University for his encouragement from the very start.

References

Abelson P. H. (1954) Organic constituents of fossils. *Carneg. Instn. Yearbook* No. 53, 97–101.

Abelson P. H. (1955) Organic constituents of fossils. *Carneg. Instn. Yearbook* No. 54, 107–109.

Abelson P. H. (1956) Paleobiochemistry. Scientific American 195, No. 1, 83–92.

Abelson P. H. (1957) Organic constituents of fossils. In Treatise on marine ecology and paleoecology–II. Paleoecology. *Geol. Soc. Amer. Mem.* **67,** 87–92.

Aberhalden E. and Brahm C. (1909) Über den Gehalt der Muskelsubstanz ägyptischer Mumien an Monoaminosäuren. *Hoppe-Seyl. Z.* **61,** 419–420.

Aberhalden E. and Heyns K. (1933) Nachweis vom Chitin in Flügoresten von Coleopteren des oberen Mitteleocän. *Biochem. Z.* **259,** 320–321.

Aberhalden E. and Weil A. (1911) Über den Gehalt ägyptischer Mumien an Eiweiss und Eiweiss-Abbauprodukten. *Hoppe-Seyl. Z.* **72,** 15–21.

Acher R., Fromageot C. and Jutisz M. (1950) Separation chromatographique d'acides aminés et des peptides—V. Les acides aminés individuels de l'insuline avec une note sur le dosage de la proline. *Biochim. Biophys. Acta* **5,** 81–88.

Barghoorn E. S. (1957) Origin of life. In Treatise on marine ecology and paleoecology—II. Paleoecology. *Geol. Soc. Amer. Mem.* **67,** 75–85.

Blake S. F. (1953) The Pleistocene fauna of Wailes Bluff and Langley's Bluff, Maryland. *Smithsonian Misc. Coll.* **121,** No. 12, 1–32.

Block R. J. and Bolling D. (1951) The Amino Acid Composition of Proteins and Foods (2nd Ed). Charles C. Thomas, Springfield, Illinois.

Block R. J., Lestrange R. and Zweig G. (1952) *Paper Chromatography: A Laboratory Manual.* Academic Press, New York.

Boyd W. C. and Boyd L. G. (1934) An attempt to determine the blood groups of mummies. *Proc. Soc. Exp. Biol., N.Y.* **31,** 671–672.

Boyd W. C. and Boyd L. G. (1937) Blood grouping tests on 300 mummies. *J. Immunol.* **32** 307–319.

Bradley W. H. (1931) Origin and microfossils of the oil shale of the Green River formation of Colorado and Utah. *U.S. Geol. Surv. Prof. Paper* A **168,** 1–58.

Brasch J. D. and Jones J. K. N. (1959) Investigation of some ancient woods. *Tappi* **42,** 913–920.

Breger I. A. (1960) *Organic Geochemistry.* (Edited by Breger I. A.) Pergamon Press, London. In press.

Cochrane A. L. (1955) Location of acid zones on paper chromatograms. *Analyst* **80,** 909.

Consden R., Gordon A. H. and Martin A. J. P. (1944) Qualitative analysis of proteins; a partition chromatographic method using paper. *Biochem. J.* **38,** 224–232.

Conway E. J. (1957) *Microdiffusion Analysis and Volumetric Error* (4th Ed.). Crosby, Lockwood, London.

Collinson E. and Swallow A. J. (1956) The radiation chemistry of organic substances. *Chem. Rev.* **56,** 471–568.

Curran H. W., Bardach J., Bowman R. I. and Lawler H. G. (1947) *A Biological Survey of Lake Opinicon.* Progress Report, Queen's University Biological Station.

Drèze A., Moore S. and Bigwood E. J. (1954) On the desalting of solutions of amino acids by ion exchange. *Analyt. Chim. Acta* **11,** 554–558.

Erdman J. G., Marlett E. M. and Hanson W. E. (1956) Survival of amino acids in marine sediments. *Science* **124,** 1026.

Ezra H. C. and Cook S. F. (1957) Amino acids in fossil human bone. *Science* **126,** 80.

Fox D. L., Updegraff D. M. and Novelli D. G. (1944) Carotenoid pigments in the ocean floor. *Arch. Biochem.* **5,** 1–23.

Fox S. W. and Middlebrook M. (1954) Anhydrocopolymerization of amino acids under the influence of hypothetically primitive terrestrial conditions. *Fed. Proc.* **13,** 211.

Gothan W. (1922) Neue Arten der Braunkohlenuntersuchung—IV. *Braunkohle* **21,** 400–401.

Graf W. (1949) Presence of a spasmogenic substance, presumably histamine, in extracts of mummy tissue. *Nature, Lond.* **164,** 701–702.

Hall A. D. and Miller N. H. J. (1908) The nitrogen compounds of the fundamental rocks. *J. Agric. Sci.* **2,** 343–345.

Hurd C. D. (1929) *The Pyrolysis of Carbon Compounds.* American Chemical Society Monograph Series. Chemical Catalogue Company, New York.

Keilin D. (1953) Stability of biological materials and its bearing upon the problem of anabiosis. *Science Progr.* **41,** 577–592.

Kernbach M. (1924) Sur la présence d'une substance albuminoide dans les ossements anciens exhumés et sur sa propriété antigène. *C.R. Soc. Biol., Paris* **90,** 1075–1077.

Kleerekoper H. (1957) Une étude limnologique de la chimie des sédiments de fond des lacs de l'Ontario méridional, Canada pp. 1–205. Thèse présentée à la Faculté des Sciences de l'Université de Paris.

Komatsu S. and Ueda H. (1923) Chemistry of Japanese plants—II. Composition of fossil wood. *Mem. Coll. Sci. Kyoto Imp. Univ.* 7A, 7–13. (Original not seen: *Chem. Abstr.* **18,** 849).

Korting G. W. and Nitz-Litzow D. (1952) Amino acid elimination at the skin surface. *Arch. Dermatol. Syphilis* **194,** 405–413. (Original not seen: *Chem. Abstr.* **46,** 11393).

Krause H. R. (1959) Biochemische Untersuchungen über den postmortalen Abbau von totem Plankton unter aeroben und anaeroben Bedingungen. *Arch. Hydrobiol.* Suppl. **24,** 297–337.

Luft F. (1930) Zur Struktur des Lignits. *Papier-Fabr.* (*Tech.-Wiss. Teil*) **28,** 787–791.

Moore S. and Stein W. H. (1954a) Procedures for the chromatographic determination of amino acids on four percent cross-linked sulfonated polystyrene resins. *J. Biol. Chem.* **211,** 893–906.

Moore S. and Stein W. H. (1954b) A modified ninhydrin reagent for the photometric determination of amino acids and related compounds. *J. Biol. Chem.* **211,** 907–913.

Pankov B. S. (1953) Amino acid composition of sweat. *Vestnik Venerol. Dermatol.* No. 3, 18–19. (Original not seen: *Chem. Abstr.* **47,** 11419).

Partridge S. M. (1948) Filter paper partition chromatography of sugars. *Biochem. J.* **42,** 238–250.

Povoledo D. (1959) Studi chimici sulle sostanze organiche azotate sedimentarie e sestoniche di alcuni laghi della Italia settentrionale. *Mem. Ist. Ital. Idrobiol.* **11,** 25–60.

Schmidt W. A. (1908) Chemische und biologische Untersuchungen von ägyptischem Mumienmaterial, nebst Betrachtungen über das Einbalsamierungsverfahren der alten Ägypter. *Z. allg. Physiol.* **7,** 369–392.

Shabarova N. T. (1955) (The chemical composition of ancient deposits) *Dokl. Akad. Nauk SSSR* **105,** 1031–1033.

Shacklock C. W. and Drakeley J. (1927) A preliminary investigation of the nitrogenous matter in coal. *J. Soc. Chem. Ind., Lond.* **46,** 478–481T.

Sinex F. M. and Faris B. (1959) Isolation of gelatin from ancient bones. *Science* **129,** 969.

Staudinger H. and Jurisch I. (1939) Ueber makromolekuläre Verbindungen. 212 Mitteilung. Ueber den Polymerizationsgrad der Zellulose in Ligniten. *Papier-Fabr.* (*Tech.-Wiss. Teil*) **37,** 181–184.

Steppuhn O. and Ljubowzowa X. (1930) Proteolytische Zellfermente von ägyptischen Mumien (etwa 3000 jährig) und Mammut (etwa 30,000 bis 100,000 jährig). *Biochem. Z.* **226,** 237–242.

Swain F. M., Blumentals A. and Millers R. (1959) Stratigraphic distributions of amino acids in peats from Cedar Creek Bog, Minnesota, and Dismal Swamp, Virginia. *Limnol. Oceanogr.* **4,** 119–127.

Tarte P. (1945) Sur l'adsorption d'acides aminés par le sulfate de baryum. *Bull. Soc. Sci. Liége* **14,** 231–242.

Thieme F. P., Otten C. M. and Sutton H. E. (1956) A blood typing of human skull fragments from the Pleistocene. *Amer. J. Phys. Anthropol.* **14,** 437–443.

Treibs A. (1934a) Über das Vorkommen von Chlorophyllderivaten in einem Ölschiefer aus der oberen Trias. *Liebigs Ann.* **509,** 103–114.

Treibs A. (1934b) Chlorophyll- und Häminderivate in bituminösen Gesteinen, Erdölen, Erdwachsen und Asphalten. Ein Beitrag zur Entstehung des Erdöls. *Liebigs Ann.* **510,** 42–62.

Treibs A. (1935a) Chlorophyll- und Häminderivate in bituminösen Gesteinen, Erdölen, Kohlen, Phosphoriten. *Liebigs Ann.* **517,** 172–196.

Treibs A. (1935b) Porphyrine in Kohlen. *Liebigs Ann.* **520,** 144–150.

Treibs A. (1936) Chlorophyll- und Häminderivate in organischen Mineralstoffen. *Angew. Chem.* **49,** 682–686.

Tyler S. A. and Barghoorn E. S. (1954) Occurrence of structurally preserved plants in pre-Cambrian rocks of the Canadian shield. *Science* **119,** 606–608.

Tyler S. A., Barghoorn E. S. and Barrett L. P. (1957) Anthracite coal from Precambrian Upper Huronian black shale of the Iron River district, northern Michigan. *Bull. Geol. Soc. Amer.* **68,** 1293–1304.

Vallentyne J. R. (1955) Sedimentary chlorophyll determination as a paleobotanical method. *Canad. J. Bot.* **33,** 304–313.

Vallentyne J. R. (1956a) A modification of the Livingstone piston sampler for lake deposits. *Ecology* **36,** 139–141.

Vallentyne J. R. (1956b) Epiphasic carotenoids in post-glacial lake sediments. *Limnol. Oceanogr.* **1,** 252–262.

Vallentyne J. R. (1957a) The molecular nature of organic matter in lakes and oceans, with lesser reference to sewage and terrestrial soils. *J. Fish. Res. Bd. Canada* **14,** 33–82.

Vallentyne J. R. (1957b) Thermal degradation of amino acids. *Carneg. Inst. Yearbook* No. 56, 185–186.

Whittaker J. R. and Vallentyne J. R. (1957) On the occurrence of free sugars in lake sediment extracts. *Limnol. Oceanogr.* **2,** 98–110.

Yamada K. (1934) Proof of lipase in Peruvian mummies. *Z. klin. Path. Hamatol. (Japan)* **3,** 867. (Original not seen: *Chem. Abstr.* **31,** 7074).

Geochimica et Cosmochimica Acta, 1960, Vol. 21, pp. 35 to 80. Pergamon Press Ltd. Printed in Northern Ireland

Ein Beitrag zur Geochemie des Schwefels

Werner Ricke
Mineralogisch-Petrographisches Institut der Universität Göttingen*

(*Received* 1 *June* 1960)

Abstract—Two chemical methods for the determination of small quantities of total and sulphide sulphur in silicate minerals and rocks are described. Sulphate sulphur, in general, is obtained as different from total and sulphide sulphur. The determination of sulphur contents down to 0·002 per cent is possible. The mean deviation lies for contents below 0·02 per cent at ±0·001 per cent; for contents between 0·02 and 0·1 per cent at ±0·0015 per cent.

Ninety-six mineral and 132 rock samples were analysed. In nearly all of them, total sulphide and sulphate sulphur were determined. The mineral analyses indicate that many rock-forming minerals contain small quantities of sulphate sulphur. In quartz up to 0·0095 per cent, in feldspars 0·022 per cent, in muscovites 0·013 per cent, in pyroxenes 0·007 per cent and in various sorosilicates up to 0·014 per cent sulphate sulphur was found.

The average total sulphur content of each mean family of igneous rocks is nearly 0·03 per cent S. The alkali rocks usually show higher contents. Sulphur occurs in igneous rocks both as sulphide and sulphate. In gabbros the sulphate portion, when present, is very small. On the average, plutonic rocks contain more sulphide sulphur and less sulphate sulphur than their effusive equivalents; silicic rocks contain less sulphide sulphur than basic rocks. The percentage of the total sulphur that is sulphate sulphur is higher in silicic rocks than in basic rocks. For three granites and one basalt, it could be shown that the feldspars are preferred hosts for sulphate sulphur.

Several possibilities for the mode of sulphate sulphur in igneous rocks are discussed. From leaching studies it seems probable that sulphate in silicate minerals appears not only in fluid inclusions, but that also replacement of SiO_4 by SO_4 in the silicate, may occur.

In sedimentary rocks the sulphur is found both as sulphide and sulphate; mainly as sulphide in shales (average: 0·22 per cent S), in greywackes (average: 0·13 per cent S) and carbonate rocks (average: 0·12 per cent S), and as sulphate in sandstones (average: 0·022 per cent S) and pelagic sediments (average: 0·13 per cent S). Metamorphous rocks also contain sulphide and sulphate sulphur.

Calculations indicate that the total sulphur contents of the oceans, of the common sedimentary rocks, and of the evaporite deposits of the earth, are almost alike, and that the sulphur in these must to a great extent have originated from degassing magmas.

Einleitung

In den magmatischen Gesteinen tritt der Schwefel am auffälligsten in Form von Sulfiden auf. Nach systematischen Untersuchungen von Newhouse (1936) und Ramdohr (1940) sind die wichtigsten Sulfidminerale in Eruptivgesteinen Pyrit, Magnetkies, Kupferkies, Pentlandit, Bornit und Cubanit. In Alkaligesteinen kann der Anteil der sulfathaltigen Feldspatvertreter der Sodalithgruppe mehrere Prozent betragen. Diese Gesteine sind aber am Aufbau der Erdkruste mengermässig nur sehr untergeordnet beteiligt.

Den ersten Wert für den durchschnittlichen Schwefelgehalt in den Eruptivgesteinen finden wir in der klassischen Arbeit von Clarke und Washington (1924). Von 5159 ausgewählten Analysen enthielten 1621 Angaben über den Gehalt an Schwefel. Mit der Annahme, dass die übrigen Proben völlig schwefelfrei sind, erhält man als Mittel für alle Proben 0,025% S. Mit der Annahme, dass die übrigen Proben im Durchschnitt den gleichen S-Gehalt haben wie die 1621, in denen Schwefel bestimmt wurde, erhält man als Mittel 0,08% S. Das arithmetische Mittel aus diesen beiden Werten, 0,052% S, wird von Clarke und Washington als am wahrscheinlichsten angenommen und wird seither häufig, z.B. von Rankama und Sahama (1950), Goldschmidt (1954) und Mason (1958) zitiert.

* Jetzige anschift: Zentrallabor für Geochemie der Isotope, Göttingen.

Tröger (1934) berechnete Durchschnittswerte für die S-Gehalte verschiedener Gruppen von Eruptivgesteinen auf der Grundlage von in der Literatur gesammelten Gesteinsanalysen.

Die Angaben über Schwefel bei Vinogradov (1956) beruhen auf den Werten von Tröger. Vinogradov berechnet hieraus für eine Mischung aus sauren und basischen Eruptivgesteinen im Verhältnis 2:1 0,09% S.

Nockolds (1954) gibt in seiner Arbeit über die mittlere Zusammensetzung einzelner Eruptivgesteinsgruppen S-Gehalte nur für Nephelinsyenite, Phonolite und Nephelinlatite an, vermutlich weil nur bei diesen Gesteinen Schwefel häufiger bestimmt wurde.

Die meisten Sedimentgesteine enthalten Schwefel als Sulfid—hauptsächlich Pyrit und Markasit—und als Sulfat—haupsächlich Anhydrit und Gips.

Clarke (1924) gibt die mittleren Schwefelgehalte der häufigsten Sedimentgesteine nach Analysen von Durchschnittsmischungen an. Den mittleren Schwefelgehalt der Sedimentgesteine berechnet er hieraus zu 0,54% SO_3 (= 0,22% S).

Die Arbeit von Vinogradov und Ronov (1956) über die Sedimentgesteine der Russischen Tafel gibt aus Analysen vieler Durchschnittsmischungen die mittleren Schwefelgehalte der Karbonat und Tongesteine und der Sandsteine der verschiedenen geologischen Formationen an. Vinogradov und Ronov berechnen den mittleren Schwefelgehalt der Gesamtsedimente der Russischen Tafel zu 2,05% SO_3 (= 0,82% S).

Mit der vorliegenden Arbeit wurde der Versuch unternommen, durch chemische Untersuchungen an Silikatmineralen, Eruptivgesteinen und Durchschnittsmischungen bestimmter Gesteinstypen zu einigen Aussagen über das Vorkommen des Schwefels in den wichtigsten Eruptivgesteinen zu kommen. Besonderer Wert wurde dabei auf die Unterscheidung von Sulfid- und Sulfatschwefel gelegt. Ferner wurde der Gehalt einiger Sedimentgesteine an Sulfid- und Sulfatschwefel bestimmt und die gewonnenen Werte mit denen anderer Autoren verglichen.

Die untersuchten Proben stammen zum größten Teil aus der geochemischen und mineralogischen Sammlung des Göttinger Mineralogisch-Petrographischen Instituts.

Methodik

Bei der chemischen Analyse der silikatischen Minerale und Gesteine wurde der Schwefel bisher, wenn überhaupt, meist gravimetrisch bestimmt, als Bariumsulfat, gelegentlich auch als Benzidinsulfat. Die Grenze der Nachweisbarkeit liegt bei diesen Methoden bei 200 μg S, d. h. bei 1 g Einwaage können gerade noch 0,02% S bestimmt werden (1,45 mg $BaSO_4$). Angaben über geringere Schwefelgehalte bei älteren Analysen haben wahrscheinlich Fehler von mindestens $\pm 100\%$, es sei denn, bei der Bestimmung wurden grössere Einwaagen verwandt und Blindwertsbestimmungen durchgeführt, um Fehler auszuschalten, die durch die Schwefelgehalte der benutzten Chemikalien entstehen (vergl. Tabelle 1).

Verfahren zur Schwefelbestimmung, mit denen Gehalte von 10 μg noch sicher erfasst werden, sind die von Wickbold (1953) beschriebene Trübungstitration von Sulfat in alkoholischer Lösung und die jodometrische Bestimmung von Schwefelwasserstoff.

Wegen der Schwierigkeit, mit chemischen Verfahren den Sulfatschwefel quantitativ zu isolieren, ohne dabei Sulfid zu oxydieren, wurde von einer direkten Bestimmung des Sulfatschwefels abgesehen und nur Gesamtschwefel und Sulfidschwefel bestimmt. Den Gehalt an Sulfatschwefel erhält man dann als Differenz aus diesen beiden Werten.

I. *Die Bestimmung des Gesamtschwefels in silikatischen Mineralen und Gesteinen*

Die Fällungstitration von Sulfat mit Bariumchlorid wurde zuerst von Gay-Lussac (1828) beschrieben. Ringbom (1941) und Frey (1952) erkannten, dass die Löslichkeit des $BaSO_4$ in Alkohol–Wasser-Gemischen wesentlich geringer ist als in Wasser und titrierten Milligramm-Mengen Sulfat mit photometrischer Endpuktsanzeige. Wickbold (1953) verfeinerte dieses Verfahren für reine Sulfatlösungen, so dass Bestimmungen von S-Mengen im Bereich von 10 μg bis 600 μg möglich wurden.

Für die hier durchgeführte Bestimmung von Schwefel in Silikatgesteinen wurde die Methode von Wickbold etwas modifiziert: Die in einer Achatkugelmühle zerkleinerte Probe wird bei *ca.*

Tabelle 1. Schwefelbestimmungen verschiedener Analytiker in Standardproben G–1 und W–1 (nach Schlecht und Stevens, 1951)

% S in Granit G–1	% S in Diabas W–1
0,01	0,04
0	0
0,02	0,03
0,04	0
0	
0,2	
0	

650°C im elektrischen Ofen mit Na_2O_2 aufgeschlossen. Dabei wird der gesamte Schwefel zu Sulfat oxydiert. Das Sulfat wird von störenden Fremdionen abgetrennt und anschliessend in methylalkoholischer Lösung durch photometrische Trübungstitration bestimmt. Von jeder Probe werden Doppelbestimmungen ausgeführt.

A. *Ausführung*

1. *Aufschluss.* Etwa 0,5 g der fein gemahlenen Probe (bei hohen S-Gehalten entsprechend weniger) werden in einen Sinterkorund-Tiegel (Degussit Al 23, 99,7% Al_2O_3) gebracht und gründlich mit 2 g Na_2O_2 vermischt, auf dieses Gemisch wird noch eine Schicht von 2 g Na_2O_2 gegeben und der Tiegel im elektrischen Simon–Müller-Ofen auf *ca.* 650°C erhitzt. Nach 10 Minuten ist der Aufschluss beendet und der gesamte Schwefel zu Sulfat oxydiert. Der erkaltete Tiegel wird in ein 200 ml H_2O enthaltendes Becherglas gegeben und dieses auf dem elektrischen Sandbad zum Sieden gebracht. In 2 Stunden ist der Schmelzkuchen ausgelaugt und alles H_2O_2 durch Kochen zerstört. Der Tiegel wird vorsichtig herausgenommen und mit H_2O abgespült. Für die nachfolgende Abtrennung des Al ist die Anwesenheit von Cl^--Ionen in der Lösung wichtig. Deshalb wird 1,5 ml konz. HCl hinzugegeben. Die Lösung wird nun durch ein Weissband-Filter abfiltriert Das Filter wird gut mit kaltem H_2O gewaschen. Das Filtrat enthält jetzt den gesamten Schwefel der Probe als Sulfat, ausserdem hauptsächlich Alkalien, Aluminium und Kieselsäure Das pH der Lösung liegt in der Gegend um 12.

2. *Kationenbeseitigung.* Da die heterometrische Sulfatbestimmung in alkoholischer Lösung nur bei geringem Fremdionengehalt möglich ist, werden zunächst die Kationen durch eine Austauscherbehandlung entfernt. Al wird hierbei mit abgetrennt, wenn die Lösung Cl^--Ionen enthält. Die Lösung wird durch eine 35 cm lange Säule von 3 cm Dürchmesser mit Ionenaustauscher I Merk gegeben (stark saurer Kationenaustauscher, Sulfosäuretyp auf Polystyrolbasis). Im oberen Teil der Säule werden nun zunächst die ein- und zweiwertigen Kationen gegen H^+-Ionen ausgetauscht, die mit den OH^--Ionen der Lösung Wasser bilden, während das Al als Aluminat vorliegt. In der Mitte der Säule erreicht das pH den Neutralpunkt und das Al fällt als Hydroxyd, z.T. als basisches Chlorid bzw. Sulfat aus. Da die Lösung aber durch die zugesetzte Salzsäure freie H^+-Ionen enthält, wird dieser Niederschlag sofort wieder aufgelöst und das Al, das jetzt im unteren Teil der Säule als Al^{3+}, genauer als $Al(H_2O)_6^{3+}$ vorliegt, gegen H^+-Ionen ausgetauscht. Die Säule wird anschliessend mit 250 ml 0,05 N HCl gewaschen. Die Austauschersäule wird zweckmäßig nach jedem Durchfluss regeneriert. Dies geschieht mit 150 ml 2 N HCl. Anschliessend muss sie mit H_2O nachgewaschen werden, bis das Filtrat pH 5 anzeigt.

3. *Bestimmung als* $BaSO_4$. Das Filtrat des Austauschers, das etwa 550 ml beträgt, wird nach Zusatz von 1,5 ml Natriumchlorid-Lösung (10 g NaCl/l.) auf dem elektrischen Sandbad zur Trockne eingedampft, die letzten Spuren HCl werden bei 120°C im elektrischen Trockenschrank beseitigt. Der Rückstand wird mit 10 ml einer Elektrolytlösung aufgenommen, die 20 g $MgCl_2 \cdot 6H_2O$ und 3,5 g NH_4Cl/l. enthält und durch Zugabe von NH_3 auf einen pH-Wert von 8 bis 8,2 gebracht wurde. Die SO_4^{2-}-haltige Lösung wird durch Filtration durch Weissband-Filter in

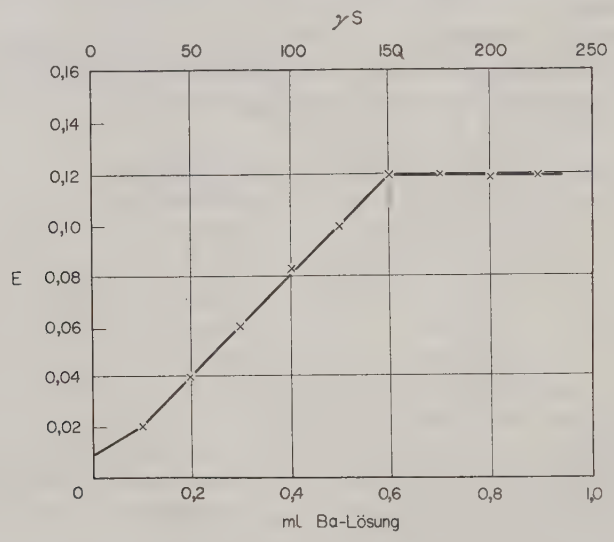

Abb. 1. Trübungstitration von 150 μg S bzw. 450 μg SO_4.

einen 100 ml-Messkolben von einem evtl. verbleibenden Rest, hauptsächlich Kieselsäure, befreit und Becherglas und Filter mit 5 ml H_2O gewaschen. Nachdem das Papierfilter nur noch Spuren Feuchtigkeit enthält, wird mit Methanol p.A. nachgewaschen, bis der Messkolben auf 100 ml aufgefüllt ist. Die so erhaltene 85% methylalkoholische Lösung wird mit Bariumchlorid-Lösung titriert, die 1,91 g $BaCl_2 \cdot 2H_2O$/l enthält, 0,1 ml Bariumchlorid-Lösung entsprechen dabei genau 25 μg S. Der Endpunkt der Titration wird heterometrisch bestimmt: Der Messkolben wird in eine 100 ml-Küvette eines Kolorimeters der Fa. Schmidt-Häntsch entleert, und mit 3 ml Methanol wird nachgespült. Dann wird laufend nach Zugabe von genau 0,1 ml Bariumchlorid-Lösung aus einer Mikrobürette die Extinktion unter Benutzung eines Farbfilters mit Durchlässigkeitsmaximum 4360 Å gemessen, nachdem man mit einem Glasstab umgerührt hat. Die Titration wird fortgesetzt, bis 4 Punkte erhalten werden, bei denen die Extinktion nicht mehr oder wesentlich weniger zunimmt als bisher. Man trägt die Messpunkte in Abhängigkeit vom Reagenzverbrauch auf Millimeter-Papier auf. Die Kurve besteht aus zwei Ästen, deren Schnittpunkt der Äquivalenzpunkt ist (Abb. 1). Die Titration kann durch Benutzung einer automatischen Titriervorrichtung und eines Magnetrührers, gekoppelt mit einem Schreiber, wesentlich vereinfacht werden. Voraussetzung hierbei ist natürlich, dass die Zugabe von Bariumchlorid-Lösung wirklich in gleichen Abständen erfolgt.

B. *Anwendungsbereich*

Die Methode eignet sich für die Bestimmung von S-Mengen zwischen 100 und 1000 μg. Bei den Bestimmungen von S-Mengen zwischen 20 und 100 μg verfährt man ebenso, nur gibt man zu dem Austauscherfiltrat eine vorgegebene Menge von 100 μg S als H_2SO_4 hinzu, die vom Analysenergebnis dann wieder abgezogen wird.

Störend bei dem Verfahren ist der S-Gehalt der benutzten Chemikalien und vor allem des Kationenaustauschers. Während die für eine Bestimmung benutzten Chemikalienmengen zwischen 10 und 15 μg S enthalten, liegt der tatsächlich gefundene Blindwert zwischen 20 und 100 μg S. Hauptursache hierfür ist, dass der Austauscher bei der Behandlung mit alkalischen Lösungen Schwefel abgibt. Man erhält trotzdem brauchbare Resultate, wenn man (a) immer die

gleichen Mengen Chemikalien verwendet, (b) möglichst immer unter gleichen Versuchsbedingungen arbeitet, d.h. in erster Linie beim Kationenaustausch gleiche Flüssigkeitsmengen mit gleichem pH-Wert verwendet, und (c) den Blindwert nach jeder zweiten Bestimmung kontrolliert und beim Ergebnis berücksichtigt.

C. *Fehlerquellen*

Da die meisten Fremdionen vor der Titration aus der Sulfatlösung entfernt wurden, kommen nur noch wenige Elemente in Frage, die die Bestimmung stören könnten. Elemente, die mit Sauerstoff Anionenkomplexe bilden, welche bei der Titration als Bariumsalze ausgefällt werden können, sind hauptsächlich Cr und P. Die Löslichkeiten der entsprechenden Salze in dem Methanol–Wasser-Gemisch wurden nicht bestimmt, als Anhaltspunkte mögen die Löslichkeiten in Wasser dienen, die in Tabelle 2 aufgeführt sind.

Tabelle 2. Löslichkeitsprodukte von Bariumsalzen bei Zimmertemperatur nach Jander und Wendt (1954)

$Ba_3(PO_4)_2$	$1{,}7 \times 10^{-4}$ Mol/l.
$BaCrO_4$	$1{,}6 \times 10^{-5}$ Mol/l.
$BaSO_4$	$8{,}6 \times 10^{-6}$ Mol/l.

Testversuche mit Mischungen aus Quarz bzw. Granit G–1 (Probe 116 aus Tabelle 7) und Cr_2O_3 bzw. $Ca_3(PO_4)_2$ konnten jedoch zeigen, dass selbst Cr_2O_3- und P_2O_5-Gehalte in den Proben, die weit über denen der normalen Gesteine liegen, die Ergebnisse der Gesamtschwefelbestimmung nicht stören (Tabelle 3).

Tabelle 3. Gesamtschwefelbestimmung in Proben mit hohen Cr- und P-Gehalten

Einwaage	In der Probe vorgegeben		In der Probe bestimmt
0,5 g SiO_2 + 0,021 g Cr_2O_3	4,03% Cr_2O_3,	<0,0020% S	<0,002% S
0,5 g SiO_2 + 0,020 g $Ca_3(PO_4)_2$	1,73% P_2O_5,	<0,0020% S	<0,002% S
0,5 g Granit + 0,030 g $Ca_3(PO_4)_2$	2,59% P_2O_5,	+0,0175% S	0,0180% S

D. *Genauigkeit*

Zur Prüfung der Methode wurden Schwefelbestimmungen in Mischungen aus Quarzmehl bzw. Gesteinspulver (Proben 116 und 157 aus Tabelle 7) mit Schwefelverbindungen bekannter Gehalte durchgeführt (Tabelle 4).

Tabelle 4. Gesamtschwefelbestimmungen in künstlichen Mischungen

Einwaage	μg S vorgegeben	μg S bestimmt	$\Delta(\mu gS)$
0,5 g SiO_2 + 0,19 mg FeS_2	101	95	−6
0,5 g SiO_2 + 1,49 mg FeS_2	795	785	−10
0,5 g SiO_2 + 0,84 mg ZnS	276	285	−9
0,5 g SiO_2 + 0,40 mg $BaSO_4$	55	60	+5
0,5 g SiO_2 + 2,56 mg $BaSO_4$	352	350	−2
0,5 g SiO_2 + 0,76 mg Fe_7S_8	318	320	+2
0,5 g Granit G–1 + 0,17 mg FeS_2	179	180	+1
0,5 g Granit G–1 + 2,40 mg $BaSO_4$	418	430	+12
0,5 g Diabas W–1 + 0,29 mg FeS_2	223	230	+7

Tabelle 5 Spalte 2 zeigt die Genauigkeit der Gesamtschwefelbestimmungen, die sich aus diesen Testversuchen und aus Analysen verschiedener Einwaagen mehrerer Gesteinsproben ergibt.

II. *Die Bestimmung des Sulfidschwefels in silikatischen Mineralen und Gesteinen*

Der Sulfidschwefel wird durch Behandeln mit Salzsäure und naszierendem Wasserstoff in Schwefelwasserstoff überführt, dieser in Cadmiumsalzlösung eingeleitet und anschliessend unter Verwendung von 0,005 N Lösungen jodometrisch bestimmt.

A. *Ausführung*

Abb. 2 zeigt die benutzte Apparatur. Sie besteht aus einer Wasserstoffbombe *A*, der konzentrierte H_2SO_4 enthaltenden Waschflasche *B*, dem Vorratsgefäss *C*, dem Hahn *D*, dem Entwicklungskolben *E* (250 ml), dem Kühler *F*, der mit 60 ml H_2O beschickten Vorlage *G* und dem 15 ml

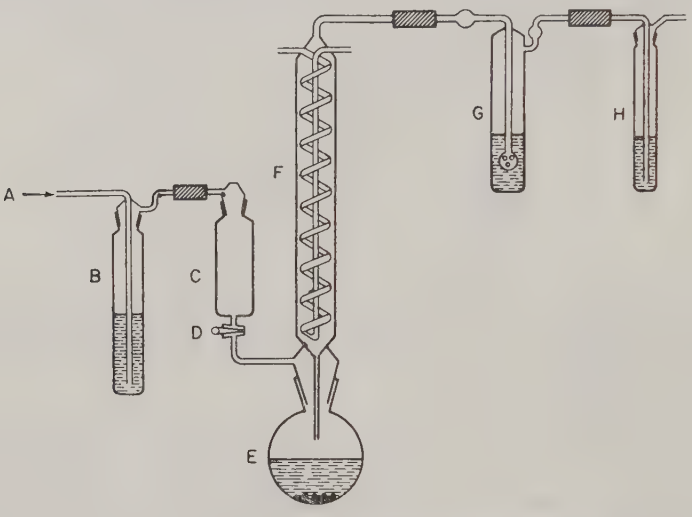

Abb. 2. Apparatur zur Sulfidschwefelbestimmung.

gepufferte Cadmiumcetat-Lösung (50 g Cd-acetat + 200 g Na-acetat/l.) enthaltenden Absorptionsgefäss *H*. Die Teile *F*, *G* und *H* sind durch PVC-Schlauch miteinander verbunden. Wegen der Lichtempfindlichkeit des CdS-Niederschlages ist das Absorptionsgefäss *H* vor Sonnenlicht geschützt.

(1) *G* und *H* sind noch nicht angeschlossen. Die feingepulverte Probe (entsprechend dem zu erwartenden Sulfidgehalt 0,1 bis 2 g) und 10 g granuliertes Zinn (S-frei) werden mit 10 ml H_2O in den Kolben *E* gebracht. Vorhandene Luft wird durch langsames Durchleiten von H_2 durch die Apparatur verdrängt.

(2) *G* und *H* werden angeschlossen. Der Hahn *D* wird geschlossen und das Vorratsgefäss *C* mit 70 ml HCl ($D = 1{,}19$) gefüllt.

(3) *D* wird geöffnet und der Entwicklungskolben mit HCl beschickt. H_2 wird weiter durch die Apparatur geleitet.

(4) Der Kolben *E* wird mit einem Bunsenbrenner langsam erwärmt, bis die Flüssigkeit in *E* siedet. Nach $4\frac{1}{2}$ Std weiterem Erwärmen ist das Sulfid der Probe vollständig aufgeschlossen. Der Brenner wird entfernt. Nach 30 Min weiterem Durchleiten von H_2 befindet sich der gesamte ausgetriebene S in der Vorlage *H* als CdS. Der im Kühler nicht kondensierte Chlorwasserstoff hat sich in der Vorlage *G* gesammelt.

(5) Der Inhalt von *H* wird sorgfältig in einen Titrierkolben überführt, in den vorher 15 ml 5 N HCl und 10 ml Kaliumjodit-Jodatlösung (entsprechend 0,005 N Jodlösung) gegeben wurden. Dabei reagiert der freiwerdende H_2S mit Jod nach der Gleichung:

$$H_2S + J_2 \rightarrow 2HJ + S$$

(6) Der Überschuss Jod wird mit 0,005 N Natriumthiosulfat zurücktitriert.

(7) Aus der verbrauchten Jodmenge wird der Sulfidschwefelgehalt berechnet.

B. *Fehlerquellen*

Während bei der Untersuchung von Sulfidmineralen, von geringen Abweichungen abgesehen, für Gesamtschwefel und Sulfidschwefel die gleichen Werte gefunden wurden, liegen die bestimmten Werte für Sulfidschwefel in Silikatmineralen und -Gesteinen häufig wesentlich unter den Gesamtschwefelergebnissen (vgl. Tabellen 6 und 7). Hauptsächlich sind sechs Fehlerquellen bei der Sulfidbestimmung möglich:

(1) Beim Mahlen wird Sulfid zu Sulfat oxydiert.
(2) Die Sulfide werden nicht quantitativ aufgeschlossen.
(3) Beim Aufschluss wird Sulfid oxydiert.
(4) Beim Aufschluss wird elementarer Schwefel reduziert.
(5) Der H_2S wird nicht quantitativ von der Cd-Lösung absorbiert.
(6) Verluste bei der jodometrischen Bestimmung.

Einige Versuche konnten zeigen, dass dies nicht die Ursachen für grössere Unterschiede zwischen den bestimmten Gesamtschwefel- und Sulfidschwefelwerten sind:

I. 10 g Quarz (S-frei) wurde mit 13,0 mg Pyrit 30 Min. in der Kugelmühle gemahlen und anschliessend in der Mischung Sulfidschwefel bestimmt. 1 g der Mischung enthält 694 μg Sulfid-S. Gefunden wurden 700 μg Sulfid-S. Dies stimmt mit den Beobachtungen von Allen und Johnston (1910) überein, die fanden, dass beim Mahlen von 5 g Pyrit in einer Achatmühle nach 1 Std nur 0,22%, nach 6 Std nur 1,1% des Pyrits zu Sulfat oxydiert wurde.

II. 5 g feingemahlener Granit Andlau Nord (Probe 109 aus Tabelle 7) werden mit 5,0 mg Pyrit (<63 μ) 30 Min in der Kugelmühle gemahlen und in der Mischung der Sulfidschwefel bestimmt. 1 g der Mischung enthält 544 μg Sulfid-S. In vier Bestimmungen wurden gefunden 530, 539, 536, 550 μg S (Mittel 539 μg S).

III. 5 g Basalt Dransberg (Probe 151 aus Tabelle 7) wurde mit 2,5 mg Magnetkies (>63 μ) 30 Min in der Kugelmühle gemahlen und in der Mischung der Sulfidschwefel bestimmt. 1 g der Mischung enthält 309 μg S. Gefunden wurden 310, 311, 318, 295 μg S (Mittel 306 μg S).

IV. 5 g eines reinen Cleavelandits mit wenig Flüssigkeitseinschlüssen (Probe 21 aus Tabelle 6) Gesamt-S: 0,0035%, Sulfid-S: $<0{,}001$%) wurde bei 100°C mit Flusssäure aufgeschlossen. Im Rückstand wurde der Gesamtschwefel zu 0,004% bestimmt, Sulfidschwefel wurde im Rückstand nicht gefunden.

V. Von 3 g Granit Andlau Nord (Gesamt-S: 0,0325%, Sulfid-S: 0,001%) wurde eine Sulfidbestimmung durchgeführt. Im Rückstand, der von der salzsauren Lösung abfiltriert und von nicht aufgelösten Zinngranalien befreit wurde, fand sich bei einer Gesamtschwefelbestimmung kein Schwefel mehr.

VI. Von 2 g Basalt Dransberg (Probe 151 aus Tabelle 7, Gesamt-S: 0,0135%, Sulfid-S: 0,0035%) wurde eine Sulfidbestimmung durchgeführt. Der Rückstand war wie bei (V) schwefelfrei.

VII. Es wurde eine Mischung von Quarz und elementarem Schwefel hergestellt. In dieser Mischung wurde S nach der Sulfidmethode bestimmt. Vorgegeben wurden 600 μg S, gefunden 603 μg S.

Für die Versuche II, III, V und VI wurden Proben ausgewählt, bei denen die Differenz zwischen gefundenem Gesamt-S und Sulfid-S besonders gross ist. Die gute Übereinstimmung zwischen Gesamtschwefel und dem bestimmten Sulfidschwefel bei den Versuchen I, II, III, V und VI schliesst die Fehlerquellen (1), (3), (5) und (6) aus. Der Versuch IV spricht gegen (2), den unvollständigen Aufschluss etwa von in Silikatpartikeln eingeschlossenen submikroskopischen oder bei der mikroskopischen Untersuchung übersehenen Sulfideinschlüssen, da Flusssäure Magnetkies unter H_2S-Entwicklung auflöst und Pyrit in Abwesenheit von größeren Mengen Eisen-III Verbindungen kaum angreift. Das Ergebnis der Versuche V und VI zeigt, dass auch hier der gesamte Sulfidschwefel ausgetrieben wurde und dass der nicht-sulfidische Schwefel dieser Proben beim Sulfidaufschluss gelöst wird. Aus Versuch VII ergibt sich schliesslich für den Punkt (4), dass etwa vorhandener elementarer Schwefel als Sulfid mitbestimmt wird.

C. *Genauigkeit*

Tabelle 5 Spalte 3 zeigt die Genauigkeit der Sulfidschwefelbestimmung bei der Ausführung von Doppelbestimmungen mit Einwaagen von 1 g bei S-Gehalten unter 0,05%, die sich aus den

Versuchen I bis III und VII und aus Analysen verschiedener Einwaagen mehrerer Gesteinsproben mit Gehalten zwischen 5 und 800 μg Sulfidschwefel ergibt.

III. *Die Bestimmung des Sulfatschwefels in silikatischen Mineralen und Gesteinen*

Der Sulfatschwefel der untersuchten Proben ergibt sich als Differenz zwischen Gesamt- und Sulfidschwefel.

Zur Prüfung der Zuverlässigkeit dieser Differenzbestimmung wurden für mehrere Konzentrationsbereiche je 10 Testanalysen an Proben ausgeführt, deren Sulfid- und Sulfatschwefelgehalte in derselben Grössenordnung liegen. In Tabelle 5 Spalte 4 sind für die verschiedenen Konzentrationsbereiche die mittleren absoluten Fehler bei der Sulfatbestimmung angegeben ($\Delta_{mittl.}$), dahinter jeweils die bei den Testbestimmungen gefundene größte Abweichung vom Mittelwert ($\Delta_{max.}$). Ist kein Sulfidschwefel vorhanden, sind die Abweichungen bei höheren Gehalten geringer als angegeben. Wird dagegen wesentlich mehr Sulfid- als Sulfatschwefel gefunden, ist die Angabe des Sulfatschwefels als Differenzbestimmung natürlich weniger zuverlässig und die Abweichungen der Ergebnisse vom Mittelwert sind grösser als die in Tabelle 5 aufgeführten.

Tabelle 5. Konzentrationsbereich und mittlerer Fehler für die Bestimmung von Gesamt-, Sulfid- und Sulfatschwefel

S-Gehalt der Probe (%)	Gesamt-S (%)		Sulfid-S (%)		Sulfat-S (%) (Sulfid-S ≃ Sulfat-S)	
	$\Delta_{mittl.}$	$\Delta_{max.}$	$\Delta_{mittl.}$	$\Delta_{max.}$	$\Delta_{mittl.}$	$\Delta_{max.}$
0,001 bis 0,002			0,0004	(0,0005)		
0,002 bis 0,01	0,0008	(0,001)	0,0004	(0,0005)	0,0010	(0,0015)
0,01 bis 0,02	0,0008	(0,001)	0,0008	(0,001)	0,0010	(0,002)
0,02 bis 0,1	0,0015	(0,002)	0,0015)	(0,002)	0,0015	(0,004)
0,1 bis 1	0,004	(0,01)	0,006	(0,01)	0,005	(0,02)

In den folgenden Tabellen werden die gefundenen Sulfatschwefelgehalte, die innerhalb der Fehlergrenzen liegen, durch Klammern gekennzeichnet.

Einschränkend zu den Daten der Tabelle 5 und den folgenden Tabellen ist zu sagen:

(1) Etwa vorhandener elementarer Schwefel fälscht die unter Sulfid-S angegebenen Werte. Da die meisten untersuchten Proben aber vermutlich keinen oder nur sehr wenig elementaren Schwefel enthalten, wurde von einer gesonderten Bestimmung abgesehen.

(2) Das Verhalten anderer Schwefelverbindungen als Sulfid, Sulfat und elementarer Schwefel bei der Sulfidbestimmung wurde aus demselben Grund nicht untersucht. (Über organisch gebundenen Schwefel in Sedimentgesteinen s.u.)

(3) Die untersuchten Minerale wurden jeweils kurz vor der Analyse gemahlen. Dagegen lag ein größerer Teil der Gesteinsproben aus der von V. M. Goldschmidt begründeten geochemischen Sammlung des Göttinger Instituts bereits als zerkleinertes Material vor. Es ist möglich, dass bei einigen dieser Proben ursprünglich vorhandenes Sulfid teilweise oxydiert ist. Die bestimmten Sulfid- und Sulfatgehalte der Proben, die bereits fein gemahlen zur Verfügung standen, werden in den Tabellen in Klammern angegeben und für die Berechnung von Durchschnittswerten nicht mit verwandt.

Die Schwefelgehalte silikatischer Minerale

In 95 Silikatmineralproben wird der Spurenelementgehalt an Schwefel bestimmt. Dass Minerale der Sodalithgruppe und Skapolithe Sulfatschwefel enthalten, ist seit langem bekannt. Doelter (1917) gibt für Hauyn S-Gehalte bis 5,49%, für Skapolithe S-Gehalte bis 1,53% an. Von der Untersuchung dieser Mineralgruppen wurde abgesehen. Die Proben stammen zum Teil aus monomineralischen Anreicherungen und Lagerstätten, teilweise wurden sie aus grobkörnigen Gesteinen mit

Hilfe einer Lupe bzw. unter dem Stereomikroskop aus dem zerkleinerten Gestein herausgelesen. Die Proben (26), (60) und (80) wurden mir freundlicherweise von Herrn Fröhlich überlassen, der die Konzentrate mit dem Frantz-Magnetscheider aus dem Basalt Probe (151) herstellte. Alle Kristalle wurden optisch auf Einschlüsse und Verwachsungen untersucht und für die Analyse, soweit es möglich war, nur solche verwandt, in denen kein Erz beobachtet wurde. Durch diese Auswahl sind die gefundenen Gesamt- und Sulfidschwefelwerte nicht immer für die Gesamtprobe charakteristisch, dafür ist die Bestimmung des Sulfatschwefels, die hier besonders interessiert, aber genauer. Grössere Sulfidgehalte konnten jedoch mikroskopisch nur in den Biotiten und Tonmineralen sicher nachgewiesen werden, so dass die in Tabelle 6 angegebenen Gesamt- und Sulfidschwefelgehalte zumindest in der Grössenordnung auch für die Gesamtproben gelten.

Quarz aus Graniten kann praktisch schwefelfrei sein (1 und 2), kann aber auch höhere Sulfatgehalte haben (0,0095% S in Probe 4). In Quarzen, die bei niederen Temperaturen gebildet wurden (5 bis 7), wurde nur wenig S gefunden.

In allen untersuchten Gerüstsilikaten (9 bis 37) wurde Sulfatschwefel nachgewiesen. Vom Hauyn (Probe 36 mit 4,81% S) abgesehen, variieren die bestimmten Sulfatgehalte zwischen 0,001 und 0,022% S. Während in Kalifeldspäten und Natronfeldspäten mit Ausnahme des Sanidin (11), der aus einem Trachyt stammt, der akzessorisch Hauyn führt, die Sulfatschwefelwerte 0,011% S nicht überschreiten, haben basische Plagioklase häufig höhere Gehalte. Auch im Nephelin und Desmin konnten relativ hohe Sulfatgehalte nachgewiesen werden.

Die untersuchten Muskovite (38 bis 42) sind sulfidfrei; die Pegmatitmuskovite (39) und (40) enthalten Sulfat. Dagegen sind Biotite und Chlorite (43 bis 51) praktisch sulfatfrei, während alle Proben mit Ausnahme der Probe (43) hohe Sulfidschwefelgehalte aufweisen. In Graniten und Pegmatiten scheinen die Sulfide bevorzugt als Verwachsungen mit Biotit vorzukommen. Während in Talk, Pyrophyllit und Chrysotil (52 bis 54) kein S gefunden wurde, können monomineralische Anreicherungen von Tonmineralen beträchtliche Sulfid- und Sulfatgehalte aufweisen, die wahrscheinlich durch Beimengungen von Pyrit, Anhydrit und Gips erklärt werden können.

Die meisten der untersuchten Pyroxene und Amphibole enthalten Sulfatschwefel. Mit einer Ausnahme sind die Gehalte nicht höher als 0,007% S. Die Hornblende (74) wurde in einem Tuff gefunden. Vermutlich ist der hohe Sulfatgehalt der Probe durch sekundäre Umwandlungen zu erklären.

Auch die Mehrzahl der untersuchten Inselsilikate enthält Sulfatschwefel. Die höchsten Gehalte dieser Gruppe wurden in Titanit (89) und Zirkon (90) mit 0,014 und 0,0125% S gefunden. In einem Beryll (96) wurde nur 0,0015% Sulfatschwefel bestimmt.

Sulfatschwefelgehalte in der Höhe, wie sie von Marinelli (1949) für Granat (0,09, 0,14 und 0,18%), Andalusit (0,16%), Topas (0,13 und 0,14%), Disthen (0,05 und 0,06%), Olivin (0,01 und 0,04%) und Epidot (0,02%) angegeben wurden, konnten nicht festgestellt werden. Marinelli prüfte auf Sulfid, indem er das Mineralpulver im Platintiegel mit Flusssäure und Schwefelsäure behandelte und entwickelten Schwefelwasserstoff mit Bleiacetatpapier über dem Tiegel nachwies. Fiel diese Probe negativ aus, so sollte kein Sulfid vorhanden sein. Da jedoch, im Gegensatz zu

Tabelle 6. Schwefel in Silikatmineralen

	Gesamt-S (%)	Sulfid-S (%)	Sulfat-S (%)
Quarz			
(1) Quarz aus Granit Grafversforsbolag (Schweden)	<0,0020	<0,0010	<0,0020
(2) Quarz aus Hornblendegranit Rautenkranz (Erzgebirge)	<0,0020	<0,0010	<0,0020
(3) Quarz aus Granit Grimstad (Norwegen)	0,0020	<0,0010	0,0020
(4) Quarz aus Granit Andlau (Vogesen)	0,0095	<0,0010	0,0095
(5) Quarz (Brasilien), Proben Trommsdorff	<0,0020	<0,0010	<0,0020
(6) Alpiner Kluftquarz, Gerstenhorn	0,0020	<0,0010	0,0020
(7) Alpiner Kluftquarz, leg. Huttenlocher	0,0030	<0,0010	0,0030
(8) Quarzsand, tertiär, Dörentrup (Lippe)	<0,0020	<0,0010	<0,0020
Gerüstsilikate			
(9) Sanidin aus Auswürfling, Wehr (Eifel)	0,0020	<0,0010	0,0020
(10) Sanidin aus Auswürfling (Eifel)	0,0040	<0,0010	0,0040
(11) Sanidin aus Trachyt Drachenfels (Siebengebirge)	0,0175	<0,0010	0,0175
(12) Orthoklas aus Granit Tröstau bei Wunsiedel (Fichtelgebirge)	0,0020	<0,0010	0,0020
(13) Orthoklas aus Kirchberger Granit Wildenau (Sachsen)	0,0025	<0,0010	0,0025
(14) Orthoklas aus Krichberger Granit Lengenfeld (Sachsen)	0,0040	<0,0010	0,0040
(15) Orthoklas aus Granit Karlsbad (Böhmen)	0,0085	<0,0010	0,0085
(16) Orthoklas aus Granit Andlau (Vogesen)	0,0075	<0,0010	0,0075
(17) Orthoklas aus Granit Grafversforsbolag (Schweden)	0,0100	<0,0010	0,0100
(18) Kalifeldspat aus Pegmatit, Caracol (Minas Geraes)	0,0020	<0,0010	0,0020
(19) Adular Haslital bei Meiringen (Schweiz)	0,0075	0,0025	0,0050
(20) Perthit aus Pegmatit, Ise (Norwegen)	0,0110	0,0035	0,0075
(21) Albit (Cleavelandit), Tatúde Itauninha de Ferros (Minas Geraes)	0,0035	<0,0010	0,0035
(22) Albit (U.S. National Bureau of Standards no. 99)	0,0030	<0,0010	0,0030
(23) Oligoklas aus Granit, Andlau (Vogesen)	0,0065	<0,0010	0,0065
(24) Oligoklas aus Granit Grafversforsbolag (Schweden)	0,0070	<0,0010	0,0070
(25) Oligoklas aus Granit Ytterby (Schweden)	0,0090	0,0030	0,0060
(26) Andesinkonzentrat (durch 8% Pyroxen, Olivin und Erz verunreinigt) aus Olivinbasalt Dransberg bei Dransfeld (Südniedersachsen) Original material Fröhlich (1960)	0,0250	0,0030	0,0220
(27) Labradorfels, Auclandsfjord (Norwegen)	0,0090	<0,0010	0,0090
(28) Labradorit, St. Paulsinsel (Labrador)	0,0140	≦0,0050	≧0,0090
(29) Labradorfels, Langenäsbach Soyndal (Norwegen)	0,0145	0,0025	0,0120
(30) Bytownitfels Italheims Klar bei Nöredal (Norwegen)	0,0100	0,0090	(0,0010)
(31) Feldspat Laaven (Norwegen)	0,0175	0,0035	0,0140
(32) Feldspat aus Granit Grimstad (Norwegen) (Orthoklas + Plagioklas)	0,0060	<0,0010	0,0060
(33) Feldspat aus Granit Rautenkranz (Erzgebirge) (Orthoklas + Plagioklas)	0,0080	<0,0010	0,0080
(34) Nephelin aus Nephelinsyenitpegmatit Miask (Ural)	0,0110	<0,0010	0,0110
(35) Nephelin aus Nephelinsyenitpegmatit Laaven, Langesundfjord (Norwegen)	0,0210	0,0085	0,0125
(36) Hauyn Niedermendig (Eifel)	4,81	n.b.	n.b.
(37) Desmin Berufjord (Island)	0,0180	<0,0010	0,0180

Tabelle 6—*Continued*

	Gesamt-S (%)	Sulfid-S (%)	Sulfat-S (%)
Blattsilikate			
(38) Muskovit aus Pegmatit, Spittal (Kärnten)	<0,0020	<0,0010	<0,0020
(39) Muskovit aus Pegmatit, Bamle (Norwegen)	0,0065	<0,0010	0,0065
(40) Muskovit aus Pegmatit, Göteborg (Schweden)	0,0135	<0,0010	0,0135
(41) Muskovit Lenkersmühle bei Windisch-Eschenbach (Oberpfalz)	<0,0020	<0,0010	<0,0020
(42) Muskovit aus Buntsandstein, Bremke bei Göttingen	<0,0020	<0,0010	<0,0020
(43) Biotit (weitgehend erzfrei) aus Granit Rautenkranz (Erzgebirge)	<0,0020	0,0010	<0,0010
(44) Biotit (mit Erzeinschlüssen) aus Granit Rautenkranz (Erzgebirge)	0,0080	0,0085	<0,0010
(45) Biotit (+etwas Hornblende) aus Granit Andlau (Vogesen)	0,0195	0,0200	<0,0010
(46) Biotit aus Granitpegmatit, Bodenmais (Bayrischer Wald)	0,0065	0,0060	(0,0005)
(47) Biotit aus Granitpegmatit, Arendal (Norwegen)	0,0260	0,0260	<0,0020
(48) Biotit aus Nephelinsyenitpegmatit Miask (Ural)	0,0460	0,0465	<0,0020
(49) Biotit aus Pegmatit Kristiansand (Norwegen)	0,0675	0,0670	(0,0005)
(50) Lepidomelan Laaven (Norwegen)	0,0190	0,0175	(0,0015)
(51) Chlorit Chester, Vermont (U.S.A.)	0,0500	0,0500	<0,0020
(52) Talk Zillertal (Österreich)	<0,0020	<0,0010	<0,0020
(53) Pyrophyllit, von Eisenerzlagerstätten, Westana Grube (Schonen)	<0,0020	<0,0010	<0,0020
(54) Chrysotil Barranco de San Juan, Sierra Nevada (Spanien)	<0,0020	<0,0010	<0,0020
(55) Halloysit Lawrence County, Missouri	0,0290	0,0025	0,0265
(56) Kaolinit Birch Pit, Macon (Georgia) Originalmaterial, American Petroleum Institute API (1951)	0,0220	<0,0010	0,0220
(57) Montmorillonit Amory (Mississippi) Originalmaterial API (1951)	0,103	0,095	0,008
(58) Montmorillonit Upton (Wyoming), Originalmaterial API (1951)	0,203	0,020	0,183
(59) Illit Morris (Illinois), Original material API (1951)	6,31	6,30	(0,01)
Kettensilikate			
(60) Pyroxenkonzentrat (durch 8% Plagioklas, Olivin und Erz verunreinigt) aus Olivinbasalt Dransberg bei Dransfeld (Südniedersachen) Originalmaterial Fröhlich (1960)	0,0020	0,0020	<0,0010
(61) Diopsid Alabel (Piemont)	0,0050	0,0030	0,0020
(62) Diopsid Schwarzenstein (Tirol)	0,0030	<0,0010	0,0030
(63) Diopsid Rotenkopf im Zillertal (Österreich)	0,0050	n.b.	n.b.
(64) Bronzit Peterlestein bei Kupferberg (Bayern)	<0,0020	<0,0010	<0,0020
(65) Bronzit Kraubath (Steiermark)	<0,0020	<0,0010	<0,0020
(66) Hypersthen Nain, Paulsinsel (Labrador)	0,0070	0,0040	0,0030
(67) Augit Firmenich bei Daun (Eifel)	0,0035	<0,0010	0,0035
(68) Augit Vesuv (Italien)	0,0025	<0,0010	0,0025
(69) Ägirin Barkewikscheeren (Norwegen)	0,0055	<0,0010	0,0055
(70) Ägirin Brewik (Norwegen)	0,0090	0,0020	0,0070

Tabelle 6—*Continued*

	Gesamt-S (%)	Sulfide-S (%)	Sulfat-S (%)
(71) Hedenbergit Nordmarken	<0,0020	<0,0010	<0,0020
(72) Diallag Figline bei Prato (Italien)	0,0020	0,0015	0,0005)
(73) Basalt. Hornblende aus Trachydolerit Kopanka (Böhmen)	0,0165	0,0130	0,0035
(74) Basalt. Hornblende aus Trachydolerit Lukow (Böhmen)	0,0175	(0,0035)	(0,0140)
(75) Hornblende Kragerö (Norwegen)	0,0045	<0,0010	0,0045
Insel- und Gruppensilikate			
(76) Olivinfels Mysäte (Norwegen)	<0,0020	<0,0010	<0,0020
(77) Olivin Björkedal (Norwegen)	<0,0020	<0,0010	<0,0020
(78) Olivinknolle aus Bombe, Dreiser Weiher (Eifel)	0,0025	<0,0010	0,0025
(79) Olivinknolle aus Olivinbasalt Hoher Hagen bei Dransfeld (Südniedersachsen)	0,0070	0,0025	0,0045
(80) Olivin-Titanomagnetit-Konzentrat aus Olivin-Basalt Dransberg bei Dransfeld (Südniedersachsen) Originalmaterial Fröhlich (1960)	0,0095	0,0065	0,0030
(81) Andalusit Lisens Alpe (Tirol)	0,0225	0,0165	0,0060
(82) Disthen aus Disthen-Glimmerschiefer St. Gotthard	0,0110	0,0040	0,0070
(83) Staurolith aus Disthen-Glimmerschiefer St. Gotthard	0,0110	0,0025	0,0085
(84) Granat (Almandin) Fort Wrangel (Alaska)	0,0100	0,0020	0,0080
(85) Granat (Andradit) Grua bei Oslo (Norwegen)	0,0105	<0,0010	0,0105
(86) Granat Luisenfelde bei Lindi (Ostafrika)	0,0065	<0,0010	0,0065
(87) Epidot Salzburg (Österreich)	0,0055	<0,0010	0,0055
(88) Epidot Arendal (Norwegen)	0,0170	0,0105	0,0065
(89) Titanit Westport (Kanada)	0,0140	<0,0010	0,0140
(90) Zirkon Ceylon	0,0150	0,0025	0,0125
(91) Turmalin Alabaschka (Ural)	0,0120	0,0040	0,0080
(92) Turmalin aus Pegmatit	0,0050	<0,0010	0,0050
(93) Topas Nakatsugawa, Mino (Japan)	<0,0020	<0,0010	<0,0020
(94) Topas Ramona (Californien)	0,0025	<0,0010	0,0025
(95) Topas aus Quarz-Topas-Turmalinfels Schneckenstein (Sachsen)	<0,0020	<0,0020	<0,0020
(96) Beryll (Brasilien)	0,0040	0,0025	0,0015

Magnetkies und anderen Sulfiden, Pyrit bei diesem Aufschluß nicht oder nur sehr langsam angegriffen wird, ist es möglich, dass Marinelli auch Sulfidschwefel als Sulfat mitbestimmte.

Die Schwefelgehalte der Eruptivgesteine

Durch die Mineralanalysen konnte gezeigt werden, dass die meisten gesteinsbildenden Minerale häufig Sulfatschwefel enthalten. Dass der Sulfatschwefel massgeblich am Schwefelgehalt der meisten Eruptivgesteine beteiligt ist, zeigt die folgende Tabelle 7, in der die Schwefelbestimmungen in 55 Gesteinsproben und 11 Durchschnittsmischungen einzelner Gesteinsgruppen aus insgesamt 123 Einzelproben aufgeführt sind. Der Wert Q in der letzten Spalte der Tabelle 7 gibt den

prozentualen Anteil des Sulfatschwefels am Gesamtschwefel an.

$$\left(Q = \frac{\text{Sulfatschwefel}}{\text{Gesamtschwefel}} \times 100.\right)$$

Aus den Werten der Tabelle 7 ist klar ersichtlich, dass die Variationsbreite sowohl der Gesamtschwefelwerte als auch der Sulfid- und Sulfatschwefelwerte innerhalb der einzelnen Gesteinstypen beträchtlich ist. Das Verhältnis Sulfatschwefel/Gesamtschwefel zeigt besonders grosse Schwankungen. Im Gegensatz zu den Harzgranitproben (98 bis 105) und den in Chemismus und Mineralbestand untereinander sehr ähnlichen Basaltproben vom Backenberg (153 bis 155) zeigt das Beispiel des Andlaugranits (Proben 109 bis 111), dass auch innerhalb eines Gesteinvorkommens Gesamt- und Sulfatschwefelgehalt durchaus wechseln können.

Aus den Ergebnissen der Eruptivgesteinsanalysen werden nun die mittleren Gehalte einzelner Gesteinsfamilien an Gesamt-, Sulfid- und Sulfatschwefel abgeschätzt.

Obwohl allein schon aus Zeitgründen bei der Auswahl der Proben zur Analyse besonderer Wert auf repräsentative Gesteine gelegt wurde—zur Bestimmung von Gesamt- und Sulfidschwefel einer Probe wurde trotz serienmässiger Durchführung der Analysen ein Tag benötigt-, können die gewonnenen Durchschnittsgehalte, besonders wegen der geringen Anzahl der untersuchten Gesteine der einzelnen Familien bei oft beträchtlichen Abweichungen der Einzelbestimmungen von den berechneten Mittelwerten, und den relativ kleinen Arealen, aus denen die Gesteine stammen, nur rohe Näherungswerte sein. Die Zuverlässigkeit der Durchschnittswerte hätte etwa durch die Verdoppelung der Analysenzahl etwas gesteigert werden können. Wesentlich genauere Aussagen kann man jedoch erst durch Analyse einer bedeutend grösseren Anzahl sorgfältig ausgewählter Gesteinsproben erhalten. Wenn in Zukunft bei der Untersuchung grösserer Gesteinskomplexe neben vielen Spurenelementen auch das relativ häufige Element Schwefel analytisch bestimmt wird, kann man sicher bald genauere Angaben über das geochemische Verhalten des Schwefels in Eruptivgesteinen erhalten.

Bei der Berechnung der Mittelwerte werden alle untersuchten Gesteine gleich berücksichtigt, die Durchschnittsmischungen entsprechend der Anzahl der Proben, aus denen sie zusammengesetzt sind. Wurden jedoch mehrere Proben, die sich nur wenig voneinander unterscheiden, aus einem Gesteinsvorkommen analysiert, so werden die Ergebnisse zu einem Wert zusammengefasst:

	Gesamt-S (%)	Sulfid-S (%)	Sulfat-S (%)	Q
Harzgranit (98 bis 105)	0,0085	0,0025	0,0060	71
Andlaugranit (109 bis 111)	0,0200	0,0030	0,0110	79*
Basalt Backenberg (153 bis 155)	0,0455	0,0055	0,0400	88

Die folgende Tabelle 8 gibt die abgeschätzten Durchschnittswerte der einzelnen Gruppen, getrennt für Tiefengesteine (T) und Ergussgesteine (E), an.

Die Berechnung der Durchschnittswerte für die kalkbetonten basischen Tiefengesteine aus den eigenen Analysen scheint mir wenig zuverlässig. Aus den

Tabelle 7. Schwefel in Eruptivgesteinen

	Gesamt-S (%)	Sulfid-S (%)	Sulfat-S (%)	Q
Saure Tiefengesteine				
Granite:				
(97) Durchschnitt von 14 deutschen Graniten (Fichtelgebirge 3; Odenwald, Bayrischer Wald, Erzgebirge, Sachsen je 2; Vogesen, Schwarzwald, Schlesien je 1) Zusammensetzung siehe Noll (1934)	0,0370	(0,0175)	(0,0195)	(53)
(98) Granit Schierke (Harz)	0,0110	<0,0010	0,0110	100
(99) Granit Brockenmassiv (Harz), Originalmaterial Degenhardt (1957) Probe Königskopf 2	0,0070	n.b.	n.b.	
(100) Granit Brockenmassiv (Harz), Originalmaterial Degenhardt (1957) Probe Königskopf 3	0,0095	n.b.	n.b.	
(101) Granit Brockenmassiv (Harz), Originalmaterial Degenhardt (1957) Probe Wurmberg 2	0,0085	n.b.	n.b.	
(102) Granit Brockenmassiv (Harz), Originalmaterial Degenhardt (1957) Probe Wurmberg 4	0,0060	n.b.	n.b.	
(103) Granit Brockenmassiv (Harz), Originalmaterial Degenhardt (1957) Probe Wurmberg 6	0,0080	n.b.	n.b.	
(104) Durchschnitt der Granitproben (99) bis (103) (Harz)	0,0080	0,0030	0,0050	62
(105) Granit Okermassiv (Harz), Originalmaterial Dreizler Probe 122	0,0105	0,0010	0,0095	90
(106) Granit Rautenkranz (Erzgebirge)	0,0065	0,0010	0,0055	85
(107) Lithionitgranit Eibenstock (Sachsen)	0,0140	0,0010	0,0130	93
(108) Porphyrischer Granit Strehlen (Schlesien)	0,0090	0 0030	0,0060	67
(109) Granit Andlau (Vogesen), Originalmaterial H. Faul Probe Andlau Mord	0,0325	(0,0010)	(0,0315)	(97)
(110) Granit Andlau (Vogesen), Originalmaterial H. Faul Probe Andlau Süd	0,0175	0,0035	0,0140	80
(111) Granit Andlau (Vogesen)	0,0105	0,0030	0,0075	71
(112) Granit "Hammergranit" Bornholm	0,0110	0,0060	0,0050	45
(113) Granit Grimstad (Norwegen)	0,0470	0,0430	0,0040	9
(114) Granit Grafversforsbolag (Schweden)	0,0075	0,0020	0,0055	28
(115) Granit "Aaregranit" Gurtnellen (Schweiz)	0,0150	0,0020	0,0130	87
(116) Granit Westerly (Rhode Island) U.S. Geol. Survey, Standardprobe G–1	0,0175	0,0060	0,0115	66
(117) Granit Eklara (Indien), Originalmaterial Köster (1956) Probe 105	0,0030	0,0030	<0,0010	0
Granodiorite:				
(118) Granodiorit (Opdalit) Ulsberg (Norwegen)	0,0160	0,0155	(0,0005)	3
(119) Granodiorit "Vanggranit" Bornholm	0,0155	0,0150	(0,0005)	3
(120) Granodiorit "Roennegranit" Bornholm	0,0475	0,0405	0,0070	15
(121) Granodiorit Schönbach (Lausitz)	0,0800	0,0790	(0,0010)	1
Quarzdiorite:				
(122) Quarzdiorit (Tonalit) Adamello (Südtirol)	0,0180	0,0060	0,0120	67

Tabelle 7.—*Continued*

	Gesamt-S (%)	Sulfid-S (%)	Sulfat-S (%)	Q
(123) Quarzdiorit "Hornblendegranit" Teufelsberg (Odenwald)	0,0410	0,0380	(0,0030)	7
Saure Ergussgesteine				
(124) Durchschnitt von 14 Lipariten, Inseln S. Pietro, S. Antioco (Sardinien) Zusammensetzung siehe v Engelhardt (1936)	0,0210	0,0020	0,0190	90
(125) Liparit Moskardshnjukar (Island) Originalmaterial Sigvaldason (1958) Probe M1	0,0155	0,0025	0,0130	84
(126) Liparit (Island) Originalmaterial Sigvaldason (1959) Probe SL1	0,0085	<0,0010	0,0085	100
(127) Durchschnitt von 8 Obsidianen (Island 4, Lipari 3, U.S.A. 1) Zusammensetzung siehe v. Engelhardt (1936)	0,0070	0,0010	0,0060	85
(128) Obsidian Roche Rossi (Lipari)	0,0065	<0,0010	0,0065	100
Kalkbetonte intermediäre Tiefengesteine				
(129) Diorit Reichenbach (Odenwald)	0,0300	0,0240	0,0060	20
Kalkbetonte intermediäre Ergussgesteine				
(130) Durchschnitt von 6 Andesiten, Aegina (griech. Insel im Saronischen Golf) Zusammensetzung siehe v. Engelhardt (1936)	0,0395	0,0035	0,0360	91
(131) Durchschnitt von 14 Andesiten, Methana (griech. Halbinsel im Saronischen Golf) Zusammensetzung siehe v. Engelhardt (1936)	0,0130	0,0015	0,0115	88
(132) Pyroxenandesit Sababurg, Reinhardswald (Hessen)	0,0735	0,0725	(0,0010)	1
(133) Pyroxenandesit Tokay (Ungarn)	0,0215	0,0010	0,0205	95
(134) Amphibolandesit Stenzelberg (Siebengebirge)	0,0145	0,0040	0,0105	72
(135) Amphibolandesit Wolkenburg (Siebengebirge)	0,0150	0,0045	0,0105	70
(136) Diabasporphyrit St. Andreasberg (Harr)	0,173	0,173	<0,002	0
Alkalibetonte intermediäre Tiefengesteine				
(137) Syenit Zitzschewig bei Dresden	0,0235	0,0075	0,0160	60
(138) Durchschnitt von 22 Nephelinsyeniten (Brasilien 5, U.S.A. 7, Kanada 2, Portugal 3, Norwegen 4, Siebenbürgen 1) Zusammensetzung siehe v. Engelhardt (1936)	0,0450	0,0325	0,0125	28
(139) Nephelinsyenit Posos de Caldas (Minas Geraes)	0,0240	0,0095	0,0145	60
Alkalibetonte intermediäre Ergussgesteine				
(140) Durchschnitt von 10 deutschen Phonoliten (Hessen 5, Eifel 2, Kaiserstuhl 2, Hegau 1) Zusammensetzung siehe v. Engelhardt (1936)	0,0320	0.0120	0,0200	62
(141) Durchschnitt von 10 böhmischen Phonoliten, Zusammensetzung siehe v. Engelhardt (1936)	0,0570	0,0250	0,0320	56
(142) Noseanphonolit Schellkopf bei Brenk (Eifel)	0,305	0,0155	0,290	95

Tabelle 7—*Continued*

	Gesamt-S (%)	Sulfid-S (%)	Sulfat-S (%)	*Q*
(143) Trachyt Hahn bei Selters (Westerwald)	0,0050	0,0010	0,0040	80
(144) Trachyt Wölferlingen (Westerwald)	0,0105	<0,0010	0,0105	100
(145) Trachyt Drachenfels (Siebengebirge)	0,113	<0,0010	0,113	100
Kalkbetonte basische Tiefengesteine				
(146) Durchschnitt von 11 deutschen Gabbros (Sachsen, Schlesien, Odenwald je 3; Harz 2) Zusammensetzung siehe Noll (1934)	0,0875	0,0880	(0,000)	0
(147) Olivingabbro Radautal bei Bad Harzburg (Harz)	0,0960	0,0960	(0,000)	0
Kalkbetonte basische Ergussgesteine				
Olivinbasalte:				
(148) Olivinbasalt Steinberg bei Barlissen (Südniedersachsen)	0,0110	0,0090	0,0020	18
(149) Olivinbasalt Bramburg bei Adelebsen (Südniedersachsen)	0,0145	0,0080	0,0065	45
(150) Olivinbasalt Hoher Hagen bei Dransfeld (Südniedersachsen) Originalmaterial Wedepohl (1950)	0,0180	0,0080	0,0100	56
(151) Olivinbasalt Dransberg bei Dransfeld (Südniedersachsen)	0,0135	0,0035	0,0100	74
(152) Trachydoleritischer Basalt Gahrenberg (Südniedersachsen)	0,0265	0,0145	0,0120	45
(153) Trachydoleritischer Basalt Backenberg (Südniedersachsen) Originalmaterial Wedepohl (1954) Probe 1	0,0430	0,0055	0,0375	87
(154) Trachydoleritischer Basalt Backenberg (Südniedersachsen) Originalmaterial Wedepohl (1954) Probe 5	0,0470	0,0055	0,0415	88
(155) Trachydoleritischer Basalt Backenberg (Südniedersachsen) Originalmaterial Wedepohl (1954) Probe 4	0,0460	0,0055	0,0405	88
Tholeiitische Basalte:				
(156) Durchschnitt von 9 Basalten Deccan (Indien) Zusammensetzung siehe v. Engelhardt (1936)	0,0310	0,0240	0,0070	23
(157) Diabas Centerville, Fairfax County U.S. Geol. Survey, Standardprobe W1	0,0135	0,0130	(0,0005)	4
Alkalibetonte basische Ergussgesteine				
(158) Melilithbasalt Hochbohl (Schwäbische Alb)	0,0255	0,0175	0,0080	31
(159) Melilithbasalt Westberg bei Hofgeismar (Hessen) Originalmaterial Ernst (1936)	0,163	0,0420	0,121	74
(160) Olivinnephelinit Mühlenberg (Eifel)	0,0270	0,0205	0,0065	24
(161) Olivinnephelinit Druseltal bei Kassel (Hessen)	0,0340	0,0150	0,0190	56
(162) Leuzitnephelintephrit Niedermendig (Eifel)	0,134	0,0025	0,131	98
(163) Leuzititschlacke Bausenberg (Eifel)	0,0365	0,0130	0,0235	65

Gabbro-Werten der Analysen (146) und (147) und den Bestimmungen an Labradorit- und Bytownitfelsen (27 bis 30) als Vertreter der Anorthosite erhält man als Mittel: 0,069% Gesamtschwefel und 0,001% Sulfatschwefel. Die Gabbro-Proben stammen aus relativ unbedeutenden kleinen Vorkommen, bei denen die Aufnahme grösserer Mengen Sedimentmaterials teils erwiesen, teils jedenfalls nicht ausgeschlossen ist. Mehr charakteristisch für diesen Gesteinstypus sind sicherlich die petrographisch und chemisch gut untersuchten Gesteine der Skaergaard Intrusion

Tabelle 8. Mittlere Häufigkeit des Schwefels in Eruptivgesteinen

Gesteinsgruppe		Gesteine, aus denen der Durchschnittswert berechnet wurde	Gesamt-S (%)	Sulfid-S (%)	Sulfat-S (%)	$\frac{\text{Sulfat-S}}{\text{Gesamt-S}} \times 100$
Saure Gesteine	T	25 Granite + 4 Granodiorite + 2 Quarzdiorite	0,029	0,016	0,006	28*
	E	16 Liparite + 8 Obsidiane	0,019	0,002	0,017	89
Kalkbetonte intermediäre Gesteine	T	1 Diorit	0,030	0,024	0,006	20
	E	24 Andesite	0,023	0,005	0,018	78
Alkalibetonte intermediäre Gesteine	T	1 Syenit + 23 Nephelinsyenite	0,044	0,031	0,013	30
	E	20 Phonolite + 1 Noseanphonolit + 3 Trachyte	0,059	0,020	0,039	66
Kalkbetonte basische Gesteine	T	vergl. Tabelle 9	0,036	0,034	0,002	6
	E	15 Basalte	0,027	0,017	0,010	37
Alkalibetonte basische Gesteine	E	2 Melilithbasalte + 2 Olivinnephelinite + 1 Leuzitnephelintephrit + 1 Leuzitit	0,070	0,018	0,052	74

* Die Proben (97) und (109) wurden wegen ihrer unsicheren Sulfid-S- und Sulfat-S-Gehalte nur zur Berechnung des Mittels für Gesamt-S verwandt.

(Grönland) und des Duluth Komplex (Minnesota). Die Arbeiten von Wager Vincent und Smales (1957) und von Snyder (1959) sind zwei der wenigen, bei denen bei der systematischen Untersuchung grösserer Gesteinskomplexe auch Schwefel bestimmt wurde. In der Tabelle 9 sind der von Wager *et al.* gegebene durchschnittliche Schwefelgehalt der Skaergaard Intrusion und der aus Schwefelbestimmungen von Snyder an vier Olivingabbros und einem Olivinnorit des "Ham brule traverse" berechnete Mittelwert für Gesteine des Duluth Komplex neben den eigenen Werten für deutsche Gabbros und Labrador- bzw. Bytownitfelse aufgeführt. Der Durchschnittsgehalt der kalkbetonten basischen Tiefengesteine an Gesamtschwefel wird als arithmetisches Mittel dieser vier Werte berechnet. Die Berechnung der Durchschnittswerte des Sulfatschwefels und des Sulfatanteils am Gesamtschwefel in dieser Gruppe wird aus den eigenen Bestimmungen nach dem üblichen Verfahren durchgeführt, der mittlere Gehalt an Sulfidschwefel wird zu 0,034% abgeschätzt.

Die in Tabelle 8 angegebenen Durchschnittswerte für alkalibetonte intermediäre Gesteine stimmen gut mit denen von Nockolds (1954) überein. Aus den von Nockolds gegebenen Daten erhält man als Durchschnittsgehalt von 48 Nephelinsyeniten: 0,036% S, als Durchschnittswert von 47 Phonoliten: 0,052% S.

Die Untersuchungen von Broderick (1935) zeigen, dass die mittleren Schwefelgehalte mehrerer grosser basaltischer Lavaströme des Keweenawan voneinander verschieden sind. Broderick erhält für den Greenstone Flow (Michigan) als Durchschnittswert von 12 Mischungen aus insgesamt 154 Einzelproben: 0,023% S,

Tabelle 9. Gesamtschwefel in kalkbetonten basischen Tiefengesteinen

		%S
Skaergaard Intrusion	nach Wager *et al.* (1957)	0,005
Duluth Komplex	nach Snyder (1959)	0,03
Mittel aus 12 deutschen Gabbros	aus Proben (145) und (146)	0,088
Mittel aus 3 Labradorfelsen + 1 Bytownitfels	aus Proben (27 bis 30)	0,012
Berechneter Durchschnitt:		0,036

für den Kearsage Flow (Michigan) von 7 Mischungen aus insgesamt 46 Einzelproben: 0,008% S. Obwohl man bei diesen Schwefelanalysen wegen des angewandten gravimetrischen Bestimmungsverfahrens keine allzu grosse Genauigkeit erwarten kann, zeigen sie sicher, dass die Schwefelgehalte dieser basaltischen Gesteine zumindest nicht wesentlich über dem berechneten Durchschnittswert aus Tabelle 8 liegen.

Wegen der Unsicherheiten bei der Abschätzung der in Tabelle 8 zusammengestellten Durchschnittsgehalte ist natürlich beim Vergleich dieser untereinander Vorsicht angebracht. Die folgenden Gesetzmässigkeiten scheinen jedoch für die aufgeführten Gesteinsgruppen vorhanden zu sein:

(1) Die mittleren Gesamtschwefelgehalte aller aufgeführten Gesteinsfamilien, mit Ausnahme der Alkaligesteine, liegen um 0,03% S.

(2) Mit Ausnahme der gabbroiden Gesteine, bei denen der Sulfatanteil, wenn überhaupt vorhanden, sehr gering ist, kommt der Schwefel als Sulfid und als Sulfat vor.

(3) Die Tiefengesteine enthalten im Mittel mehr Sulfidschwefel und weniger Sulfatschwefel als ihre Ergussgesteinsäquivalente. Der Anteil des Sulfatschwefels am Gesamtschwefel ist bei den Tiefengesteinen im Mittel geringer as bei den entsprechenden Ergussgesteinen.

(4) Die sauren Tiefengesteine enthalten im Mittel weniger Sulfidschwefel als die basichen Tiefengesteine.

(5) Die sauren Ergussgesteine enthalten im Mittel weniger Sulfidschwefel als die basischen Ergussgesteine.

(6) Der prozentuale Anteil des Sulfatschwefels am Gesamtschwefel ist bei den sauren Gesteinen im Mittel grösser als bei den basischen Gesteinen. (Für die Alkaligesteine konnte dieser Gang nicht gezeigt werden.)

Eine weitere Gesetzmässigkeit ist möglich, durch die vorhandenen Daten aber noch nicht gesichert:

(7) Tiefengesteine enthalten im Mittel etwas mehr Gesamtschwefel als ihre Ergussgesteinsäquivalente.

Die Punkte (4) und (5) stehen in Einklang mit den Beobachtungen von Newhouse (1936), der durch die systematische mikroskopische Untersuchung der Erzminerale in den wichtigsten Tiefen- and Ergussgesteinen fand, dass "the more femic rocks contain a larger proportion of sulphides than do the salic ones."

Die Feststellung Trögers (1934), dass basische Gesteine im Durchschnitt wesentlich mehr Gesamtschwefel enthalten als saure, kann durch die gewonnenen Ergebnisse nicht bestätigt werden. Während der von Tröger angegebene Durchschnittsgehalt der Alkaligranite, Alkalikalkgranite, Granodiorite und Quarzdiorite (0,05% S) immerhin nur etwas höher als der neuberechnete (0,029% S) liegt, sind die Differenzen bei den Anorthositen (nach Tröger: 0,01% S), Dioriten (nach Tröger: 0,1% S), Gabbros (nach Tröger: 0,2% S) und Peridotiten (nach Tröger: 0,25% S) beträchtlich. So wertvoll eine Berechung der mittleren Häufigkeiten selten analytisch bestimmter Elemente aus Literaturdaten einzelner Analysen ist, wenn noch keine systematischen Untersuchungen hierüber vorliegen, so ist die Berechnungsart doch mit zahlreichen Fehlermöglichkeiten behaftet. Für das Element Schwefel ist sicher eine der schwerwiegendsten, dass es vom Gesteinsanalytiker in vielen Fällen nur dann bestimmt wird, wenn im Gestein sulfidisches Erz makroskopisch oder mikroskopisch festgestellt wurde. Durch eine bevorzugte Berücksichtigung dieser Analysen müssen systematische Plusfehler entstehen. Da die basischen Tiefengesteine teilweise sehr niedrige, teilweise sehr hohe Schwefelgehalte haben (vgl. Tabelle 9), ist hier die Gefahr der Überbewertung der schwefelreichen Gesteine besonders gross.

Die bisherigen Untersuchungen zeigten, dass viele Silikatminerale und Eruptivgesteine häufig Sulfatschwefel enthalten. In den Hauptbestandteilen von drei Graniten und einem Basalt als Vertreter der wichtigsten Gesteinsgruppen wurden die Sulfatschwefelgehalte bestimmt. Die folgende Zusammenstellung (Tabelle 10) soll zeigen, in welchen Mineralen sich der Sulfatschwefel in den Eruptivgesteinen hauptsächlich befindet.

Die Tabelle 10 zeigt, dass die Feldspäte zumindest in den hier angeführten Gesteinen die Hauptträger des Sulfatschwefels sind. Dieser Befund wird durch die übrigen Mineralanalysen der Tab. 6 erhärtet, bei denen die Feldspäte die höchsten Sulfatschwefelgehalte aufweisen. Bei den Graniten von Andlau und Grafversforsbolag konnte gezeigt werden, dass sich die Sulfatschwefelgehalte von Orthoklas und Plagioklas aus dem gleichen Gestein nicht wesentlich voneinander unterscheiden. Ebenfalls in Übereinstimmung mit den übrigen Mineralanalysen zeigt die Tabelle 10 aber, dass die Feldspäte nicht die alleinigen Sulfatträger in den Gesteinen sind.

Betrachtungen über die Art des Vorkommens von Sulfatschwefel in Eruptivgesteinen

Ehe die verschiedenen Möglichkeiten für das Vorkommen von Sulfatschwefel in Eruptivgesteinen diskutiert werden, sollen die Ergebnisse einiger ausgeführter Lösungsversuche mitgeteilt werden.

Einige Minerale, deren S-Gehalte in Tabelle 6 aufgeführt sind, wurden in der Kugelmühle auf die Korngrösse $<3_{\mu}$ gebracht. Jeweils 2 g des Pulvers (bei Hauyn nur 0,12 g) wurden in 250 ml Wasser suspendiert und 4 Stunden bei 25°C in einer Plastikflasche geschüttelt. Anschließend wurde durch ein Membranfilter abfiltriert, der Rückstand mit 250 ml Wasser ausgewaschen und im Rückstand und im Filtrat getrennt der Gesamtschwefel bestimmt.

Tabelle 10. Sulfatschwefelgehalte der Hauptkomponenten einiger Gesteine

Gestein	Mineral	Gew. (%)	Sulfat-S im Mineral (%)	Beitrag zum Sulfat-S des Gesteins (%)	Sulfat-S im Gestein direkt bestimmt (%)
Granit Andlau (111)	Quarz (4)	24	0,0095	0,0023	
	Orthoklas (16)	27	0,0075	0,0020	
	Plagioklas (23)	40	0,0065	0,0026	
	Biotit (45)	6	0,0005	<0,0001	
				0,0069	0,0075
Granit Grimstad (113)	Quarz (3)	30	0,0020	0,0006	
	Feldspat (32)	65	0,0060	0,0039	
				0,0045	0,0040
Granit Grafversforsbolag (114)	Quarz (1)	30	<0,0020	<0,0006	
	Orthoklas (17)	30	0,0100	0,0030	
	Plagioklas (24)	30	0,0070	0,0021	
				0,0051	0,0055
Olivinbasalt Dransberg (151)	Plagioklas (26)	45	0,0220	0,0099	
	Pyroxen (60)	35	<0,0010	<0,0003	
	Olivin + Titanomagnetit (80)	20	0,0030	0,0006	
				0,0105	0,0100

Die Ergebnisse dieser Lösungsversuche sind in Tabelle 11 dargestellt. Die Lösungsversuche wurden im allgemeinen an sulfidfreien Mineralen ausgeführt, nur vier Proben enthielten Sulfidschwefel. Für die Angaben des ungelösten und des gelösten Sulfatschwefels bei diesen Proben wurde angenommen, dass das Sulfid quantitativ im Rückstand verblieb. Grössere Fehler können jedenfalls durch etwaige teilweise Oxydation des Sulfidschwefels dieser Proben nicht entstanden sein. Wichtig sind in Tabelle 11 die Werte der letzten Spalte, die angeben, wieviel % des ursprünglich in der Probe vorhandenen Sulfatschwefels gelöst wurden.

Einige Lösungsversuche wurden noch etwas modifiziert:

I. Das Andesinkonzentrat (26) wurde anstatt 45 Minuten jetzt 3 Stunden

gemahlen. Der gelöste Sulfatschwefel wurde zu 0,0097% bestimmt, d.h. anstatt 41% wurde jetzt 44% des Sulfats gelöst.

II. Feldspat (33) wurde anstatt 45 Minuten jetzt 3 Stunden gemahlen. Der gelöste Sulfatschwefel wurde zu 0,0050% bestimmt, d.h. anstatt 50% wurde jetzt 62% des Sulfats gelöst.

III. Orthoklas (16) wurde anstatt 4 Stunden 16 Stunden mit Wasser geschüttelt. Der gelöste Sulfatschwefel wurde zu 0,0015% bestimmt, d.h. anstatt 15% wurde jetzt 20% des Sulfats gelöst.

Tabelle 11. Bestimmung des löslichen Anteils am Sulfatschwefel mehrerer Minerale

Probe	Gesamt-S (%)	Sulfid-S (%)	Sulfat-S (%)	Gesamt-S ungelöst (%)	Sulfat-S ungelöst (%)	Sulfat-S gelöst (%)	Löslicher Anteil des Sulfat-S (%)
Quarz (4)	0,0095	<0,0010	0,0095	<0,0020	<0,0020	0,0091	96
Quarz (7)	0,0030	<0,0010	0,0030	<0,0020	<0,0020	0,0031	100
Orthoklas (16)	0,0075	<0,0010	0,0075	0,0060	0,0060	0,0011	15
Cleavelandit (21)	0,0035	<0,0010	0,0035	0,0017	0,0017	0,0020	57
Perthit (20)	0,0110	0,0035	0,0075	0,0079	0,0044	0,0023	31
Oligoklas (23)	0,0065	<0,0010	0,0065	0,0040	0,0040	0,0020	31
Andesinkonzentrat (26)	0,0250	0,0030	0,0220	0,0150	0,0120	0,0090	41
Feldspat (33)	0,0080	<0,0010	0,0080	0,0040	0,0040	0,0040	50
Hauyn (36)	4,81	n.b.	4,81	n.b.	n.b.	0,38	7,8
Muskovit (39)	0,0065	<0,0010	0,0065	0,0025	0,0025	0,0040	62
Kaolinit (56)	0,0220	<0,0010	0,0220	<0,0020	<0,0020	0,0228	100
Montmorillonit (57)	0,103	0,095	0,008	0,095	0	0,0082	100
Augit (67)	0,0035	<0,0010	0,0035	0,0020	0,0020	0,0020	57
Hornblende (74)	0,0175	0,0035	0,0140	0,0032	0	0,0140	100
Olivin (78)	0,0025	<0,0010	0,0025	(0,0010)	(0,0010)	0,0020	80
Granat (85)	0,0105	<0,0010	0,0105	0,0055	0,0055	0,0045	43

IV. Oligoklas (23) wurde anstatt 4 Stunden 16 Stunden mit Wasser geschüttelt. Es konnten keine Unterschiede festgestellt werden.

Während der Sulfatschwefel in Quarz, Kaolinit, Montmorillonit, Olivin und Hornblende (74) durch Ausschütteln der gemahlenen Proben mit Wasser praktisch vollständig herausgelöst werden konnte, wurde bei den übrigen Proben nur ein Teil des Sulfatschwefels gelöst (zwischen 15 und 62%). Auch durch weiteres Zerkleinern der Proben oder längeres Ausschütteln konnte nur wenig mehr gelöst werden. Das Sulfat des Hauyn konnte nur zu einem geringen Teil in Lösung gebracht werden (7,8%).

Ähnliche Lösungsversuche wurden von Faber (1941), Behne (1953) und Kuroda und Sandell (1953) beschrieben. Prinzipiell ähnliche Verfahren benutzten Roedder (1958) und Ames (1958) zur Untersuchung von Flüssigkeitseinschlüssen in Mineralen.

Zum Vergleich mit den in dieser Arbeit bestimmten Gehalten an Gesamtsulfat und löslichem Sulfat seien einige Ergebnisse der erwähnten Autoren wiedergegeben:

Faber zerkleinerte die Proben auf <0,25 mm, behandelte das Pulver mehrere Tage bzw. Wochen mit lauwarmem Wasser, filtrierte und bestimmte in der Lösung Sulfat und andere Ionen. Faber fand so in Quarz aus Granitpegmatiten 0,0016 und 0,0029%, in Feldspat aus Granitpegmatiten 0,0046 und 0,0065% löslichen Sulfatschwefel, in 12 Graniten zwischen 0,0012 und 0,0073% (Mittel 0,0031%) und in einem Olivinbasalt 0,0037% löslichen Sulfatschwefel.

Behne zerkleinerte sein Material auf <3 μ, schüttelte 2 bzw. 4 Stunden bei Zimmertemperatur mit Wasser und bestimmte das Gesamtchlor der Proben und gelöstes Chlorid. Behne fand, dass das gesamte Chlor, das der Feldspat aus Granit Rautenkranz enthält (0,0060%) so gelöst werden konnte. Für diese Arbeit wurde aus derselben Granitprobe Feldspat ausgelesen und hierin 0,0080% Gesamtsulfatschwefel und 0,0040% löslicher Sulfatschwefel bestimmt (vgl. Tab. 11). Behne fand im Biotit desselben Gesteins 0,0650% Chlor, von dem jedoch nur 0,0060% in Lösung ging. Sulfatschwefel konnte in diesem Biotit nicht nachgewiesen werden.

Kuroda und Sandell zerkleinerten die Proben auf 100-mesh Korngrösse und bestimmten das bei Zimmertemperatur durch Schütteln mit Wasser oder wässriger Kaliumnitratlösung herausgelöste Chlor. Aus einem Perthit, der ursprünglich 0,0070% Chlor enthielt, konnten 0,0058% gelöst werden, aus verschiedenen Gesteinen wurden maximal 0,0070% Chlor in Lösung gebracht.

Roedder fand in 12 einzelnen Quarzkristallen zwischen 0,0002 und 0,0033% löslichen Sulfatschwefel (im Mittel 0,0012%). Ames bestimmte in pegmatitischem Quarz 0,0002% und in Fluoritkristallen 0,0097 und 0,0024% löslichen Sulfatschwefel.

Grundsätzlich gibt es für das Vorkommen von Sulfatschwefel in Gesteinen 4 Möglichkeiten:

(1) Das Sulfat kommt in Sulfatmineralen wie Baryt oder Anhydrit oder in Sulfatsilikaten wie Nosean und Hauyn vor.

(2) Die Sulfatgruppe ersetzt andere Radikale in Kristallgittern.

(3) Das Sulfat ist in Flüssigkeitseinschlüssen gelöst in Silikatmineralen enthalten.

(4) Sulfat liegt in glashaltigen Gesteinen in fester Lösung im Glas vor.

Zu (1): Obwohl mehrere Sulfate, hauptsächlich Baryt und Anhydrit, daneben auch Gips und Alunit, häufig als Hydrothermalbildungen auftreten, ist deren Vorkommen in normalen Eruptivgesteinen nicht bekannt. Diese Minerale kommen also üblicherweise wohl nicht in mikroskopisch gut sichtbaren Kristallen vor. Dagegen kann die Möglichkeit, dass diese Sulfate submikroskopisch, etwa an Korngrenzen oder in den Spaltrissen mancher Minerale vorhanden sind, nicht ausgeschlossen werden. Etwa so vorhandenes Sulfat würde—grössere Mengen Baryt ausgenommen—bei den Lösungsversuchen als gelöstes Sulfat bestimmt werden.

Zu (2): Zur Erklärung der gefundenen Sulfatschwefelgehalte durch den Ersatz anderer Elemente durch Schwefel bzw. anderer Radikale durch die Sulfatgruppe in Mineralen der Eruptivgesteine kommen nur solche Elemente bzw. Radikale in Frage, die in Mengen vorhanden sind, die in der Grössenordnung der gefundenen Sulfatschwefelgehalte oder darüber liegen. Dem S^{6+} vergleichbare Ionenradien finden wir unter diesen Elementen nur beim P^{5+} und Si^{4+}. Die Tabelle 12 zeigt die Ionenradien R_z nach Pauling und die Atomabstände Z—O von ZO_4-Gruppen in verschiedenen Mineralen.

Das weitaus wichtigste Phosphatmineral in Eruptivgesteinen ist der Apatit. Die Analysenzusammenstellung von Doelter (1917) gibt bei 5 Apatiten S-Gehalte zwischen 0,05 und 0,07% an. Kind (1939) isolierte Apatite aus 7 zum Teil sulfathaltigen magmatischen Gesteinen, fand aber bei der Analyse keinen Schwefel. Als mineralogische Raritäten gelten dagegen Apatite mit hohen Sulfatgehalten, wie sie z.B. von Brauns (1917) vom Laacher See (Eifel) mit 0,45 bis 0,54%

Sulfatschwefel und von McConell (1937) mit 8,28% Sulfatschwefel und Vasileva (1958) mit 0,14 bis 1,50% Sulfatschwefel aus kontaktmetamorphen Kalken beschrieben wurden. Nach den Untersuchungen von McConell und Vasileva werden bei sulfathaltigen Apatiten die Positionen des PO_4^{3-} teilweise durch SO_4^{2-} und SiO_4^{4-} ersetzt.

Wegen des geringen Apatitgehaltes der meisten Gesteine kann der Apatit als Sulfatträger nur in den Fällen massgeblich zum Sulfatgehalt eines Eruptivgesteins beitragen, wenn er einen aussergewöhnlich hohen Schwefelgehalt besitzt.

Tabelle 12. Atomabstände Z—O in einigen Mineralen mit Gruppen ZO_4

Atomgruppe	Z	R_z (Å)	Mineral	Abstände Z—O (Å)	
SO_4^{2-}	S^{6+}	0,29	Gips	1,54 bis 1,65	nach Strukturbericht II (1937)
PO_4^{3-}	P^{5+}	0,34	Apatit	1,49 bis 1,82	nach Strukturbericht II (1937)
SiO_4^{4-}	Si^{4+}	0,41	Orthoklas	1,66 bis 1,70	nach Chao *et al.* (1940)
			Anorthit	1,62 bis 1,72	nach Sörum (1953)
			Olivin	1,60 bis 1,79	nach Belov *et al.* (1951)

Die Raumbeanspruchung der Sulfatgruppe in selbständigen Sulfatmineralen ist etwa die gleiche wie die der SiO_4-Tetraeder in Silikatmineralen. So ist jedenfalls aus räumlichen Gründen ein Einbau von SO_4^{2-} anstelle von SiO_4^{4-} in Silikatgitter möglich. Der Ladungsausgleich könnte dabei durch einen weiteren Ersatz des Si^{4+} durch Al^{3+} erfolgen:

$$3Si^{4+} \rightarrow S^{6+} + 2Al^{3+}$$

oder z.B. bei den Feldspäten durch Ersatz des Ca^{2+} durch Na^{+}:

$$Si^{4+} + 2Ca^{2+} \rightarrow S^{6+} + 2Na^{+}$$

oder dadurch, dass einzelne Kationengitterplätze, etwa des Ca^{2+} in Feldspäten nicht besetzt sind:

$$Si^{4+} + Ca^{2+} \rightarrow S^{6+}$$

Zur Erklärung eines Sulfatschwefelgehaltes von 0,01% im Feldspat muss von etwa 6000 (Si, Al)O_4-Tetraedern eins durch SO_4 ersetzt sein. Sind in einem Silikatmineral die anstelle von SiO_4-Tetraedern eingebauten Sulfatgruppen statistisch verteilt, so sollte nur ein geringer Teil des Sulfats durch Behandlung des Mineral pulvers mit Wasser gelöst werden. Befindet sich das Sulfat jedoch hauptsächlich an Spaltrissen, Zwillingsgrenzen und anderen Stellen, an denen das Gitter gestört ist, so wird ein grösserer Teil des Sulfats in Lösung gehen können, denn beim Zerkleinern der Kristalle werden diese Stellen besonders leicht an die Oberfläche gelangen.

Besitzen Silikatgitter besonders grosse Hohlräume, wie die Zeolithe und Beryll, so können Sulfatgehalte dieser Minerale auch dadurch erklärt werden, dass sich einzelne Sulfatgruppen in diesen Hohlräumen befinden.

Zu (3): In den meisten der untersuchten Minerale konnten zahlreiche, wenn auch meist sehr kleine Flüssigkeitseinschlüsse beobachtet werden. Die Untersuchungen von Wahler (1956) zeigen, dass der Gewichtsanteil der Flüssigkeitseinschlüsse in einzelnen Mineralen 0,05 bis 0,5% betragen kann. Während die

höchsten von Wahler in Einschlüssen in Quarz, Beryll und Topas bestimmten Sulfatkonzentrationen nur etwa 0,04% S bei Gesamtsalzkonzentrationen in der Grössenordnung zwischen 2 und 20% betragen, können die Sulfatgehalte in Einschlüssen anderer Bildungsbedingungen wesentlich höher sein. Dies geht besonders aus den von Faber, Roedder und Ames und den in dieser Arbeit bestimmten Sulfatgehalten verschiedener Quarze hervor, die man wohl nur durch Flüssigkeitseinschlüsse erklären kann. Dass Faber auch aus Feldspäten Chlorid und Sulfat lösen konnte und dass von dem Sulfatschwefel des Feldspat aus Granit Rautenkranz (0,0080%) die Hälfte in Lösung ging, während Behne das gesamte Chlor desselben Materials (0,0060%) als Chlorid lösen konnte, spricht dafür, dass bei den Feldspäten häufig zumindest ein Teil des löslichen Sulfatschwefels mit dem Chlor in Flüssigkeitseinschlüssen vorliegt. Ähnliche Betrachtungen lassen sich auch für andere Minerale anstellen. So bestimmten z.B. Kuroda und Sandell in einem Hypersthen von Nain (Labrador) 0,0220% Chlor. In dieser Arbeit wurden in einem Hypersthen derselben Lokalität (Probe 66) 0,0030% Sulfatschwefel gefunden. Es ist möglich, dass auch hier das Sulfat zusammen mit Chlorid in Flüssigkeitseinschlüssen gelöst ist.

Bei den ausgeführten Lösungsversuchen geht mit Sicherheit das Sulfat in Lösung, das sich in Einschlüssen befindet, deren Grösse $> 3\ \mu$ ist. Es ist jedoch wahrscheinlich, dass beim Mahlen der Proben auch der weitaus grösste Teil wesentlich kleinerer Einschlüsse freigelegt wird, so dass sich praktisch das gesamte Sulfat aus Flüssigkeitseinschlüssen in der Lösung befindet.

Zu (4): Das Vorkommen von Sulfat in Gesteinsglas ist auf glashaltige Ergussgesteine beschränkt. Die untersuchten Olivinbasalte aus der Umgebung von Göttingen (Proben 147 bis 154) enthalten nur wenig Glas. Der Sulfatschwefel dieses Glases müsste mehrere Prozent betragen, um die hier gefundenen Sulfatschwefelgehalte (z.B. 0,0415% in Probe 153) zu erklären. In der Durchschnittsmischung von 8 Obsidianen (Probe 128) wurde jedoch nur 0,006% Sulfatschwefel bestimmt. Auch in drei weiteren Proben natürlicher Gläser aus verschiedenen Vorkommen konnten keine hohen Sulfatschwefelgehalte festgestellt werden:

	Gesamt-S (%)	Sulfid-S (%)	Sulfat-S (%)
Obsidian Hekla (Island)	0,014	0,002	0,012
Tachylit Bobenhausen (Vogelsberg, Hessen)	0,022	0,021	(0,001)
Nephelinführender Tachylit Steinberg bei Feldbach (Steiermark)	0,048	0,045	(0,003)

Die Sulfatschwefelgehalte einiger Eruptivgesteine können durch das Vorkommen küstenfernen Tiefseesedimenten kommt der Schwefel—jedenfalls in geringen Tieten auch durch das Auftreten von Sulfatapatit erklärt werden. Durch die ausgeführten Mineralanalysen konnte aber nachgewiesen werden, dass die meisten Silikatminerale kleine Mengen Sulfatschwefel enthalten. Es ist möglich, dass dies Sulfat teilweise an submikroskopische Einschlüsse von Sulfatmineralen in Silikaten gebunden ist. Quarze enthalten mit Sicherheit häufig Sulfat in Flüssigkeitseinschlüssen. Für andere Minerale konnte diese Erklärung wahrscheinlich gemacht

werden. Da jedoch bei den meisten Mineralen nur ein Teil des Sulfatschwefels gelöst werden konnte, bleibt ausserdem die Möglichkeit eines Einbaus von Sulfat in Silikatgitter bestehen. Besonders wegen des grossen Ladungsunterschiedes zwischen Si^{4+} und S^{6+} ist ein solcher Einbau am ehesten in locker gepackten Silikatstrukturen zu erwarten. Die relativ hohen Sulfatschwefelwerte in den Gerüstsilikaten entsprechen dieser Annahme.

Die Schwefelgehalte der Sedimentgesteine

Das Element Schwefel wird bei der chemischen Analyse von Sedimentgesteinen häufig bestimmt. Die analytische Bestimmung des Gesamtschwefels bereitet hier meist keine Schwierigkeiten, wenn man nicht Wert auf Präzisionsanalysen legt. Wegen der inhomogenen Verteilung des Schwefels in vielen dieser Gesteine sind die Abweichungen vom Durchschnittsgehalt, die durch die Probeentnahme entstehen, meist höher als die Fehler bei der Analyse, so dass eine allzu grosse Genauigkeit bei diesen Bestimmungen meist gar nicht erforderlich ist.

Obwohl in einzelnen Gesteinen oft Sulfide und Sulfate beobachtet wurden, wissen wir quantitativ über die Verteilung von Sulfid- und Sulfatschwefel in den Sedimentgesteinen noch sehr wenig. Aus diesem Grunde wurden mit der oben beschriebenen Methode in 46 Sedimentproben und 12 Durchschnittsmischungen aus insgesamt 226 Einzelproben die Gehalte an Gesamt,- Sulfid- und Sulfatschwefel bestimmt.

Elementarer Schwefel, der gelegentlich in Sedimenten vorkommt, mengenmässig aber nur sehr selten ins Gewicht fällt, wurde dabei als Sulfidschwefel mitbestimmt. Viele Sedimentgesteine enthalten organische Substanz ("Bitumen"), die hauptsächlich aus Kohlenwasserstoffen besteht, wahrscheinlich aber auch geringe Mengen verschiedener Schwefelverbindungen enthalten kann. Forsman und Hunt (1958), die die Zusammensetzung der unlöslichen organischen Substanz in Sedimentgesteinen untersuchten, gelang zwar die Abtrennung dieses Materials von den wichtigsten Mineralen der Gesteine, sie konnten es aber nicht von dem immer vorhandenen Pyrit isolieren und deshalb auch nicht den organisch gebundenen Schwefel bestimmen. Je nach der Art dieser Verbindungen wird dieser Schwefel bei der Sulfidbestimmung reduziert und als Sulfid mitbestimmt werden oder im Rückstand bleiben und als Sulfat angegeben werden. Mehrere Erdölproben mit Schwefelgehalten zwischen 0,10 und 0,88% S, die mir Herr Dr. Füchtbauer von der Gewerkschaft Elverath, Hannover, freundlicherweise überließ, wurden nach der Sulfidmethode behandelt. Hierbei wurden die im Öl vorhandenen Schwefelverbindungen nicht in Schwefelwasserstoff überführt.

Die Angaben der Sulfid- und Sulfatschwefelgehalte in der folgenden Tabelle können also bei einigen Gesteinen durch das Vorkommen von elementarem Schwefel und organisch gebundenem Schwefel verfälscht sein. Vermutlich werden aber diese Fehler in den meisten Fällen unbedeutend sein.

In Tabelle 13 sind die gefundenen Schwefelgehalte der untersuchten Sedimentgesteine aufgeführt. Der Wert Q gibt wieder den prozentualen Anteil des Sulfatschwefels am Gesamtschwefel an.

Die Schwefelgehalte der verschiedenen Sedimentgesteine unterscheiden sich

Tabelle 13. Schwefel in Sedimentgesteinen

	Gesamt-S (%)	Sulfid-S (%)	Sulfat-S (%)	Q
Verwitterungsbildungen und Tonminerale				
(164) Bauxit Arkansas, Metal Grade	0,0330	0,0050	0,0280	85
(165) Bauxit Originalmaterial U.S. National Bureau of Standards Probe 69 A	0,0295	<0,0010	0,0295	100
(55) Halloysit Lawrence County (Missouri)	0,0290	0,0025	0,0265	91
(56) Kaolinit Birch Pit, Macon (Georgia) Originalmaterial API (1951)	0,0220	<0,0010	0,0220	100
(57) Montmorillonit Amory (Mississippi) Originalmaterial API (1951)	0,103	0,095	(0,008)	8
(58) Montmorillonit Upton (Wyoming) Originalmaterial API (1951)	0,203	0,020	0,183	90
(59) Illit Morris (Illinois) Originalmaterial API (1951)	6,31	6,30	(0,01)	0
Pelitische Sedimente				
(166) Durchschnitt von 36 europäischen paläozoischen Tonschiefern (Silur 9, Devon 12, Karbon 13, Rotliegendes 2) Zusammensetzung siehe Noll (1934)	0,296	0,242	0,054	18
(167) Durchschnitt von 14 japanischen paläozoischen Tonschiefern (Hauptinsel Honschu) Originalmaterial Minami (1935)	0,117	0,056	0,061	52
(168) Wissenbacher Schiefer, Devon, Goslar (Harz)	1,00	0,62	0,38	38
(169) Dachschiefer Raumland, Devon (Rothaargebirge)	0,50	0,50	(0,00)	0
(170) Kulmtonschiefer Waldenburg (Schlesien)	0,0350	0,0120	0,0230	66
(171) Kulmtonschiefer Okertal (Harz) Originalmaterial Dreizler Probe 39	0,0135	0,0045	0,0090	67
(172) Kulmtonschiefer Okertal (Harz) Originalmaterial Dreizler Probe 41	0,155	0,153	(0,002)	1
(173) Kulmtonschiefer Okertal (Harz) Originalmaterial Dreizler Probe 42	0,0140	<0,0010	0,0140	100
(174) Kulmtonschiefer Okertal (Harz) Originalmaterial Dreizler Probe 42A	0,0155	<0,0010	0,0155	100
(175) Kulmkieselschiefer Wallau (Hessen) Originalmaterial Hoss (1957) Probe Wallau 8	0,0270	0,0270	(0,000)	0
(176) Ton Hardegsen bei Göttingen, Röt	0,0280	<0,0010	0,0280	100
(177) Ton Hünstollen bei Göttingen, Röt, Originalmaterial Lippmann	0,0240	<0,0010	0,0240	100
(178) Ton Grossalmerode (Hessen), tertiäre Süsswasserbildung. Originalmaterial Lippmann (1952)	0,380	0,380	(0,000)	0
(179) Ton Limburg (Lahn), Originalmaterial Köster	0,0205	<0,0010	0,0205	100
(180) Entsalztergrauer Salzton (Zechstein) Reyershausen bei Göttingen, Originalmaterial Niemann (1960) Probe 2937	n.b.	0,337	n.b.	

Tabelle 13—*Continued*

	Gesamt-S (%)	Sulfid-S (%)	Sulfat-S (%)	*Q*
(181) Entsalzter grauer Salzton (Zechstein) Reyershausen bei Göttingen, Originalmaterial Niemann (1960) Probe 2941	n.b.	0,029	n.b.	
(182) Entsalzter grauer Salzton (Zechstein) Reyershausen bei Göttingen, Originalmaterial Niemann (1960) Probe 3348	n.b.	0,0510	n.b.	
(183) Entsalzter roter Salzton, (Zechstein) Reyershausen bei Göttingen. Originalmaterial Braitsch Probe 2994	n.b.	1,26	n.b.	
(184) Entsalzter roter Salzton (Zechstein) Reyershausen bei Göttingen, Originalmaterial Braitsch Probe 3167	n.b.	1,80	n.b.	
(185) Entsalzter Tonrückstand aus anhydritischem Hartsalz (Zechstein) Reyershausen bei Göttingen, Originalmaterial Braitsch Probe 2949b $<60\mu$	n.b.	0,84	n.b.	
(186) Entsalzter Ton aus Carnallitgestein (Zechstein) Reyershausen bei Göttingen, Originalmaterial Braitsch Probe 2983	n.b.	<0,0020	n.b.	
(187) Durchschnitt von drei Proben Tiefseeton (Meteor-Stationen 248, 250 und 251, Brasilianisches Becken; Sedimenttiefe: 31 bis 38 cm)	0,153	<0,0020	0,153	100
(188) Tiefseeton Lamont Station A160 8 (Nordamerikanisches Becken; Sedimenttiefe 5 m)	n.b.	<0,0010	n.b.	
(189) Tiefseeton Lamont Station A160 8 (Nordamerikanisches Becken; Sedimenttiefe 8,50 m)	0,078	0,0150	0,063	81
(190) Tiefseeton Lamont Station 172 14/19 (Nordamerikanisches Becken; Sedimenttiefe 3 m)	n.b.	<0,0010	n.b.	
Psammitische Sedimente				
(191) Durchschnitt von 11 deutschen Karbonsandsteinen. Zusammensetzung siehe v. Engelhardt (1936)	0,0255	0,0140	0,0115	45
(192) Durchschnitt von 23 deutschen Buntsandsteinen. Zusammensetzung siehe v. Engelhardt (1936)	0,0230	0,0030	0,0200	87
(193) Durchschnitt von 12 deutschen Kreidesandsteinen. Zusammensetzung siehe v. Engelhardt (1936)	0,0280	0,0040	0,0240	86
(194) Unterer Buntsandstein, Freden (Leine)	0,0190	<0,0010	0,0190	100
(195) Sandstein, oberer Keuper, Bovenden bei Göttingen	0,0135	<0,0010	0,0135	100
(8) Tertiärer Quarzsand, Dörentrup (Lippe)	<0,0020	<0,0010	<0,0020	
(196) Durchschnitt von 10 deutschen Quarziten. Zusammensetzung siehe v. Engelhardt	0,0125	0,0030	0,0095	76

Tabelle 13—*Continued*

	Gesamt-S (%)	Sulfid-S (%)	Sulfat-S (%)	*Q*
(197) Durchschnitt von 17 Graüwacken (vorwiegend Devon, z. T. Kulm) Zusammensetzung siehe v. ENGELHARDT (1936)	0,124	0,119	(0,005)	4
(198) Grobkörnige Kulmgrauwacke Steimkertal (Harz) Originalmaterial MATTIAT (1960) Probe 4	0,160	0,154	(0,006)	4
(199) Mittelkörnige Kulmgrauwacke Steimkertal (Harz) Originalmaterial MATTIAT (1960) Probe 5	0,147	0,147	(0,000)	0
(200) Feinkörnige Kulmgrauwacke Steimkertal (Harz) Originalmaterial MATTIAT (1960) Probe 6	0,251	0,252	(0,000)	0
Chemische und Biogene Sedimente				
(201) Durchschnitt von 32 deutschen Devonkalken, Zusammensetzung siehe v. ENGELHARDT (1936)	0,0980	0,0900	0,0080	8
(202) Durchschnitt von 45 deutschen Jurakalken, Zusammensetzung siehe v. ENGELHARDT (1936)	0,166	0,130	0,036	22
(203) Durchschnitt von 16 deutschen Kreidekalken, Zusammensetzung siehe v. ENGELHARDT (1936)	0,0985	0,0860	0,0125	13
(204) Kulmkieselkalk, Bromberg bei Küstelberg (Hessen)	0,0715	0,0125	0,0590	83
(205) Wellenkalk aus Muschelkalk mu_2, Hoffmannshof bei Göttingen	0,0125	0,0060	0,0065	52
(206) Dolomit, Muschelkalk mu_3, Nikolausberg bei Göttingen	0,0450	0,0180	0,0270	60
(207) Dolomitischer Mergel, Muschelkalk mm, Kerstlingeröder Feld bei Göttingen	0,0310	0,0085	0,0225	73
(208) Trochitenkalk, Muschelkalk mo_1, Reckershausen bei Göttingen	0,0210	0,0020	0,0190	90
(209) Ceratitenkalk, Muschelkalk mo_2, Hainberg bei Göttingen	0,0400	0,0055	0,0345	86
(210) Dolomit, Hauptdolomit des Zechstein, Scharzfeld (Harz)	0,0120	<0,0010	0,0120	100
(211) Dolomit, Originalmaterial U.S. National Bureau of Standards Probe 88A	0,0290	0,0110	0,0180	62
(212) Toniger Kalk, Originalmaterial U.S. National Bureau of Standards Probe 1A	0,302	0,286	0,016	5
(213) Durchschnitt aus 8 Tiefseeproben: Globigerinenschlamm (Stephan Stationen 68 bis 70, 72, 77 bis 80, Brasilianisches Becken, Sedimenttiefe 0 bis 45 cm)	0,122	<0,0010	0,122	100
(214) Eisenoolith, Lias, Echte bei Northeim (Südniedersachsen)	0,345	0,345	(0,000)	0
(215) Feuerstein aus Kreide, Stevns Klint (Dänemark)	<0,0020	<0,0010	<0,0010	.

zum Teil beträchtlich voneinander, auch innerhalb der einzelnen Gesteinsgruppen. Ebenso zeigt die Verteilung von Sulfid und Sulfatschwefel starke Schwankungen.

Die unterschiedlichen Schwefelgehalte der monomineralischen Tonmineralanreicherungen (55 bis 59) sind sicher auf verschiedene Bildungsbedingungen zurückzuführen. Für zwei Tonmineralproben (56 und 57) wurde gezeigt, dass der gesamte Sulfatschwefel mit Wasser ausgeschüttelt werden kann (vgl. Tab. 11). Das heisst, das Sulfat liegt hier in selbständigen Sulfatmineralen vor oder, wenn eine Bindung im Silikatgitter vorhanden sein sollte, ist diese jedenfalls nicht fest.

In den Tonen und Tonschiefern kommt der Schwefel teils nur als Sulfid oder nur als Sulfat, teils aber auch in beiden Oxydationsstufen vor. Bei den Tonschiefern gehen hohe Sulfidgehalte häufig mit hohen Bitumengehalten parallel. Von den von Dreizler (1960) untersuchten Kulmtonschieferproben (171 bis 174) hat nur die sulfidreiche Probe 171 einen erhöhten Gehalt an organischer Substanz. Dieselbe Beziehung zeigen die von Forsman und Hunt (1958) angegebenen Gehalte an Schwefel und organischem Kohlenstoff von 17 verschiedenen Sedimentgesteinen. Inwieweit hier der Schwefel direkt aus den Organismen stammt oder durch die Anhäufung organischer Substanz nur die Bedingungen zur Reduktion von Sulfaten und Ausfällung von Sulfiden gegeben wurden, lässt sich nicht ohne weiteres entscheiden.

Die Sulfidbestimmungen in Toneinlagerungen in anhydritführenden Salzgesteinen (Proben 180 bis 185) zeigen, dass auch hier beträchtliche Sulfidgehalte auftreten können.

Die Tiefseesedimente (Proben 187 bis 190 und 213) enthalten Schwefel vorwiegend als Sulfat. Das Porenvolumen dieser Proben bei der Entnahme aus dem Ozeanboden ist leider nicht bekannt. Wenn wir mit einem Gehalt von 50 Gewichtsprozent Meerwasser rechnen, müssen die bei 110°C getrockneten Proben 0,09% Sulfatschwefel enthalten, der von diesem Porenwasser herrührt. Die bestimmten Gehalte (0,063 bis 0,153%) liegen in dieser Grössenordnung. Eine beträchtliche Anreicherung des Sulfats in diesen Sedimenten findet demnach nicht statt. In den küstenfernen Tiefseesedimenten kommt der Schwefel—jedenfalls in geringen tieten im Sediment—als Sulfat vor. Der Sulfidschwefel in Probe (189), die aus dem Nordamerikanischen Becken, jedoch von einem Punkt etwa 180 km östlich der Insel Guadeloupe stammt, ist vermutlich durch die Nähe der Inselgruppe der Kleinen Antillen bedingt.

Während die untersuchten Sandsteine aus verschiedenen geologischen Formationen im Mittel niedrige Schwefelgehalte haben (um 0,02% S), vorwiegend als Sulfat, zeigen die Grauwacken wesentlich höhere Werte (um 0,13% S) mit einem starken Überwiegen des Sulfidanteils. Die Unterschiede zwischen den mittleren Schwefelgehalten dieser beiden Gesteinstypen sind wohl durch die verschiedenen Bildungsweisen verständlich. Während die untersuchten Sandsteine hauptsächlich aus Quarz bestehen, liegt bei den Grauwacken neben Eruptivgesteinsbruchstücken auch ein beträchtlicher Anteil wenig aufgearbeiteten Sedimentmaterials vor. Besonders deutlich wird das, wenn man die Schwefelwerte der von Mattiat (1960) näher untersuchten Proben (198 bis 200) betrachtet: Der Sulfatschwefelgehalt der grobkörnigen Probe (198) ist hier vielleicht an Quarze und Feldspäte gebunden; der Schwefelgehalt der feinkörnigen Probe (200) liegt dem Durchschnittsvert der Tonschiefer nahe.

In den untersuchten Karbonatgesteinen überwiegt der Sulfidschwefel, teilweise liegt hier auch Sulfat vor. Der Sulfatanteil kann in Kalken und Dolomiten aber auch überwiegen, besonders wohl bei Proben mit niedrigen Gesamtschwefelgehalten (204 bis 211).

In Kieselschiefer (Probe 175) und Kieselkalk (Probe 204) wurde wenig, in einem Feuerstein (Probe 215) kein Schwefel gefunden. Hoss (1957) fand bei der Analyse einer Reihe Kieselschiefergesteine ebenfalls durchweg niedrige Schwefelgehalte.

Tabelle 14. Mittlere Häufigkeit des Schwefels in Sedimentgesteinen (aus eigenen Analysen berechnet)

Gesteinsgruppe	Gesamt-S (%)	Sulfid-S (%)	Sulfat-S (%)	$\frac{\text{Sulfat-S}}{\text{Gesamt-S}} \times 100$
Mittel aus 67 Tonen und Tonschiefern (Proben 55 bis 59, 166 bis 179)	0,22	0,17	0,05	23
Mittel aus 59 Sandsteinen (Proben 8, 191 bis 196)	0,022	0,005	0,017	77
Mittel aus 20 Grauwacken (Proben 197 bis 200)	0,13	0,13	0,004	3
Mittel aus 102 Karbonatgesteinen (Proben 201 bis 212)	0,12	0,10	0,024	19
Mittel aus 12 rezenten Tiefseesedimenten (Proben 187, 189, 213)	0,13	0,001	0,13	99

Aus den Analysendaten der Tabelle 13 werden nun die mittleren Schwefelgehalte der wichtigsten Sedimentgesteinsgruppen berechnet. Dabei werden alle untersuchten Gesteine aus einer Gruppe gleichstark berücksichtigt, die Durchschnittsmischungen entsprechend der Anzahl der Proben, aus denen sie zusammengesetzt sind. Bei der geringen Anzahl der untersuchten Gesteine können diese Angaben nicht sehr genau ein, sie können aber als Anhaltspunkte dienen. Tabelle 14 zeigt die aus den eigenen Analysen berechneten Mittelwerte.

Zum Vergleich mit den aus den eigenen Analysen berechneten Durchschnittswerten der einzelnen Gesteinsgruppen werden nun einige Literaturdaten über die Häufigkeit des Schwefels in Sedimentgesteinen in den Tabellen 15 bis 19 zusammengestellt und diskutiert. Dabei handelt es sich teilweise um Schwefelbestimmungen in Durchschnittsmischungen (M) und teilweise um Bestimmungen in mehreren Einzelproben, aus denen entweder die Autoren Mittelwerte berechnet haben oder die Durchschnittswerte als arithmetisches Mittel aller aufgeführten Analysen neu berechnet werden (E). Bei vielen Analysen wurde der Schwefel nur als SO_3 oder nur als FeS_2 angegeben. Meistens handelt es sich dabei um das Ergebnis von Gesamtschwefelbestimmungen. Es ist aber nicht gesagt, dass wirklich der gesamte Schwefel immer in der angegebenen Form auftritt. Deshalb werden die Literaturangaben immer auf % Gesamtschwefel umgerechnet. Geht aus den betreffenden Arbeiten eindeutig hervor, dass Sulfid- und Sulfatschwefel in den einzelnen Proben nebeneinander bestimmt wurden, so wird aus diesen Werten der prozentuale Anteil des Sulfatschwefels berechnet und unter *Q* in den folgenden Tabellen 15 bis 19 aufgeführt.

Der Schwefelgehalt der Böden hängt natürlich vom Ausgangsgestein und den

Verwitterungsbedingungen ab. Die von CLARKE (1924) angegebenen Analysen von Durchschnittsmischungen amerikanischer Böden zeigen niedere Schwefelgehalte als die meisten Eruptiv- und Sedimentgesteine. Der Schwefel der verwitterten Gesteine wird demnach sicher zum grossen Teil zu Sulfat oxydiert und so durch die Flüsse ins Meer gelangen. Nach CONWAY (1942) beträgt der mittlere Gehalt der Flußwässer an gelöstem Sulfatschwefel 0,0006% S, der allerdings nur zu einem Teil aus der Verwitterung der Gesteine stammt, zum anderen Teil als "zyklisches Salz" aus dem Meer in die Niederschläge und dann in die Flüsse gelangt ist.

Dass auch Rückstände intensiver chemischer Festlandsverwitterung Schwefel enthalten, zeigen z.B. die Bauxitanalysen (164) und (165).

Tabelle 15. Angaben verschiedener Autoren über Schwefelgehalte in Verwitterungsbildungen

			% S	Q
CLARKE (1924)	466 Böden humider Gebiete der U.S. Südstaaten	(M)	0,02	
	313 Böden der ariden Gebiete von Californien, Washington und Montana	(M)	0,02	
GOLDSCHMIDT (1933)	78 norwegische Glaziallehme (0,07% Sulfid-S + 0,03% Sulfat-S)	(M)	0,10	30

Der Schwefelgehalt der von GOLDSCHMIDT (1933) analysierten norwegischen Lehme, Produkte einer vorwiegend mechanischen Verwitterung von Eruptivgesteinen, ist höher als der Durchschnittswert der Eruptiva. Es ist möglich, dass die Ausgangsgesteine hier teilweise erhöhte Schwefelgehalte haben, man muss aber auch damit rechnen, dass ein beträchtlicher Teil des Schwefels aus der Verwitterung sulfidischer Lagerstätten kommen kann oder dass diese Sedimente vielleicht das Sulfat, das mit den Niederschlägen zugeführt wird, teilweise absorbieren. (Das Regenwasser enthält, nach CONWAY (1942), im Mittel etwa 0,0001% S).

Eine ganze Reihe der in Tabelle 16 aufgeführten Durchschnittswerte bestätigen, dass das vorher berechnete Mittel für Tone und Tonschiefer mit 0,22% ungefähr richtig ist. Die Tabelle 16 zeigt aber zugleich die wichtigsten Probleme, die zur Ermittlung des wirklichen Durchschnittswertes gelöst werden müssen, nämlich (1) die Frage, mit welcher Häufigkeit salinare Bildungen den Tongesteinen eingelagert sind (Bei den Sandsteinen und Karbonatgesteinen tritt das gleiche Problem wieder auf); und (2) die Frage nach dem Anteil der stark bituminösen Tonschiefer und Schiefer.

Fast alle Proben aus den von URBAIN (1951) beschriebenen Profilen enthalten geringe Mengen Gips, darunter befindet sich eine Probe mit extrem hohem Gipsgehalt von etwa 42%. Berücksichtigt man diese Probe nicht bei der Mittelwertsbildung, so erhält man anstatt 0,99% S ($Q = 69$) nur 0,65% S ($Q = 55$). Das Auslassen dieser Probe ist berechtigt, wenn man z.B. nur Einzelproben mit weniger als 10% Gips oder Anhydrit zu den Tongesteinen zählt. Will man aber den mittleren Schwefelgehalt eines grösseren Sedimentkomplexes bestimmen, der zum überwiegenden Teil aus tonigen Komponenten besteht, dann muss man zweifellos z.B. Einschaltungen von Gips- oder Anhydritlagen in ein solches Gesteinspaket mitberücksichtigen.

Die Bedeutung der Inhomogenität grösserer Sedimentkomplexe für die geochemische Verteilung von Spurenelementen in den Sedimentgesteinen ist hier am Beispeil des Schwefels besonders auffällig demonstriert, wo in Form von Gips- und

Tabelle 16. Angaben verschiedener Autoren über Schwefelgehalte in tonigen Gesteinen

			% S	
Eckel (1904)	36 praekambrische Schiefer	(E)	0,20	
Clarke (1924)	51 paläozische Tonschiefer	(M)	0,23	
	27 mesozoische und känozoische Tonschiefer	(M)	0,31	
	6 Dachschiefer	(E)	0,25	
Minami (1935)	10 mesozoische japanische Tonschiefer	(M)	0,20	
Urbain (1951)	21 meist karbonatreiche französiche Tone aus zwei Profilen (darunter eine Probe mit 42% Gips) (0,31% Sulfid-S + 0,68% Sulfat-S)	(E)	0,99	69
	20 meist karbonatreiche französiche Tone aus zwei Profilen. (0,29% Sulfid-S + 0,36% Sulfat-S)	(E)	0,65	55
	18 praekambrische Schiefer	(E)	0,18	
	7 Tonschiefer	(E)	0,04	
Nanz (1953) Shaw (1956) Vinogradov und Ronov (1956)	252 Durchschnittsmischungen von insgesamt 6804 Tongesteinen der Russischen Tafel (Praekambrium bis Känozoikum) (Mittlerer Gehalt an org. C: ≈ 0,67% nach Ronov, 1958)	(M)	0,25	
	9 Durchschnittsmischungen von insgesamt 253 Tongesteinen der Russischen Tafel (Oberdevon, Famennien) (Mittlerer Gehalt an org. C: ≈ 0,44% nach Ronov, 1958)	(M)	2,64	
	28 Durchschnittsmischungen von insgesamt 730 Tongesteinen der Russischen Tafel (Perm) (Mittlerer Gehalt an org. C: ≈ 0,30% nach Ronov, 1958)	(M)	0,62	
	215 Durchschnittsmischungen von insgesamt 5821 Tongesteinen der Russischen Tafel (alle Formationen ausser Famennien und Perm)	(M)	0,12	
	17 marine Tonschiefer	(E)	0,55	62
Tourtelot (1957)	15 marine Tonschiefer	(E)	0,92	
Keith und Degens (1959) Ricke	Mittel aus Analysen von Einzelproben und Mischungen von insgesamt 67 Tonen und Tonschiefern (vgl. Tabelle 14)		0,22	24
Forsman und Hunt (1959)	9 Tonschiefer (Mittlerer Gehalt an org. C: 2,50%)	(E)	1,27	
Le Riche (1959)	29 Südenglische Lias-Tone (Mittlerer Gehalt an org. C: 3,64%)	(E)	2,72	
James (1954)	13 pyritische bituminöse Schiefer der Pyritlagerstätte des Iron River District (Michigan) (Mittlerer Gehalt an org. C: 7%)	(E)	19,8	

Anhydritzwischenlagen in Tonen, Kalken und Sandsteinen oft beträchtliche Mengen Schwefel angereichert sein können. In den meisten Fällen wohl weniger augenscheinlich, gibt es ähnliche Konzentrationen aber auch bei einer Reihe anderer Spurenelemente, etwa bei der Anreicherung zahlreicher Schwermetalle in der

Nähe organischer Substanz oder der lokalen Anhäufung von Strontium als Coelestin in Klüften und Hohlräumen in Kalken. Während hier zwar genetisch andere Verhältnisse vorliegen, ist ihre Auswirkung auf die Bestimmung der Spurenelemente in einem grösseren Gesteinskomplex doch die gleiche.

In der Arbeit von VINOGRADOV und RONOV (1956) sind die mittleren Schwefelgehalte der tonigen, sandigen und karbonatischen Sedimentgesteine der Russischen

Tabelle 17. Angaben verschiedener Autoren über Schwefelgehalte in Sandsteinen und Grauwacken

			% S	Q
CLARKE (1924)	253 Sandsteine	(M)	0,03	
	371 Sandsteine für Bauzwecke	(M)	0,04	
VINOGRADOV und RONOV (1956)	158 Durchschnittsmischungen von insgesamt 3709 Sandsteinen der Russischen Tafel (Praekambrium bis Känozoikum)	(M)	0,28	
	6 Durchschnittsmischungen von insgesamt 110 Sandsteinen der Russischen Tafel (Oberdevon, Famennien)	(M)	0,60	
	16 Durchschnittsmischungen von insgesamt 564 Sandsteinen der Russischen Tafel (Perm)	(M)	1,59	
	136 Durchschnittsmichungen von insgesamt 3035 Sandsteinen der Russischen Tafel (alle Formationen ausser Famennien und Perm)	(M)	0,11	
RICKE	Mittel aus Analysen von Einzelproben und Mischungen von insgesamt 59 Sandsteinen (vgl. Tabelle 14)		0,022	77
PETTIJOHN (1957)	9 Grauwacken	(E)	0,14	
HUCKENHOLZ (1959)	2 Grauwacken	(E)	0,20	
RICKE	Mittel aus Analysen von Einzelproben und Mischungen von insgesamt 20 Grauwacken (vgl. Tabelle 14)		0,13	3

Tafel aus den verschiedenen geologischen Formationen berechnet. Ein Vergleich dieser Schwefelgehalte mit den Angaben von LOTZE (1958) über die Salzbildung der geologischen Vergangenheit zeigt, dass im allgemeinen die Schwefelgehalte in den Formationen relativ hoch sind, in denen die Salzausscheidung in diesem Gebiet beträchtlich ist. Wahrscheinlich werden also die teilweise hohen Schwefelwerte in der Zusammenstellung von VINOGRADOV und RONOV auf beträchtliche Beimengungen von Gips und Anhydrit zurückzuführen sein. Besonders hoch sind die Schwefelgehalte in den Gesteinen der oberdevonischen Famennien-Stufe und des Perm. Führt man die Mittelwertsbildung für die tonigen Sedimente der Russischen Tafel in der von VINOGRADOV und RONOV angegebenen Weise—nach rein stratigraphischen Gesichtspunkten—aus, lässt dabei aber die hohen Werte des Famennien und Perm aus, so erhält man als Durchschnitt aus nun 5821 Einzelproben anstatt 0,25% nur 0,12% S. Da vermutlich bei diesen Gesteinen aber auch Salinarbildungen eine Rolle spielen, wird der mittlere Schwefelgehalt der "reinen" Tongesteine aus diesem Gebiet noch niedriger liegen.

Bei einigen Werten der Tabelle 16 ist der mittlere Gehalt an organischem Kohlenstoff angegeben. Auf die erhöhten Sulfidschwefelgehalte in kohlenstoffreichen Gesteinen wurde bereits hingewiesen. Die letzten Werte der Tabelle 16 zeigen, wie beträchtlich die Schwefelgehalte in bituminösen Schiefern sein können.

Der berechnete Durchschnittswert für Sandsteine aus Tabelle 14 stimmt gut mit den von Stokes analysierten Dürchschnittsmischungen (Clarke, 1924)

Tabelle 18. Angaben verschiedener Autoren über Schwefelgehalte in Karbonatgesteinen

			% S	Q
Clarke (1924)	345 Kalksteine (0,09% Sulfid-S + 0,02% Sulfat-S)	(M)	0,11	18
	498 Kalksteine für Bauzwecke (0,07% Sulfid-S + 0,03 + Sulfat-S)	(M)	0,10	30
Schucht (1935)	6 Kalksteine des unteren Muschelkalk (Göschwitz bei Jena)	(E)	0,09	
Stout (1941)	284 paläozoische Dolomite und Kalksteine von West Ohio (0,13% Sulfid-S + 0,05% Sulfat-S)	(E)	0,18	28
Urbain (1951)	11 gipshaltige französiche Mergel (0,45% Sulfid-S + 0,48% Sulfat-S)	(E)	0,93	52
Muir und Hardie (1956)	141 Schottische Kalksteine	(E)	0,23	
Vinogradov und Ronov (1956)	198 Durchschnittsmischungen von insgesamt 8847 Karbonatgesteinen der Russischen Tafel (Praekambrium bis Känozoikum)	(M)	1,65	
	31 Durchschnittsmischungen von insgesamt 1963 Karbonatgesteinen der Russichen Tafel (Oberdevon, Famennien)	(M)	3,48	
	21 Durchschnittsmischungen von insgesamt 988 Karbonatgesteinen der Russischen Tafel (Perm)	(M)	4,65	
	146 Durchschnittsmischungen von insgesamt 5896 Karbonatgesteinen der Russischen Tafel (alle Formationen ausser Famennien und Perm)	(M)	0,83	
Vinogradov und Ronov (1956) (aus Literaturdaten)	4268 Karbonatgesteine der Russischen Tafel (Praekambrium bis Känozoikum)		1,24	
Ricke	Mittel aus Analysen von Einzelproben und Durchschnittsmischungen von insgesamt 102 Karbonatgesteinen (vgl. Tabelle 14)		0,12	19

überein. Vinogradov und Ronov (1956) finden in russischen Sandsteinen wesentlich höhere Schwefelgehalte. Obwohl es durchaus möglich ist, dass Sandsteine mit so niedrigen Schwefelgehalten wie die amerikanischen und deutschen in Russland selten sind, sind die starken Differenzen wohl doch hauptsächlich auf die unterschiedliche Art der Probenahme zurückzuführen. Ebenso wie bei den Tongesteinen kann auch hier gezeigt werden, dass ausserordentlich hohe Schwefelgehalte besonders in den salzreichen Formationen bestimmt wurden, so dass auch hier die erhöhten Schwefelgehalte wahrscheinlich auf Gips- und Anhydriteinlagerungen zurückzuführen sind.

Schwefel wurde in Grauwacken nur selten bestimmt. Der aus neun von Pettijohn (1959) zusammengestellten Analysen berechnete Durchschnittswert stimmt gut mit dem neuberechneten überein und bestätigt, dass die Schwefelgehalte der Grauwacken im Mittel beträchtlich höher sind als die reinen Sandsteine.

Der berechnete Wert für die mittlere Häufigkeit des Schwefels in Karbonatgesteinen (0,12% S) ist ungefähr richtig, wenn man ihn auf relativ reine Kalke und Dolomite beschränkt und stimmt gut mit dem von Clarke (1924) angegebenen

Tabelle 19. Angaben verschiedener Autoren über Schwefelgehalte in rezenten Tiefseesedimenten

			% S	*Q*
Clarke (1924)	11 Tiefseeproben der Challenger Expedition	(E)	0,11	
	52 Proben landnahe abgelagerter Tone (Meerestiefen: 250 bis 3900 m)	(M)	0,13	
Edginton und Byers (1942)	28 Tiefseeproben des Nordatlantik aus 13 Lotkernen (Meerestiefen: 1280 bis 4900 m, mittlerer Chlorgehalt = 1,38%)	(E)	0,13	
Ricke	Mittel aus Analysen von Einzelproben und Durchschnittsmischungen von insgesamt 12 Tiefseesedimenten (vgl. Tabelle 14)		0,13	99
Correns (1937)	8 Blauschlickproben der Meteor Expedition (Meerestiefen: 2787 bis 5156 m) Sulfidschwefel:	(E)	0,06	
Oustromov und Shilov (1956)	68 Tiefseeproben landnaher Sedimente der Nordwestpazifik aus 10 Lotkernen (Meerestiefen: 4240 bis 6910 m, mittlerer Gehalt an org. C = 0,80% Sulfidschwefel:	(E)	0,02	

Mittelwert überein. Bildet man das arithmetische Mittel aus den von Stout (1941) und Muir und Hardie (1956) veröffentlichten Analysen, erhält man etwas höhere Werte.

Die Gehalte, die von Vinogradov und Ronov (1956) als Mittel für russische Karbonatgesteine angegeben werden, liegen jedoch, ebenso wie die Schwefelgehalte der von Urbain (1951) untersuchten gipshaltigen Mergel, eine Grössenordnung höher. Zur Erklärung dieser Differenz müssen hier beträchtliche Anhydrit- und Gipsgehalte in den russischen Gesteinen angenommen werden.

Der Vergleich der eigenen Analysenwerte mit den von Clarke (1924) zitierten Schwefelbestimmungen von Brazier in Proben der *Challenger*-Expedition, dem ebenfalls bei Clarke angegebenen Schwefelgehalt der von Steiger analysierten Durchschnittsmischung aus 53 "terrigeneous clays" und den Werten von Edgington und Byers (1942) zeigt, dass die Schwefelgehalte dieser Tiefseeablagerungen ziemlich einheitlich sind.

In zwei von Correns (1937) beschriebenen Tiefseeproben der *Meteor*-Expedition wurde von Brünger löslicher Sulfatschwefel zu 0,12 bzw. 0,17% S und Chlorid zu 0,73 bzw. 1,43% Cl bestimmt. Hieraus ergibt sich für S/Cl in diesen Proben 0,16 bzw. 0,12, während das Verhältnis S/Cl im Meerwasser im Mittel 0,042 beträgt.

Bramlette und Bradley (1942) wiesen auf das relativ hohe Verhältnis S/Cl in

den von Edgington und Byers chemisch untersuchten Sedimenten hin, das sich in den meisten dieser Proben etwa um den Faktor 2 vom Verhältnis S/Cl im Meerwasser unterscheidet. Sie fanden, dass das Sulfat der Proben, darunter 3 Fraktionen eines Globigerinenschlammes, durch Behandeln mit Wasser quantitativ ausgelaugt werden konnte und schlossen daraus, dass dieses nicht in Foraminiferenschalen eingebaut sei und die Sedimente lösliche Sulfate, vermutlich Gips, enthielten.

Die Untersuchungen von Behne (1953) haben gezeigt, dass Tonminerale durch Behandeln mit verdünnter Salzsäure Chlor aufnehmen können. Auch dieser

Tabelle 20. Schwefel in metamorphen Gesteinen

	Gesamt-S (%)	Sulfid-S (%)	Sulfat-S (%)	Q
(191) Durchschnitt von 10 deutschen Quarziten	0,0125	0,0030	0,0095	76
(217) Glimmerschiefer Ehrenfriedersdorf (Sachsen)	0,0260	0,0135	0,0125	48
(218) Amphibolit Byholme (Norwegen)	0,0210	0,0010	0,0200	95
(219) Amphibolit Minnesota	0,0160	0,0030	0,0130	81
(220) Orthogneis Muggenbrunn (Schwarzwald)	0,0155	0,0040	0,0115	74
(221) Paragneis Muggenbrunn (Schwarzwald)	0,203	0,201	(0,002)	1
(222) Eklogit Weissenstein (Fichtelgebirge)	0,0825	0,0810	(0,0015)	2

Effekt kann für die Abweichungen im Verhältnis löslicher Sulfatschwefel/lösliches Chlorid eine Rolle spielen.

Locher (1952) bestimmte lösliches Sulfat und Chlorid in 5 Tiefseeton-Proben der *Albatross*-Expedition. Auch hier ist das Verhältnis S/Cl mit 0,064 bis 0,090 höher als S/Cl in Meerwasser (0,042). Behne (1953) fand in Tiefseesedimenten höhere Chlorgehalte als Edgington und Byers, als Mittel von 8 Proben der *Albatross*-Expedition 2,1% Cl.

Die im Anschluss an Tabelle 13 durchgeführte Abschätzung zeigt, dass bei den in der vorliegenden Arbeit untersuchten Tiefseeproben der Faktor einer möglichen Sulfatanreicherung kaum den Wert 2 übersteigt.

Die von Pralow an Blauschlicken der *Meteor*-Expedition ausgeführten Sulfidschwefelbestimmungen (Correns, 1937) und die Sulfidanalysen an den Sedimenten aus einer landnahen Grabenzone des Nordwestpazifik von Oustromov und Shilov (1956) zeigen, dass auch in beträchtlichen Meerestiefen Sulfid auftreten kann. Der Küsteneinfluss wird durch den hohen Gehalt an organischem Kohlenstoff in diesen Proben deutlich.

Aus den in dieser Arbeit durchgeführten Sulfidbestimmungen an küstenferneren Tiefseeproben geht jedoch hervor, dass in den mehr verbreiteten langsam sedimentierten Tiefseeablagerungen Schwefel im allgemeinen nur als Sulfat vorkommt.

Schwefelgehalte metamorpher Gesteine

In der Tabelle 20 sind die Ergebnisse der Schwefelbestimmungen in einigen metamorphen Gesteinen zusammengestellt.
Auf Grund dieser wenigen Bestimmungen kann man natürlich keine allgemeinen

Aussagen machen. Die Analysen der Proben (191) und (217 bis 222) zeigen jedoch, dass auch die Schwefelgehalte metamorpher Gesteine recht unterschiedlich sein können und dass neben Sulfidschwefel auch hier Sulfatschwefel von Bedeutung ist.

Zum Schluss sind noch die Schwefelbestimmungen in den Zersatzprodukten zweier Gesteine aufgeführt, die von SIGVALDASON (1958) und BOLTER näher untersucht wurden (Proben 223 bis 228). In beiden Fällen wird die Umwandlung der Ausgangsgesteine durch hydrothermale Lösungen angenommen.

	Gesamt-S (%)	Sulfid-S (%)	Sulfat-S (%)	Q
(125) Liparit Moskardshnjukar (Island) Originalmaterial SIGVALDASON (1958) Probe M1	0,0155	0,0025	0,0130	84
(232) Zersetzter Liparit Moskardshnjukar (Island) Originalmaterial SIGVALDASON (1958) Probe M6	0,0790	0,0345	0,0445	56
(224) Zersetzter Liparit Moskardshnjukar (Island) Originalmaterial SIGVALDASON (1958) Probe M7	0,0315	<0,0010	0,0315	100
(152 bis 154) Trachydoleritischer Basalt Backenberg	0,0450	0,0055	0,0395	88
(225) Schwach zersetzter Basalt Backenberg Originalmaterial BOLTER Probe 4	0,0035	<0,0010	0,0035	100
(226) Stark zersetzter Basalt Backenberg Originalmaterial BOLTER Probe 1	0,0070	<0,0010	0,0070	100
(227) Stärker zersetzter Basalt Backenberg Originalmaterial BOLTER Probe 2	0,0080	<0,0010	0,0080	100
(228) Sehr stark zersetzter Basalt Backenberg Originalmaterial BOLTER Probe 10	<0,0020	<0,0010	<0,0020	

Die Analysen zeigen, dass das Verhalten des Schwefels hierbei nicht einheitlich zu sein braucht, bei dem isländischen Liparit ist der Schwefel in den Umwandlungsprodukten angereichert, im Falle des Basalts vom Backenberg wird der Schwefel offenbar weggeführt.

Der Mittlere Schwefelgehalt der oberen Lithosphäre Bilanz und Kreislauf

Aus den abgeschätzten Durchschnittsgehalten der einzelnen Eruptivgesteinsgruppen aus Tabelle 8 ergibt sich als mittlerer Schwefelgehalt der Eruptivgesteine der oberen Lithosphäre etwa der der Granite, Granodiorite und Quarzdiorite, da sich die mittleren Gehalte der übrigen wichtigen Gesteinsgruppen nicht wesentlich von diesen unterscheiden. Unter Berücksichtigung der diskutierten Fehlerquellen kann man 0,03% S als gesicherten Mittelwert betrachten. Die an magmatische Gesteine geknüpften Sulfidlagerstätten wurden hierbei nicht berücksichtigt. Obwohl die bekannten Erzlagerstätten lokal beträchtliche Sulfidanreicherungen darstellen, ist ihr Anteil an den Eruptivgesteinen mengenmässig, jedenfalls in der zugänglichen Kruste, doch sehr gering, so daß sich der angegebene Durchschnittsgehalt der Eruptivgesteine durch die Sulfidlagerstätten wohl nicht wesentlich erhöhen wird.

Die Berechnung des mittleren Schwefelgehaltes der Sedimentgesteine ist wesentlich unsicherer, besonders wegen der Schwierigkeit, den Anteil des an Evaporite gebundenen Sulfatschwefels zu bestimmen.

Zunächst wird der mittlere Gehalt der Sedimente ohne den Evaporitanteil aus den in Tabelle 14 zusammengestellten Durchschnittswerten der Tone und Tonschiefer, der Sandsteine und der Kalke und Dolomite unter Verwendung der von Correns (1948) bestätigten Anteilabschätzungen von Goldschmidt (siehe v. Engelhardt, 1936) berechnet.

Tabelle 21. Berechnung des mittleren Schwefelgehalts der Sedimentgesteine. (ohne Tiefseesedimente und Evaporite)

	Anteil (%)	S (%)	Anteilmässige Häufigkeit
Tone und Tonschiefer	79,6	0,22	0,175
Sandsteine	11,9	0,022	0,004
Kalke und Dolomite	8,5	0,12	0,010
Durchschnitt der Sedimente:			0,19% S

Dieser Wert stimmt gut mit dem von Clarke (1924) angegeben Mittel (0,22%) überein. Der mittlere Schwefelgehalt der untersuchten Tiefseesedimente (0,13% S) liegt in derselben Grössenordnung, so dass dieser Sedimentdurchschnitt auch bei Berücksichtigung der Tiefseesedimente ungefähr erhalten bleiben wird.

Führt man eine entsprechende Rechnung mit den von Vinogradov und Ronov (1956) angegebenen Durchschnittswerten der einzelnen Gesteinsgruppen für die Gesteine der Russischen Tafel, jedoch mit den von Goldschmidt berechneten Anteilen dieser Gesteine an den Gesamtsedimenten durch, so erhält man als Mittel $0{,}35_5$%.

Nehmen wir an, die Differenz dieser Werte sei auf Einlagerungen von Anhydrit und Gips in die entsprechenden russischen Gesteine zurückzuführen, und diese Gesteine seien für die Sedimente der ganzen Erde charakteristisch, so beträgt der Schwefelgehalt dieser Einlagerungen an den Gesamtsedimenten $0{,}16_5$%, also etwa ebenso viel wie die der häufigsten Sedimentgesteine. Daneben treten aber auch mächtige Anhydrit- und zum Teil auch Gipsbildungen auf, die sicher in den russischen Durchschnittsmischungen nicht enthalten sind. Der Anteil des Evaporitschwefels an den Gesamtsedimenten würde also noch beträchtlich grösser als $0{,}16_5$% sein. Nun sind Salinarbildungen in Russland weit verbreitet und der Anteil des Evaporitsulfats in diesem Gebiet an den Sedimentgesteinen ist wahrscheinlich grösser als in den Sedimenten der ganzen Erde. Ein Gehalt von 0,2% S Evaporitschwefel an den Gesamtsedimenten wird deshalb vielleicht den wirklichen Verhältnissen nahe kommen.

Ault und Kulp (1959) führten eine Abschätzung des gesamten Evaporitschwefels unter Zugrundelegung der von Krumbein (1951) zusammengestellten Sulfatlagerstätten Nordamerikas durch und fanden 1×10^{21} g Evaporitschwefel mit einem Unsicherheitsfaktor 3 (nach Sloss, siehe Ault und Kulp). Dies entspricht, wenn man die durchschnittliche Sedimentbedeckung der Erdoberfläche

nach GOLDSCHMIDT mit 170 kg/cm² animmt, einem Anteil von 0,12% (bis 0,36%) an den Gesamtsedimenten. Diese Abschätzung bestätigt, dass der angenommene Wert 0,2% ungefähr richtig ist.

An einem Beispiel soll gezeigt werden, welche Bedeutung die Anhydritbildungen in relativ kleinen Arealen haben können: MACFADYEN (1933) beschreibt mitteleozäne Anhydrite aus Britisch-Somaliland und gibt als mittlere Mächtigkeit 300 bis 350 m und ihr Volumen mit über 21 000 km³ an. Der Anteil des Schwefels dieser Anhydrite, die in einem Horizont eines Areals von nur 65 000 km² angereichert sind, an den Sedimentgesteinen der ganzen Erde beträgt etwa:

$$\frac{\text{Volumen Anh. (cm}^3) \times \text{Dichte Anh. (g/cm}^3) \times \%\text{ S im Anhydrit}/100}{\text{Masse der Gesamtsedimente/cm}^2\text{ (g/cm}^2) \times \text{Erdoberfläche (cm}^2)} \times 100$$

$$= \frac{2{,}1 \times 10^{19} \times 3 \times 0{,}235}{170 \times 10^3 \times 5{,}1 \times 10^{18}} \times 100 = 0{,}0017\%\text{ S}$$

mit anderen Worten etwa 1/115 des angenommenen Evaporitschwefels.

Sedimentäre Sulfidlagerstätten—ebenso wie magmatisch entstandene—sind in diesem Ausmasse nicht bekannt. Eine der grössten bekannten Sulfidlagerstätten

Tabelle 22. Berechnung des Anteils Schwefel und Chlor in Meerwasser und Sedimentgesteinen aus der Verwitterung der Eruptivgesteine

	Masse n. GOLDSCHMIDT (kg/cm²)	% S	S (kg/cm²)	% Cl	Cl (kg/cm²)	H_2O (kg/cm²)
Meerwasser	279	0,09	0,25	1,93	5,4	
ohne Evaporite		0,19	0,32			
Sedimentgesteine	170			0,0154	0,026	
Evaporitanteil		0,2	0,34			
			0,91		5,43	280
Verwitterte Eruptivgesteine	160	0,03	0,048	0,0150	0,024	2
(Meerwasser + Sedimentgesteine) — verwitterte Eruptivgesteine			0,86		5,41	278

ist die des Iron River District, Michigan (vgl. Schluss der Tabelle 16), die JAMES (1954) als rein sedimentär ansieht und deren Schwefelvorrat er mit 25×10^9t angibt. Dies ist jedoch nur 1/600 der Schwefelmenge, die an den vorher erwähnten Anhydrit aus Somaliland gebunden ist. Die sedimentären Sulfidlagerstätten werden also am Schwefelgehalt der Gesamtsedimente quantitativ nur sehr untergeordnet beteiligt sein.

Wie schon durch die hohen Schwefelgehalte der Sedimentgesteine deutlich geworden ist, spielt das Meer im Kreislauf des Schwefels eine sehr wichtige Rolle. Der mittlere Schwefelgehalt des jetzigen Meerwassers beträgt nach KALLE (1943) etwa 0,09% S.

Um zu zeigen, wie gross der Anteil des aus der Verwitterung der Eruptivgesteine stammenden Schwefels an dem Schwefelgehalt der Verwitterungsprodukte ist, sind in der Tabelle 22 die gewonnenen Werte zusammengestellt und unter Verwendung der Angaben von GOLDSCHMIDT (1933) auf kg/cm² Erdoberfläche umgerechnet. Zum Vergleich sind die entsprechenden Werte für Chlor nach BEHNE (1953) und die Werte für Wasser nach GOLDSCHMIDT (1954) mit aufgeführt.

Etwa 0,91 kg/cm² Schwefel im Meerwasser und den Sedimentgesteinen stehen nur etwa 0,048 kg/cm², das ist ungefähr 1/20 dieses Betrages, in den verwitterten Eruptivgesteinen gegenüber. Die Hauptmenge des Schwefels im Meer und in den Sedimenten stammt also nicht aus der Verwitterung der Eruptivgesteine, sondern aus Entgasungen des Erdmantels und der Erdkruste. Rubey (1951) hat besonders darauf hingewiesen, dass neben den vulkanischen Exhalationen auch heisse Quellen bei der Entgasung der Magmen eine grosse Rolle spielen und sieht diese als die wichtigsten Förderquellen der leichtflüchtigen Bestandteile an.

Die Tabelle 22 zeigt, dass sich der grösste Teil des Schwefels aus den Entgasungen nicht im Meerwasser befindet, sondern an die Sedimente gebunden ist.

Nimmt man mit Rubey (1951) an, dass die Wasser-, Schwefel- und Chlormengen der Primitiven Atmosphäre (und Hydrosphäre) im Verhältnis zu den im Laufe der geologischen Geschichte von der Erde ausgestossenen Wasser-, Schwefel- und Chlormengen gering waren, dann kann man das Verhältnis zwischen Schwefel und Chlor aus diesen Entgasungen berechnen.

$$(S/Cl)_{Entgasung} = \frac{(S_{Meer} + S_{Sedimente}) - S_{verw.\ Eruptivgest}}{(Cl_{Meer} + Cl_{Sedimente}) - Cl_{verw.\ Eruptivgest}} = \frac{0{,}86}{5{,}41} = 0{,}16 = 1{:}6{,}3$$

Entsprechend erhält man für das Verhältnis zwischen Chlor und Wasser:

$$(Cl/H_2O)_{Entgasung} = \frac{5{,}41}{278} = 0{,}020$$

Das Verhältnis S/Cl ist in den in der Natur beobachteten Entgasungsprodukten sehr variabel. Es hängt sicher von den Gehalten der Stammagmen und von den Bedingungen, unter denen die Gase bis zur Erdoberfläche aufgestiegen sind, ab. Zies (1929) schätzt den Anteil der Entgasungen des Vulkans Katmai (Alaska) im Jahr 1919 an S und Cl auf 0,3 × 10^6 t H_2S und 1,25 × 10^6 t HCl, das entspricht einem Verhältnis S/Cl = 1:4,3. Rubey (1951) berechnetejdie Durchschnittsgehalte an Schwefel und Chlor aus 23 Gasproben aus Fumarolen der Katmai-Gegend (nach Allen und Zies, 1923) und heisser Quellen aus Californien und Wyoming (nach Allen und Day, 1927) zu 0,3% S und 0,12% Cl. Das Verhältnis S/Cl ist hier 1:4. Ellis (1957) gibt als mittleren Gehalt von 4 Fumarolen aus White Island (Neuseeland) 0,16% H_2S und 0,91% HCl an, hier ist das Verhältnis S/Cl = 1:5,9. Die beobachteten Verhältnisse stimmen bei diesen Beispielen wenigstens in der Grössenordnung mit den berechneten überein. Es gibt jedoch auch zahlreiche Fälle, in denen ganz andere Verhältnisse auftreten. So hat ebenfalls Rubey (1951) die Ergebnisse von 26 Analysen Shepherds (1938) von Gasen der Hawaiischen Vulkane Kilaüea und Mauna Loa in Gewichtsprozente umgerechnet und erhält 12,6% S und nur 0,1 % Cl, das Verhältnis ist hier 1:0,008.

Zum Schluss sei noch eine rohe Überschlagsrechnung durchgeführt, um zu zeigen, dass der Anteil der Schwefelverbindungen an der magmatischen Gasphase im allgemeinen verhältnismässig gering ist.

Nimmt man an:

(1) Die Mengen H_2O, Cl und S, die nicht aus der Verwitterung stammen und sich heute im Meer und in den Sedimentgesteinen befinden, stammen zum überwiegenden Teil aus Entgasungen und zwar aus den gleichen Entgasungen, und

(2) die entgasten Magmen hätten ursprünglich 4% H_2O enthalten und lägen jetzt als Eruptivgesteine mit 1% H_2O vor, so erhält man aus den Verhältnissen

$$(Cl/H_2O)_{Entgasung} = 0{,}020 \text{ und } (S/Cl)_{Entgasung} = 0{,}16:$$

$$H_2O_{(entgast)} = 4\% - 1\% = 3\%$$

$$Cl_{(entgast)} = 0{,}020 \times 3 = 0{,}06\%$$

$$S_{(entgast)} = 0{,}16 \times 0{,}06 = 0{,}01\%$$

Der Gehalt dieses "Urmagmas" an H_2O, Cl und S wäre also:

$$H_2O_{(\text{"Urmagma"})} = H_2O_{(Gestein)} + H_2O_{(entgast)} = 1 + 3 = 4\%$$

$$Cl_{(\text{"Urmagma"})} = Cl_{(Gestein)} + C_{(entgast)} = 0{,}015 + 0{,}06 = 0{,}075\%$$

$$S_{(\text{"Urmagma"})} = S_{(Gestein)} + S_{(entgast)} = 0{,}03 + 0{,}01 = 0{,}04\%$$

Während dieses hypothetische Magma viel Chlor und Wasser verlor, blieb der Schwefel bei der Kristallisation zum grossen Teil im Gestein.

Obwohl bei der oben ausgeführten Berechnung eine Reihe von Hilfsannahmen gemacht wurden, so zeigt diese wohl doch, dass trotz der grossen Schwefelmengen, die wir heute im Meer und in den Sedimenten vorfinden, der Schwefel bei der Kristallisation von Magmen im allgemeinen zum grössten Teil im Gestein bleibt, es sei denn, die ursprünglichen Schwefelgehalte seien erheblich höher gewesen und der Schwefel sei—vermutlich als entmischte Sulfidschmelze—in grössere Tiefen abgesunken.

Der Kreislauf des Schwefels ist—in grossen Zügen gesehen—folgender:

Das Element Schwefel kommt in den Eruptivgesteinen als Sulfid und als Sulfat vor. Der mittlere Gehalt der Eruptivgesteine beträgt etwa 0,03% S (davon 1/3 als Sulfat).

Bei der Verwitterung dieser Gesteine wird das Sulfid zu Sulfat oxydiert und zum grossen Teil durch die Flüsse ins Meer transportiert.

Auch aus der Verwitterung magmatischer Sulfidlagerstätten gelangt Schwefel ins Meer. Die Schwefelmenge in den bekannten Sulfidlagerstätten magmatischen Ursprungs ist jedoch gegenüber der in den Eruptivgesteinen gering.

Der weitaus grösste Teil des Schwefels, der sich jetzt im Meer und in den Sedimenten befindet, stammt aus Entgasungen der Magmen und wurde in Form vulkanischer Exhalationen—vorwiegend als SO_2 und H_2S—und durch heise Quellen an die Erdoberfläche befördert. Dieser Schwefel gelangt letzten Endes zum grossen Teil als Sulfat ins Meer.

Bei der Eindunstung abgeschlossener Meeresbecken kommt es zur Sulfatausscheidung. Ein grosser Teil des Schwefels befindet sich in den hieraus entstandenen Anhydritgesteinen und Anhydrit- und Gipsschichten, die anderen Sedimenten, besonders den Karbonatgesteinen, eingelagert sind.

In den häufigeren Flachseesedimenten kommt der Schwefel als Sulfid und Sulfat vor, am höchsten sind die Gehalte hier in den Tonen und Tonschiefern. Die Sulfide stammen dabei teilweise aus dem—vorwiegend bakteriellen—Abbau organischer Substanzen (in erster Linie der Proteine), zum grössten Teil sind sie aber

wohl durch die bakterielle Reduktion von Sulfat unter anaeroben Bedingungen entstanden. Ein Teil des Schwefels gelangt in die Tiefseesedimente, in denen er vorwiegend als Sulfat vorliegt.

Zusammenfassung

Es werden zwei chemische Methoden zur Bestimmung kleiner Mengen Gesamtschwefel und Sulfidschwefel in silikatischen Mineralen und Gesteinen beschrieben. Den Sulfatschwefel erhält man im allgemeinen als Differenz aus Gesamt- und Sulfidschwefel. Man kann so Schwefelgehalte bis herunter zu 0,002% bestimmen. Der mittlere Fehler liegt für Gehalte unter 0,02% bei $\pm$0,001%, für Gehalte zwischen 0,02 und 0,1% bei $\pm$0,0015%.

96 Mineral- und 132 Gesteinsproben wurden analysiert, in fast allen wurde Gesamt-, Sulfid- und Sulfatschwefel bestimmt.

Die Mineralanalysen zeigen, dass Sulfatschwefel in vielen gesteinsbildenden Mineralen in geringen Mengen vorhanden ist. In Quarzen wurde bis zu 0,0095%, in Feldspäten bis zu 0,022%, in Muskoviten bis zu 0,013%, in Pyroxenen bis zu 0,007% und in verschiedenen Inselsilikaten bis zu 0,014% Sulfatschwefel gefunden.

Der mittlere Gesamtschwefelgehalt der wichtigsten Eruptivgesteinsfamilien liegt um 0,03% S, nur die Alkaligesteine haben meist höhere Gehalte. Mit Ausnahme der gabbroiden Gesteine, bei denen der Sulfatanteil, wenn überhaupt vorhanden, sehr gering ist, kommt der Schwefel in den Eruptivgesteinen als Sulfid und als Sulfat vor. Die Tiefengesteine enthalten im Mittel mehr Sulfidschwefel und weniger Sulfatschwefel als ihre Ergussgesteinsäquivalente. Die sauren Gesteine enthalten im Mittel weniger Sulfidschwefel als die basischen Gesteine. Der prozentuale Anteil des Sulfatschwefels am Gesamtschwefel ist bei den sauren Gesteinen im Mittel grösser als bei den basischen Gesteinen. Für drei Granite und einen Basalt konnte gezeigt werden, dass hier die Feldspäte die Hauptträger des Sulfatschwefels sind.

Verschiedene Möglichkeiten für die Art des Vorkommens von Sulfatschwefel in Eruptivgesteinen werden diskutiert. Lösungsversuche machen es wahrscheinlich, dass Sulfat in Silikatmineralen nicht nur in Flüssigkeitseinschlüssen vorliegt, sondern auch ein Ersatz von SiO_4 durch SO_4 im Silikatgitter stattfinden kann.

In den Sedimentgesteinen kommt das Element Schwefel hauptsächlich als Sulfid und als Sulfat vor; vorwiegend als Sulfid in Tonen und Tonschiefern (Mittel: 0,22% S), in Grauwacken (Mittel: 0,13% S) und in Karbonatgesteinen (Mittel: 0,12% S), vorwiegend als Sulfat in Sandsteinen (Mittel: 0,022% S) und in landfernen Tiefseesedimenten (Mittel: 0, 13% S).

Auch in metamorphen Gesteinen wurde Sulfid- und Sulfatschwefel gefunden.

Der Schwefel, der sich heute—etwa zu gleichen Teilen—im Meer, in den Evaporiten und in den häufigeren Sedimentgesteinen befindet, stammt zum grossen Teil aus Entgasungen der Magmen.

Anerkennungen—Für die Überlassung des Themas, das Interesse am Fortgang dieser Arbeit und für zahlreiche wertvolle Anregungen danke ich meinem hochverehrten Lehrer, Herrn Professor Dr. C. W. Correns, sehr. Allen Angehörigen der Mineralogischen Anstalten danke ich für

ihre Unterstützung; besonders danke ich Fräulein Dr. P. Schneiderhöhn, Herrn Professor Dr. J. Zemann, Herrn Dozenten Dr. K. H. Wedepohl für viele gute Ratschläge, sowie Herrn Dr. M. Ziegler vom Anorganisch-Chemischen Institut.

Literatur

Allen E. T. und Day A. L. (1927) Hot springs of the Yellowstone National Park. *Publ. Carneg. Inst.* 466.

Allen E. T. und Johnston J. (1910) Die genaue Bestimmung von Schwefel in Pyrit und Markasit. *Z. anorg. Chem.* **69,** 102–121.

Allen E. T. und Zies E. G. (1923) A chemical study of the fumaroles of the Katmai Region. *Nat. Geograph Sc. Contr. Tech. Papers* 2

American Petroleum Institute (API) (1951) Preliminary Reports Reference, Research Project 49, Columbia Universität, New York.

Ames L. L. (1958) Chemical analyses of fluid inclusions in a group of New Mexico minerals. *Econ. Geol.* **53,** 473–480.

Ault W. U. und Kulp J. L. (1959) Isotopic geochemistry of sulphur. *Geochim. et Cosmochim. Acta* **16,** 201–235.

Behne W. (1953) Untersuchungen zur Geochemie des Chlor und Brom. *Geochim. et Cosmochim. Acta* **3,** 186–214.

Belov N. V., Belova E. N., Andrianova N. H. und Smirnova P. F. (1951) Determination of the parameters in the olivine (forsterite) structure with the harmonic three-dimensional synthesis. *Dokl. Akad. Nauk. SSSR* **81,** 399–402.

Bramlette M. N. und Bradley W. H. (1942) Geology and biology of North Atlantic deep-sea cores between Newfoundland and Ireland. Lithologic and geologic interpretations. *U.S. Geol. Survey Prof. Paper* 196, 1–32.

Brauns R. (1917) Über den Apatit aus dem Laacher Seegebiet. Sulfatapatit Carbonatapatit. *Neues Jahrbuch Min. Geol. Pal. Beil.* **41,** 60–92.

Broderick T. M. (1935) Diferentiation in lavas of the Michigan Keweenawan. *Bull. Geol. Soc. Amer.* **46,** 503–558.

Chao S. H., Hargreaves A. und Taylor W. H. (1940) The structure of orthoclase. *Miner. Mag.* **25,** 498–512.

Clarke R. W. (1924) The data of geochemistry. *Bull. U.S. Geol. Surv.* 770.

Clarke R. W. und Washington H. S. (1924) The composition of the earth's crust. *U.S. Geol. Survey Prof. Paper* 127.

Conway E. J. (1942) Mean geochemical data in relation to oceanic evolution. *Proc. R. Irish. Acad.* **48,** 119–159.

Correns C. W. (1937) Die Sedimente des Äquatorialen Atlantischen Ozeans. Deutsche Atlantische Expedition *Meteor* III, 3. Walter de Gruyter, Berlin und Leipzig.

Correns C. W. (1948) Die geochemische Bilanz. *Naturwiss.* **1,** 7–12.

Degenhardt H. (1957) Untersuchung zur geochemischen Verteilung des Zirkoniums in der Lithosphäre. *Geochim. et Cosmochim. Acta* **11,** 279–309.

Doelter C. (1917) *Handbuch der Mineralchemie.* Theodor Steinkopff, Dresden und Leipzig.

Dreizler I. (1960) Petrographische Untersuchungen der westlichen Kontaktzone des Okergranits (Harz). Vorgesehen für *Bei tr. Min. Pet.*

Eckel (1904) On American shales and roofing slates. *J. Geol.* **12,** 25–29.

Edgington G. und Byers H. G. (1942) Geology und Biology of North Atlantic deep-sea cores between Newfoundland and Ireland. Selenium content and chemical analysis. *U.S. Geol. Survey Prof. Paper* 196, 151–155.

Ellis A. J. (1957) Chemical equilibrium in magmatic gases. *Amer. Sci.* **255,** 416–431.

Engelhardt W. von (1936) Geochemie des Bariums *Chem. Erde* **10,** 187–246.

Ernst T. (1936) Der Melilithbasalt des Westberges bei Hofgeismar, nördlich von Kassel, ein Assimilationsprodukt ultrabasischer Gesteine. *Chem. Erde* **10,** 631–666.

Faber H. (1941) On the salt-solutions in microscopic cavities in granites. *Danm. Geol. Unders.* 2. Raek. **67,** 45–89.

Forsman J. P. und Hunt J. M. (1958) Insoluble organic matter (kerogen) in sedimentary rocks. *Geochim. et Cosmochim. Acta* **15,** 170–182.

Frey H. (1952) Titration von Sulfat bis zur maximalen Trübe. Semimikrobestimmung von Gesamtschwefel in vulkanisierten Gummimischungen. *Analyt. Chim. Acta* **6,** 28–30.

Fröhlich F. (1960) Die geochemische Verteilung von Chrom in der Erdkruste. Vorgesehen für *Geochim. et Cosmochim. Acta.*

Gay-Lussac M. (1828) Essai des potasses des commerce. *Ann. Chim. Phys.* **39,** 337–368.

Goldschmidt V. M. (1933) Grundlagen der quantitativen Geochemie. *Fortsch. Min. Krist. Pet.* **17,** 112–156.

Goldschmidt V. M. (1954) *Geochemistry.* Oxford University Press.

Hoss H. (1957) Untersuchungen über die Petrographie kulmischer Kieselschiefer. *Beitr. Min. Pet.* **6,** 59–88.

Huckenholz H. G. (1959) Sedimentpetrographische Untersuchungen an Gesteinen der Tanner Grauwacke. *Beitr. Min. Petr.* **6,** 261–298.

James H. L. (1954) Sedimentary facies of iron-formation. *Econ. Geol.* **49,** 235–293.

Jander G. und Wendt H. (1954) *Lehrbuch der analytischen und präparativen anorganischen Chemie* (2 Auflage). S. Hirzel Verlag, Leipzig.

Kalle K. (1943) *Der Stoffhaushalt des Meeres.* Becker und Erler, Leipzig.

Keith M. L. und Degens E. T. (1959) Geochemical indicators of marine and fresh water shales. In Abelson P. H. (1959) *Researches of Geochemistry* pp. 38–61. John Wiley, New York and London.

Kind A. (1939) Der magmatische Apatit. *Chem. Erde* **12,** 50–81.

Köster H. (1956) Beitrag zur Kenntnis indischer Laterite. *Heidelberg Beitr. Min. Pet.* **5,** 23–64.

Krumbein W.C. (1951) Occurrence and lithologic associations of evaporites in the United States. *J. Sed. Petrology* **21,** 63–81.

Kuroda K. und Sandell E. B. (1953) Chlorine in igneous rocks. *Bull. Geol. Soc. Amer.* **64,** 879–896.

Le Riche H. H. (1959) Trace elements in the Lower Lias of Southern England. *Geochim. et Cosmochim. Acta* **16,** 101–122.

Lippmann F. (1952) Mineralogische Untersuchungen an einigen niederhessischen Tertiärtonen. (unter besonderer Berücksichtigung der Differentialthermoanalyse) *Heidelberg Beitr. Min. Pet.* **3,** 219–252.

Locher F. W. (1952) Sedimentpetrographische Untersuchungen zweier Lotkerne der Albatross-Expedition. *Heidelberg Beitr. Min. Pet.* **3,** 193–218.

Lotze F. (1957) *Steinsalz und Kalisalze* Bd. I. Gebruder Bornträger, Berlin.

MacFadyen (1933) *Geology of British Somaliland* Bd. I.

McConell D. (1937) The substitution of SiO_4- and SO_4-groups for PO_4-groups in the Apatite structure; Ellestadite, the end-member. *Amer. Min.* **22,** 977-986.

Marinelli A. (1949) Sulla presenza del radicale solforico in alcuni neosilicati. *R.C. Accad. Naz. Lincli.* (*Cl. Sci. Fis. Mat. Nat.*) Ser. 8 **6,** 487–491.

Mason B. (1958) *Principles of Geochemistry.* John Wiley, New York and London.

Mattiat B. (1960) Beitrag zu Petrographie der Kulmgrauwacke. Vorgesehen für *Beitr. Min. Pet.*

Minami E. (1935) Selengehalte von europäischen und japanischen Tonschiefern. *Nachr. Ges. Wiss. Göttingen, Math. Nat. Kl.* 1, **12,** 143–145.

Muir A. und Hardie H. G. M. (1956) The Limestones of Scotland. Chemical Analyses and Petrography. *Memoirs of the Geological Survey. Special reports on the mineral resources of Great Britain No.* 37.

Nanz R. H. (1933) Chemical composition of pre-cambrian slates with notes on the geochemical evolution of lutites. *J. Geol.* **61,** 51–64.

Newhouse W. H. (1936) Opaque oxides and sulphides in common igneous rocks. *Bull. Geol. Soc. Amer.* **47,** 1–52.

Niemann H. (1960) Untersuchungen am Grauen Salzton der Grube "Königshall-Hindenburg", Reyershausen bei Göttingen. Vorgesehen für *Beitr. Min. Pet.*

Nockolds S. R. (1954) Average chemical composition of some igneous rocks. *Bull. Geol. Soc. Amer.* **65,** 1007–1032.

Noll W. (1934) Geochemie des Strontium. *Chem. Erde* **8,** 507–600.
Oustromov E. A. und Shilov V. V. (1956) Distribution of sulphurous iron and hydrogen sulphide in sediments of deepwater depressions of the northwestern part of the Pacific Ocean. *Geochimija* **7,** 25–38.
Pettijohn F. J. (1957) *Sedimentary Rocks* (2 Auflage). Harper, New York.
Pralow W. (1938) Mikroskopische und chemische untersuchungen einiger Proben des estländischen Tons. *Chem. Erde* **11,** 480–497.
Proske O. und Blumenthal H. (1949) *Analyse der Metalle* Bd. I. *Schiedsverfahren.* S. 428. Berlin, Göttingen und Heidelberg.
Ramdohr P. (1940) Die Erzminerale in gewöhnlichen magmatischen Gesteinen. *Abh. preuss. Akad. Wiss. Berlin* **2,** 1–43.
Rankama K. und Sahama T. G. (1950) *Geochemistry.* Chicago University Press.
Ringbom A. (1941) Über photoelektrische Fällungstitrationen. *Z. Anal. Chem.* **122,** 263–279.
Roedder E. (1958) Technique for the extraction and partial chemical analysis of fluid-filled inclusions from minerals. *Econ. Geol.* **53,** 235–269.
Ronov A. B. (1958) Organic carbon in sedimentary rocks (in relation to the presence of petroleum). *Geochimija* **5,** 510–536.
Rubey W. W. (1951) Geologic history of sea water. *Bull. Geol. Soc. Amer.* **62,** 1111–1148.
Schlecht W. G. und Stevens R. E. (1951) A cooperative investigation of precision and accuracy in chemical, spectrochemical and modal analysis of silicate rocks—II. Results of chemical analysis of samples of granite and diabase. *Bull. U.S. Geol. Surv.* **980,** 7–24.
Schucht F. (1935) *Die Muschelkalkböden Mitteldeutschlands und ihre land- und forstwirtschaftliche Nutzung.* Reichsnährstand Verlags, Berlin.
Shaw D. M. (1956) Geochemistry of pelitic rocks –III. Major elements general geochemistry. *Bull. Geol. Soc. Amer.* **67,** 919–934.
Shepherd E. S. (1938) The gases in rocks and some related problems. *J. Sci.* 5. Ser. **35Ä,** 311–351.
Sigvaldason G. E. (1958) Das Liparitvorkommen der Moskardshnjukar auf Island. *Beitr. Min. Pet.* **6,** 100–107.
Sigvaldason G. E. (1959) Min. Untersuchungen über Gesteinszersetzung durch postvulkanische Aktivität in Island. *Beitr. Min. Pet.* **6** 405–426.
Snyder I. L. (1959) Distribution of certain elements in the Duluth Complex. *Geochim. et Cosmochim. Acta* **16,** 243–277.
Sörum H. (1953) The structure of plagioclase felspars—II. *Acta Cryst.* **6,** 413–417.
Stout W. (1941) Dolomites and limestones of western Ohio. *Bull. Geol. Surv. Ohio* **4,** 42.
Strukturbericht II (1937) Bearbeitet von Hermann C., Lohrmann O. und Philipp H. S. 97–102. Akademische Verlags, Leipzig.
Tourtelot H. A. (1957) Chemical composition of the Pierre Shales and equivalent rocks of late cretaceous age, Great Plains Region. *Program Seventieth Annual Meeting of the Geological Society of America* p. 136.
Tröger E. (1934) Der Gehalt an selteneren Elementen bei Eruptivgesteinen. *Chemie Erde* **9,** 286–310.
Urbain P. (1951) *Recherches petrographiques et geochimiques sur deux series de roches argileuses.* T.1: *Lias et Oolithique du Calvados;* T. 2. *Eocene et Oligocene de la region de Paris.* Imprimerie Nationale, Paris.
Vasileva (1958) On sulphur-containing apatites. *Geochimija* 368–373.
Vinogradov A. P. (1956) Distribution of chemical elements in the earth's crust. *Geochimija* **1,** 3–52.
Vinogradov A. P. und Ronov A. B. (1956) Composition of sedimentary rocks of the Russian Platform in connection with the history of its tectonic movements. *Geochimija* **6,** 3–24.
Wager L. R., Vincent E. A. und Smales A. A. (1957) Sulphides in the Skaergaard Intrusion, East Greenland. *Econ. Geol.* **52,** 855–895.
Wahler W. (1956) Über die in Kristallen eingeschlossenen Gase und Flüssigkeiten. *Geochim. et Cosmochim. Acta* **9,** 105–135.
Wedepohl K. H. (1950) Der Feldspatbasalt des "Hohen Hagen" bei Dransfeld. *Heidelberg Beitr. Min. Pet.* **2,** 378–382.

Wedepohl K. H. (1954) Der trachydoleritische Basalt des Backenberges bei Güntersen, westl v. Göttingen. *Heidelberg Beitr. Min. Pet.* **4,** 217–232.

Wickbold R. (1953) Die photometrische Trübungstitration zur Bestimmung kleinster Sulfatmengen. *Angew. Chem.* **65,** 159–161.

Zies E. G. (1929) The Valley of the Ten Thousand Smokes. *Nat. Geogr. Soc. Techn. Papers Katmai Series* 4, Washington.

Geochimica et Cosmochimica Acta, 1960, Vol. 21, pp. 81 to 98. Pergamon Press Ltd. Printed in Northern Ireland

Minor element abundance in a part of the Brazilian shield*

N. Herz† and C. V. Dutra‡
†U.S. Geological Survey, Belo Horizonte, Minas Gerais, Brazil, and
‡Instituto de Tecnologia Industrial, Belo Horizonte, Minas Gerais, Brazil

(*Received* 11 *February* 1960)

Abstract—Thirty-nine samples of granitic rocks from the Quadrilátero Ferrífero, Minas Gerais, Brazil, representing "mixed" ages and at least three distinct Pre-Cambrian ages were analysed for seventeen minor elements. The rocks are placed in five groups: (1) 2400 million year old group; (2) Bação complex younger, a group of mixed rocks derived from (1) and (3); (3) 1350 million year old group; (4) a 500 million year old gneissic group; (5) a 500 million year old silicic group, a later differentiate of a 500 million year old magma.

Compared to granitic rocks elsewhere, these Brazilian rocks are about average in Ba, Sc, Zr, Pb, Nb, Co, Ni, Be and Mo; above average in La and Y; and below average in Cu, Sr, Ga, Sn, V and Cr. Compared to metasedimentary rocks elsewhere in the world, metasedimentary rocks of this region are about average in all seventeen minor elements.

Sr has its greatest abundance in the 2400 million year old rocks; Ba, V, Co, Sc, Cr, Ni and Cu in the 1350 million year; and La, Nb, Sn, Zr, Y and Ga in the 500 million year silicic. These abundances are in accord with the petrology and chemistry of the rocks. The 1350 million year rocks are the most mafic of the group and should logically concentrate Ba, V, Co, Sc, Cr, Ni and Cu which are most abundant in earlier crystallates. The 500 million year old silicic rocks are the most felsic and should concentrate La, Nb, Sn, Zr, Y and Ga, which are all most abundant in the latest fractions of granitic magma crystallization.

The trace elements also lend support to the idea that the Bação complex rocks developed by anatexis of 2400 million year rocks during the 1350 million year orogeny. Cu, Sc, Ga, Zr, Sn and Nb have about the same magnitude in the Bação and the 2400 million year rocks and Sr, V, Co, Cr and Ni are lower in the Bação than either the 2400 or the 1350 million year old rocks. This lower abundance is a probable effect of "debasification" which is also brought out by the analysis of major constituents.

The effects of a geochemical migration of the elements in this part of the earth's crust may be indicated by the increased abundance of Y in successively younger rock types. The increase of La, Nb, Pb, Sn, Y and Zr in the 1350 million year rocks compared to the 2400 million year rocks might also be an effect of a secular migration.

Introduction

This paper presents geochemical data from the comparatively little known Pre-Cambrian shield area of central Brazil. Most theories of the geochemistry of Pre-Cambrian rocks or of the crust in general and most estimates of abundance of elements in the crust have been formulated largely on the basis of data from the northern hemisphere, especially the Fennoscandian and the Canadian shields. The data presented here afford an opportunity to test check some of these ideas and estimates in one of the major shield areas of the world.

Since 1946 a detailed geologic mapping program has been in progress in the Quadrilátero Ferrífero, an area of some 7000 km² in central Minas Gerais, Brazil (Sociedade Brasileira de Geologia, 1958) by the Departamento Nacional da Produção Mineral of Brazil and the U.S. Geological Survey. The United States part of the study is presently under the auspices of the International Cooperation Administration of the Department of State. The results presented in this article are the product of a co-operative programme of trace element studies, started in 1957 by the U.S. Geological Survey and the Instituto de Technologia Industrial, Minas Gerais, Brazil. These studies were initiated on selected granitic rocks to

* Published by permission of the Directors of the Departamento Nacional da Produção Mineral do Brazil and the United States Geological Survey.

determine whether distinctive trace element suites had been formed during different tectonic periods or in specific geologic environments. The principal aim of this study was the correlation of granitic bodies which are separated either by great distances or by intervening formations. Part of this phase of the work, as well as the techniques of spectrochemical analysis used, have been described elsewhere (Herz and Dutra, 1958). In this present paper, data based on these and other analyses are given for the abundance of seventeen minor elements in the Pre-Cambrian granitic rocks of the Quadrilátero Ferrífero of central Minas Gerais, Brazil (Table 2).

The trace elements of the granites were determined by spectrographic methods without using internal standards and with the following apparatus and working conditions:

Spectrograph. Grating spectrograph with a 3 m focal length, Eagle mount, and dispersion of 5 Å/mm. Slit 0·025 mm.

Cathode. Graphite electrode, 3 mm diameter.

Anode. Graphite electrode of high purity (United Spectrographic Graphite), 6 mm diameter, with a cavity 3 mm wide by 7 mm deep and with a wall of 0·5 mm thickness. The external cut extended 9 mm below the lip of the cavity.

Analytical gap. A 4 mm gap, maintained throughout the excitation period.

Excitation source. Manufactured by Baird Associated, adjusted to furnish a direct current of 250 V and 15 A.

Length of exposure. Total consumption of the sample in arc ($\pm$110 sec).

Wavelength range and photographic emulsion. Region (a) from 2460 to 3870 Å, Kodak plate SA-1. Region (b) 3980 to 5400 Å, Kodak plate III-F. (The exposures in region (b) were made with a rotating two-step sector, on the secondary focus of the spectrograph).

Lines used. Ba, 4934·09 Å. Be, 3131·07 Å. Co, 3453·50 Å. Cr, 4254·35 Å. Cu, 3273·96 Å Ga, 2943·64 Å. La, 4333·73 Å. Mo, 3170·35 Å. Nb, 3163·40 Å. Ni, 3050·83 Å. Pb, 2833·07 Å. Sc, 4246·33 Å. Sn, 3262·33 Å. Sr, 4607·33 Å. V, 4384·72 Å. Y, 4374·93 Å.* Zr, 3391·97 Å.

Microphotometer. Jarrell–Ash comparator–projector (model 200).

Sample preparation. The samples were thoroughly homogenized then mixed with half of their weight of powdered graphite of high purity. Twenty-five milligrams of each mixture was transferred to the anode crater and volatilized in the arc to total consumption. All the exposures were made in duplicate.

Standards. A series of six standards containing all the trace elements was made using a base called "synthetic granite" (SiO_2 72·3 per cent, Al_2O_3 15·5 per cent, Fe_2O_3 1·5 per cent, $CaCO_3$ 1·2 per cent, $MgCO_3$ 0·5 per cent, Na_2CO_3 3·5 per cent, and K_2CO_3 5·5 per cent, sintered at 900°C). All the components of the standards are spectrographically pure products, except SiO_2 which was added in the form of finely ground clear quartz crystal. The trace elements added range from 1 to 333 p.p.m., except Ba and Sr which range from 10 to 3330 p.p.m.

An idea of the accuracy of the spectrographic determination was obtained by analysing G–1 (Ahrens, 1954, pp. 20–21). Abundance values for elements in these samples were obtained from analytical curves set up by known standards (Herz and Dutra, 1958, pp. 85–86). Our values for the granite G–1 obtained in two different plates and analysed on different days are shown in Table 1. The values recommended by Green (1959) are also shown for comparison. Curves for the determination of strontium were corrected in every plate by taking into account the value 233 p.p.m. recommended by Herzog and Pinson (1955) for G–1.

* Mn 4374·497 can interfere with this yttrium line. However, no granite sample that was analysed showed an amount of manganese higher than the limits of interference.

Determinative curves for V were made using the values recommended by AHRENS (1954) for G–1 and W–1 in different mixtures.

Ar^{40}/K^{40} age determinations were carried out in the laboratories of the Department of Geology and Geophysics of the Massachusetts Institute of Technology, under the direction of Professor P. M. HURLEY, on either biotite or muscovite or both of different rock samples (HERZ *et al.*, 1960). On the basis of these determinations, the granites are assigned to three distinct ages of intrusion or formation: 2400 million year, 1350 million year and 500 million year. The greatest age is

Table 1. Results of analysis of G–1 compared with the recommended values of GREEN (1959) in p.p.m. (For V and Sr see text)

	Plate A	Plate B	GREEN (1959)
Co	2·0	2·3	2·0
Ni	1·3	1·3	1·5
Sn	6·4	3·9	2·0?
Mo	6·5	8·0	9·0
Zr	200	185	190
Y	21	16	19
Cu	9	6·6	13
Pb	41	55	48
Ga	15	18·5	20
Be	2·6	2·2	3·3
Nb	15	22	19
Sc	4·5	4·5	6
Cr	18	24	27
La	153	132	140
Ba	1340	1250	1300

based on three analyses that range from 2310 to 2510 million years; the intermediate age on two analyses, 1340 and 1360 million year; and the youngest on ten analyses that range from 450 to 550 million years. A fourth group of rocks with ages between 1080 and 595 million years are considered to be "mixed," that is, older rocks that were affected to some extent by later orogenies.

The writers acknowledge the assistance of the Conselho Nacional de Pesquisas do Brasil which made available the laboratory instruments used in this study.

Granitic rocks sampled

The granitic rocks described in this article have been placed in five groups: (1) a 2400 million year age group; (2) the Bação complex younger; (3) a 1350 million year age group; (4) a 500 million year old gneissic group; and (5) a 500 million year old silicic group. Samples of the 2400 million year age group (Engenheiro Corrêa granodiorite) were collected from the type locality in the Bação complex, near the town of Engenheiro Corrêa (see index map). The "Bação complex younger" samples consist of mixed granitic rocks 1350 million years old and younger, that may have been derived by palingenesis or anatexis of the

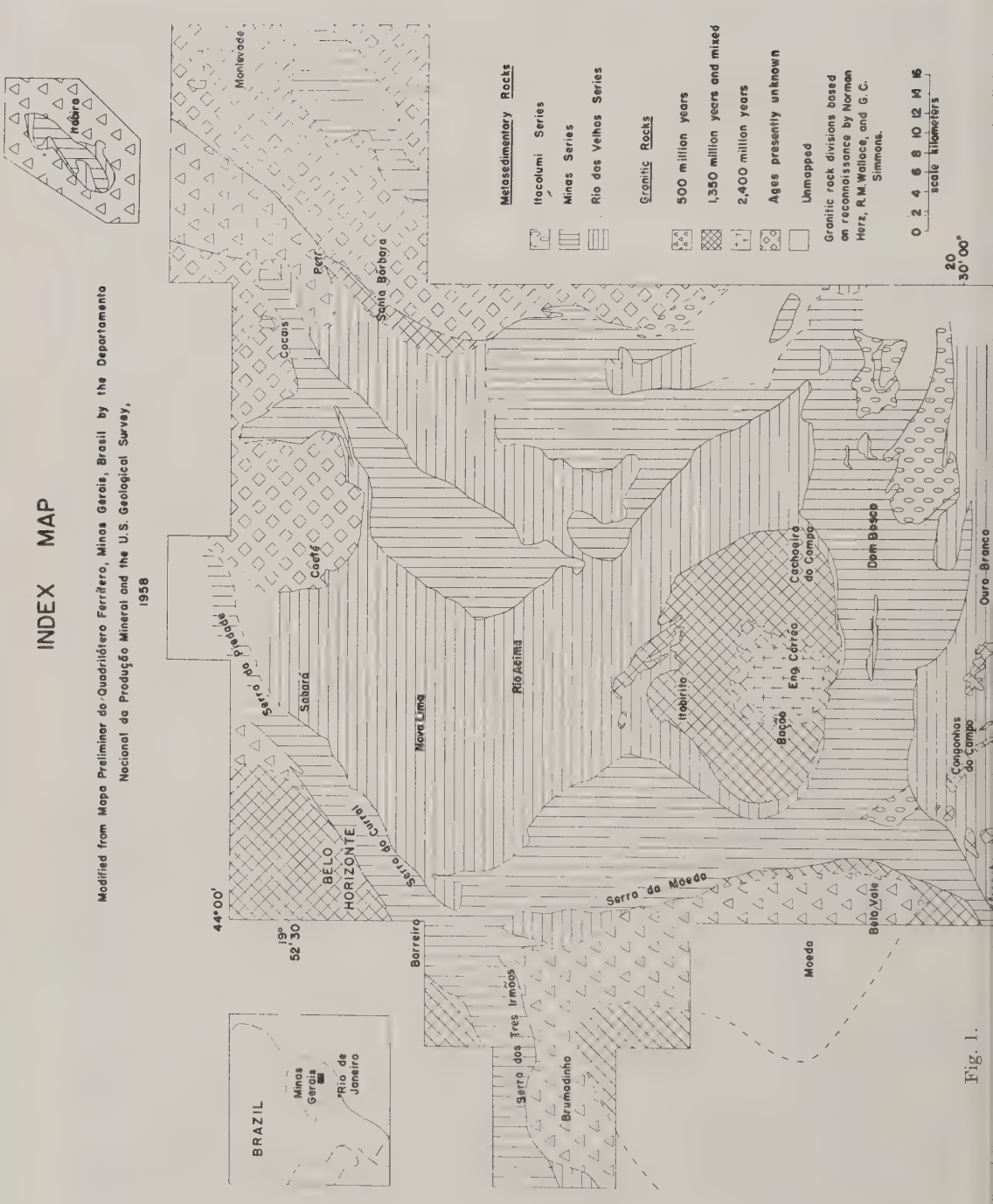
INDEX MAP
Modified from Mapa Preliminar do Quadrilátero Ferrífero, Minas Gerais, Brasil by the Departamento Nacional da Produção Mineral and the U.S. Geological Survey, 1958
Metasedimentary Rocks
Itacolumi Series
Minas Series
Rio das Velhas Series
Granitic Rocks
500 million years
1,350 million years and mixed
2,400 million years
Ages presently unknown
Unmapped
Granitic rock divisions based on reconnaissance by Norman Herz, R.M. Wallace, and G.C. Simmons.
0 2 4 6 8 10 12 14 16
scale kilometers
Ribeirão
Monlevade
Santa Bárbara
Cocais
Caeté
Sabará
Serra do Piedade
Rio Acima
Nova Lima
Serro do Curral
BELO HORIZONTE
Barreiro
Serra dos Três Irmãos
Brumadinho
Serra da Moeda
Moeda
Bela Vale
Congonhas do Campo
Itabirito
Bação
Eng. Correa
Cachoeira do Campo
Dom Bosco
Ouro Branco
20 30' 00"
44°00'
19° 52' 30
BRAZIL
Minas Gerais
Rio de Janeiro

Fig. 1.

Engenheiro Corrêa granodiorite, all found within the Bação complex. The Bação younger rocks have, in general, a more felsic composition than either their parent rock, the 2400 million year granodiorite or the 1350 million year granites found outside the Bação complex which were apparently not derived from the 2400 million year old rock. Samples of the 1350 million year age group, used for the averages of Table 2, were collected north of Belo Horizonte, in the extreme northern part of the Bação complex, and south of Congonhas do Campo. Some of these samples yield ages that are mixed, but their geologic environment and composition suggest that no chemical influence was exerted on these rocks by any later intrusions. The 1350 million year old granite is the most mafic of all the granitic rocks of the area, and contains the highest amount of biotite of any of the rocks and also, in many places, abundant amphibole and chlorite.

The 500 million year rocks are divided into two groups: a "gneissic" and a "silicic," although the two grade into each other. The gneissic rocks, used for the averages of Table 2, were collected near Itabira, from the Serra de Ouro Branco, and south of the Serra do Curral and west of the Serra da Moeda. Two general modes of origin have been ascribed to these rocks, one a mixing of either older sediments or igneous rocks with a later "granitizing" medium, and the other an early differentiation of a granitic magma. For the purposes of analysis of the trace element behaviour, the second origin will be considered the only one, although it must be recognized that both processes were at work throughout the area. The rocks used for the average of the 500 million year silicic rocks are from Itabira and the Petí dam in the north-eastern part of the Quadrilátero Ferrífero, and possess many features recognized as being purely igneous in origin. These rocks seem to have differentiated and separated at a later magmatic stage than the gneissic, are commonly rich in fluorite, and show an enrichment of SiO_2 (Table 3) and rare earth elements (Table 2) compared to the gneissic rocks. The gneissic rocks, on the other hand, are enriched in Ba and Sr which suggests a higher temperature of formation for them.

Explanation of tables

Table 2 shows the results of spectrochemical analyses of some granitic rocks from the Quadrilátero Ferrífero, Minas Gerais, Brazil, for seventeen elements, shown as the arithmetic mean for each rock group. The range for each element is given below each average. The data used for the calculations are based both on published (Herz and Dutra, 1958, Table 1) and previously unpublished analyses.

The number of samples shown under "all samples" is greater than the sum of the analyses used to obtain the data for the five rock types of Table 2. Only those rocks whose ages or whose facies are well established were used for the rock type averages; the mixed rocks and gradational rocks comprise the remainder. The averages for "all samples" are not weighted on the basis of the area covered by each rock type but are only the arithmetic mean of the samples. The estimates of Vinogradov (1956) for each element's abundance in "acidic rocks" are also shown for comparison.

Table 3 shows the average results of rapid rock analysis of some of the granitic

Table 2. Spectrochemical analyses of granitic rocks; Quadrilátero Ferrífero, Minas Gerais, Brazil (in p.p.m.)
(Analyst: C. V. DUTRA, Instituto de Tecnologia Industrial)

Rock type	Number of samples	Cu	Ba	Sr	Sc	La	Y	Ga	Zr	Sn	Pb	Nb	V	Cr	Co	Ni	Number of samples	Be	Mo
2400 million years	2	2·3	860	300	2·8	n.d.	11	19	105	7·1	12	11	21	3·6	3·0	4·7	1	3·6	3·3
	range	0·6–4·0	825–900	290–305	1·3–4·3	n.d.	9·4–12	15–22	96–115	6·3–7·9	4·6–19	7·0–15	14–29	3·4–3·8	2·8–3·1	2·7–6·7			
Baçao Complex younger	3	3·4	1040	190	3·8	17	19	19	94	5·6	25	11	9·7	2·1	n.d.	2·9	0		
	range	1·2–7·2	700–1430	145–240	3·6–4·2	n.d.–51	11–23	17–21	59–110	2·0–10	21–28	7·0–15	7·5–14	1·4–3·1	n.d.	2·3–4·0			
1350 million years	7	13	1250	280	8·8	98	59	17	270	36	28	26	41	25	8·2	19	4	3·3	1·8
	range	1·8–36	895–1610	72–575	7·2–15	62–210	24–87	7·4–21	185–370	7·0–61	15–50	11–49	20–68	2·1–55	5·2–17	2·2–70	range	n.d.–5·2	n.d.–3·7
500 million years gneissic	6	1·2	710	98	4·3	63	87	15	190	25	16	19	10	1·6	2·0	3·5	1	4·0	3·7
	range	0·5–2·0	450–1030	52–130	2·5–8·0	n.d.–110	24–245	13–16	96–290	3·5–68	10–29	11–28	1·3–29	0·9–2·9	n.d.–4·4	2·0–6·3			
500 million years silicic	2	3·2	230	28	n.d.	175	260	24	340	47	28	85	4·1	0·4	n.d.	3·4	0	—	—
	range	2·0–4·4	12·5–450	14–42	n.d.	120–230	200–315	24	275–410	17–7	23–33	57–110	n.d.–8·1	n.d.–0·8	n.d.–	2·7–4·0			
Average all samples	39	11	860	160	6·5	76	82	16	220	25	26	25	29	7·7	3·8	8·3	19	4·1	1·9
VINOGRADOV (1956)		30	830	300	7	46	20	30	200	45	20	20	40	25	5	8		5·5	1·9

n.d. = not detected.

Table 3. Chemical analyses of granitic rocks, Quadrilátero Ferrífero, Minas Gerais, Brazil
(Rapid rock analysis, methods similar to those described in U.S. Geological Survey Bulletin 1036-C)
(Analysts: P. L. D. Elmore, S. D. Botts, I. H. Barlow, M. D. Mack, H. W. Thomas and G. Chloe; F by S. M. Berthold U.S. Geological Survey)

Rock type	Number of samples analysed	SiO_2	Al_2O_3	Fe_2O_3	FeO	MgO	CaO	Na_2O	K_2O	TiO_2	P_2O_5	MnO	H_2O	CO_2	F	sum
2400 million years	1	72·1	15·0	0·9	1·1	0·52	1·8	4·7	2·6	0·24	0·09	0·06	0·61	0·14	n.d.*	99·9
Bação complex younger	3	74·9	14·4	0·3	0·64	0·20	1·5	4·0	3·5	0·11	0·03	0·04	0·42	0·07	0·03*	100·1
1350 million years	2	67·8	14·6	1·1	2·6	1·5	2·6	3·8	3·8	0·57	0·25	0·09	0·72	0·09	0·07†	99·6
500 million years gneissic	6	74·2	13·6	0·7	1·1	0·43	0·93	3·2	4·8	0·25	0·07	0·05	0·66	0·17	0·04‡	100·2
500 million years silicic	2	76·0	12·2	0·7	1·1	0·01	0·76	3·6	4·6	0·11	0·01	0·04	0·44	0·10	0·45†	99·7

* 1 analysis.
† 2 analyses.
‡ 4 analyses.
n.d. = not detected.

Table 4. Semiquantitative spectrographic analysis of metasedimentary rocks of the Quadrilátero Ferrífero
(Figures are reported to nearest number in the series 1, 3, 10, 30 etc., in p.p.m.)
(Analyst: Helen W. Worthing, U.S. Geological Survey)

Specimen number	Cu	Ba	Sr	Sc	La*	Y	Ga	Zr	Sn†	Pb	Nb†	V	Cr	Co	Ni	Be	Mo†	Location and description
J-10	30	300	300	10	n.d.	30	10	100	n.d.	3	n.d.	300	1000	30	300	1	10	Cachoeira do Campo quad., Nova Lima "roof pendant", qz-bi-amphibolite
J-84b	30	1000	100	10	30	30	30	100	n.d.	3	n.d.	300	300	10	100	3	n.d.	Cachoeira do Campo quad., Caraça chlord-musc-qz-schist
J-155c	30	300	300	30	n.d.	30	30	100	n.d.	3	n.d.	300	300	10	30	1	10	Dom Bosco quad., Nova Lima epidote-amphibole rock
J-211	3	300	300	10	30	30	30	300	n.d.	10	n.d.	300	300	10	100	1	10	Dom Bosco quad., Piracicaba, iron-bearing qz-ser-chlor-schist
J-341	10	300	30	10	30	30	30	100	n.d.	3	n.d.	300	300	10	100	3	10	Dom Bosco quad., Piracicaba, qz-ser-chlord-chlor schist

Table 4 (*continued*)

Specimen number	Cu	Ba	Sr	Sc	La*	Y	Ga	Zr	Sn†	Pb	Nb†	V	Cr	Co	Ni	Be	Mo†	Location and description
J-682b	10	3000	100	3	100	30	30	300	3	3	n.d.	100	30	10	100	3	n.d.	Dom Bosco quad., Piracicaba, limon-qz-ser-schist
J-693	10	1000	30	3	30	30	10	300	n.d.	3	n.d.	100	30	3	30	1	3	Ouro Branco quad., Ouro Branco sub-graywacke, feld-ser-quartzite
A-4953	30	1000	300	10	n.d.	30	30	100	n.d.	10	n.d.	300	300	10	100	1	10	Nova Lima quad., Sabará, staur-gar-bi-schist
JG-241	30	1000	3000	10	30	10	30	100	n.d.	3	n.d.	100	30	3	30	1	3	Rio Acima quad., Nova Lima, gray-wacke ep-chlor-feld-ser-qz rock

Notes: visual detection limit below n.d. = not detected
* 30 p.p.m.
† 3 p.p.m.
Quadrangles and sedimentary formations described in Sociedade Brasileira de Geologia, 1958.
Mineral abbreviations: bi, biotite; chlor, chlorite; chlord chloritoid; ep, epidote; feld, feldspar; gar, garnet; limon, limonite; musc, muscovite; qz, quartz; ser, sericite; staur, staurolite.

samples. Table 4 shows the results of semiquantitative spectrographic analysis of some metasedimentary rocks from the Quadrilátero Ferrífero.

The trace elements are arranged in terms of their periodic table groups.

Interpretation of results of analyses of granitic rocks

Copper. According to Ahrens (1953, p. 16) copper is concentrated in the earliest stages of magmatic crystallization and then again in the pegmatitic and pneumatolytic stages.

In the rocks under consideration, copper is lowest in the 500 million year old gneissic rocks, 1·2 p.p.m., and highest in the 1350 million year old group, 13 p.p.m. However, in all rocks except the 1350 million year old group the copper content is fairly uniform, from 1·2 to 3·4 p.p.m. This distribution is in accord with Sandell and Goldich's observation (1943, p. 175) that the amounts of silica and copper in magmatic rocks are inversely proportional, for the 1350 million year old rocks have by far the lowest SiO_2, 67·8 per cent as against from 72·1 to 76·0 per cent for all other rocks (Table 3).

Magmatic rocks from localities in the United States that average 72 per cent SiO_2 have 16 p.p.m. of copper (Sandell and Goldich, 1943, p. 175); these Brazilian rocks with an average SiO_2 content of 73·5 per cent have only 11 p.p.m. copper.

Beryllium. Beryllium is said to concentrate more in silicic than subsilicic rocks and to be most abundant in alkali-rich granites (Sandell, 1952, p. 211). The total range of beryllium in the rocks of this part of Brazil is not great, and seems to be of the same order of magnitude, from 3 to 4 p.p.m., in the different rock types.

The average of all samples, 4·1 p.p.m., is higher than that given by Sandell (1952, p. 212), 3 p.p.m., for "granites and related rocks."

Barium and strontium. Rankama and Sahama (1950, p. 472) state that both barium and strontium are concentrated in earlier, high-temperature granitic magma crystallates. In the latest crystallates of a granitic magma, barium becomes enriched in comparison to strontium, but the total amount of both elements decreases. According to Turekian and Kulp (1956, p. 265) the strontium content is strongly controlled by the calcium throughout the course of granitic crystallization.

The Sr/Ca ratio (Table 5) is fairly uniform (from 15·1 to 23·0) in the older rocks and lower (14·8 and 5·2) in the 500 million year granites. Turekian and Kulp (1956, p. 290) found an average ratio of 16·7 to 23·0 for granitic rocks and the Sr/Ca ratio increasing with increasing Ca content. The higher Ba/Sr ratio and lower Sr/Ca ratio show that the 500 million year silicic group is impoverished in strontium in comparison to the 500 million year old gneissic rocks and other granites as would be expected in a late differentiate. The Bação younger granites also have a higher Ba/Sr ratio than either the 2400 or the 1350 million year old rocks. This higher ratio may be an effect of "debasification" during the anatexis of the 2400 million year old rocks in the 1350 million year old orogeny.

The average barium content of these rocks, 860 p.p.m. is somewhat higher than Goldschmidt's estimate (1954, p. 252) of 480 p.p.m. for granite and liparite,

but is in agreement with VINOGRADOV's figure (1956) of 830 p.p.m. for acidic rocks. However, the average strontium content of these rocks, 160 p.p.m., is considerably lower than VINOGRADOV's figure (1956) of 300 p.p.m.

Scandium. Scandium substitutes diadochically for magnesium and for ferrous iron in mafic minerals and so is said to be more abundant in mafic and ultramafic rocks than in granites (GOLDSCHMIDT, 1954, p. 304). In the pneumatolytic and

Table 5. Ba/Sr and Sr × 1000/Ca ratios

Rock type	Ba/Sr	Sr × 1000/Ca
2400 million years	2·9	23
Bação younger	5·5	18
1350 million years	4·5	15
500 million years gneissic	7·2	15
500 million years silicic	8·2	5

pegmatitic stage of a granite magma, scandium substitutes for these elements in biotite.

The scandium content is fairly uniform in the different rocks; the maximum, 8·8 p.p.m., is found in the 1350 million year granite; the minimum, in the 500 million year silicic; the latter is not determinable. The 1350 million year old is generally richer in mafic minerals and the 500 million year silicic, a late-stage crystallate, is low in mafic minerals.

The average abundance of scandium in all samples, 6·5 p.p.m., agrees with VINOGRADOV's figure (1956) of 7 p.p.m.; GOLDSCHMIDT's figure (1954, p. 305) of 2 p.p.m. for granite is probably low.

Lanthanum and yttrium. Lanthanum and yttrium are concentrated in the residual liquors of a magma (RANKAMA and SAHAMA, 1950, p. 518). These elements tend to form independent minerals that are exceptionally rich in rare earths, such as xenotime, allanite, fluorite and apatite, which are all common in the post-2400 million year old rocks (Table 2, HERZ *et al.*, 1960).

With one minor exception, the values for lanthanum and yttrium are in accord with RANKAMA's observation (1946, p. 12) that the granites richest in rare earths are the youngest ones. The minimum values for both lanthanum and yttrium are found in the 2400 million year old rocks, not determinable and 11 p.p.m., respectively. Rocks of the Bação complex derived from the 2400 million year old granodiorite have only a little more than this (17 and 19 p.p.m., respectively). The yttrium content is higher in successively younger rocks; lanthanum also increases in younger rocks except that it is higher in the 1350 million year old rocks than in the 500 million year old gneissic rocks.

The average abundances of both lanthanum and yttrium in the granitic rocks of Minas Gerais is considerably higher than in granitic rocks elsewhere in the world. Thus, the average lanthanum content in Minas Gerais is 76 p.p.m.; RANKAMA and SAHAMA (1950, p. 528) cite 43 and 60 p.p.m. in granites and VINOGRADOV (1956) cites an average of 46 p.p.m. for acidic rocks but a range from 30 to 80 p.p.m. The average yttrium content of 82 p.p.m. is higher than FLEISCHER's

range (1955, pp. 151) of from 36 to 45 p.p.m. for rocks with more than 65 per cent SiO_2.

Gallium. According to Ahrens (1953, pp. 11–12), gallium is closely associated with aluminium throughout the course of magmatic crystallization and there is a slight tendency for the Ga/Al ratio to increase during fractionation.

The gallium content in the different rock types and even the different samples shows very little variation. However, it can be seen (Table 6) that the Bação

Table 6. Ga × 1000/Al ratio

Rock type	Ga × 1000/Al
2400 million years	0·24
Bação younger	0·25
1350 million years	0·22
500 million years gneissic	0·21
500 million years silicic	0·37

younger rocks have a higher Ga/Al ratio than both the 2400 million year old and the 1350 million year old rocks and that the 500 million year old silicic rocks have a higher ratio than the 500 million year old gneissic rocks. In both cases, the data suggest that the Bação younger and the 500 million year old silicic rocks are later differentiates than their associated facies.

The average abundance for all rocks, 16 p.p.m., is in excellent agreement with the figure of 16·5 p.p.m. for rocks with more than 65 per cent of SiO_2; cited by Fleischer (1955, p. 150).

Zirconium. Zirconium is concentrated largely in the later differentiation of a granitic magma (Degenhardt, 1957, p. 289). Much of it occurs in zircon, but some is also found in the dark minerals.

In the rocks studied, the total zirconium is largely related to the zircon content. Thus, zircon was not seen in thin sections of the 2400 million year old rocks, and they and their derivatives, the Bação younger rocks, have the lowest contents of zirconium, 105 and 94 p.p.m., respectively. Zircon is fairly abundant in many thin sections of the 1350 million year old rocks and both 500 million year old granites. In the 1350 and 500 million year old rocks, zirconium ranges from 190 to 340 p.p.m., a two- to three-fold increase over the 2400 million year old rocks.

The average abundance of zirconium in all of these rocks, 220 p.p.m., is somewhat higher than Degenhardt's average (1957, p. 306) of 175 p.p.m. for granite.

Tin and lead. Both tin and lead are enriched in late crystallates of a granitic magma and are at a maximum in pneumatolytic rocks (Rankama and Sahama, 1950, p. 733). In addition, according to Wedepohl (1956, p. 99) lead should be slightly more abundant in rocks of younger age because of the introduction of lead of radiogenic origin to the crust through geologic time. Tin seems to be especially enriched in certain geographic areas and during certain geologic epochs (Onishi and Sandell, 1957, p. 263).

Tin has its lower values in the 2400 million year rocks and the 2400 million year derived rocks of the Bação complex, 7·1 and 5·6 p.p.m., respectively. It

is more abundant in the later rocks by a factor of from 3 to 6 which suggests that the area changed from one poor in tin to one richer in tin. The 500 million year old silicic rocks are enriched over the 500 million year old gneissic rocks in both tin and lead, a probable effect of later differentiation. The minimum value for lead is found. in the 2400 million year old rock, 12 p.p.m.; possible contributing factors for this low value are its great age and low radioactivity (note its lower rare earth content, Table 2).

Table 7. Nb × 100/Ti and Nb/Nr ratios

Rock type	Nb × 100/Ti	Nb/Zr
2400 million years	0·8	0·10
Bação younger	1·7	0·12
1350 million years	0·8	0·096
500 million years gneissic	1·3	0·10
500 million years silicic	13	0·25

The statement of Wedepohl (1956, p. 137) that lead increases with metamorphism is apparently borne out by the metasedimentary rock analyses (Table 4). The rocks with the highest lead content, J–211 and A–4953, are both closely associated with granitic intrusion. Sample J–211 is of rock that was in contact with rocks that show granitization phenomena and sample A–4953 shows contact metamorphism. Sample J–10, however, is from a root pendant and has about the same amount of lead as the lower grade metamorphic samples.

Onishi and Sandell (1957, p. 262) give an average value of 3 p.p.m. tin in granites: the data in Table 2 show 25 p.p.m. Vinogradov (1956) cites 45 p.p.m. for acidic rocks and Goldschmidt (1954, p. 395) 80 p.p.m. In relation to the data of Vinogradov and Goldschmidt, the Quadrilátero Ferriféro is a relatively tin-poor area; this is also borne out by the analyses of the metasedimentary rocks (Table 4).

The average lead abundance of 26 p.p.m. is similar to Wedepohl's figure (1956, p. 110) of 20 p.p.m. for "Saure Gesteine."

Niobium and vanadium. Niobium is concentrated in the later differentiates of a granitic magma, and vanadium in the earliest (Goldschmidt, 1954, pp. 489, 500). Niobium takes the place of titanium in biotite, rutile and sphene, and is also closely related to zirconium; the average niobium content of igneous rocks is one-tenth that of zirconium (Goldschmidt, 1954, p. 504). These relations are generally substantiated by the analyses of granitic rocks of the Quadrilátero Ferriféro as is shown in Table 7.

Table 7 shows that the excess of niobium over titanium and zirconium is greater in the Bação younger rocks than in both the 2400 million year and the 1350 million year old rocks; the 500 million year old silicic rocks are also greatly enriched in niobium over the 500 million year gneissic. The data for vanadium show a maximum in the 1350 million year with 41 p.p.m. and a minimum in the 500 million year silicic with 4·1 p.p.m.

The average abundance of niobium in these rocks, 25 p.p.m., is in agreement with the 30 p.p.m. cited by Rankama and the 20 p.p.m. by Goldschmidt for

granites (cited in Rankama and Sahama, 1950, p. 606). The abundance of vanadium, 29 p.p.m., is about the same as Lundegardh's 30 p.p.m. for acidic igneous rocks of central Roslagen Sweden and higher than Sahama's 17 p.p.m. for granites of southern Lapland (cited in Rankama and Sahama, 1950, p. 596).

Chromium and molybdenum. Chromium is concentrated in the earliest crystallates of a magma (Rankama and Sahama, 1950, p. 620). Kuroda and Sandell (1954, p. 49) state that molybdenum shows little variation in different igneous rock types, but has a slight tendency to concentrate in alkali-rich differentiates.

Table 8. Co/Ni ratio

Rock type	Co/Ni ratio
2400 million years	0·64
Bação younger	*
1350 million years	0·43
500 million years gneissic	0·57
500 million years silicic	*
Average, all samples	0·45

* Co not determinable.

The maximum concentration of chromium, 25 p.p.m., is found in the 1350 million year old rocks, and is greater by a sevenfold factor than the next highest value, 3·6 p.p.m. in the 2400 million year old rocks. The Bação complex younger rocks have less chromium than both the 2400 million year old rocks and the 1350 million year old rocks, another sign of their "debasification" from the original 2400 million year old rocks. The minimum value for chromium in all these rocks, 0·4 p.p.m., is found in the 500 million year old silicic rocks, as is expected in a late-stage differentiate.

The abundance of molybdenum is about the same order of magnitude in all rocks, and the maximum for any one sample is only 6 p.p.m.

The average abundance of 7·7 p.p.m. of chromium agrees with Goldschmidt's range (1954, p. 548) of from 2 to 10 p.p.m. in granites and liparites. The average of 1·9 p.p.m. molybdenum agrees with the 1·1 p.p.m. of Kuroda and Sandell (1954, p. 45) for granitic rocks.

Cobalt and nickel. Both nickel and cobalt are more abundant in mafic rocks than in granitic, though the Co/Ni ratio is said to increase from mafic to granitic (Rankama and Sahama, 1950, p. 682). The Co/Ni ratio is shown in Table 8 for these rocks; the lowest value is in the 1350 million year old rocks as is to be expected from its more mafic composition.

The absolute abundance of nickel is actually rather close to that of cobalt. The maximum for both elements is in the 1350 million year old rocks. The younger Bação rocks have less of both metals than have the 1350 and the 2400 million year old rocks which shows a loss of these metals in the palingenesis of the older rocks; the 500 million year old silicic rocks have less than the 500 million year old gneissic rocks. The ratio obtained for all samples, 0·45, is in good agreement with that of Sandell and Goldich (1943, p. 182) for American silicic rocks, 0·52.

The average abundance of 3·8 p.p.m. cobalt in all samples is in good agreement

with SANDELL and GOLDICH's figure (1943, p. 182) of 3 p.p.m. in American silicic rocks. The nickel abundance average, 8·3 p.p.m., is somewhat higher than SANDELL and GOLDICH's estimate of 5·8 p.p.m.

Results of semiquantitative spectrographic analysis of metasedimentary rocks

Table 4 shows the results of semiquantitative spectrographic analysis of some metasedimentary rocks of the Quadrilátero Ferrífero. In Table 9, the average for each element is compared with the results from other parts of the world. SHAW's data (1954) are on rocks from the Devonian Littleton formation of New Hampshire; MACPHERSON's (1958) are largely from Pre-Cambrian Canadian argillaceous rocks. Since the results of the Quadrilátero Ferrífero rocks are semiquantitative, the averages cited in the table should be considered as an order of magnitude only.

There are no startling conclusions to be drawn from the data. The minor elements are about as abundant in these rocks as they are in other metasedimentary and sedimentary rocks in different parts of the world. It is interesting to note, however, that despite the enrichment of the igneous rocks in rare earth elements, there is no enrichment of these elements in the metasedimentary rocks. Apparently, the rare earth minerals present in the granites were destroyed either during the deposition and lithification of the sediments derived from them or during the later metamorphism of the sediments.

CONCLUSIONS

Compared to the data of VINOGRADOV (1956) on abundances in "acid" rocks of the world, the granitic rocks of the Quadrilátero Ferrífero are about average in Ba, Sc, Zr, Pb, Nb, Co, Ni, Be and Mo; below average in Cu, Sr, Ga, Sn, V and Cr; above average in La; and much above average (greater than four times) in Y. If these data prove to be about normal for the Brazilian shield as a whole, then the abundance presently accepted for Y in granites will have to be greatly increased.

In the rocks of this present study, Sr has its greatest value in the 2400 million year old suite; Ba, V, Co, Sc, Cr, Ni and Cu in the 1350 million year suite; and La, Nb, Sn, Y, Zr, and Ga in the 500 million year silicic. Pb has the same value in both the 1350 million year and the 500 million year silicic rocks. The data for Mo and Be show no great variation. These trace element abundances supplement data obtained from field and petrographic studies and from chemical analysis of the major constituents. From these other studies, we know that the 1350 million year old rocks are the most mafic of all. These rocks have the highest contents of iron, magnesium and calcium, and the lowest of silicon. In addition to this, a high degree of regional and contact metamorphism is associated with these rocks, all of which points to a high temperature of formation for them. The 500 million year old rocks, on the other hand, are the richest of all in silicon and sodium and the lowest in aluminium, magnesium and calcium, and in many places the intruded sediments show only limited contact metamorphic effects. This is evidence of a comparatively lower temperature, late-magmatic stage of formation for these younger rocks.

The elements whose maximum abundance is found in the 1350 million year old rocks are generally believed to concentrate in the earlier, higher temperature

Table 9. Averages of semiquantitative spectrographic analyses of metasedimentary rocks of Quadrilátero Ferrífero compared with elsewhere

	Cu	Ba	Sr	Sc	La	Y	Ga	Zr	Sn	Pb	Nb	V	Cr	Co	Ni	Be	Mo
Quadrilátero Ferrífero, Table 4	20	900	400*	9	30	30	30	200	n.d.	5	n.d.	200	300	9	100	1	6
Shaw, 1954	18		710	14		45	19	200		24		120	110	18	64		
MacPherson, 1958	47	441										175	212		108		
Others	40 – 65	690	300	6·5	26	15·8	50	160	4	20		120	410 – 680	8	24	1	0·5 – 4·5
Reference†	2	1	6	1	1	1	3	8	5	4		7	1	1	1	1	2

* -200 excluding JG-241.

† References: (1) "Al-rich schists," So. Lapland, Sahama, 1945; quoted in Rankama and Sahama (1950).
(2) "European and Japanese shales," Kuroda and Sandell (1954), p. 56.
(3) "Russian clay," Borovick, Prokopenko and Pokrovskaya, (1939), quoted in Rankama and Sahama (1950), p. 728.
(4) "Tonschiefer," Wedepohl (1956), p. 133.
(5) "European and Japanese shales," Onishi and Sandell (1957), p. 263.
(6) "Average shale," Turekian and Kulp (1956), p. 284.
(7) "Clays and shales," Joost (1932), quoted in Rankama and Sahama (1950), p. 601.
(8) "Tonschiefer," Degenhardt (1957), p. 306.

n.d. = not detected.

stages of granitic magma crystallization. The elements whose maximum is in the 500 million year old silicic rocks on the other hand are ones that should concentrate in the later, lower-temperature stages of magmatic crystallization. Thus both sets of trace elements behave as predicted by their known geochemical behaviour in a crystallizing and fractionating magma.

The maximum value for Sr is found in the 2400 million year old rocks. This may be an effect of a high temperature of formation, but whatever the reason, these oldest rocks are clearly enriched in Sr compared to both Ba and Ca (Table 5).

Trace elements also lend support to the idea that many rocks of the Bação complex represent rocks of 2400 million years age that were remobilized in the 1350 million years orogeny. Thus, Cu, Sc, Ga, Zr. Sn and Nb, are about as abundant in the Bação rocks as they are in the 2400 million year rocks, and Ba, Y and La are intermediate in value between the 2400 million year and the 1350 million year rocks. Sr, V, Co, Cr and Ni are lower in the Bação than either of the other rocks, and Pb has about the same value in the Bação rocks as in the 1350 million year rocks. The lower values for Sr, V, Co, Cr and Ni in the Bação compared to the abundance of these elements in the other rocks may be an effect of "debasification" during the anatexis of the 2400 million year old rocks. This effect has already been noted in the higher ratios for Ba/Sr (Table 5), Ga $\times$ 1000/Al (Table 6), and Nb $\times$ 100/Ti (Table 7) in the Bação rocks compared to the others. The phenomenon of "debasification" is also brought out by the analysis of the major constituents (Table 3) for the Bação rocks have higher SiO_2 and lower Al_2O_3, iron, MgO and CaO than either of the other rocks. Equal values for lead in the Bação and the 1350 million year rocks may be due in part to the general increase in lead by the contribution of radiogenic sources to the crust in geological time (Wedepohl 1956, p. 99).

Rankama (1946) has discussed at length the idea that a geochemical migration of elements takes place on a global scale. According to this idea, the granitophile elements, such as Li, Be, Rb, Cs, Ba, rare earths, Ta and Pb, tend to concentrate in the outermost parts of the earth's crust and the siderophile, represented by Y, are pushed downwards towards the basaltic substratum owing to a secular geochemical migration. The time involved in the history of the different granites of the Quadrilátero Ferrífero is sufficiently great so that if any secular process is at work in this area, its effect should be shown in the abundances of the different elements. This effect, however, will be modified to a great degree by such processes as differentiation of each magma and fractionation of each granitic rock which have also been operative in this area.

The increasing abundance for Y in each succeeding rock type (Table 2) might be a result of this geochemical migration. This increase of Y with geological time is opposite to that predicted by Rankama (1946, p. 19) though his conclusion was drawn from the limited data available at the time. Y is classified as lithophilic (for instance Goldschmidt, 1954, p. 25) and so should become more abundant with time. On the other hand, Sr shows a decreasing abundance with time, but this may be an effect of decreasing temperature of formation in succeeding rocks, for Sr is generally conceded to be lithophilic (for instance Green, 1959).

Another probable temporal effect may be shown by the relative abundances of

minor elements in the 2400 million year and the 1350 million year old rocks. Except for Sr, Ga, Be and Mo, all the elements are more abundant in the 1350 million year than the 2400 million year old rock. It is easy to understand why Ba, V, Co, Sc, Cr, Ni and Cu should be more abundant in the younger rock because of its more mafic nature. The concomitant increase of La, Nb, Pb, Sn, Y and Zr in the younger rock, however, may be due to a secular geochemical enrichment in this part of the earth's crust. At any rate, this increase cannot be explained on the basis of the known behaviour of these elements in a crystallizing melt, for these elements should logically concentrate in the more felsic rock. Their increased abundance in a rock which is the most mafic of the group can perhaps best be explained by the phenomenon of secular geochemical enrichment.

References

Ahrens L. H. (1953) The use of ionization potentials—II. Anion affinity and geochemistry. *Geochim. et Cosmochim. Acta* **3,** 1–29.

Ahrens L. H. (1954) *Quantitative Spectrochemical Analysis of Silicates.* Pergamon Press, London.

Degenhardt H. (1957) Untersuchungen zur geochemischen Verteilung des Zirkoniums in der Lithosphäre. *Geochim. et Cosmochim. Acta* **11,** 279–309.

Fleischer M. (1955) Estimates of the abundances of some chemical elements and their reliability. In *Crust of the Earth.* Geol. Soc. America Special Paper 62, 145–154.

Goldschmidt V. M. (1954) *Geochemistry.* Clarendon Press, Oxford.

Green J. (1959) Geochemical table of the elements for 1959. *Bull. Geol. Soc. Amer.* **70,** 1127–1184.

Herz N. and Dutra C. V. (1958) Preliminary spectrochemical and age determination results on some granitic rocks of the Quadrilátero Ferrífero, Minas Gerais, Brazil. *Soc. Brasileira de Geol. Bol.* **7,** 81–95.

Herz N., Hurley P. M., Pinson W. H. and Fairbairn H. W. (1960) Age measurements from a part of the Brazilian Shield. Report in preparation.

Herzog L. F. and Pinson W. H. Jr. (1955) The Sr and Rb contents of the granite G–1 and diabase W–1. *Geochim. et Cosmochim. Acta* **8,** 295–298.

Kuroda P. K. and Sandell E. B. (1954) Geochemistry of molybdenum. *Geochim. et Cosmochim. Acta* **6,** 35–63.

MacPherson H. G. (1958) A chemical and petrographic study of Precambrian sediments. *Geochim. et Cosmochim. Acta* **14,** 73–92.

Onishi Hiroshi and Sandell E. B. (1957) Meteoric and terrestrial abundance of tin. *Geochim. et Cosmochim. Acta* **12,** 262–270.

Rankama Kalervo (1946) *On the Geochemical Differentiation in the Earth's Crust.* Bull 137, Comm. Geol. de Finlande.

Rankama Kalervo and Sahama T. G. (1950) *Geochemistry.* University of Chicago Press, Chicago.

Sandell E. B. (1952) The beryllium content of igneous rocks. *Geochim. et Cosmochim. Acta* **2,** 211–216.

Sandell E. B. and Goldich S. S. (1943) The rarer metallic constituents of some American igneous rocks. *J. Geol.* **51,** 99–115, 167–189.

Shaw D. M. (1954) Trace elements in pelitic rocks—I. Variation during metamorphism. *Bull. Geol. Soc. Amer.* **65,** 1151–1166.

Sociedade Brasileira de Geologia (1958) *Guia Geológico do Quadrilátero Ferrífero de Minas Gerais, para o XII Congresso Anual,* Belo Horizonte.

Turekian K. K. and Kulp J. L. (1956) The geochemistry of strontium. *Geochim. et Cosmochim. Acta* **10,** 245–296.

Vinogradov A. P. (1956) The regularity of distribution of chemical elements in the earth's crust. *Geokhimiya* **1,** 1–52.

Wedepohl K. H. (1956) Untersuchungen zur Geochemie des Bleis. *Geochim. et Cosmochim. Acta* **10,** 69–148.

Geochimica et Cosmochimica Acta, 1960, Vol. 21, pp. 99 to 109. Pergamon Press Ltd. Printed in Northern Ireland

Synthesis fields of some aluminium silicates

R. M. Carr and W. S. Fyfe
University of Otago, New Zealand, and University of California, Berkeley

(*Received* 27 *April* 1960; *Revised* 15 *June* 1960)

Abstract—The P—T field in which a phase or assemblage of phases may be synthesized need not be identical with that in which it is stable. This proposition is illustrated by studies in the system Al_2O_3–$4SiO_2$ under hydrothermal conditions. Three different starting materials have been used (amorphous Al_2O_3–quartz, kaolinite–amorphous silica, kaolinite–quartz) and three significantly different synthesis diagrams result. None can be said to represent stable equilibrium but petrological observations indicate that results using kaolinite and quartz (the closest approach to natural starting materials) may approach most closely to equilibrium conditions. With this starting material at 30,000 lb/in^2 kaolin passes to pyrophyllite at 420°C, pyrophyllite to an andalusite-like phase (here called X-andalusite, possibly the "AS(H)-II" of Aramaki and Roy) at 470°C and X-andalusite to mullite at 525°C. The writers believe that, due to prohibitive kinetic aspects of boundary reversal, it may be impossible to establish the equilibrium relations between sillimanite and andalusite by synthetic methods.

Introduction

Hydrous and anhydrous aluminosilicates are of importance in many metamorphic rocks including representatives of a variety of metamorphic facies. The low-temperature dehydration of clays to micas and mica-like minerals takes place between the zeolite and greenschist facies while micas persist through to the amphibolite facies, where the anhydrous aluminosilicates (kyanite, andalusite and sillimanite) appear. Kyanite and sillimanite also occur in the granulite facies. Petrological observations indicate the following reaction sequence in response to rising temperatures:

$$\underset{\text{kaolinite}}{Al_2Si_2O_5(OH)_4} + 2SiO_2 \leftrightharpoons \underset{\text{pyrophyllite}}{Al_2Si_4O_{10}(OH)_2} + H_2O$$

$$\underset{\text{pyrophyllite}}{Al_2Si_4O_1\text{-}(OH)_2} \leftrightharpoons \underset{\substack{\text{andalusite}\\ \text{kyanite}\\ \text{sillimanite}}}{Al_2SiO_5} + 3SiO_2 + H_2O$$

$$\underset{\substack{\text{andalusite,}\\ \text{etc.}}}{3Al_2SiO_5} \leftrightharpoons \underset{\text{mullite}}{Al_6Si_2O_{13}} + SiO_2$$

Recent work by Roy and Osborn (1954) indicates that kaolinite dehydrates with the formation of pyrophyllite near 400°C at water pressures of from 150 to 2000

bars and that pyrophyllite decomposes to mullite and quartz at temperatures between 550°C and 600°C for the same pressure range. Kennedy (1955) has, in general, confirmed the decomposition conditions quoted above but states that the high temperature phase in the pressure range 400–3000 bars is a solid solution of mullite and sillimanite. The decomposition of pyrophyllite to sillimanite plus quartz (1000 bars and 500°C, 14,500 bars and 700°C) is reported by Griggs and Kennedy (1956). Roy (1954) has reported the synthesis of andalusite from seeded mixes and from natural kaolinite. A stability field for andalusite of 450–650°C at water pressures of 10,000–30,000 lb/in^2 was suggested. Andalusite has also been synthesized by Hemley (1959) at 450°C in the system K_2O–Al_2O_3–SiO_2–H_2O. Since Aramaki and Roy (1959) have suggested that synthetic material previously reported as andalusite is actually a new related phase which they designate AS(H)-II, all "andalusite" synthesis may be of questionable significance.

Since natural pyrophyllite and the anhydrous aluminosilicates are commonly associated with quartz, stability relations of aluminosilicates in the presence of excess silica should be of special significance in interpretation of metamorphic conditions. In other studies in this laboratory, Coombs *et al.* (1959), it was found that starting materials may have a profound influence on products. As this system is of such petrological importance, a more detailed study of this aspect of the system has been undertaken. In particular, the effect of varying the silica activity by adding the silica as quartz or in the amorphous state has been examined.

Method of Investigation

"Test tube" bombs of stainless steel were used for most of the runs below 600°C while a nimonic alloy was used for higher temperature runs. The bombs were heated in electric furnaces controlled by Sunvic energy controllers and errors in control and temperature measurement were within ± 7°C.

Kaolinite–quartz mixes proved to be reasonably reactive and represent a possible natural assemblage. Natural kaolinite (sample 15082, Geology Department, University of Otago) and finely ground quartz were mixed in the molecular proportion $Al_2O_3.4SiO_2$ for the majority of the runs. Amorphous (chromatographic) alumina–quartz and amorphous silica–kaolinite mixes were also used to test the effect of starting material on fields of syntheses.

The sample was placed in a silver capsule with ends pinched off but not sealed. Temperatures were measured with chromel–alumel thermocouples and pressures with a Bourdon gauge. Runs were terminated by release of pressure and air quenching. Under these conditions hydration is impossible and extensive dehydration of hydrous phases is unlikely. Separate experiments indicated that pyrophyllite does not dehydrate under these conditions. It may also be noted that with air quenching the first 100°C fall in temperature at 350°–600°C is extremely rapid. Products were examined with a Philips X-ray diffractometer using filtered Cu radiation.

Experimental Results

Table 1. Phases produced from amorphous alumina–quartz ($Al_2O_3 + 4SiO_2$) at various temperatures and pressures

Run no.	Temp. (°C)	Water pressure (lb/in^2)	Time (days)	Products
PM31	376	15,000	5	Quartz + kaol.
PM56	384	15,000	11	Quartz + kaol. + pyroph.
PM42	398	15,000	7	Quartz + pyroph.
PM43	434	15,000	6	Quartz + pyroph.
PM45	446	15,000	12	Quartz + cor.
PM33	498	15,000	14	Quartz + cor.
PM34	589	15,000	14	Quartz + cor.
PM41	724	10,000	7	Quartz + cor.
PM32	693	10,000	14	Quartz + cor.
PM27	756	7,500	7	Quartz + mull.
PM71	377	30,000	7	Quartz + kaol. + boeh. + mont.
PM69	392	30,000	7	Quartz + kaol. + boeh. + pyroph.
PM52	418	30,000	7	Quartz + pyroph. + mont.
PM208	460	30,000	10	Quartz + pyroph.
PM68	467	30,000	7	Quartz + cor.
PM49	498	30,000	7	Quartz + cor.
PM67	390	45,000	4	Quartz + kaol. + boeh.
PM59	402	45,000	4	Quartz + kaol. + pyroph.
PM74	419	45,000	4	Quartz + pyroph.
PM54	439	45,000	4	Quartz + pyroph.
PM75	470	45,000	4	Quartz + cor.
PM203	545	45,000	21	Quartz + cor.
PM225	407	60,000	2	Quartz + kaol. + boeh.
PM226	425	60,000	$2\frac{1}{2}$	Quartz + kaol. + pyroph.
PM193	443	60,000	$2\frac{1}{2}$	Quartz + pyroph.
PM229	467	60,000	3	Quartz + pyroph.
PM230	479	60,000	2	Quartz + cor.

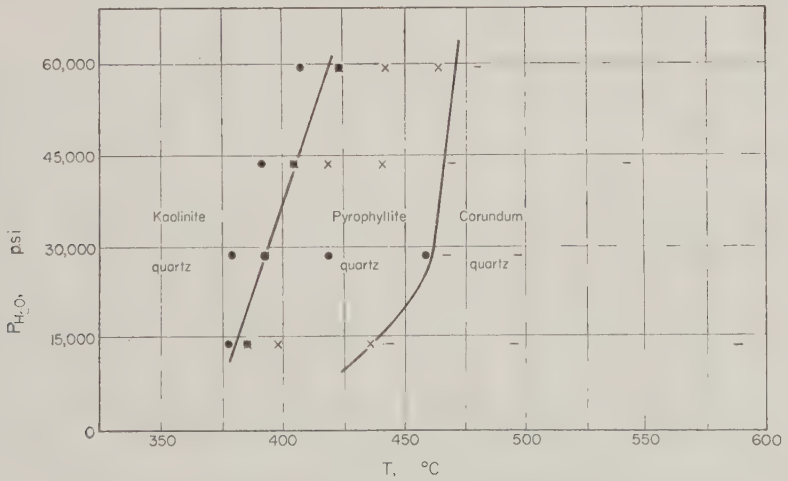

Fig. 1. Fields of synthesis of phases formed from amorphous alumina and quartz. Minor amounts of boehmite were present in some low-temperature runs indicating sluggish reaction between this phase and quartz (cf. Table 1). ● represents kaolinite or montmorillonite, × represents pyrophyllite, □ represents X-andalusite, ○ represents mullite, — represents corundum.

Table 2. Phases produced from amorphous silica–kaolinite ($Al_2O_3 + 4SiO_2$) at various temperatures and pressures

Run No.	Temp. (°C)	Water pressure (lb/in^2)	Time (days)	Products
PM125	342	15,000	11	Kaol. + crist. + mont.
PM128	356	15,000	8	Kaol. + pyroph. + crist.
PM122	363	15,000	10	Pyroph. + crist.
PM121	426	15,000	9	Pyroph. + crist.
PM133	535	15,000	6	Pyroph. + crist.
PM162	565	15,000	6	X-and. + mull. + crist. + quartz
PM124	347	30,000	7	Kaol. + crist. + mont.
PM127	362	30,000	7	Pyroph. + ?crist.
PM123	385	30,000	7	Pyroph. + crist.
PM129	496	30,000	7	Pyroph. + crist.
PM163	527	30,000	6	Pyroph. + crist.
PM161	542	30,000	6	Mull. + quartz
PM132	351	45,000	7	Kaol. + ?crist. + mont.
PM136	361	45,000	5	Pyroph. + kaol. + ?crist.
PM138	381	45,000	5	Pyroph. + ?crist.
PM126	506	45,000	8	Pyroph. + crist.
PM135	535	45,000	4	Pyroph. + crist.
PM137	545	45,000	3	Pyroph. + quartz + mull. + ?X-and.

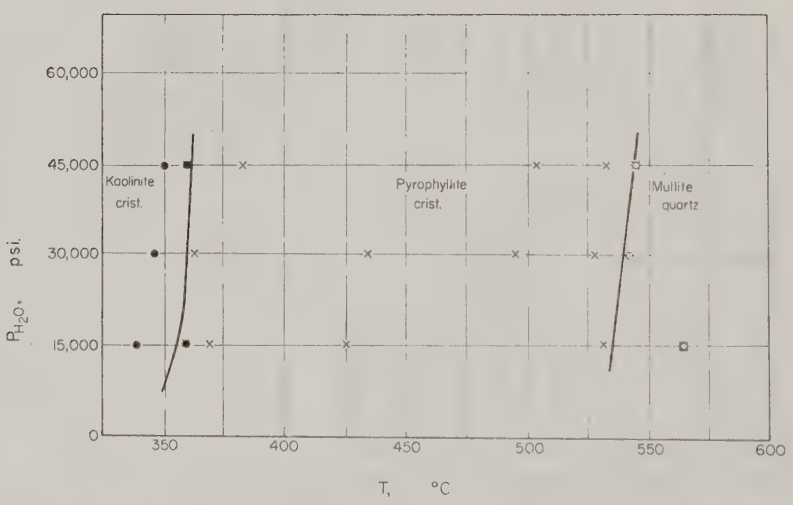

Fig. 2. Fields of synthesis of phases formed from kaolinite and amorphous silica (cf. Table 2). See caption to Fig. 1 for explanation of symbols.

Table 3. Phases produced from kaolinite–quartz ($Al_2O_3 + 4SiO_2$) at various pressures and temperatures

Run no.	Temp. (°C)	Water pressure (lb/in^2)	Time (days)	Products
PM83	396	15,000	9	Quartz + kaol. + mont.
PM73	414	15,000	7	Quartz + kaol. + pyroph.
PM79	418	15,000	9	Quartz + pyroph.
PM115	465	15,000	14	Quartz + pyroph.
PM107	475	15,000	14	Quartz + pyroph. + X-and.
PM99	500	15,000	7	Quartz + pyroph. + X-and.
PM100	511	15,000	14	Quartz + X-and.
PM141	520	15,000	14	Quartz + X-and. + mull.
PM116	539	15,000	15	Quartz + mull.
PM78	695	15,000	7	Quartz + mull.
PM76	407	30,000	7	Quartz + kaol.
PM86	421	30,000	7	Quartz + pyroph.
PM80	454	30,000	7	Quartz + pyroph.
PM88	471	30,000	6	Quartz + pyroph. + X-and.
PM117	474	30,000	2	Quartz + pyroph. + X-and.
PM95	499	30,000	7	Quartz + X-and.
PM119	506	30,000	9	Quartz + pyroph. + X-and.
PM140	526	30,000	7	Quartz + X-and. + mull.
PM143	547	30,000	7	Quartz + mull. + X-and.
PM84	402	45,000	6	Quartz + kaol.
PM90	426	45,000	5	Quartz + pyroph.
PM87	460	45,000	6	Quartz + pyroph.
PM89	480	45,000	6	Quartz + pyroph. + X-and.
PM114	506	45,000	14	Quartz + pyroph. + X-and.
PM98	523	45,000	5	Quartz + X-and. + pyroph.
PM150	540	45,000	7	Quartz + mull. + X-and.

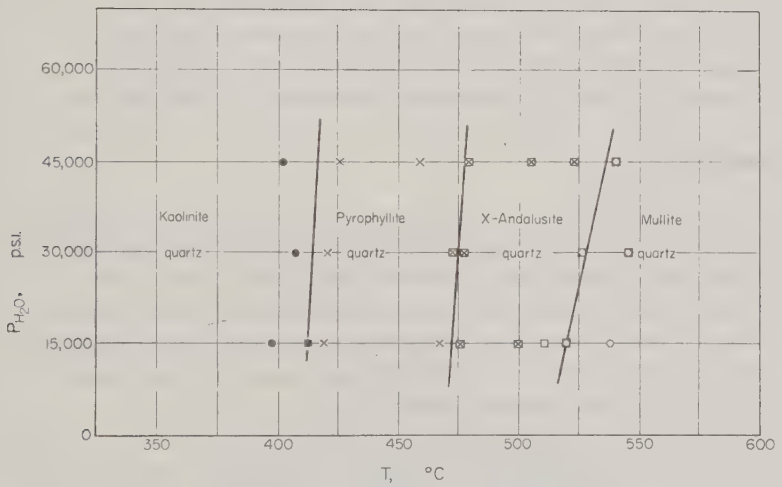

Fig. 3. Fields of synthesis of phases formed from kaolinite and quartz (cf. Table 3). It will be noted that pyrophyllite is present in most runs containing X-andalusite. See caption to Fig. 1 for explanation of symbols.

Table 4. Phases produced from decomposition of synthetic assemblages at various temperatures and pressures

Run no.	Starting material	Temp. (°C)	Water pressure (lb/in²)	Time (days)	Products
PM156	Pyroph. + quartz	467	15,000	8	Quartz + pyroph. + ?X-and.
PM157	Pyroph. + quartz	483	15,000	14	Quartz + pyroph. + ?X-and.
PM155	Pyroph. + quartz	488	15,000	9	Quartz + pyroph. + X-and.
PM148	Pyroph. + quartz	507	15,000	14	Quartz + pyroph. + X-and.
PM154	Pyroph. + quartz	514	15,000	7	Quartz + pyroph. + X-and.
PM158	Pyroph. + quartz	486	25,000	7	Quartz + pyroph. + X-and.
PM149	Pyroph. + quartz	498	30,000	12	Quartz + pyroph. + X-and.
PM152	Pyroph. + quartz	516	30,000	7	Quartz + pyroph. + ?X-and.
PM145	Pyroph. + quartz	548	30,000	8	Quartz + pyroph. + X-and. + mull.
PM160	Pyroph. + quartz	478	45,000	8	Quartz + pyroph. + X-and.
PM159	Pyroph. + quartz	499	45,000	11	Quartz + pyroph. + C-and.
PM153	Pyroph. + quartz	525	45,000	5	Quartz + pyroph. + X-and.
PM142	X-and. + quartz	439	20,000	7	Quartz + pyroph. + X-and.
PM118	X-and. + quartz	490	25,000	12	Quartz + X-and.
PM146	Mull. + quartz	515	15,000	14	Quartz + mull.
PM147	Mull. + quartz	519	45,000	7	Quartz + mull.

Abbreviations used: kaol. = kaolinite, pyroph. = pyrophyllite, cor. = corundum, X-and. = X-andalusite, boeh. = boehmite, mull. = mullite, crist. = cristobalite, mont. = Al montmorillonite, ? signifies doubtful presence.

Discussion

The kaolinite synthesis and breakdown field

The kaolinite–pyrophyllite boundary is markedly dependent on starting material; amorphous alumina–quartz and amorphous silica–kaolinite mixes lead to lower boundary temperatures than quartz kaolinite mixes. The appearance of montmorillonite near the kaolinite–pyrophyllite boundary is not unexpected since Roy and Osborn (1954) have synthesized an aluminium montmorillonite in this system and have suggested that it may be stable up to 420°C in the presence of excess silica and water. No attempt has been made in the present investigation to resolve the stability relations between kaolinite, montmorillonite and pyrophyllite.

The pyrophyllite synthesis field

Pyrophyllite was successfully synthesized from all three starting materials. When silica is present in the starting material as quartz, the pyrophyllite field is noticeably smaller than that determined by Kennedy (1955) and by Roy and Osborn (1954) and that determined by the present writers using amorphous silica. For example at 1000 bars the field of pyrophyllite is narrower by 100°C.

The dependence on the nature of the starting material can be simply explained by reference to the silica content of pyrophyllite.

$$\text{Pyrophyllite} = Al_2Si_4O_{10}(OH)_2$$
$$\text{Kaolinite} = Al_2Si_2O_5(OH)_4$$
$$\text{Andalusite} = Al_2SiO_5$$
$$\text{Mullite} = Al_6Si_2O_{13}$$

Pyrophyllite contains more silica relative to alumina than any of the other aluminium silicates synthesized. Hence the starting material capable of producing the highest silica activity in solution should give the broadest pyrophyllite field. The field produced from amorphous silica–kaolinite is twice as broad as the fields produced from starting materials containing comparatively insoluble quartz as the principal source of silica. Amorphous silica rapidly crystallizes to cristobalite from solutions in super-critical water (Carr and Fyfe, 1958), but will be more soluble than quartz. The pyrophyllite synthesis fields obtained from amorphous alumina–quartz and kaolinite–quartz are approximately of the same extent and shape. Since a high alumina activity should be provided by the amorphous alumina–quartz mix one might expect kaolinite to be favoured. But once the alumina has all disappeared with the formation of kaolinite then the reaction will take place under the same conditions as for the starting material kaolinite–quartz.

Although the effect of silica activity provides a reasonable explanation for the broad pyrophyllite field in Fig. 2, differences in nucleation rates can also modify the synthesis fields as may be the case for the andalusite–mullite relations discussed below.

The corundum synthesis field

Corundum was synthesized from amorphous alumina–quartz at temperatures above 470°C and persisted to 750°C at 7500 lb/in² water pressure when mullite was formed. Aramaki and Roy (1958) have reported indications of a stability field for the assemblage quartz–corundum in a P–T area centring around 600°C and 4000 atm. Without reliable data on heats of reaction (which are probably very small) it is not possible on thermodynamic grounds to eliminate this possibility but petrological evidence suggests that this is a metastable assemblage. If the rate of formation of corundum is faster than the rate of formation of aluminosilicates and if the free energy of the reaction

$$\text{corundum} + \text{quartz} \leftrightarrows \text{andalusite}$$

is small, then the degree of supersaturation necessary for rapid nucleation of aluminium silicates may never be achieved. Long runs with synthetic corundum–quartz did not give anhydrous aluminosilicates. The lack of readily available alumina in the other two starting materials used probably precludes the facile nucleation of corundum and hence favours the synthesis of anhydrous aluminosilicates.

X-andalusite: description and synthesis field

An andalusite-like phase (designated X-andalusite) was synthesized from kaolinite–quartz and pyrophyllite–quartz. Microscopic examination of all synthetic samples showed the phase to occur in cloudy, amorphous-looking aggregates, lacking appreciable birefringence and with a refractive index of about 1·62–1·63. X-ray diffraction data for natural andalusite from Clooney, Donegal, Ireland and X-andalusite are presented in Table 5. The stronger lines ascribed to X-andalusite are consistently close to andalusite lines, but have slightly larger spacings. Some important andalusite lines (e.g. 4·54 Å) are missing. Weak lines ascribed to X-andalusite which do not match andalusite lines may be of doubtful significance.

Aramaki and Roy (1959) suggest that their AS(H)-II may possibly have the same relation to andalusite as mullite has to sillimanite. It is also conceivable that X-andalusite may have hydroxyl substituting for SiO_4 as in the grossularite-hydrogrossular series in which the substitution is accompanied by lowering of refractive index and expansion of cell dimensions (Yoder, 1950).

In all except three of the runs where kaolinite–quartz was used, pyrophyllite

Table 5

Andalusite			X-andalusite		
d (Å)	I	2θ	d (Å)	I	2θ
5·54	100	15·98	5·58	100	15·89
4·54	40	19·56	4·14	10	21·44
3·93	15	22·62	3·96	35	22·41
3·52	10	25·25	3·52	15	25·30
3·50	30	25·47	2·83	10	31·63
2·78	100	32·26	2·79	60	32·10
2·495	20	35·995	2·521	10	35·60
2·486	20	36·13	2·359	15	38·14
2·469	15	36·40	2·335	10	38·56
2·375	5	37·84	2·228	15	40·48
2·353	10	38·24	2·213	10	40·76
2·348	5	38·33	2·182	10	41·39
2·276	10	39·59	2·145	10	42·13
2·272	10	39·66			
2·254	35	39·98			
2·248	20	40·10			
2·183	20	41·37			
2·172	25	41·57			

persisted throughout the field in which X-andalusite was synthesized. X-andalusite, in turn, appeared to persist into the mullite field. Many runs not listed in Table 3 were conducted in order to resolve this problem of mixtures but run times were not sufficiently long for metastable phases to disappear from such mixes. A quartz–pyrophyllite–X-andalusite mixture could be produced in 2 days and persisted in runs of 14 days. However, the observed partial decomposition of the assemblage pyrophyllite–quartz to pyrophyllite-X-andalusite-quartz (see Table 4) indicates that X-andalusite–quartz is more stable than pyrophyllite–quartz in most of its synthesis field of Fig. 3. Further, the formation of pyrophyllite from X-andalusite (Table 4) confirms the relative stability pyrophyllite in Fig. 3.

The results presented here indicate a positive boundary slope between the synthesis fields of X-andalusite and mullite. As neither the composition nor density of X-andalusite are known, no predictions regarding this slope can be made. Aramaki and Roy (1958), and Clark, *et al.* (1957) have suggested a negative slope for the boundary between andalusite and mullite. As mullite + quartz is the high-temperature assemblage it must also be the high-entropy assemblage. Although there are large differences in the reported values of the

density of mullite, all indicate a small positive ΔV for the reaction andalusite to mullite and quartz and hence a positive boundary slope seems more likely.

The importance of starting material

Using the arguments of Coombs *et al.* (1959) it is possible to make qualitative predictions of the magnitude of the effect of amorphous starting materials on synthesis fields if the position of the synthesis field determined with a crystalline mix is known.

Consider the effect of silica activity on the pyrophyllite–X-andalusite boundary. Data from synthesis and decomposition experiments indicate that the reaction:

$$\underset{\text{pyrophyllite}}{Al_2(Si_4O_{10})(OH)_2} \rightarrow \underset{\text{X-andalusite}+\text{quartz}+\text{water}}{\text{“}Al_2SiO_5\text{”} + 3SiO_2 + H_2O}$$

proceeds reversibly at 475°C and 30,000 lb/in². For this reaction, if at equilibrium $\Delta G = 0$, and the ΔS of dehydration might be of the order of 10–15 cal/°C per H_2O molecule. Therefore ΔH at 475°C can be determined and, to a first approximation, is assumed to be independent of temperature. If cristobalite (produced by the rapid crystallization of amorphous silica) is substituted for quartz the above reaction will have a ΔG of the order of +900 cal (Rossini *et al.*, 1952) and equilibrium would be shifted to a temperature 60–90°C higher. The expected boundary displacement is demonstrated both in direction and order of magnitude by the data in Tables 2 and 3.

It might be argued that high silica activity would also favour andalusite rather than mullite since andalusite (and probably X-andalusite also) has the larger silica content. This is not borne out by the results. The assumption that nucleation rates of all possible phases are comparable is implied in the above argument but may not be the case. In a mixture with low activity of starting materials, a metastable product such as mullite may not be able to form in the andalusite field. If the starting materials are amorphous and active then the expected ready nucleation of the high-temperature phase (and hence high-entropy phase), mullite, may obliterate the expected expansion of the field of andalusite.

The identification of mullite

Mullite cannot be easily distinguished from sillimanite by X-ray methods and the presence of either of these phases in synthetic products always constitutes a major problem of identification. De Keyser (1951) reports that it is possible to distinguish the minerals by observing X-ray reflections in the 65–77° 2θ range. Unfortunately the samples produced in the present investigation were too poorly crystalline to be examined satisfactorily in this region. Hence small, but significant, differences between lattice spacings in the 31–41° range of 2θ were used. De Keyser gives the following spacings for certain corresponding lines in sillimanite and mullite:

	Sillimanite		Mullite	
	d (Å)	2θ	d (Å)	2θ
(1)	2·885	31·0	2·885	31·0
(2)	2·667	33·6	2·683	33·4
(3)	2·536	35·4	2·536	35·4

The angular distances between these lines were measured for three mullite samples from fire bricks and refractory tube, and two sillimanite samples. Average values (in $\Delta 2\theta$ for Cu $K\alpha$ radiation) are as follows:

	Sillimanite	Mullite
$\Delta 2\theta$, 1–2	2·46°	2·29°
$\Delta 2\theta$, 2–3	1·87°	2·00°

All of the mullite-like samples synthesized in the present experiments were examined and average values for three of them are given below:

	PM78	PM116	PM143
$\Delta 2\theta$, 1–2	2·33°	2·22°	2·21°
$\Delta 2\theta$, 2–3	2·00°	2·03°	2·06°

The high-temperature phase synthesized in the present investigation is thus much closer to mullite than to sillimanite.

Conclusions

The use of quartz and natural kaolinite or pyrophyllite as starting materials for synthesis should result in a closer approach to natural conditions than is attained with amorphous mixes, the possibility of metastable crystallization being reduced. Nevertheless, the formation of mixtures and the appearance of X-andalusite instead of a geologically common phase such as andalusite or sillimanite suggest that equilibrium was not obtained in the present experiments.

The reversible decomposition of pyrophyllite to X-andalusite fixes an upper limit to the stability field of pyrophyllite. The breakdown to andalusite or sillimanite should occur at lower temperatures at the same pressure. The data in Fig. 1 set an upper limit to the stability of kaolinite or montmorillonite.

It is apparent from the present results that, in this system, the least reactive starting materials produce phases more compatible with geological observations.

Acknowledgements—The writers are greatly indebted to Professor D. S. Coombs for his constant advice during this work and critical reading of the manuscript. Thanks are also due to Professor R. R. Nimmo and S. Hughes of the physics department for assistance with X-ray facilities. Invaluable technical assistance was furnished by V. G. Tyrrell and L. Wylie. The work was made possible by support from New Zealand University Research Fund and the Mellor Fund. One of the writers (R. M. C.) held an I.C.I. fellowship.

References

Aramaki S. and Roy R. (1958) Further equilibrium studies in the system Al_2O_3 SiO_2—H_2O under hydrostatic and uniaxial pressure. *Bull. Geol. Soc. Amer.* **69**, 1530 (Abstract).

Aramaki S. and Roy R. (1959) Detailed X-ray data on mullite and two new anhydrous aluminosilicates AS(H)-II and high-temperature sillimanite. *Bull. Geol. Soc. Amer.* **70**, 1562 (Abstract).

Carr R. M. and Fyfe W. S. (1958) Some observations on the crystallization of amorphous silica. *Amer. Min.* **43**, 908–916.

Clark S. P., Robertson E. C. and Birch F. (1957) Experimental determination of kyanite–sillimanite equilibrium relations at high temperatures and pressures. *Amer. J. Sci.* **255**, 628–640.

Coombs D. S., Ellis A. J., Fyfe W. S. and Taylor A. M. (1959) The zeolite facies, with comments on the interpretation of hydrothermal synthesis. *Geochim. et Cosmochim. Acta* **17**, 53–107.

Griggs D. T. and Kennedy G. C. (1956) A simple apparatus for high pressures and temperatures. *Amer. J. Sci.* **254**, 722–735.

Hemley J. J. (1959) Some mineralogical equilibria in the system K_2O—Al_2O_3—SiO_2—H_2O. *Amer. J. Sci.* **257**, 241–270.

Kennedy G. C. (1955) Pyrophyllite–sillimanite–mullite equilibrium relations to 20,000 bars and 800°C. *Bull. Geol. Soc. Amer.* **66**, 1584 (Abstract).

Keyser W. L. de (1951) Study of sillimanite and mullite by X-rays. *Trans. Brit. Ceram. Soc.* **50**, 349–364.

Rossini F. D., Wagman D. D., Evans W. H., Levine S. and Jaffe I. (1952) *Selected Values of Chemical Thermodynamic Properties.* National Bureau of Standards Circular 500. Superintendent of Documents, Washington, D.C.

Roy D. M. (1954) Hydrothermal synthesis of andalusite. *Amer. Min.* **39**, 140–143.

Roy R. and Osborne E. F. (1945) The system Al_2O_3—SiO_2—H_2O. *Amer. Min.* **39**, 853–885.

Yoder H. S. (1950) Stability relations of grossularite. *J. Geol.* **58**, 221–253.

Geochimica et Cosmochimica Acta, 1960, Vol. 21, pp. 110 to 126. Pergamon Press Ltd. Printed in Northern Ireland

Carbon isotope fractionation during photosynthesis

R. Park* and S. Epstein
Division of Geological Sciences, California Institute of Technology,
Pasadena, California

(*Received* 1 *September* 1959)

Introduction

Systematic differences in the C^{13}/C^{12} ratio of various reservoirs in the carbon cycle have been known since the work of Nier and Gulbransen (1939). Isotopic variations between these reservoirs are a consequence of the differences in chemical and physical properties of different isotopic species of a molecule (Urey, 1947). Various aspects of C^{13}/C^{12} ratio variations in natural materials have been considered by Craig (1953), who made a thorough survey of carbon isotope variations using a precise mass spectrometer, by Wickman (1952), by Baertschi (1953), and others. From these researches it is apparent that one of the important steps in the carbon cycle which contributes both directly and indirectly to C^{13}/C^{12} variation of carbon-containing materials in nature is the photosynthetic fixation of carbon by marine and terrestrial plants.

Although it is known that photosynthesis is accompanied by an isotopic fractionation which favours the fixation of C^{12} into the plants, the mechanism for this fractionation is not known. As a result, the reasons for the large variations in the C^{13}/C^{12} ratio between various plants are not understood. It is desirable to understand the reasons for isotopic fractionation in photosynthesis and the various factors controlling it, because such knowledge should contribute to the elucidation of the CO_2 fixation process *per se* and, at the same time, provide information which is pertinent to the interpretation of C^{13}/C^{12} ratios of fossil carbon deposits.

Some data pertinent to the above problem are the measured differences between the C^{13}/C^{12} ratios of atmospheric carbon dioxide and plant material in the controlled laboratory experiment done by Baertschi (1953). Baertschi observed an isotope fractionation between CO_2 and fixed plant carbon of 1·026. Baertschi (1952) also demonstrated that the difference in rate of collision of the two carbon isotopic species of carbon dioxide against the absorbing surface of the leaf can not explain the C^{13}/C^{12} fractionation associated with photosynthesis. In addition he concluded that the respired CO_2 has the same C^{13}/C^{12} ratio as the plant (Baertschi, 1953). Wickman (1952) analysed a wide taxonomic variety of plants collected from different ecological environments and concluded that the variations in the C^{13}/C^{12} ratio between different plants were due to variations in the C^{13}/C^{12} ratio of atmospheric carbon dioxide. Wickman suggested that local carbon cycles of relatively low C^{13}/C^{12} ratio could form under certain conditions, thereby giving rise to plants of unusual C^{13}/C^{12} ratio. Keeling's (1958) results on the variation

* Present address: University of California Radiation Laboratory, Berkeley, California.

of the C^{13}/C^{12} ratio in atmospheric CO_2 collected at a variety of localities showed that the C^{13}/C^{12} ratio in atmospheric CO_2 goes through a diurnal cyclic variation in which C^{12} rich CO_2 is added to the atmosphere during the night due to plant respiration and is absorbed during the day due to preferential fixation of $C^{12}O_2$ during photosynthesis. However, these variations were not sufficiently great to account for the existing ranges in values of the isotope ratio of plants and also did not explain the reason why, in many cases, adjacent plants can still be isotopically different. Craig (1954) argued against the explanation of Wickman. Craig favoured the reasonable possibility that some fractionation of the carbon isotopes takes place in the internal reactions of the plant and that the environment may influence the magnitude of these fractionations.

Analytical Techniques

(a) *Mass spectrometer analysis*

The CO_2 samples were analysed in a Nier sixty-degree sector-type mass spectrometer which incorporates the improvements described by McKinney *et al.* (1950) for determining C^{13}/C^{12} and O^{18}/O^{16} ratios to $\pm 0{\cdot}1$ per mil. All values obtained were corrected for mixing of the standard and sample gas, and for the O^{17} contribution to the mass-45 peak. The corrections are described in detail by Craig (1957). The results are presented as per mil deviations of the C^{13}/C^{12} ratio of the sample, from CO_2 prepared from a Cretaceous belemnite, *Belemnitella americana*, from the Peedee formation of South Carolina. This standard (PDB) is the one which has been used at the University of Chicago.

The relative isotopic composition (δ) of a sample is then given as follows:

$$\delta, ‰ = \left(\frac{(C^{13}/C^{12}\ \text{sample})}{(C^{13}/C^{12}\ \text{standard})} - 1 \right) \times 10^3.$$

Thus, samples enriched in C^{12} as compared to the standard assume negative values while samples enriched in C^{13} as compared to the standard assume positive values. The precision of the δ is $\pm 0{\cdot}1$ per mil.

The enrichment factor or fractionation factor between two compounds, A and B, is defined as:

$$\alpha = \frac{C^{13}/C^{12}A}{C^{13}/C^{12}B}$$

also
$$\alpha \simeq \frac{1 + \delta_A/1000}{1 + \delta_B/1000}$$

or
$$\alpha \simeq 1 + \frac{\delta_A - \delta_B}{1000}.$$

Thus if
$$\delta_A - \delta_B = 10‰$$
the fractionation factor between A and $B \simeq 1{\cdot}010$.

(b) *Combustion of samples*

Plant materials were converted to CO_2 according to the procedure described by Craig (1953). In this procedure samples are combusted over copper oxide in an

oxygen atmosphere at 800-900°C. After cycling the gases through the combustion tube with an automatic Toepler pump for 30 min, the CO_2 produced is collected in a liquid nitrogen trap and excess oxygen is pumped away. The trap is then warmed in a dry-ice bath and the CO_2 is distilled into a sample tube which is at liquid nitrogen temperature. Water and most other contaminants remain in the trap at the dry-ice temperature.

(c) *Preparation of* CO_2 *from calcium carbonate*

Carbon dioxide was prepared from calcium carbonate according to the procedure described by McCrae (1950). Phosphoric acid (100%) is placed in the side arm of a reaction vessel and the calcium carbonate sample is placed in the central portion of the vessel. After evacuation, the acid is tipped into the calcium carbonate and is allowed to react for 1 hr. The volume of CO_2 is then measured manometrically and transferred into a sample tube.

Experimental Procedures and Results

(a) *Determination of the fractionation factor between* CO_2 *and fixed plant carbon under controlled conditions*

As an initial step in an investigation of C^{13}/C^{12} fractionation during photosynthesis it seemed desirable to repeat and extend the experiments of Baertschi

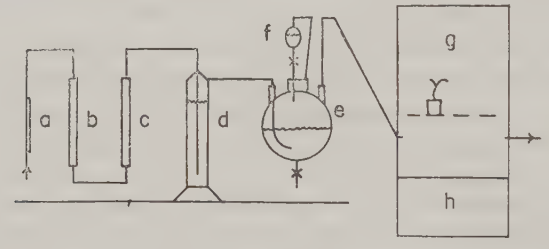

Fig. 1. Temperature controlled booth and CO_2 generating apparatus. (a) flowmeter, (b) tube filled with anhydrous $CaCl_2$ plus ascarite, (c) ascarite-filled tube, (d) $Ba(OH)_2$ trap, (e) flask containing $CaCO_3$ slurry, (f) hydrochloric acid, (g) booth containing growing plants, (h) temperature controlling mechanism and fan.

using tomato rather than bean plants. Tomato seeds are small and contribute little carbon to the final plant. Therefore the carbon harvested should be, for all practical purposes, that which is photosynthetically fixed under controlled conditions.

Tomato seeds (var. Extra Early) were germinated on moist vermiculite at 26°C for 5 days in the dark. At the end of this time the etiolated seedlings were removed from the dark, planted in individual cups and placed in the temperature-controlled lucite booth shown in Fig. 1. Booth temperature was maintained at 26°C during the day and at 22°C during the night, both constant to ± 1°C. A bank of fluorescent bulbs over the booth gave a light intensity of 1000 ft-candles at the level of the plants, and was controlled by a central time clock in the Earhart Plant Research Laboratory to give a 12 hr photoperiod. In several experiments sunlight was used as the light source.

Carbon dioxide of known C^{13}/C^{12} ratio was admitted to the booth by acidification of $CaCO_3$ with HCl. Carbon dioxide derived in this way was generated at a rate 200 times faster than the photosynthetic fixation capacity of the plants at maximum size. The CO_2 was diluted to the desired concentration by adding air from which atmospheric CO_2 had been removed. Such air was prepared from Earhart Laboratory compressed air which was first dried with anhydrous $CaCl_2$. It was then passed through tubes 1·5 cm in diameter and 80 cm in length containing NaOH coated asbestos (Ascarite) and finally through a $Ba(OH)_2$ trap. Air

Table 1. The effect of the drying method on the C^{13}/C^{12} ratio of tomato leaves

CO_2 source	δ of fresh leaves (per mil)	δ of dried leaves (per mil)
Air	−29·9	−30·1
$CaCO_3$	−25·6	−26·0

washed in this way contains no CO_2 when assayed with an infrared CO_2 analyser or when passed through a series of liquid nitrogen traps. The ability of ascarite to remove CO_2 under experimental conditions was also demonstrated by the fact that the $Ba(OH)_2$ solution never became cloudy. Variations in air flow rate and acidification rate of $CaCO_3$ gave a 10 per cent error in the concentration of CO_2 being given to the plants during an experiment.

Dark-germinated seedlings were placed in the booth during the evening, which allowed 12 hr for the booth to flush with CO_2 of known isotopic composition and concentration before the lights were turned on. During this time the booth was flushed with seven times its own volume of new atmosphere. Calcium carbonate and HCl were added as necessary to the CO_2 generation chamber. The ascarite and $CaCl_2$ tubes were replaced every 12 hr even though the white zone, indicating Na_2CO_3, was present only a few centimetres down the tube.

The plants were watered with nutrient solution (Hoagland's) once per day by removing the rubber cork containing the air outlet tube and inserting a metal hose. This operation took less than 1 min and was performed in the evening so that any contamination with atmospheric CO_2 would be flushed from the booth before the lights were turned on.

At the end of 13 days, the young plants were removed from the booth and dried in a vacuum desiccator over H_2SO_4. Any loss of volatile compounds from the plants under these conditions was not sufficient to change, significantly, the isotopic composition. This was shown by analysing plants directly without the drying process. These results are given in Table 1.

In the initial experiments, 1·5 per cent CO_2 (by volume) of known isotopic composition was used as the carbon supply for photosynthesis. This CO_2 concentration represents an unnatural condition since the CO_2 content of normal air is only 0·03-0·04 per cent. Further experiments were therefore run using CO_2 concentrations approximating those which are present in nature. Experiments to determine the effects of light intensity on photosynthetic fractionation were also carried out.

The $CaCO_3$ which was used as a source of CO_2 was analysed according to the procedure described by McCrea (1950). The δ-value for this carbon was found to be 2·6 per mil.

Nineteen plants were grown for 13 days in an atmosphere containing 1·5 per cent CO_2 and were prepared for analysis as described above. The initial etiolated seedlings averaged 1·7 mg dry weight and had a δ-value of −24·9 per mil. The final plants weighed (dry) from 42 to 68 mg. The leaves, stems and roots (excluding the cotyledons) from three plants were analyzed separately. These results are given in Table 2.

Table 2. C^{13}/C^{12} ratios of tomato plants grown in 1·5% CO_2 (δ = 2·6‰)

Plant no.	Dry wt. (mg)	δ of leaves (per mil)	δ of stems (per mil)	δ of roots (per mil)
AP-2	67·5	−25·3	−25·0	−24·7
AP-4	41·8	−25·0	−24·7	−24·7
AP-5	54·1	−24·5	−24·2	−24·2
Average		−24·9	−24·6	−24·5

The C^{13}/C^{12} ratio of the stems may be used as the average value for that of the plant as a whole. The enrichment factor is:

$$\frac{C^{13}/C^{12}CO_2}{C^{13}/C^{12}\text{ plant}} = 1{\cdot}0279.$$

The experiment was then repeated and the results from the repeat experiment are given in Table 3. Again taking the δ-value for the stems as the average value, the enrichment factor may be calculated:

$$\frac{C^{13}/C^{12}CO_2}{C^{13}/C^{12}\text{ plant}} = 1{\cdot}0285.$$

Table 3. C^{13}/C^{12} ratios of tomato plants grown in 1·5% CO_2 (δ = 2·6‰)
(Repeat experiment)

Plant no.	Dry wt. (mg)	δ of leaves (per mil)	δ of stems (per mil)	δ of roots (per mil)
BP-2	50·0	−26·1	−25·1	−24·6
BP-3	47·4	−25·8	−25·4	−24·4
BP-4	37·0	−26·1	−25·2	−24·3
Average		−26·0	−25·2	−24·4

The preceding experiments were next repeated using lower CO_2 concentrations. The results of these experiments are given in Table 4, and a summary of the fractionation factors at different CO_2 concentration is given in Table 6.

Table 4. C^{13}/C^{12} ratio of a tomato plant grown in low concentrations of CO_2 ($\delta = 2{\cdot}6‰$)

CO_2 concentration (%)	Dry wt. (mg)	δ of leaves (per mil)	δ of stems (per mil)	δ of roots (per mil)	δ of cotyledons (per mil)	Whole plant
0·05	35·1	−23·4	−22·8	−23·1	−22·8	—
0·015	9·3	—	—	—	—	−21·6

(c) *Effects of high light intensities on the fractionation factors of photosynthesis*

This experiment was designed to determine whether light intensities greater than 10^3 ft-candles influence the fractionation factor of tomato plants grown in 1·5 per cent CO_2 (δ of $CO_2 = 2{\cdot}6$ per mil). High light intensities were obtained by moving the booth and carbon dioxide generating unit into a greenhouse exposed to natural sunlight. Under these conditions a light intensity of 2000 ft-candles was recorded inside the booth during midday. The experiment was run during late April and early May so that the day-length exceeded 12 hr. The experiment was run for 13 days. Results are given in Table 5. By taking the stems as an average value, the fractionation factor may be computed:

$$\frac{C^{13}/C^{12}CO_2}{C^{13}/C^{12}\text{ plant}} = 1{\cdot}0277.$$

Table 5. C^{13}/C^{12} ratio of a tomato plant grown at high light intensity in 1·5% CO_2 ($\delta = 2{\cdot}6‰$)

Plant no.	Dry wt. (mg)	δ of leaves (per mil)	δ of stems (per mil)	δ of roots (per mil)
HP-1	48·4	−24·7	−24·4	−24·1

The data of the foregoing experiments are summarized in Table 6. It is seen that greater C^{12} enrichment occurs at high CO_2 concentrations, and that light intensity is not important over the intensity range studied.

Table 6. Summary of fractionation factors for tomato plants grown in different CO_2 concentrations

CO_2 conc. (vol. %)	Av. plant wt. (mg)	Fractionation factor ±0·0001
1·5 ± 0·15	50·1	1·0279
1·5 ± 0·15	42·1	1·0285
0·05 ± 0·005	35·1	1·0263
0·015 ± 0·002	9·3	1·0247
1·5 ± 0·15 (high light intensity)	48·4	1·0277

(d) *The C^{13}/C^{12} ratio of CO_2 respired by tomato plants of known C^{13}/C^{12} ratio*

The carbon dioxide respired by tomato plants in the dark was obtained using the apparatus of Fig. 2. In this case the chamber was shielded from the light by aluminium foil and the respired CO_2 was flushed from the chamber by a stream of CO_2 free air. The CO_2 was trapped in series of liquid-nitrogen cooled traps. The chamber was of such size that the gas within it was displaced every 20 min. In the case when a sample was taken 10 min after the initiation of the experiment, higher flow rates were used. The δ-values for the respired CO_2 and for the plant are

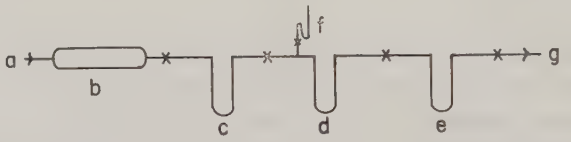

Fig. 2. Apparatus for collection of respired CO_2. (a) air from which CO_2 has been removed, (b) respiratory chamber, (c) dry-ice trap, (d), (e) liquid nitrogen traps, (f) manometer, (g) vacuum pump preceded by liquid-nitrogen trap.

shown in Table 7. The relationship between the δ-values for respired CO_2 and the time of collection relative to the beginning of the dark period is also shown in Fig. 3. It is evident that the C^{13}/C^{12} ratio of respired CO_2 changes with time, the

Table 7. δ-Values for CO_2 respired by tomato plants in which the fixed carbon has the δ-value of $-32{\cdot}4‰$

Elapsed time from start of dark period	δ of respired CO_2 (per mil)
10 min	−24·3
2 hr	−25·8
4 hr	−27·2
6 hr	−27·6
16 hr	−28·2
40 hr	−30·0

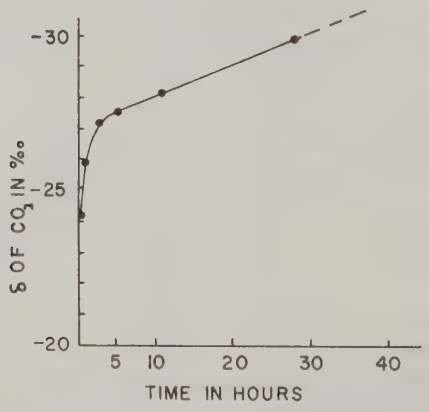

Fig. 3. C^{13}/C^{12} ratios of CO_2 respired by tomato plants in which the fixed carbon has the C^{13}/C^{12} ratio $\delta = -32{\cdot}4‰$.

ratio being largest during the initial stages of respiration. These results are discussed in detail elsewhere (PARK and EPSTEIN 1960) and in the discussion at the end of this paper.

(e) *The δ-values of* CO_2 *dissolved in plant during photosynthesis and respiration*

As indicated in the introduction, the inability to explain the observed fractionation by a process occurring outside the leaf surface suggests that some precursor must exist in the leaf which has a C^{13}/C^{12} ratio intermediate between the plant and atmospheric carbon dioxide. Since the fixation of the CO_2 into carbohydrates

Table 8. Contamination of CO_2 dissolved in tomato leaves by dry ice purposely added to the system
(δ of dry ice = −40‰; δ of plant = −30‰)

Sample no.	Time pumped at −78°C (hr)	Amt. CO_2 (cm^3)	δ of CO_2 (per mil)
1	1	1·0	−33·3
2	3	0·45	−13·3
3	12	0·66	−11·3

occurs in the aqueous matter of plant cells (cytoplasm) it appeared desirable to sample the CO_2 dissolved in the leaf cytoplasm during photosynthesis to determine if this CO_2 is indeed of intermediate isotopic composition.

The procedure used to isolate the dissolved CO_2 of leaves in steady-state photosynthesis was the following. Leaves were removed from a plant in bright light and rapidly frozen. The best freezing method consisted of plunging the leaves under liquid nitrogen immediately upon their removal from the plant. The leaves were then transferred to a precooled flask (−78°C) and the evacuated at dry-ice temperature. Pumping was continued for about 1 hr. The leaves were thawed by pouring 10 ml of 3% H_2SO_4 from a side arm. The CO_2 freed from the pulpy residue of the leaves was collected and analysed. Some precautionary measures had to be taken to ensure that the sample of CO_2 was actually that dissolved in the cytoplasm. To determine the necessary precautions the following series of experiments were done.

After tomato leaves are frozen to liquid nitrogen temperature it is necessary to transfer the leaves to a precooled flask. During this exposure to air, CO_2 could condense on the cold surface of the leaf and not be completely removed by evacuation of the flask at dry-ice temperature. To test this possibility, three frozen tomato leaf samples were prepared and 200 mg of dry-ice added to each sample. The 200 mg of dry ice should represent about one hundredfold more CO_2 than could come in contact with the frozen plant in the normal experimental procedure. Each sample was then pumped for varying lengths of time and a comparison of the yields and C^{13}/C^{12} ratios is given in Table 8. These data show that 3 hr pumping is necessary to remove 200 mg of solidified CO_2 from an evacuated flask at dry ice temperature. The δ-value obtained after this time is very close to that obtained in most of the samples run. It is estimated that a maximum of 60 min of pumping is enough for samples ordinarily prepared. This experiment also shows that little

or no exchange of CO_2 occurs between the leaf and the surrounding atmosphere when the leaf is frozen. This means that exposure of a leaf to air CO_2 after initial freezing in liquid N_2 will not result in appreciable contamination.

A major source of contamination of dissolved CO_2 might be the decarboxylation of keto acids by 3% H_2SO_4. After dilution with the aqueous phase of the plants, the concentration of H_2SO_4 is reduced to about 0·5 N. This concentration of acid undoubtedly decarboxylates some of the more unstable β-keto acids. A number of α-keto acids such as α-keto glutarate exist in plant tissues. Fairly

Table 9. Yields and δ-values of CO_2 released from tomato leaves by various acidification procedures

Acid	CO_2 yield (cm^3/g dry weight of plant tissue)	δ of CO_2 (per mil)
1 N H_2SO_4	1·7	−15·2
1 N Lactic	1·1	−15·4
0·1 M KH_2PO_4	2·1	−16·9
0·1 M KH_2PO_4	4·9	−26·8
(allowed to react 15 hr)	0·9	−25·5
None		
"	0·9	−30·5

rigorous conditions are needed to decarboxylate an α-keto acid. For this reason CO_2 from α-keto acids is probably not an important contaminant. However, β-keto acids exist in small quantities in plants, and, in addition, yield CO_2 under very mild conditions. Virtanen, cited by Thimann and Bonner (1950), reports the presence of 30-40 mg oxaloacetic acid per 100 g of pea plant. This concentration of β-keto acid in tomato leaf samples could produce about 0·2 ml of CO_2. This approximate calculation suggests, therefore, that the observed values for dissolved CO_2 may be a combination of the dissolved CO_2 and the CO_2 derived from plant carbon. Thus the "dissolved CO_2" in tomato leaves may be richer in C^{13} than the values reported in Tables 9, 10 and 11.

One method used to check for possible contamination of dissolved CO_2 by CO_2 from decomposition of organic compounds was to use different acids of varying strength, and to consider the δ-values and yields of CO_2 per unit weight of plant. Table 9 gives the result of such an experiment with field-grown tomato leaves. The amount and δ-value of CO_2 obtained with 0·1 M KH_2PO_4 as the acid was found to be very variable. In one case the phosphate-acidified mixture was permitted to stand overnight. Under these conditions, the yield of CO_2 was very large and the δ-value for the evolved CO_2 was the same as the leaves. This result is apparently due to persistence of enzymic decarboxylation activity under these conditions. Strong acids such as lactic and sulphuric acids consistently gave the highest C^{13}/C^{12} ratios and the lowest CO_2 yields indicating that strongly-acidic conditions denature CO_2 liberating enzymes rapidly while milder conditions allow enzymically evolved CO_2 to contaminate the system. When no acid is added, the yield of CO_2 is small and has a δ-value similar to that of the plant, suggesting that the CO_2 evolved is also the result of enzymic decarboxylation. The strongly-acidified plant leaves, when left over a long period of time, showed no increase in

yield nor any change in δ-values. Thus it is necessary to use strong acid both to destroy enzymic activity and to remove the "dissolved CO_2".

Another method used to check the validity of acidification as a means of isolating "dissolved CO_2" was to analyse the "dissolved CO_2" of respiring plants and compare this value with the C^{13}/C^{12} ratio of respired CO_2. The plants were

Table 10. CO_2 dissolved in respiring tomato plants

Plant no.	δ of dissolved CO_2 (per mil)	δ of respired CO_2 (per mil)
1	−25·8	−29·3
2	−25·9	−20·8
3	−20·4	−20·8
4	−21·3	−28·5
Average	−23·4	−25·8

swept with CO_2-free air in the respiration line so that no re-equilibration with air could occur. After 12 hr the respiring plants were frozen in darkness in a dry-ice bath and the dissolved CO_2 isolated as described above. Data from such experiments are given in Table 10.

The C^{13}/C^{12} ratio of dissolved CO_2 in respiring tomato leaves lies well within the range of δ-values obtained for respired CO_2 of tomato leaves. The CO_2 obtained by

Table 11. CO_2 dissolved in photosynthesizing tomato leaves
(δ leaves $\approx$ −30‰; δ atmospheric $CO_2 \approx$ −7‰)

Sample no.	δ (‰) of CO_2 dissolved in leaves during photosynthesis
LD-19	−15·4
LD-22	−17·5
LD-31*	−12·3
LD-32*	−12·0
LD-33*	−12·3
LD-36	−15·2
LD-37	−9·6
LD-71	−14·1
Average	−13·6

* Samples collected from the same group of plants at the same time.

acidification of respiring leaves must be largely an expression of the CO_2 dissolved in leaf cytoplasm because the surrounding atmosphere is continuously kept CO_2-free by stream of CO_2 free air.

C^{13}/C^{12} ratios of the dissolved CO_2 of photosynthesizing tomato leaves are reported in Table 11. An average δ-value of −13·6 per mil is obtained for the C^{13}/C^{12} ratio of CO_2 dissolved in tomato leaves during photosynthesis. The δ-values in Table 11 are all intermediate between plants and atmospheric CO_2. They have a range in δ-values much greater than the precisions of measurements.

However, such a range may be real and will be considered in the discussion section. Assuming that air CO_2 has a δ-value of -7, and using the average δ-value of "dissolved CO_2" ($-14‰$), the enrichment factor between air CO_2 and "dissolved CO_2" is:

$$\frac{C^{13}/C^{12}CO_2}{\overline{C^{13}/C^{12}\text{ ``dissolved } CO_2\text{''}}} = 1{\cdot}007$$

(f) *The relationship between the δ-values of "dissolved CO_2" and the δ values of fixed carbon*

Calvin (1954) has shown that the principal CO_2 fixation reaction in photosynthesis is the carboxylation of ribulose 1:5-diphosphate (RuDP) to yield two 3-phosphoglyceric acids (PGA) (shown in Fig. 4).

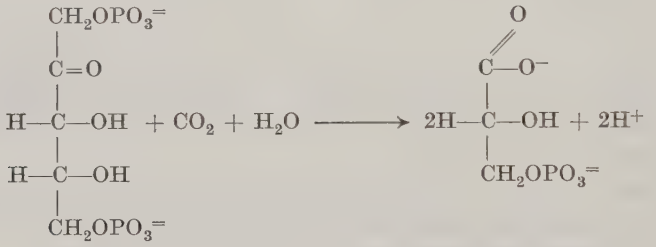

Fig. 4. The carbon fixation reaction of photosynthesis

Both Jakoby *et al.* (1956) and Weissback *et al.* (1956) have purified the enzyme which catalyses this reaction. Horecker's system was chosen for investigation of carbon isotope fractionation during the enzymic fixation of "dissolved CO_2" into sugars during photosynthesis.

Ribulosecarboxylase was prepared according to the method described by Horecker (1956). The only modification of the method was to suspend the final enzyme preparation in 0·1 M carbonate buffer (pH 7·4) rather than in phosphate buffer. The catalytic efficiency of the enzyme was established by fixation of $C^{14}O_2$ into ribulose diphosphate to yield C^{14}-labelled phosphoglyceric acid. The enzyme was highly active and carried out a stoichiometric conversion of RuDP* to PGA.

The reaction mixture, containing a trace of enzyme, bicarbonate salt and RuDP, was now allowed to react for about 60 min at 25°C. At this time all the RuDP was converted to PGA (as was shown by preliminary C^{14}-labelled fixation experiments). The reaction mixture was acidified to release the three hundredfold excess of bicarbonate. The PGA was then isolated as the insoluble barium salt. The PGA was purified by chromatographic techniques and converted to CO_2 by combustion. The details of this procedure are well described in the biological literature (Weissbach, 1956). The data are given in Table 12.

Only one-sixth of the carbon atoms in the isolated PGA are derived from dissolved CO_2 in solution. The remaining five-sixths of the carbon atoms were

* Ribulose 1:5-diphosphate was obtained as the barium salt from B. L. Horecker at the National Institute of Health.

derived from RuDP. The isotopic composition of the fixed carbons is given by the material balance expression:

$$\tfrac{5}{6}(-13{\cdot}7‰) + \tfrac{1}{6}(x) = -15{\cdot}2‰$$

where x = the δ value of the carbon fixed into sugar, $x = -22{\cdot}8‰$.

Table 12. C^{13}/C^{12} ratios of the reactants and products of the enzymatic CO_2 fixation reaction of photosynthesis

Material	δ-value of carbon (per mil)	
	Experiment 1	Experiment 2
Ribulose 1:5-diphosphate	−13·7	−13·7
Total CO_2 dissolved in reaction mixture	−5·4	−0·2
3-Phosphoglyceric acid	−15·2	−13·9

The difference in per mil (Δ) of the CO_2 in solution and that fixed during carboxylation is then given by: $\Delta = -(22{\cdot}8) - (-5{\cdot}4)^* = -17{\cdot}4‰$.

$$\frac{C^{13}/C^{12} \text{ dissolved } CO_2}{C^{13}/C^{12} \text{ fixed carbon}} \simeq 1{\cdot}017.$$

Since $$\frac{C^{13}/C^{12}CO_2}{C^{13}/C^{12} \text{ plant}} = \frac{C^{13}/C^{12}CO_2}{C^{13}/C^{12} \text{ dissolved } CO_2} \times \frac{C^{13}/C^{12} \text{ dissolved } CO_2}{C^{13}/C^{12} \text{ plant}}$$

then, by substituting into this equation the experimentally-determined values,

$$\frac{C^{13}/C^{12}CO_2}{C^{13}/C^{12} \text{ plant}}$$

may be calculated to be: $(1{\cdot}007)(1{\cdot}017) = 1{\cdot}024$.

When the preceding result is compared with the approximate values for the naturally-occurring fractionation factor for tomato plants, the two fractionation factors agree remarkably well. The naturally-occurring fractionation factor for tomato plants is estimated by taking a δ-value of −7 per mil for atmospheric CO_2 and a δ value of −30 per mil for tomato plants.

Discussion

Experiments on the extraction of "dissolved CO_2" and on the enzymic fixation of carbon dioxide suggest that the major fractionation of carbon isotopes in the photosynthetic fixation of atmospheric carbon dioxide is due to two steps. The first step involves the preferential uptake of C^{12} from the atmosphere and the second step the preferential conversion of C^{12} rich "dissolved CO_2" to phosphoglyceric acid which is known to be the first product of photosynthesis.

Subsequent metabolism of photosynthetic products is also accompanied by isotope fractionation (Park and Epstein, 1960). However, these fractionations

* δ of bicarbonate = 5·4‰.

affect the isotopic composition of only a few minor constituents of the plant as a whole. Graphically the model can be pictured as follows:

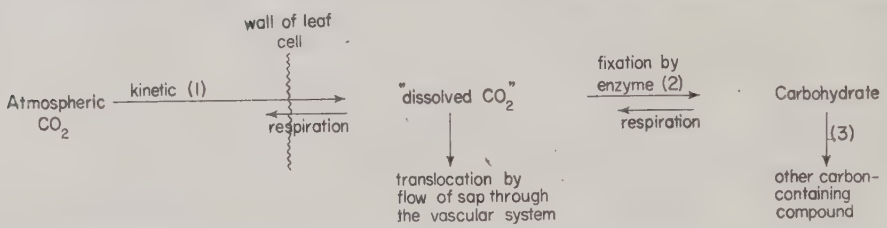

The fractionation accompanying the first step (1) can vary over a wide range. Under conditions of rapid CO_2 absorption into the leaf where no back diffusion of CO_2 into the atmosphere takes place, it is reasonable to assume that such a process would be approximated by the absorption of CO_2 into a $Ba(OH)_2$ solution. Such an absorption is known to be accompanied by a fractionation factor of about 1·014 (Baertschi, 1953; Craig, 1953).

This would result in a δ-value for "dissolved CO_2" of -21 per mil. On the other hand, if the other extreme is considered, namely if exchange between the atmospheric CO_2 and "dissolved CO_2" in cytoplasm (pH of cytoplasm ≈ 7) is relatively rapid, then the "dissolved CO_2" in the cytoplasm would have a δ-value of -1 per mil (δ of atmosphere $CO_2 \simeq -7$), the relationship observed between ocean "dissolved CO_2" and atmospheric CO_2 (Craig, 1954). The fractionation factor for step (1) obtained in the experiments reported in this paper ranges between 1·002 and 1·010 (average 1·007) and the δ-values for "dissolved CO_2" in the range -9 to -14, which are well within the expected range, show that C^{13}/C^{12} ratio of the "dissolved CO_2" is primarily controlled by kinetic effects. It is also evident that the δ-values of "dissolved CO_2" and thus the δ-values for plants can vary over a wide range depending only on the efficiency of CO_2 uptake by plants. The second step which affects the isotopic composition is the conversion of "dissolved CO_2" to phosphoglyceric acid. In this step $C^{12}O_2$ is preferentially fixed into the primary photosynthetic product which is ultimately converted to carbohydrate. Clearly, if all the "dissolved CO_2" were fixed, then no difference in the C^{13}/C^{12} ratio would exist between the dissolved CO_2 and the carbohydrate produced. It is therefore necessary that a portion of the unreacted and C^{13}-enriched "dissolved CO_2" must be eliminated from the plant. The more efficient the elimination, the greater will be the fractionation in step (2). In our enzymic experiment, only a small fraction of the "dissolved CO_2" was converted and thus a maximum fractionation was realized.

Similarly the relationship between the δ of field tomato plants and the "dissolved CO_2" in these plants gives a similar fractionation value. It must be true, then, that an important fraction of the CO_2 taken up by leaves must be eliminated by translocation (by water circulation through plants). The recent experiment of Harris and Van Bavel (1957) shows that plants evolve CO_2 from the roots at a rapid rate during the light period. We have attempted to sweep isolated roots of bean plants with CO_2-free air and trap the evolved CO_2 in light and dark periods. Although we have found that the δ-values for CO_2 evolved during the light period are

some 13 per mil (or more) greater than mean δ-values for the plants, the difficulty in arranging an airtight system around roots while they are attached to the leaves makes our results unreliable.

The third stage contributing to the fractionation of plant carbon involves chemical steps during which plant metabolism affects the isotopic composition of the final plant to only a slight degree. Measurements have been made on the δ-values of lignin, cellulose, pectins and lipids extracted from tomato plants. All but the lipid fraction are isotopically similar to the whole plant. The lipid fraction is enriched in C^{12}. The details of these experiments are given elsewhere (Park and Epstein, 1960).

It is of interest to test the validity of the simple model, proposed for the fractionation in photosynthetic fixation of carbon dioxide, by determining whether the model will explain various observed carbon isotopic ratios:

(1) The fractionation factor between atmospheric CO_2 and plant carbon appears to be a function of the concentration of CO_2 in the atmosphere (see Table 6). Lower CO_2 concentrations are accompanied by smaller fractionation factors. There can be several reasons for this observation. (a) With a low concentration of CO_2 in the atmosphere the rate of back diffusion from leaf to the atmosphere becomes more important and the kinetic effect is thus decreased. (b) The immediate atmosphere around the leaves may be depleted more efficiently at low CO_2 concentrations so that some of the local C^{13} enriched atmospheric CO_2 is incorporated into the plant. The above two considerations would tend to make the leaves richer in C^{13} and thus less different from the atmospheric CO_2, thereby resulting in a lower fractionation factor.

(2) The respiration experiments are of interest here because the average δ-value for CO_2 respired in the first 10 min is richer in C^{13} than plant carbon by about $+10$ per mil. In a few hours the change in δ-value of respired CO_2 with time is much slower. The C^{13}/C^{12} ratio of the respired CO_2 becomes smaller and more similar to the δ-values of the fixed plant carbon. Since the "dissolved CO_2" is eliminated from the cytoplasm during the early stages of respiration, it is reasonable that the initial respired CO_2 should have a higher C^{13}/C^{12} ratio than that of the subsequently respired CO_2. The nature of the respiration curve over periods of time longer than several hours is associated with lipid formation and destruction. This point is discussed elsewhere (Park and Epstein, 1960).

(3) There are certain terrestrial plants such as lichens which lack a vascular system. In such plants translocation of solutes over long distances is negligible. Since these plants lack this mechanism for removal of "dissolved CO_2" from photosynthetic cells, they should acquire a unique δ-value. If only step (1) (the kinetic fractionation step) was operative, and back diffusion was small, then all the "dissolved CO_2" would have to be totally converted to the carbohydrate and the maximum fractionation factor would be 1·014, i.e. the δ-value for the plant would be -21 per mil. On the other hand, if the back diffusion were rapid from the plant and the "dissolved CO_2" equilibrated with atmospheric CO_2, the enzymic fractionation could be operative since the C^{13}-rich fraction could be eliminated by the back diffusion. In this case the "dissolved CO_2" would have a δ-value of -1 per mil (6 per mil heavier than atmospheric CO_2) and the plant

could have a δ-value of -18 per mil. Thus the photosynthetic fractionation factor for lichens should be in the range of 1·010 to 1·014 relative to atmospheric CO_2 and the range of δ-values for these plants should be about -18 to -21 per mil. This range would increase somewhat if the δ-values for atmospheric CO_2 deviate from the -7 per mil values. The assigned range for the δ-values for lichens is unique in that most terrestrial plants lie within the range of about -23 per mil to -30 per mil (Craig, 1953; Wickman, 1952). In other words, the absence of a

Table 13. A comparison of the C^{13}/C^{12} ratios of lichens and higher plants

Sample	δ (in per mil)
Ramalina sp.‡	−18·0
Lichen A*	−18·6
Lichen B*	−21·1
Lichen C*	−21·0
Lichen D†	−18·9
Lichen E†	−18·1
Lichen F†	−20·5
Leaf of *Quercus agrifolia**	−26·0
Annual grass (unidentified)*	−28·3

* Samples collected within several feet of one another in the San Gabriel Mountains near Altadena, California.
† Samples collected in Tick Canyon, California.
‡ Sample collected near Point Conception, California.

translocation system in terrestrial plants should reduce the fractionation accompanying the photosynthetic process. Several lichens of different species, collected from several localities were analysed. In addition several higher plants growing close to some of the lichens were also analysed. The results are shown in Table 13. The results are remarkably consistent with the predicted ones. In addition it is of interest to note the difference between the δ-values of the vascular plants and lichens collected within a few feet of each other.

(4) As a result of the consideration of the model it was interesting to analyse a plant which could be grown either terrestrially or under water. Two *Hygrophila polysperma* plants, a common aquarium specimen, were grown side by side under water and in a moist atmosphere. Both systems were ventilated with the same air supply. The δ-value for new growth on the underwater sample was $-21·7$. Delta-values for the air grown leaves were $-25·5$, $-27·0$ and $-29·0$. In both cases air was passed through the growing medium to maintain good circulation. The above four data can be interpreted on the basis of the model since, in the water-grown sample, the first kinetic step was eliminated and thus the isotope fractionation between plant and atmospheric CO_2 was decreased.

(5) It is of interest to consider the carbon isotopic data for marine algae in relation to the proposed model. The data of Craig and Wickman show that δ-values of marine algae are about -8 to -18 per mil and about -7 to -17 per mil relative to "dissolved CO_2" in the oceans. If the communication between the "dissolved CO_2" in the cytoplasm of algae and "dissolved CO_2" in the ocean water is rapid, then the δ-value of "dissolved CO_2" in the algae should be about -1 per

mil. Fractionation by the algae should then be due to the second step of the model, namely the enzyme-catalysed fixation. In this case the minimum δ-value of the algae should be -18 per mil. If the rate of exchange between the "dissolved CO_2" in the ocean and the "dissolved CO_2" in the cytoplasm is slow relative to the CO_2 fixation rate, then the difference between the δ-values for ocean "dissolved CO_2" and the δ-values of algae should be correspondingly smaller. It is interesting that the most negative δ-values for normal marine algae are about -18 per mil (-17 per mil relative to dissolved CO_2 in ocean water) which would correspond to the -18 per mil minimum value predicted from the fractionation factor obtained for the laboratory enzyme catalyzed reaction. It is realized that some exceptions to the predicted δ-values may arise. In these cases it would appear, however, that such factors as unusual fixation pathways and unusual ecological conditions should be considered.

One of the unexpected ratios found in natural materials is that of the calcium carbonate of calcareous algae (Craig, 1953). The δ-values in nearly all the samples observed are more positive than the δ-values of slowly precipitated invertebrate shells. The isotopic composition of oxygen in the carbonates are nearly always lower in O^{18} than the invertebrate shells (Lowenstam and Epstein, 1954). The oxygen isotope data suggest that the algae carbonate is precipitated under non-equilibrium conditions, whereas the invertebrate shells are laid down in equilibrium with ocean water. Under equilibrium conditions the C^{13}/C^{12} ratio of the algae carbonate should be about the same as that for invertebrate shells. This contradiction can be explained by the above model if we consider that algae incorporate the carbon into the carbonate which has been partially depleted of C^{12} rich CO_2 by the enzymatic fixation of CO_2 during photosynthesis.

Many aspects of the variation of the C^{13}/C^{12} ratio of photosynthetic materials have been explained on the basis of a two step model. The first step is the fractionation involved in absorption of the CO_2 from the atmosphere by the leaf. The second step is the enzymatic conversion of "dissolved CO_2" in the cytoplasm to carbohydrates. Using this model it was possible to explain:

(1) The difference between the C^{13}/C^{12} ratio of atmospheric CO_2 and plants.
(2) The variation in the C^{13}/C^{12} ratio in naturally-occurring plants.
(3) The nature of the variation of the C^{13}/C^{12} ratio of respired CO_2, particularly during the beginning of dark period.
(4) The C^{13}/C^{12} ratio of CO_2 extractable by acid from the plant.
(5) The C^{13}/C^{12} ratio difference between land plants and marine plants.
(6) The C^{13}/C^{12} ratio of calcareous skeleton of algae.
(7) The difference in C^{13}/C^{12} ratio between lichens and higher plants.

The model presented here is necessarily in its simplest form and as such, does not define in detail mechanisms responsible for the C^{13}/C^{12} fractionation in CO_2 fixation. On the other hand, even in this simple form, it has permitted the design and interpretation of the experiments described here. It also explains many published results and predicts the unusual C^{13}/C^{12} ratio of lichens and other plants that could be grown under specified conditions.

Acknowledgement—The writers wish to thank Dr. F. Went and Dr. J. Bonner for making their facilities available and for their interest in this work. We also wish to acknowledge the assistance of Mrs. I. Vidziunas. This research was financed in part by AEC contract AT(11-1) 208.

References

Baertschi P. (1952) Die Fractionierung der Kohlenstoffisoptopen bei der Absorption von Kohlendioxyd. *Helv. Chim. Acta* **35,** 1030–1036.

Baertschi P. (1953) Die Fractionierung der natürlichen Kohlenstoffisotopen im Kohlendioxydstoffwechsel grüner Pflanzen. *Helv. Chim. Acta* **36,** 773–781.

Craig H. (1953) The geochemistry of the stable carbon isotopes. *Geochim. et Cosmochim. Acta* **3,** 53–92.

Craig H. (1954) Carbon-13 in plants and the relationship between carbon-13 and carbon-14 variations in nature. *J. Geol.* **62,** 115-149.

Craig H. (1957) Isotopic standards for carbon and oxygen and correction factors for mass-spectrometric analysis of carbon dioxide. *Geochim. et Cosmochim. Acta* **12,** 133–149.

Harris D. G. and van Bavel C. H. M. (1957) Root respiration of tobacco, corn, and cotton plants. *Agron. J.* **49,** 182–184.

Jakoby W. B., Brummond D. O. and Ochoa S. (1956) Formation of 3-phosphoglyceric acid by carbon dioxide fixation with spinach leaf enzymes. *J. Biol. Chem.* **218,** 811–822.

Keeling C. D. (1958) The concentration and isotopic abundances of atmospheric carbon dioxide in rural areas. *Geochim. et Cosmochim. Acta* **13,** 322–334.

Lowenstam H. A. and Epstein S. (1957) On the origin of sedimentary aragonite needles of the Great Bahama Bank. *J. Geol.* **65,** 364–375.

McCrea J. M. (1950) On the isotopic chemistry of carbonates and a paleotemperature scale. *J. Chem. Phys.* **18,** 849–857.

McKinney C. R., McCrea J. M., Epstein S., Allen H. A. and Urey H. C. (1950) Improvements in mass spectrometers for measurements of small differences in isotopic abundance ratios. *Rev. Sci. Instrum.* **21,** 724–730.

Nier A. O. and Gulbransen E. A. (1939) Variations in the relative abundance of the carbon isotopes. *J. Amer. Chem. Soc.* **61,** 697–698.

Park R. and Epstein S. (1960) *Plant Physiol.* In press.

Quayle J. R., Fuller R. C., Benson A. A. and Calvin M. (1954) Enzymatic carboxylation of ribulose diphosphate. *J. Amer. Chem. Soc.* **76,** 3610–3611.

Thimann K. V., and Bonner W. D. (1950) *Ann. Rev. Plant Physiol.* **1,** 75–108.

Weissbach A., Horecker B. L. and Hurwitz J. (1956) The enzymatic formation of phosphoglyceric acid from ribulose diphosphate and carbon dioxide. *J. Biol. Chem.* **218,** 795–810.

Wickman F. E. (1952) Variations in the relative abundance of the carbon isotopes in plants. *Geochim. et Cosmochim. Acta* **2,** 243–254.

Urey H. C. (1947) The thermodynamic properties of isotopic substances. *J. Chem. Soc.* 562 -581.

Geochimica et Cosmochimica Acta, 1960, Vol. 21, pp. 127 to 144. Pergamon Press Ltd. Printed in Northern Ireland

A description of the meteorite which fell near Abee, Alberta, Canada*

K. R. Dawson, J. A. Maxwell
Petrological Sciences Division, Geological Survey of Canada
and
D. E. Parsons
Physical Metallurgy Division, Mines Branch, Ottawa

(*Received* 11 *April* 1960)

Abstract—The Abee meteorite, which fell at 54°13′ N, 113°00′ W, north of Edmonton, Alberta, on 9 June 1952, is described for the first time in this paper. The surface features and internal structures are those of a black polymict chondritic breccia. Chemical analyses have been made of the matrix and of the stony fragments, and these have been recalculated to give a mineralogical norm which corresponds with mineral identifications by X-ray diffraction. The stone consists mainly of enstatite and kamacite–taenite, with minor troilite, and accessory oldhamite, alabandite, α-cristobalite, and quartz. The metallurgical study of the nickel–iron of the meteorite indicates that relatively coarse grains of a kamacite–cohenite intergrowth resembling pearlite with marginal areas and islands of α-2-iron are the dominant phases present. Taenite is present only as an accessory constituent. The exterior of the fusion crust contains droplets of δ-iron and very fine-grained magnetite whereas the interior of the crust contains martensite grains produced by the heating and quenching of the kamacite.

Introduction

History

The Abee meteorite was seen to fall at 1105 hours M.S.T., on 9 June 1952 at a point 54°13′ N, 113°00′ W, near Abee, just north of Edmonton, Alberta. It was recovered on 14 June from a wheat field belonging to Mr. H. Buryn where it rested in a fresh hole from 2 to 3 ft in diameter, 6 ft deep and inclined at 65° to the horizontal. After purchase by the Geological Survey of Canada it was shipped to Ottawa, stored for a short interval and then subjected to an intensive study which is being reported for the first time in this paper. The description of the meteorite is based upon: (1) megascopic and microscopic characteristics; (2) identification of the mineral species by X-ray diffraction; (3) chemical and spectrographic analysis of selected material: and (4) metallurgical heat treatments, etches, and microhardness determinations.

Shape, size and weight

The Abee meteorite is an angular block 30·5 × 40·6 × 47·0 cm in dimensions The volume is 28,400 cm^3, the specific gravity is 3·5 and the mass weighed 107 kg on recovery. The general shape is characterized by planar surfaces and angular corners which have been rounded by its passage through the atmosphere (see Plates 1 and 2). Locally, the surface exhibits a variety of irregularities which include a triangular-shaped scar, areas of spalled crust, piezoglyphs, flutings and a pebbled surface texture.

* Publication authorized by the Directors, Geological Survey of Canada and Mines Branch, Department of Mines and Technical Surveys.

Preparation procedure

The meteorite was submitted to the staff of the National Museum for the preparation of a mould from which plaster models were made. These models, painted to simulate the colour of the original, were prepared as part of the record of the meteorite and for display at a later date.

The meteorite was studied to determine suitable sawing directions which would facilitate the detailed examination. The meteorite was first sawed in half in the equatorial position, and on completion of the first cut a second was made parallel with the first which produced a triangular plate approximately 1 in. thick. This plate has been the source of the material used in this study. The cut face of one of the original halves was polished to bring out the internal structure and the distribution of the coarser-grained constituents. The plate was then cut into fragments of a variety of sizes for study by several different techniques.

All stages of the work have been recorded photographically beginning with pictures of the uncut meteorite. These illustrate the general shape and the nature of the surface of the stone. The polished surface was photographed to show the structural features and the distribution of the visible constituents. Numerous other photographs have been taken of polished sections and polished thin sections at magnifications up to $\times 1000$.

Fragments of the plate have been submitted for preparation as polished sections, thin sections, and for tritium analyses (Begemann *et al.*, 1959).* Two cubes (see Fig. 1) were cut from the plate to represent material from both the matrix and the fragments, and submitted for chemical analysis. The cube representing the matrix most certainly contained minute fragments; whether or not the cube cut from the fragment contained matrix material could not be determined. The cubes were cleaned of surficial grease and rust and then crushed in a large steel mortar until all material passed through a 100-mesh sieve. Each sample was thoroughly mixed in a mechanical mixer prior to the start of the analytical work.

The petrology and mineralogy are the responsibility of the senior writer, the geochemistry was done by Maxwell, the metallurgy by Parsons.

Surficial Features

The surface of the meteorite is covered by a black lustreless crust with the exception of spalled areas and the scar area (see Plates 1 and 2). This crust, although generally smooth, is not vitreous in appearance and it has been moulded around a variety of surface features. It averages 2 mm in thickness and locally surrounding the spalled areas there is evidence of two distinct layers. The crust is the same colour as the fresh interior of the meteorite and does not show any mottling effects. Close examination permits the identification of some stony fragments and iron grains, features that are readily apparent on fresh polished surfaces.

The triangular scar area, approximately 15 $\times$ 25 cm, is characterized by a rough hackly surface surrounded by the fusion crust of the meteorite. The scar is the

* Begemann *et al.* found the H^3 and He^3 contents to be the same both at the centre and the surface (see Fig. 1). The He^3 content was measured to be $(0{\cdot}13 \pm 0{\cdot}01) \times 10^{-6}$ cm^3/g at standard temperature and pressure. This amount of He^3 and the H^3 decay rate give a maximum radiation age of 30×10^7 years.

Plate 1. View of the exterior of the Abee meteorite showing its form, areas from which the fusion crust was spalled, and piezoglyphs with delicate flow lines. Maximum diameter 40 cm. GSC 109341–B.

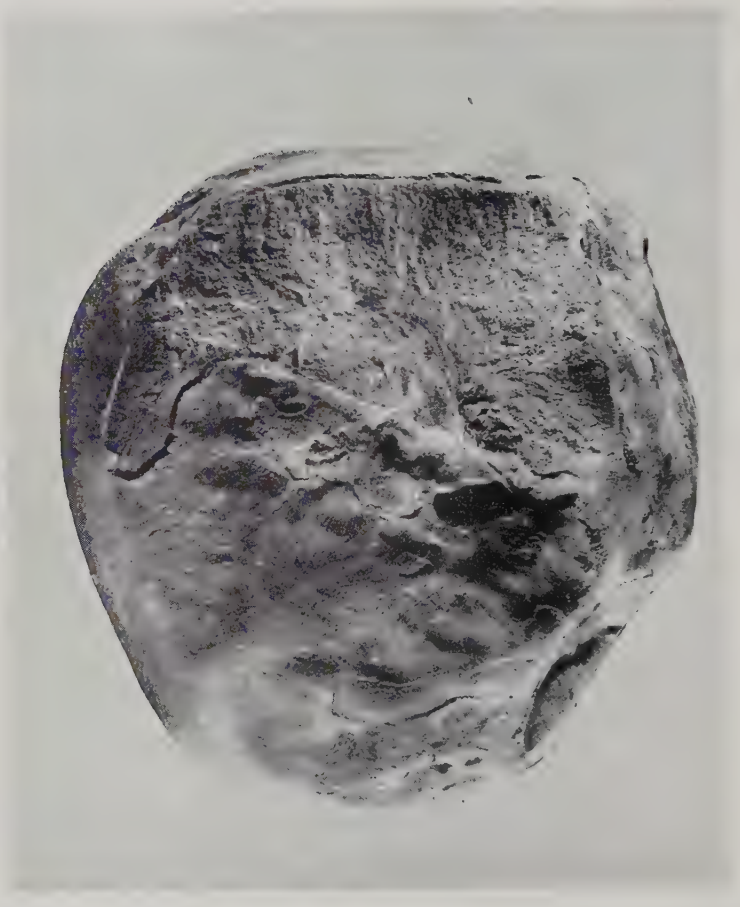

Plate 2. View of the exterior of the Abee meteorite showing the form, the scar area, piezoglyphs, flow lines, and areas from which the fusion crust was spalled. Maximum diameter 40 cm. GSC 109341–C.

same colour as the fresh interior of the meteorite and its surface is sufficiently rough to mask the details of the internal structure and the distribution of the kamacite–taenite grains. The fusion crust is terminated abruptly at the edge of the area and there is no evidence that it started to re-form before impact. The characteristics of the feature suggest that it represents the site from which a piece was broken shortly before impact.

Fig. 1. Plan of the medial plate cut from the Abee meteorite showing the distribution of specimens supplied to Dr. Begemann (I, II) and those supplied for chemical analysis (III, IV). Maximum diameter 40 cm.

Spallation of the fusion crust has taken place on many of the surface angularities of the meteorite. Such areas have relatively smooth surfaces by comparison with the scar area but not so smooth that the internal structures are readily identified on them. The smooth surface suggests that the fusion crust consisted of an outer and an inner layer. The spalled areas are attributed to attrition by the atmosphere just prior to impact or to the thermal shock as the meteorite entered the soil. The edges of such areas have not been smoothed by further burning, suggesting that the passage through the atmosphere must have been complete, or nearly so, before the event took place.

Piezoglyphs, or surface pits resembling thumb prints, are a common feature of the surface. They vary in depth to a maximum of 3·8 cm and in shape from

relatively symmetrical to asymmetrical. Asymmetry is characteristic of the deep piezoglyphs that occur in the vicinity of the scar area. They are characteristically covered by the fusion crust and some exhibit delicate flutings which are radially distributed relative to the bottom of the feature. These structures are attributed to the uneven burning of the surface of the meteorite in the atmosphere (Williams, 1959). They may represent areas of materials which were more combustible than the silicates, or points at which atmospheric eddies were generated by surface irregularities.

Delicate flutings or ridges have been recognized on the surface of the fusion crust in some of the piezoglyphs and in the vicinity of the scar area. They rarely exceed a fraction of a millimetre in height or width and from 25 to 50 mm in length. They exhibit a radial development in the piezoglyphs and are directed away from the scar area. The flutings have been attributed to the flow of molten material in the incandescent layer surrounding the meteorite in the atmosphere (Williams, 1959).

The crust although generally smooth, is characterized by roughness and ridging, the ridges being less than 0·1 mm high and having a maximum width of from 3 to 4 mm. The roughness contributes locally to the formation of flutings because fine tails have formed in the lee of resistant material. The ridging outlines some of the large stony fragments as well as some of the smaller iron-clad fragments. The relief texture can be correlated with concentrations of granular kamacite–taenite either in the margins of the stony fragments or in the iron-clad fragments. This is interpreted as evidence that the iron was more resistant to burning than the enclosing or associated silicate minerals.

Mineralogy

The Abee meteorite consists for the most part of enstatite and kamacite–taenite with minor troilite and accessory plessite, cohenite, oldhamite, quartz, α-cristobalite, plagioclase, alabandite and graphite. Because of the opacity of normal thin sections it was necessary to resort to the use of polished sections and polished thin sections to study textural relationships. The constituent minerals, which are generally very fine-grained, have been identified by X-ray diffraction techniques and because of the grain size, most powder patterns showed lines of two or more species. Both quartz and cristobalite, which are rarely identified in stony meteorites, were identified in powder patterns (see Table 2), and since the X-ray mounts were made without grinding there has been no opportunity to introduce either mineral from another source such as an agate mortar.

Enstatite

The enstatite, which gives an X-ray diffraction pattern corresponding to nearly pure enstatite, is the dominant silicate constituent of the meteorite and it occurs in subhedral to euhedral grains that vary from very fine-grained to microscopic. The subhedral grains are present in the very fine-grained aggregate which makes up much of the matrix and the stony fragments. Such aggregates also carry coarser individuals which show oriented grey inclusions in the dark grey host

material. The individual grains are usually opaque but a few sparsely disseminated grains transmit light.

Euhedral enstatite grains occur in the iron-rich peripheral zones of the stony fragments, in the mixed fragments (see Plate 3), in the chondrules (see Plate 4(a), and rarely in the iron spheres (see Plate 4(b) and fragments. The enstatite in the peripheral zones also occurs as embayed relicts. A pseudo-ophitic texture is locally developed by the euhedral enstatite and the interstitial grains of kamacite–taenite; the enstatite occurs as inclusions in, or may protrude from silicate aggregates into, the kamacite–taenite areas. In such occurrences the grains exhibit excellent crystal form which can be seen in polished sections. Some crystals of this type of occurrence may be coated by troilite and/or oldhamite and some fractured crystals have microfractures occupied by these minerals.

In the mixed fragments the enstatite is associated with kamacite–taenite as described above and also as coarse grains or mosaic aggregates of relatively coarse grains.

The enstatite, which occurs in chondrules (see Plate 4(a)), consists mainly of relatively coarse-grained radiating aggregates of prisms, fine-grained aggregates or a combination of both. It may or may not be associated with accessory inclusions of the metallics and in one or two cases relict crystals remain in circular areas of kamacite–taenite. In the latter, the iron may have replaced a siliceous chondrule.

Enstatite grains, which occur as minor accessory inclusions in kamacite–taenite aggregates, have been observed both in circular and angular areas of the latter.

Kamacite–taenite

Kamacite or α-iron, the nickel-poor alloy of iron, is the most abundant metallic constituent of the meteorite (Urey and Mayeda, 1959) on the basis of X-ray data. It is associated with taenite or γ-iron, the nickel-rich alloy, and some plessite which is an intergrowth of kamacite and taenite. Taenite was identified in a single chondrule by means of the X-ray diffraction technique (see Table 1). These iron minerals occur in microscopic grains disseminated through the matrix and in the chondrite fragments that make up this meteorite. They form granular aggregates in the peripheral zones of many stony fragments, and occur in spherical grains (see Plate 5(a)), and in iron silicate fragments. They appear white in polished sections, show no crystal outlines, and vary in size from a few millimetres in diameter to much less. Kamacite–taenite grains are commonly surrounded by rims (see Plato 5(b)) and are cut by veinlets of troilite and oldhamite.

Peripheral concentrations of the alloys surround many of the stony fragments, These zones are characterized by a noticeable reduction in the silicate and sulfide constituents and the appearance of a more or less continuous distribution of the kamacite–taenite.

Kamacite–taenite also occurs as spherical grains (see Plate 5(b)) as a coating on the silicate chondrules (see Plate 4(a)), or as a replacement of these chondrules (see Plate 4(b)). These occurrences may represent three stages of development of the spherical grains of the alloy. Certain chondrules are coated with kamacite–taenite which contains a few small silicate inclusions; other chondrules consist of kamacite containing radially distributed relicts of enstatite. A number of circular areas of

nearly pure kamacite–taenite occur in the stony fragments and these may represent chondrules which have been completely replaced.

Kamacite–taenite fragments range in composition from pure kamacite to silicate– or sulphide–kamacite mixtures. The mixed fragments exhibit the most variable distribution of the kamacite–taenite.

Troilite

Troilite, which is the most abundant sulphide constituent of the meteorite, is characterized by a variety of occurrences (see Plate 5(b)). In polished sections it appears as a yellowish-grey mineral and its identification has been confirmed by X-ray diffraction. Troilite characteristically occurs at the margins of kamacite–taenite aggregates and in fine-grained enstatite aggregates and exhibits scalloped contacts against both. Less commonly it forms thin festoon-like veinlets in the kamacite–taenite. Troilite surrounds the larger iron areas, sometimes in company with the unidentified dark grey metallic phase. Some troilite grains commonly carry small round kamacite inclusions. Troilite also occupies the interstices among the small enstatite crystals, again accompanied by dark grey metallic phase.

Oldhamite

Oldhamite, the calcium sulphide, which has been identified by X-ray diffraction but not by optical means, has been identified in fine-grained mixtures of alabandite and orthopyroxene. Oldhamite was identified in two of thirty-six powder mounts prepared for the X-ray diffraction technique and is considered to be an accessory constituent of the meteorite.

Alabandite

Alabandite, the manganese sulphide, was identified in a single chondrule by means of an X-ray diffraction pattern and optically as round grey metallic inclusions in kamacite–taenite areas. Alabandite has not been reported in meteorites before (Merrill, 1930) and consequently the pattern was measured and compared with a standard alabandite pattern (see Table 1). The agreement between the patterns is good except for a slight difference in the cell edge.

Quartz and α-cristobalite

Both quartz and α-cristobalite have been identified by the X-ray powder pattern technique. Both have rarely been reported from meteorites and the patterns of both have been measured and tabulated for comparison with standard patterns (see Table 2). Both minerals have been identified in several chondrules and in mixed fragments having a white-coloured constituent; α-cristobalite has been identified along with enstatite in residues from the chemically analysed specimens. Neither mineral has been detected by optical means.

Plagioclase

Plagioclase lines have been identified by X-ray diffraction patterns obtained from a single chondrule. It has not been identified by optical means and appears to be quite restricted in its distribution. Recalculation of the chemical analysis

Plate 3. Polished surface of a mixed fragment showing the textural and mineralogical characteristics of such fragments. Millimetre scale. GSC 109425.

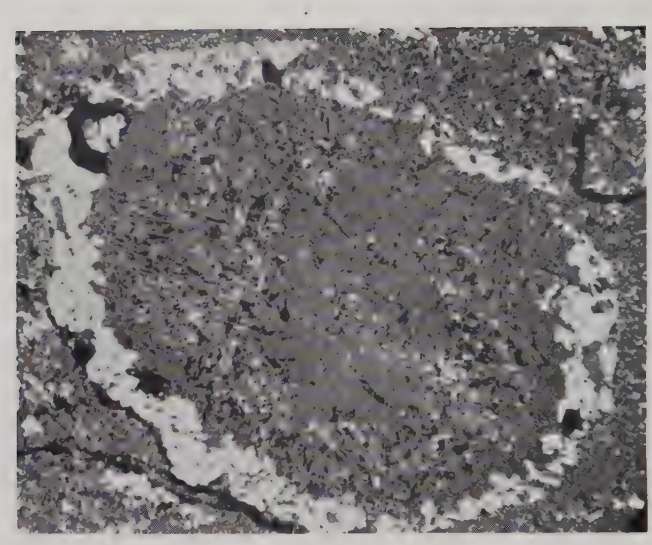

Plate 4(a). Polished section of a chondrule which consists mainly of enstatite with accessory disseminated troilite and a kamacite–taenite rim. ×35.

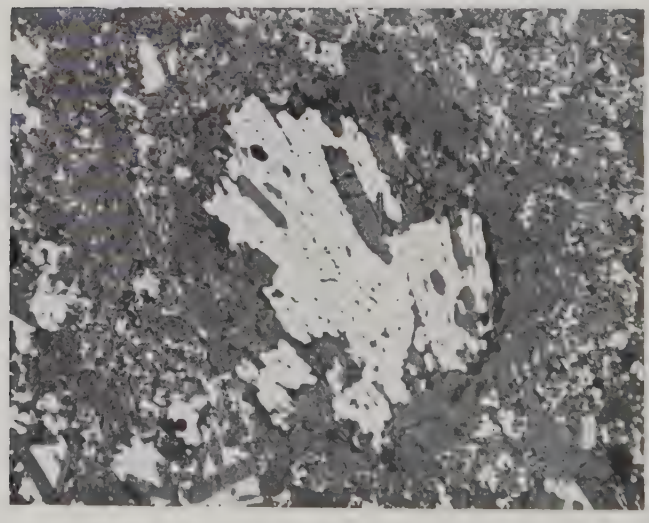

Plate 4(b). Polished section of a chondrule in which the radiating enstatite crystals have been largely replaced by kamacite–taenite. ×56.

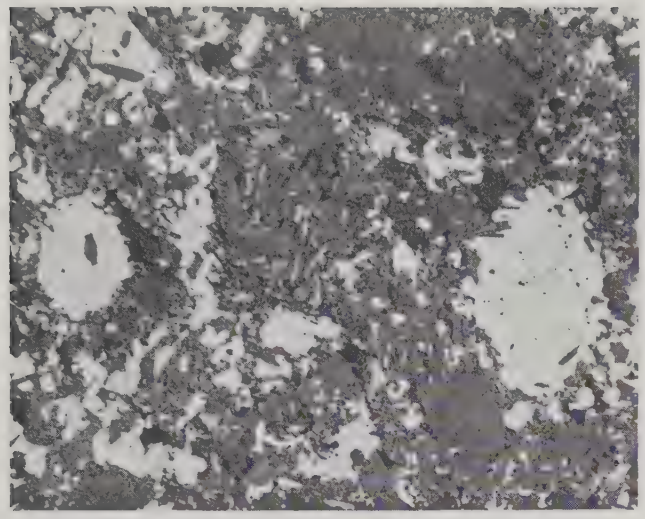

Plate 5(a). Polished section of spherical grains of kamacite–taenite in the enstatite aggregate. Enstatite inclusions preserved. ×56.

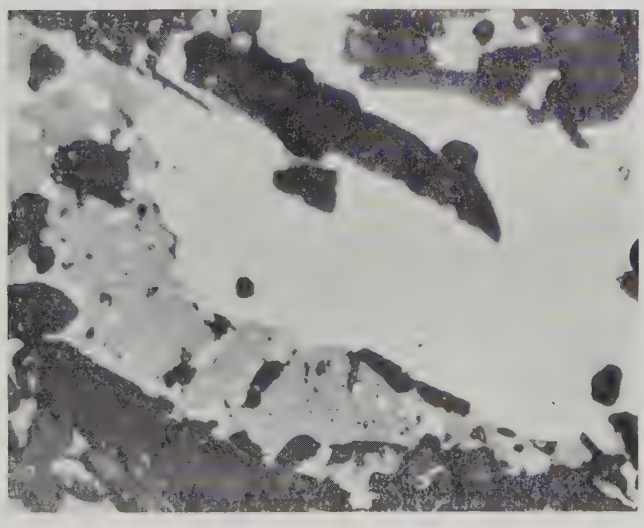

Plate 5(b). Polished section of kamacite–taenite (white) partly surrounded by oldhamite (dark grey) with troilite inclusions (medium grey). The enstatite crystals are nearly black. ×560.

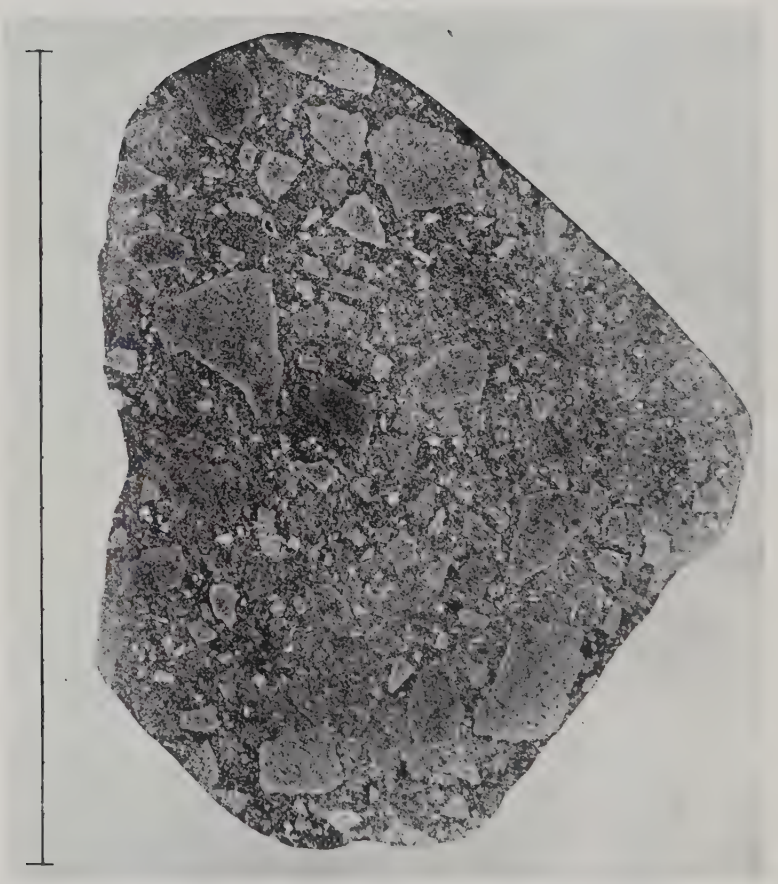

Plate 6. Polished surface of the equatorial slice showing textural and mineralogical variation of both the fragments and the matrix. Maximum diameter 40 cm. GSC 109341–D.

suggests that a small amount of albite and potash feldspar is present in both the matrix and in the fragment.

Graphite

Chemical analysis has established the presence of a small quantity of carbon in both the specimen of the matrix and of the fragment. A few grains have been

Table 1. Alabandite: X-Ray patterns

G.S.C. 10335 (mixture)		Alabandite, Nagyac, Transylvania	
d(meas.)	*I*	*d*(meas.)	*I*
3·30*	2		
3·15†	3		
2·98‡	4		
2·85*†	4	2·85	1
2·58	10	2·60	10
2·47†	1		
2·09§	5		
2·00*	3		
1·914‡	1		
1·827§	7	1·848	7
1·725	1	1·768	1
1·647*	1		
1·600	2	1·581	1
1·488†	5		
1·381†	1		
1·304	1	1·306	3
1·281*	2		
1·268‡	1		
1·216§	1		
1·157*	4	1·166	4
1·052	3	1·064	4

* Oldhamite. † Orthopyroxene.
‡ Unidentified, 2·98 possibly troilite. § Taenite.
Underlined numbers have been correlated with corresponding lines in standard albandite.
Patterns were made using a 57·3 mm camera, and Cu radiation with a Ni filter.

tentatively identified as graphite in polished sections but the distribution of the mineral is not fully understood.

Structural Features and Petrography

The Abee meteorite is a polymict breccia (Wahl, 1952), (see Plate 6) with no detectable bedding or other concentration of the constituent debris. The fragments include pieces of black chondrite, kamacite–taenite mixed with silicates, and kamacite–taenite, all embedded in a matrix consisting of a fine-grained aggregate of enstatite locally cemented by poikiloblastic aggregates of kamacite–taenite

both in the stony fragments and the matrix. This basic distribution of constituents is varied by the occurrence of spherical black chondrules in the stony fragments, and kamacite–taenite spheres. The meteorite is without fractures and veins and

Table 2. Cristobalite and quartz: X-ray patterns

Quartz*		G.S.C. 16206		G.S.C. 9724		Cristobalite†	
d(meas.)	*I*	*d*(meas.)	*I*	*d*(meas.)	*I*	*d*(meas.)	*I*
				4·51‡	1		
4·26	35	4·25	7				
		4·04	3	4·06	10	4·04	100
		3·71‡	2				
3·343	100	3·33	10	3·36	1		
		3·14	2	3·14	2	3·138	12
		2·97§	3	2·97§	1		
		2·85	3	2·85	3	2·845	14
		2·68§	2	2·71§	2		
		2·52	1	2·49	5	2·489	18
2·458	12	2·46	4			2·468	6
				2·38	1	2·342	21
2·282	12	2·28	3	2·30	1		
2·237	6	2·22	3				
2·128	9	2·12	4	2·11	2	2·121	4
		2·09§	3				
		2·00	1	2·02	2	2·024	3
1·980	6	1·977	5				
				1·941	2	1·932	4
		1·922‡	2				
		1·914‡	2				
				1·877	2	1·874	4
1·817	17	1·814	6	1·824	1		
				1·747	1	1·756	1
		1·737	1			1·736	1
		1·722§	1				
				1·698	2	1·692	3
1·672	7	1·666	3				
1·659	3						
				1·647	1	1·642	1
				1·613	3	1·612	5
		1·599	1			1·604	2
				1·575	1	1·574	1

* Swanson *et al.* (1954).
† Swanson and Tatge (1953).
‡ Unidentified.
§ Troilite pattern.
Patterns were made using a 57·3 mm camera and Cu radiation with a Ni filter.

it breaks across rather than around the chondrules. The shape of the coarser fragments and the lack of sorting suggests that the meteorite is an explosion breccia.

The large angular pieces of uniformly fine-grained black chondrite range in

size up to 8 × 6 cm. They contain sparsely disseminated black chondrules, a few microscopic spheres of iron and iron-rich peripheral zones. The iron-rich peripheral zones average 3 mm in width and with few exceptions they characterize these fragments. The inner margins of such zones are gradational whereas the outer margins are sharp. A 60-sec. etch with picral revealed the granular nature of the kamacite–taenite and also the presence of some areas of plessite (PERRY, 1944). The peripheral enrichment is obvious but the explanation for its genesis is not. However, concentric development relative to the shape of the fragments suggests that it formed after the fragments were broken from their source and likely before the breccia was compacted to its present condition.

The iron-silicate fragments (see Plate 7(a)) range in size up to a maximum of 20 mm and most approximate the maximum size. They vary in shape from angular to sub-rounded with contacts which vary from sharp to indistinct from fragment to fragment and around the periphery of a single fragment. They also tend to be more equidimensional than the chondrite fragments. The relative distribution of kamacite–taenite, troilite, oldhamite, enstatite and the other silicate minerals is highly variable, from completely heterogeneous to quite highly ordered concentrations of iron relative to the silicates. Several fragments contain a white translucent silicate (see Plate 7(b)) with enstatite and kamacite. The grains of the white constituent are anhedral and have been distributed in a variety of ways relative to the other constituents. Some mixed fragments have large areas of iron (see Plate 3) in which euhedral grains of enstatite occur. Moreover, these fragments contain a greater variety of mineral constituents than does the matrix, including plagioclase, alabandite, quartz and α-cristobalite.

The iron fragments vary from 15 mm down to microscopic grains. The average size appears to be 0·5 mm. They vary in shape from angular to sub-rounded and are mainly structureless. They do not exhibit peripheral zones and most contain some included silicate grains. Their contacts with the matrix are sharply defined.

The matrix is a microbreccia composed of fine-grained debris similar in colour and composition to the fragments. It consists of subhedral to anhedral grains of enstatite in a hypidiomorphic granular aggregate without visible cement other than the areas of metallic constituents. The enstatite grains, which occur mainly in disorganized aggregates, locally show radial organization or simulate the ophitic texture of gabbro. Isolated grains of kamacite–taenite occur in enstatite aggregates in areas several times the size of individual silicate grains. In the latter case, the silicates are fractured and veined by iron on a microscopic scale. Euhedral inclusions of the silicates persist in the former or protrude into it. Margins of the larger iron areas have been coated by troilite and less frequently by oldhamite.

The black chondrules, which are most common in the stony fragments, occur as black spheres 1·5 mm or less in diameter. They are sparsely and irregularly disseminated through the chondrite fragments. When examined in thin section they are found to be nearly opaque and the internal structures are difficult to observe. One chondrule observed in polished section shows crystals of enstatite radiating from the side of the structure, and a second consists mainly of kamacite–taenite with enstatite relicts distributed in a similar manner. The margins may be diffuse or sharply defined and in a few cases the chondrules have been coated

with kamacite–taenite. Those with diffuse margins are difficult to detect in polished sections although the chondrule appears as a circular area poor in iron with or without oriented grains of enstatite and little or no metallics. The sharply defined chondrules may be rich or poor in metallics and with or without visible orientation of the constituent silicates. Some such chondrules contain irregularly distributed zones of troilite and possible minor oldhamite. Other sharply defined chondrules have been coated by kamacite–taenite in a continuous layer with varying amounts of silicate crystals as inclusions within it (see Plate 4(a)). The composition and microstructures of the chondrules exhibit a considerable degree of variation.

The crust (see Plate 7(b)) is characterized by an inner dense siliceous layer and an outer zone comprised of both silicates and metallics. The inner zone is continuous having gradational contacts with the unfused interior and with the outer zone. The silicate crystals are commonly fractured and veined by metallics along the interface between the crust and the unfused rock. The inner zone is a continuous aggregate of fused silicate material with little or no metallic material. The outer zone is discontinuous with areas of fine-grained metallic inclusions as its most characteristic feature.

Chemistry

Chemical and spectrographic analyses of the matrix and of a fragment are given in Table 3. The methods used in the chemical analyses are briefly described in Appendix I. A discussion of the chemical evidence for the distribution of iron, nickel, sulphur, phosphorus and carbon is included here.

Iron is present in the ferrous state as troilite and, possibly, as cohenite; it is also abundantly present as metallic iron. The close correspondence obtained between the values for total iron and those for metallic and ferrous iron indicates that little, if any, ferric iron is present. Analysis of the black acid-insoluble silicate residue yielded only a small amount of iron and this is thought to have been derived from unattacked iron carbide coating the silicates. Only the small amount of ferric iron is believed to be in the silicates (see Table 3); the bulk of the iron is found in the sulphide and metallic phases.

Nickel occurs for the most part in the metallic phase of the meteorite. Qualitative tests made with dimethylglyoxime on the solutions resulting from the determination of iron in the magnetically-separated portions revealed that most of the nickel was in the magnetic portion and only a trace of it was found in the solution of the non-magnetic part. Although determination of the "sulphide" sulphur content of these separated portions indicated that there was sufficient sulphur in the magnetic part to combine with the nickel, no millerite (NiS) could be found by mineralogical examination and Rankama and Sahama (1950, p. 677) state that nickel is pronouncedly siderophile in its geochemical behaviour. It is therefore placed in the metallic phase.

Sulphur is present as a sulphide only, as indicated by the close correspondence between the values for the "sulphide" sulphur and total sulphur determinations. Phosphorus is included among the silicate constituents and may be present as merrillite (Wahl, 1950, p. 417) although no mineralogical evidence has been found

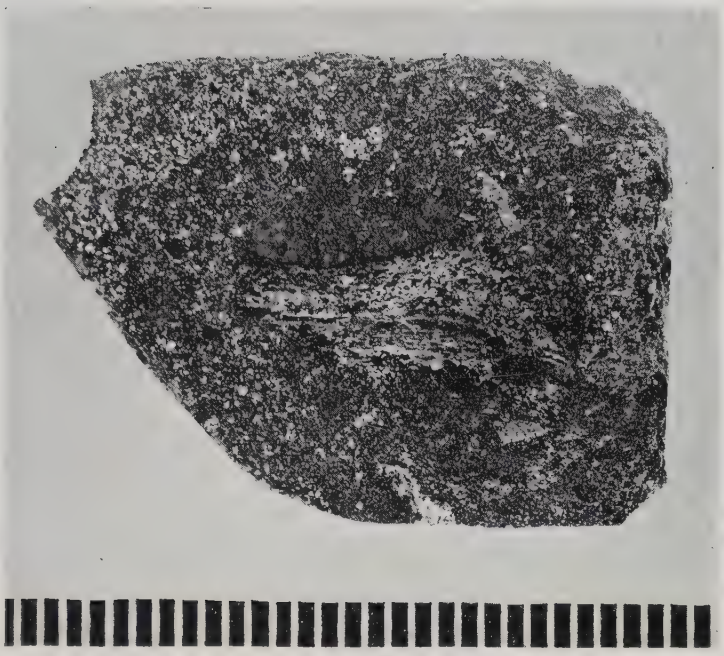

Plate 7(a). Polished surface of a mixed fragment showing the mineralogical and textural characteristics. Millimetre scale. GSC 109425.

Plate 7(b). Polished cross-section of the crust showing three gradational zones, the inner cracked enstatite aggregate, the intermediate metallic free zones, and the outer zone characterized by fine-grained disseminated metallics. ×175.

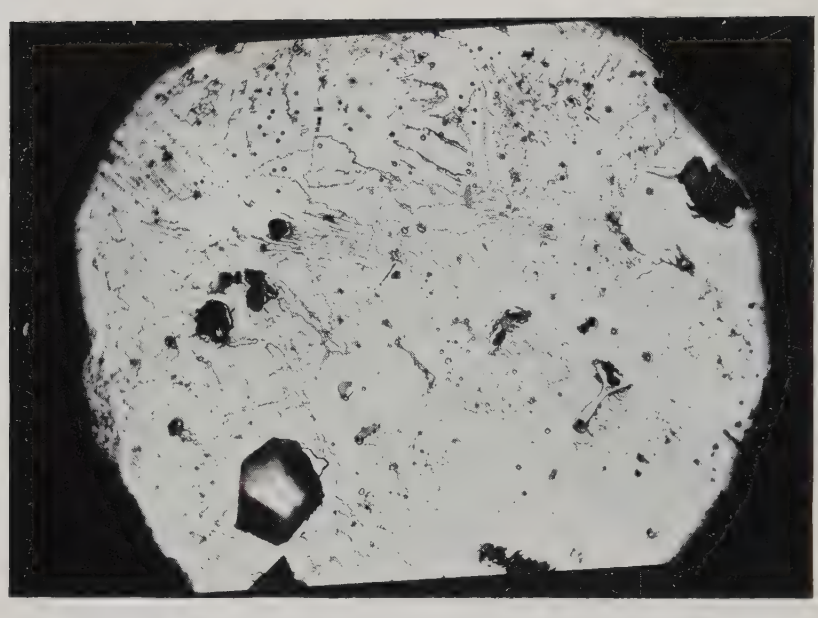

Plate 8(a). Untreated lamellar kamacite–cohenite intergrowth resembling pearlite. 4 per cent picral etch. ×300.

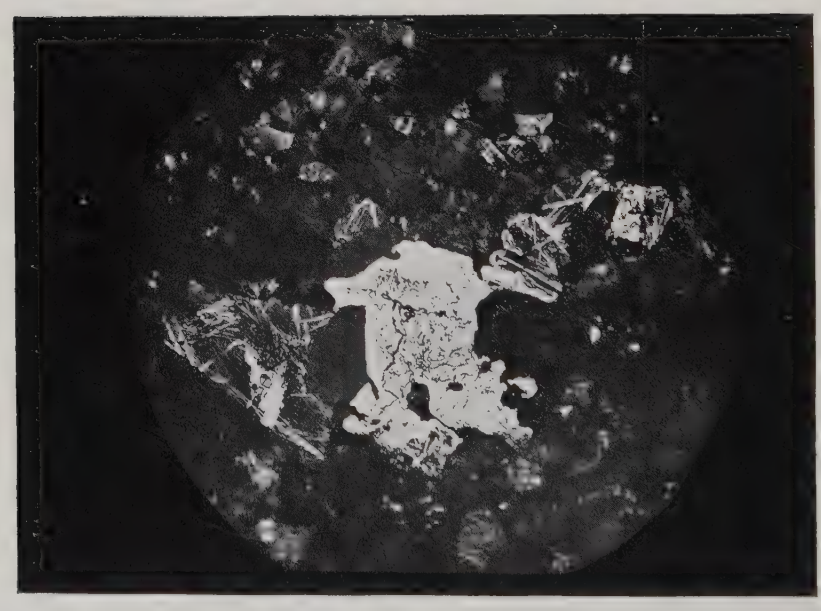

Plate 8(b). Untreated α-2-iron in grains at the margin of the larger kamacite grains and isolated within the enstatite aggregate. Etched 1½ min in boiling alkaline sodium picrate. ×300.

Table 3. Chemical analyses (wt.%) of the matrix and a fragment*

Oxide or element	Matrix	Fragment
SiO_2	37·78	41·26
Al_2O_3	1·34	2·67
Fe_2O_3	0·42	0·23
CaO	0·06	0·20
MgO	19·04	18·33
Na_2O	1·01	1·35
K_2O	0·10	0·15
H_2O^+	0·22	0·15
H_2O^-	0·21	0·06
TiO_2	0·08	0·04
P_2O_5	0·60	0·51
Cr_2O_3	n.f.	tr.
CO_2	0·04	0·08
Silicates	60·90	65·03
Fe	22·15	17·38
Ni	1·66	1·23
Metallic	23·81	18·61
Fe	7·91	7·95
Ca	0·70	0·44
Mn	0·20	0·55
S	6·12	7·83
C	0·38	0·25
Sulphides	15·31	17·02
Total	100·02	100·66
Powder density†	$3·252^{(23·8/4°C)}$	$3·506^{(24·7/4°C)}$
Spectrographic analysis‡ (p.p.m.)		
Co	700	700
Ba	500	100
Cu	100	100
V	<100	n.f.

* Analysts, S. Courville and J. A. Maxwell, Geological Survey of Canada.

† Powder density determinations by K. G. Hoops, using an Ellsworth fused silica pycnometer.

‡ Semiquantitative spectrographic analysis by W. H. Champ, Geological Survey of Canada.

to support this, and it could be present as apatite or even in the non-silicate phase as schreibersite, $(Fe, Co, Ni)_3P$.

It is reported by Rankama and Sahama (1950, p. 533) that carbon occurs in

meteorites chiefly as cohenite, Fe_3C, and as graphite. Although the physical nature of the powdered sample suggests the presence of considerable graphite, there is no definite mineralogical evidence to support this observation. Leaching of the samples with hydrochloric acid yielded a black acid-insoluble residue. Digestion of this residue with hydrofluoric acid decomposed it, with the formation of a black sludge and the liberation of much iron. Filtration and ignition of this sludge showed part of it to be carbon, which suggests that the latter is combined with the iron in some form, possibly as cohenite. Metallurgical evidence (see Appendix II) confirms the presence of cohenite in the kamacite grains.

Table 4. Recalculated mineralogical analysis (wt.%) of the matrix and the fragment

Mineral	Matrix	Fragment
Enstatite	48·8	46·8
Albite	6·4	9·0
Orthoclase	0·5	1·0
Cristobalite and quartz	3·9	6·3
Merrillite	1·3	1·3
Alabandite	0·4	1·2
Oldhamite	0·6	0·2
Troilite	11·2	14·2
Cohenite	1·6	1·3
Kamacite–taenite	25·3	18·6
	100·0	99·9

Normative calculations

The chemical data were recalculated, using standard formulae, to the appropriate normative silicates, sulphides and native iron and nickel. Water and carbon dioxide were omitted and the small amount of Fe_2O_3 was recalculated to Fe and added to the sulphide constituents. Enstatite and orthoclase were calculated to use all available MgO and K_2O. Soda was divided between sufficient merrillite to satisfy the available P_2O_5, as proposed by Wahl (1950), and albite. The remaining silica became the quartz and α-cristobalite identified by X-ray diffraction. Sulphur was combined in a 1:1 ratio with available manganese, the balance of the lime, and sufficient iron to form alabandite, oldhamite and troilite, respectively. The remaining iron was combined with carbon in the ratio 3:1 to form cohenite. All of the nickel was combined with metallic iron to form kamacite–taenite. The recalculated mineralogical analyses of the matrix and fragment are given in Table 4.

Conclusions

(1) The Abee meteorite exhibits such surficial structures as the fusion crust, spallation scars, piezoglyphs, flutings and pebbled surface.

(2) The meteorite is a polymict chondritic breccia containing angular fragments of black chondrite in a matrix of similar material. The fragments include smaller pieces of pure iron and iron–silicate mixtures.

(3) The matrix is a microbreccia without any primary structure.

(4) Chondrules are present in many fragments. They are black, spherical bodies which rarely exceed 1 mm in diameter. They do not break free from the matrix.

(5) The mineral species include abundant kamacite–taenite and enstatite, minor troilite and accessory oldhamite, alabandite, plagioclase, quartz, α-cristobalite, taenite and plessite. Alabandite, quartz and α-cristobalite, which have not been previously reported in stony meteorites, have been identified by X-ray diffraction.

(6) Fine-grained opaque enstatite occurs in the matrix, fragments, and in the chondrules.

(7) Kamacite occurs in disseminated grains among the silicates, as a more or less continuous granular aggregate with enstatite inclusions at the periphery of silicate fragments, in spheres 1 mm in diameter, and in small mixed fragments.

(8) Iron occurs as troilite, metallic iron, and possibly as cohenite; nickel is considered to be present in the metallic phase, probably as kamacite with some taenite.

(9) Sulphur occurs as sulphides only, and is present as troilite, alabandite and oldhamite.

(10) Carbon is believed to be present chiefly as cohenite, although some graphite may also occur.

(11) Kamacite–cohenite intergrowths resembling pearlite are the dominant phase of the meteoric iron. It is associated with marginal grains and disseminated islands of α-2-iron.

(12) The fusion crust exhibits droplets of δ-iron on its exterior and disseminated grains of martensite within itself.

(13) The lack of Neumann lines, the veination of the enstatite by kamacite, and the ballation of the kamacite are interpreted as evidence that the meteorite was heated subsequent to brecciation of the parent body and prior to passage through the earth's atmosphere.

Acknowledgements—The writers wish to express their appreciation of the interest shown, and assistance given, by Dr. E. Poitevin, formerly of the Geological Survey of Canada, and Dr. P. Millman of the Astrophysical Division of the National Research Council of Canada. The assistance rendered by their colleagues, Dr. S. C. Robinson and Dr. R. J. Traill, in critically reading the manuscript is gratefully acknowledged.

Appendix I

The Methods of Chemical Analysis Used

SiO_2, Al_2O_3, CaO, MgO, P_2O_5, MnO, NiO, Cr_2O_3, H_2O^+, H_2O^- and CO_2 were determined by the "classical" methods of rock analysis. A Perkin–Elmer Model 146 flame photometer was used for the final determination of Na_2O and K_2O; the results were obtained by direct reading without internal standard, after addition of a "radiation" buffer to sample and standard solutions.

The TiO_2 content was obtained spectrophotometrically, using the yellow complex formed with hydrogen peroxide, after mercury cathode electrolysis of the solutions to eliminate the interference due to the large amount of iron present (Maxwell and Graham, 1949).

Various methods were used to determine the total sulphur, including ignition of the sample in a Parr peroxide bomb, but the most satisfactory method was that

described by Kolthoff and Sandell (1952, p. 335) involving the decomposition of the sample with nitric acid and bromine. The standard evolution method, in which the liberated S^{2-} is finally titrated with standard potassium iodate–iodide solution in the presence of starch as indicator, was used to measure the amount of sulphur present in the form of sulphide.

Attempts to determine the carbon content of the samples by total combustion of the sample in oxygen gave results that were consistently high, probably because of the absorption of the sulphur compounds formed during combustion by the ascarite in the carbon dioxide absorption bulb. The addition to the train of a chromic acid trap finally eliminated the sulphur interference.

Potentiometric titration, with a standard solution of potassium dichromate, of the ferrous and total iron gave good results for the latter but the presence of sulphide, carbon and metallic iron made the ferrous iron value unreliable. Metallic iron was determined by the method described by Riott (1941); the sample is digested with an acidified cupric chloride–potassium chloride solution and filtered; the Cu^{+} present in the solution is precipitated with powdered aluminium metal, the solution again filtered and the Fe^{2+} titrated with standard potassium dichromate, using diphenylamine as indicator.

Removal of the metallic iron was necessary in order to permit the determination of ferrous iron; after unsuccessful attempts to do this with a Frantz isodynamic separator, it was finally achieved with a small hand magnet. The magnetic and non-magnetic portions obtained in this way are as follows:

	Magnetic (%)	Non-magnetic (%)
Matrix	32	68
Fragment	27	73

While the separation was not entirely complete, satisfactory results were obtained for the ferrous and total iron, and sulphide sulphur, on the magnetic and non-magnetic portions of both samples.

The amount of Ca present as oldhamite, CaS, was obtained by digesting the samples in very dilute acetic acid, as suggested by Wahl (1950, p. 424).

Appendix II

Iron Metallurgy

The iron present in the Abee meteorite contains an average nickel content of 4·5% and a minimum of 0·2% carbon combined as Fe_3C (cohenite) (see Table 5). No Neumann lines have been preserved in the kamacite grains and no graphite flakes have been identified in the kamacite. Etching with boiling alkaline sodium picrate demonstrates the widespread development of an irregular lamellar intergrowth of cohenite in all kamacite grains (see Plate 8(a)), and reveals small quantities of a hard acicular α-2-form of iron (Uhlig, 1954) as small grains and as

projections from some kamacite grains (see Plate 8(b)). A search of the polished sections revealed a few small grains of taenite marginal to the kamacite.

An attempt was made to separate the metallic from the non-metallic portion of the Abee meteorite using an iodine–methanol reflux reaction. This separation yielded a soluble portion of 44·29 ± 0·92 per cent (based on six determinations). The analysis of the soluble portion is shown in Table 5.

Methods used in Table 5

(1) The carbon was determined by combustion, a manganese dioxide trap being used to eliminate the sulphur compounds.

Table 5. Analysis of the iodine–methanol soluble portion
(Analysts: L. G. Ripley and R. G. Sabourin, Mineral Sciences Division, Mines Branch.)

Element	%	No. of determinations
C	0·19 ± 0·05*	2
Fe	72·19 ± 0·16	3
Ni	4·53 ± 0·07	2
Co	0·25 ± 0·01	2
Mn	0·37 ± 0·01	2
S	13·54*	1
P_2O_5	0·80*	1

* These values are obtained by calculation using the difference between the total ion concentration in the bulk sample and the quantity of this ion which was found in the iodine–methanol insoluble portion.

(2) Iron was determined titrimetrically by a classical method.

(3) Nickel, cobalt and manganese were determined by classical spectrophotometric methods.

(4) Sulphur was determined by wet oxidation followed by a barium sulphate precipitation.

(5) Phosphorus was determined by the classical ammonium molybdate precipitation.

The iron in the outer fusion crust is characterized by the development of iron oxide, probably magnetite (see Plate 7(b)), and a few small grains of δ-ferrite (or taenite) (see Plate 10). Martensite grains occur along the inner margin of the fusion crust.

Two sulphide minerals were observed in relatively large quantities at the surface of the kamacite (see Plate 5(b)). These were attacked and removed by the etchant.

The identity of the cohenite in the kamacite was confirmed by chemical analysis (see Table 5) and by laboratory treatments. Metallographic examination, microhardness tests (see Table 6) and laboratory heat treatments were made to determine the response of the lamellar cohenite (see Table 7) to conventional hardening, tempering, spheroidizing, and annealing treatments. Heating at 842°C for 20 min. followed by water quenching resulted in the complete solution of the cohenite in the kamacite which was transformed to martensite by the quench (see Plate 9(a)).

Table 6. Results of microhardness tests

Description of phase	Rockwell C hardness*
Specimens as received	
Kamacite	35–44
Kamacite–cohenite intergrowth	42–48
α-2–iron	58–63
Granular α-2–phase	57
Sulphides combined	47
Enstatite crystals	67–70
Black silicate phase	too brittle
Fusion crust—iron oxides	39–59
α-2-iron	56
decarburized kamacite	37–38
martensite (slightly tempered near surface)	58–61
Heat-treated specimens	
A.† Martensite	60
B. Slightly tempered martensite	62
C. Tempered martensite	42–45
D. Enveloping bainite or plessite	56–58
E. Pearlite	41
enveloping bainite or plessite	56
pearlite	44–47
F. Decarburized areas of α-2-iron	33
α-2-iron not decarburized	38
pearlite—partly dissolved	44–45

* 100 g load, 10·25 objective. Hardness obtained by conversion from Knoop hardness and checked against Rc 64, Rc 47, and Rc 27 standard calibration blocks.

† Letters A–F designate laboratory heat treatments (see Table 7).

Table 7. Summary of heat treatment tests

Sample	Heat treatment
A.	Heated in vacuum at 842°C for 20 min and water quenched to room temperature.
B.	Half of sample A was tempered 2 hr at 149°C in air.
C.	Half of sample B was additionally tempered 1 hr at 648°C in air.
D.	Heated in vacuum at 871°C for 30 min and cooled to room temperature in the furnace.
E.	Same as for D except that the vacuum was broken.
F.	Heated for 120 hr in air at 593°C.

Subsequent tempering treatments at 149°C and at 648°C accomplished the normal breakdown of the martensite to kamacite and cohenite. Heating in vacuum at 871°C with slow cooling in the furnace reproduced a kamacite–cohenite distribution similar to that of the natural meteoric iron except that considerable "bainite"

Plate 9(a). Light coloured areas of martensite synthesized from kamacite–cohenite grains by heating and quenching. Etched $1\frac{1}{2}$ min in boiling alkaline sodium picrate. $\times 300$.

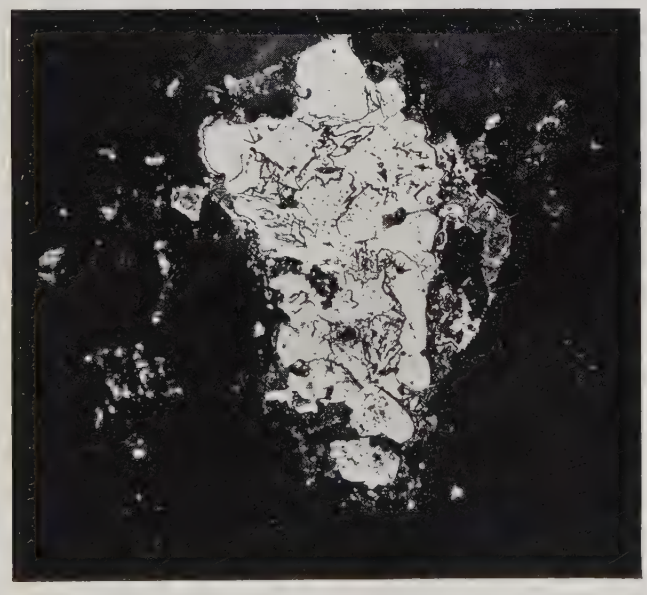

Plate 9(b). Discontinuous marginal zone of synthesized bainite surrounding kamacite cohenite grains. Etched $1\frac{1}{2}$ min in boiling alkaline sodium picrate. $\times 300$.

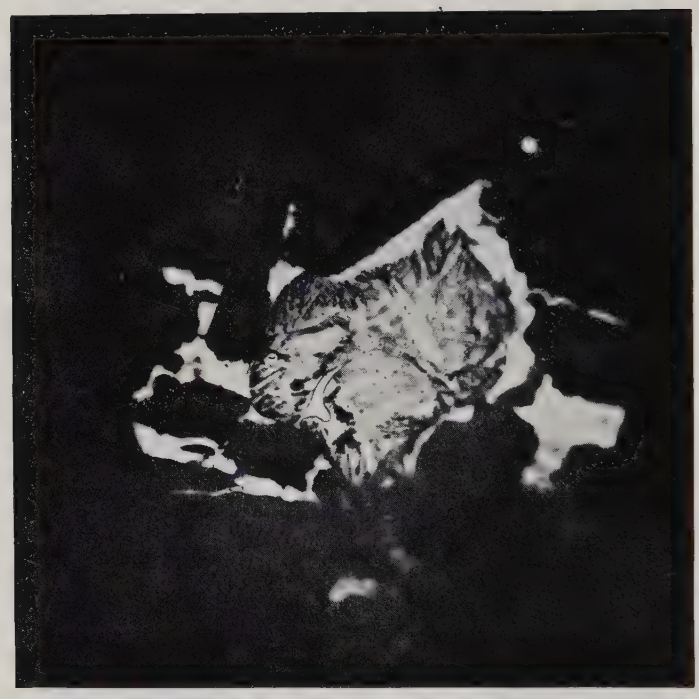

Plate 10. White drops of δ-iron in α-2-iron exposed at the surface of the fusion crust and embedded in silicate glass. 4 per cent picral etch. $\times 1050$.

(plessite) formed in a discontinuous peripheral zone surrounding the kamacite (see Plate 9(b)).

Heating at 871°C in air, with slow cooling in the furnace developed a similar structure and resulted in oxidation of iron at the surface of the specimen to produce a thicker scale than the primary fusion crust. Heating at 593°C for 120 hr resulted in partial solution of some of the cohenite lamellae and complete spheroidization in some grains. Where kamacite grains were exposed to the air, diffusion zones (nickel–oxygen) developed and the kamacite was almost completely decarburized.

The absence of Neumann lines, the veining of the fractured silicate crystals by kamacite, and the balling of kamacite are interpreted as evidence that the meteorite was heated subsequent to fragmentation of the parent body. The temperature reached was sufficient to remobilize the iron and destroy the Neumann lines.

The α-2-areas are interpreted as evidence of a peripheral enrichment of nickel in the kamacite grains sufficient to permit transformation to martensite at a cooling rate which simultaneously produced the kamacite–cohenite intergrowth. Reheating had failed to homogenize the nickel content, and subsequent cooling had not caused complete spheroidization of the cohenite lamellae. Peripheral concentrations of nickel in the kamacite suggested by the formation of "bainite" have not been corroborated by chemical means. Calculations predict that the nickel content of the pure iron after complete separation will be increased from the 4·53% reported to about 7%. However, laboratory annealing treatment by slow cooling from 871°C did develop a hard acicular phase, which formed a discontinuous peripheral zone surrounding the kamacite grains. The hardness of this phase is only slightly lower than that of the α-2-phase and corresponds to that of "bainite" or low-carbon martensite whereas that of the α-2-phase corresponds to martensite in hardened steel containing about 0·45% carbon.

The δ-ferrite or taenite and iron oxide in the outer fusion crust and the martensite grains in the inner crust are interpreted as products of fusion of the surface of the meteorite during its passage through the atmosphere. The δ-ferrite is retained in quenched droplets of molten iron (see Plate 9), the magnetite is the product of oxidation of the iron by the atmosphere, and the martensite results from the quenching action of the cold meteorite on the surficial grains heated during flight.

References

Begemann F., Eberhardt P. and Hess D. C. (1959) ^{3}He-^{3}H- Strahlungsalter eines Steinmeteoriten. *Z. Naturf.* **14**a, 500–503.

Kolthoff I. M. and Sandell E. B. (1952) *Textbook of Quantitative Inorganic Analysis* (3rd Ed.), MacMillan, New York.

Maxwell J. A. and Graham R. P. (1949) The mercury cathode and its applications. *Chem. Rev.* **46,** 471–498.

Merrill G. P. (1930) Composition and structure of meteorites. *Bull. U.S. Nat. Mus.* **149.**

Perry S. H. (1944) The metallurgy of meteoritic iron. *Bull. U.S. Nat. Mus.* **184,** 1–93.

Rankama K. and Sahama Th. G. (1950) *Geochemistry.* University of Chicago Press, Chicago.

Riott J. P. (1941) Determining metallic iron in iron oxides and slags. *Industr. Engng. Chem. (Anal.)* **13,** 546–549.

Swanson H. E., Fuyat R. K. and Ugrinic G. M. (1954) NBS Circular 539, vol. III, p. 25.

Swanson H. E. and Tatge E. (1953) NBS Circular 539, Vol. I, p. 41.

Uhlig H. H. (1954) Contribution of metallurgy to the origin of meteorites. I—Structure of metallic meteorites, their composition and the effect of pressure. *Geochim. et Cosmochim. Acta* **6,** 282–301.

Urey H. C. and Mayeda T. (1959) The metallic particles of some chondrites. *Geochim. et Cosmochim. Acta.* **17,** 113–125.

Wahl W. (1950) The statement of chemical analyses of stony meteorites and the interpretation of the analyses in terms of minerals. *Miner. Mag.* **29,** 416–426.

Wahl W. (1952) The brecciated stony meteorites and meteorites containing foreign fragments. *Geochim. et Cosmochim. Acta* **2,** 92–117.

Williams D. J. (1959) A fluid-dynamic mechanism of meteorite pitting. *Smithsonian Contributions to Astrophysics* **3,** 47–67.

Geochimica et Cosmochimica Acta, 1960, Vol. 21, pp. 145 to 150. Pergamon Press Ltd. Printed in Northern Ireland

Meteoritic abundance of ruthenium

T. Hara* and E. B. Sandell
University of Minnesota, Minneapolis, Minn.

(*Received* 25 *May* 1960)

Abstract—The ruthenium content of fifteen chondrites (all "finds") averaged 1·0 p.p.m., with a range from 0·7 to 1·3 p.p.m. The metal phase of chondrites contains, on the average, 4–5 p.p.m. Ru, and the troilite phase a similar amount. Ruthenium varies widely in iron meteorites, the range of seventeen extending from less than 1 p.p.m. to 15 p.p.m., with an average of approximately 7 p.p.m. Ruthenium tends to vary inversely with nickel (and palladium) in irons. There seems to be a relation between the ruthenium content and the structure of iron meteorites.

Most of the data on the abundance of ruthenium in meteorites was obtained more than 25 years ago. Goldschmidt (1954) has summarized these values. Iron meteorites contain approximately 10 p.p.m. Ru (Goldschmidt and Peters, 1931) and the metal phase of chondrites 10·6 p.p.m. according to a calculation of Goldschmidt based on an atomic ruthenium abundance of $2{\cdot}95 \times 10^{-7}$ (Σ elements = 1) in chondrites (Noddack and Noddack, 1934). Widely different values for the ruthenium content of the troilite of iron meteorites have been reported: 1 p.p.m. (Goldschmidt and Peters, 1931), 4·2 p.p.m. (Noddack and Noddack, 1930), and 7 p.p.m. (Noddack and Noddack, 1931). The troilite of stony meteorites contains 20 p.p.m. Ru according to the Noddack and Noddack (1931). The analytical values of Goldschmidt and Peters were obtained by arc spectrography, those of Noddack and Noddack by X-ray spectrography, after concentration of the platinum metals. Recently, Herr *et al.* (1958) reported $42{\cdot}4 \pm 1{\cdot}5$ p.p.m. Ru in the iron meteorite Carbo (medium octahedrite, 8·68% Ni).

Since ruthenium is an element that can readily be isolated and determined by absorption spectrophotometry it seemed worth while to obtain additional data on the abundance and distribution of ruthenium in meteorites.

Analytical Method

Both iron and silicate meteorites were heated with hydrochloric acid to bring the metal and sulphide phases into solution. Chloride was removed by fuming with sulphuric acid and, after taking up in water, the residue was filtered off. This was fused with sodium peroxide. The combined solutions from the acid and peroxide decompositions were distilled after addition of potassium permanganate and sodium bismuthate. Ruthenium and osmium are thus separated from all the other constituents of the sample. Ruthenium was determined spectrophotometrically in the distillate with 1:4-diphenylthiosemicarbazide as reagent (Hara and Sandell, 1960). A red-violet complex is formed, which can be extracted with chloroform. Osmium gives no coloration and does not interfere.

One gramme samples of iron and 2·5 g samples of chondrites were usually taken

* Present address, Doshisha University, Kyoto, Japan.

for analysis. The reproducibility of the determination of ruthenium in siderites was tested by drilling amounts of several grammes from six points on a slab of the San Angelo iron, approximately 1·5 cm apart. The six samples showed 11·2, 11·0, 10·9, 10·9, 11·1 and 11·3 p.p.m. Ru, respectively.

Analyses of synthetic samples indicated a ruthenium recovery of 95 per cent in the analysis of irons, and 90–95 per cent in the analysis of chondrites. The values reported in the tables have not been corrected for the generally slightly low recoveries.

Results and Discussion

Siderites

The ruthenium contents of seventeen iron meteorites* and of the metal phase of two pallasites are listed in Table 1. Variation over a wide range, from less than 1 p.p.m. to 15 p.p.m. Ru, is shown. The average of approximately 7 p.p.m. Ru

Table 1. Ruthenium content of siderites

Meteorite	Type*	Group†	Ru (p.p.m.)
Ainsworth	Og		3·8, 3·8
Altonah	Of	IV	3·6
Arispe	Og	II	9·7, 10·3
Canyon Diablo	Og	I–II	5·9, 5·9
Costilla Peak	Om	III	12·5, 12·2
Coya Norte	H	II	14·2, 15·3
Deport	Og	II	4·4
Duchesne	Of	IV	1·9, 2·3
Edmonton	Of	III	0·8, 0·7
Goose Lake	Om	II	4·5, 4·6
Henbury	Om	II	3·5, 3·7
Mount Joy	H	II	9·1
Sacramento Mtns.	Om	III	9·8
San Angelo	Om	III	11·1 (avg.)
Sandia Mtns.	H	II	7·4, 7·5
Spearman	Om	III	4·8
Willow Creek	Om	III	3·6
Admire (metal phase)	P	III	0·7
Brenham (metal phase)	P		4·6

* According to Lovering *et al.* (1957).
† Gallium (or germanium) group according to Goldberg *et al.* (1951) and Lovering *et al.* (1957).

can therefore have little exact significance. Almost one half (seven) of the samples have ruthenium contents falling between 3·5 and 5 p.p.m. (cf. Fig. 1).

There is a general tendency for ruthenium to decrease as the nickel content increases (Fig. 2). Below 8–9% Ni, the ruthenium content rises sharply with decreasing nickel concentration. It appears that in this region the content of ruthenium depends on the structure of the iron as well as on the nickel content.

* We are indebted to Dr. Harrison Brown and Dr. W. Nichiporuk for most of the irons analysed. A sample of the Canyon Diablo iron, in the form of turnings, was kindly furnished by Dr. J. D. Buddhue.

The hexahedrites apparently give a branch lying at lower nickel contents than does the branch representing the medium octahedrites (but one of the latter, Henbury, is out of line). The coarse octahedrites seem to lie on a branch of their own between the hexahedrites and the medium octahedrites. The fine octahedrites have high

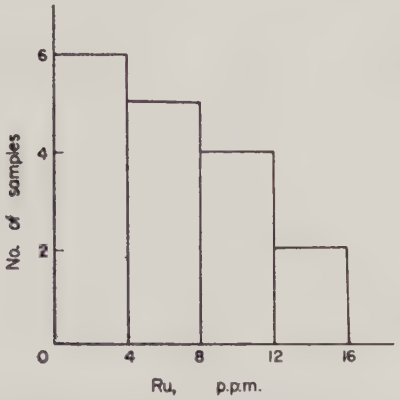

Fig. 1. Frequency diagram of ruthenium in seventeen siderites.

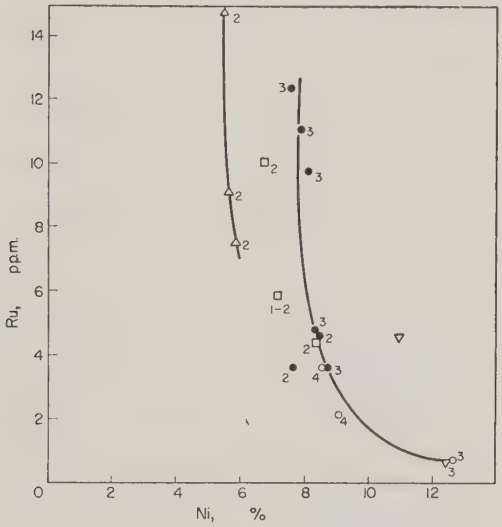

Fig. 2. Relation between nickel and ruthenium contents of sixteen siderites and the metal phase of two pallasites. Numbers 1, 2, 3 and 4 refer to gallium groups I, II, III and IV of Goldberg *et al.* (1951) and Lovering *et al.* (1957). Nickel values are from Lovering *et al.* (1957). ○ Of. ● Om. □ Og. △ H. ▽ P (metal phase).

nickel and low ruthenium contents. Inasmuch as relatively few siderites are represented in these correlations, the conclusions must be considered tentative.

No direct relation between the ruthenium contents of iron meteorites and the gallium–germanium groups of Lovering *et al.* (1957) is apparent.

Since, as shown by Goldberg *et al.* (1951), palladium generally increases with nickel in siderites, a plot of ruthenium against palladium shows a rough inverse

relationship between these two elements (Fig. 3).* The average content of ruthenium is almost twice that of palladium (6·1 p.p.m. Ru, 3·3 p.p.m. Pd) in the thirteen irons in which both elements have been determined.

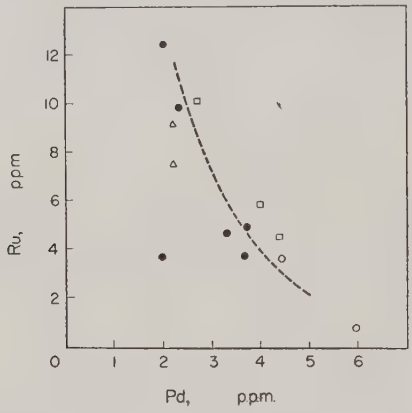

Fig. 3. Relation between palladium and ruthenium contents of thirteen siderites. Palladium values are from Goldberg *et al.* (1951). ○ Of. ● Om. □ Og. △ H.

Chondrites

Ruthenium was determined in fourteen chondrites, which are all "finds" (Table 2). The values fall in a narrow range (Fig. 4) from 0·7 to 1·3 p.p.m. Ru. The average is 0·95 p.p.m., which may as well be rounded off to 1·0 p.p.m. The atomic abundance is approximately 1·5 (Si = 10^6).

Table 2. Ruthenium content of chondrites

	Ru (p.p.m.)
Alamogordo, N. Mex.	1·2
Arriba, Colo.	0·7
Cope, Colo.	1·1
Estacado, Texas	1·3
Gladstone, N. Mex.	1·1
Gruver, Tex.	1·1
Haven, Kan.	1·2
Kingfisher, Okla.	0·8
Ladder Creek, Kan.	0·7
Melrose, N. Mex.	0·8
Morland, Kan.	0·9
Ness County, Kan.	0·7
Plainview, Tex.	1·1
Potter, Nebr.	0·8
Roy, N. Mex.	0·8

* The seemingly aberrant point in Fig. 3 at Ru = 3·6 and Pd = 2·0 p.p.m. represents the Henbury iron, the ruthenium content of which is thus low with respect to palladium as well as to nickel.

Determinations of ruthenium in the separated metal and troilite phases gave the following results:

	Ru in metal (p.p.m.)	Ru in FeS (p.p.m.)
Cope, Estacado, Haven, Ladder Creek, Melrose, Plainview	4·3	6·3
Alamogordo, Arriba, Gladstone, Gruver, Kingfisher, Morland, Ness County, Potter, Roy	5·3	5·2

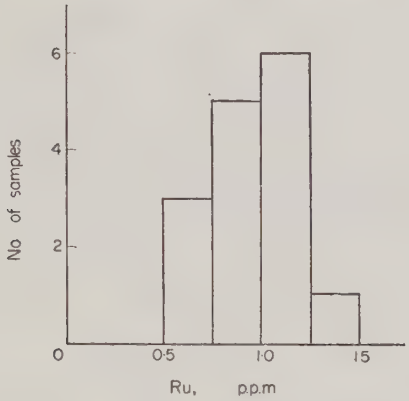

Fig. 4. Frequency diagram of ruthenium in fifteen chondrites.

These values should be looked upon as approximate only, even though recorded to the first decimal, because of the difficulty of obtaining clean separations and because of the relatively small quantities of material analysed. However, it may be concluded that the ruthenium content of the troilite of chondrites is comparable to that of the iron phase. On this basis ruthenium is roughly as strongly chalcophilic as it is siderophilic.

It is of interest to compare the meteoritic abundance of ruthenium ($Z = 44$) with that of its neighbours of even atomic number in the fifth series of the periodic table, as far as these abundances are known. Molybdenum ($Z = 42$) is probably slightly more abundant than ruthenium in chondrites (1·6 p.p.m. Mo according to Kuroda and Sandell, 1954). No chondritic average for palladium ($Z = 46$) is available, but from the sideritic values of Goldberg *et al.* (1951), the meteoritic abundance of palladium may be estimated as roughly one half that of ruthenium. There are no reliable values for cadmium ($Z = 48$) in meteorites, but possibly its abundance does not exceed that of palladium. The abundance curve for the elements of even atomic number rises slightly at tin ($Z = 50$), for which the average in chondrites is not far from 1 p.p.m. (Onishi and Sandell, 1957), or much the same as the value for ruthenium.

Suess and Urey (1956) have adopted the atomic abundances Ru:Rh:Pd = 1·49:0·214:0·675, based on Si = 10^6, which give the atomic ratios 10:1·44:4·5, compared to the Goldschmidt ratios 10:5:9 for meteorites. Cameron (1959) takes the abundances of Ru, Rh and Pd as 0·87, 0·15 and 0·675 (Si = 10^6), thus making palladium almost as abundant as ruthenium.

Acknowledgement—This work was made possible by a postdoctoral research grant from the du Pont de Nemours Company.

References

Cameron A. G. W. (1959) *Astrophys. J.* **129,** 676.

Goldberg E., Uchiyama A. and Brown H. (1951) The distribution of nickel, cobalt, gallium, palladium and gold in iron meteorites. *Geochim. et Cosmochim. Acta*, **2,** 1–25.

Goldschmidt V. M. (1954) *Geochemistry* p. 682. Oxford University Press.

Goldschmidt V. M. and Peters C. (1931) *Nachr. Akad. Wiss. Göttingen, Math.-Physik. Kl.* 165.

Hara T. and Sandell E. B. (1960) *Anal. Chim. Acta.* In press.

Herr W., Merz E., Eberhardt P., Geiss J., Lang C. and Signer P. (1958) Search for decay products of natural technetium. *Geochim. et Cosmochim. Acta* **14,** 158 (Abstract).

Kuroda P. K. and Sandell E. B. (1954) Geochemistry of molybdenum. *Geochim. et Cosmochim. Acta* **6,** 35–63.

Lovering J. F., Nichiporuk W., Chodos A. and Brown H. (1957) The distribution of gallium, germanium, cobalt, chromium and copper in iron and stony-iron meteorites in relation to nickel content and structure. *Geochim. et Cosmochim. Acta* **11,** 263.

Noddack I. and Noddack W. (1930) *Naturwissenschaften* **18,** 757.

Noddack I. and Noddack W. (1931) *Z. phys. Chem.* A **154,** 207.

Noddack I. and Noddack W. (1934) *Svensk Kem. Tidskr.* **46,** 173.

Onishi H. and Sandell E. B. (1957) Meteoric and terrestrial abundance of tin. *Geochim. et Cosmochim. Acta* **12,** 262–270.

Suess H. E. and Urey H. C. (1956) *Rev. Mod. Phys.* **28,** 53.

Geochimica et Cosmochimica Acta, 1960, Vol. 21, pp. 151 to 155. Pergamon Press Ltd. Printed in Northern Ireland

GEOCHEMICAL NOTE

Separation of n-octadecane-1-C^{14} from asphaltic* mixtures by elution chromatography

Bartholomew Nagy, Paulette Hamway, G. C. Gagnon and M. Cefola
Fordham University, New York 58, New York

(*Received in final form*, 13 *June* 1960)

Abstract—It is often assumed that the *n*-heptane chromatographic fraction represents the total saturated hydrocarbon content of asphaltic matter. This assumption, however, is based on an approximation rather than on an analytically rigorous finding. C^{14}-labelled *n*-octadecane was mixed with the semi-solid Athabasca petroleum and the mixture was eluted with a series of solvents. The majority, but not all, of the radioactive material was recovered with *n*-heptane from aluminium oxide and silica gel columns. For example, combined counts equivalent to 2·32 per cent of the *n*-heptane eluate counts were recorded in consecutive eluate fractions (such as in the pyridine fractions) from a Fisher alumina column. It is recommended in routine geological studies that the chromatographic fractions be analysed by suitable means to ascertain their composition and to identify their impurities.

Introduction

Chromatography is one of the principal methods of separating the components of organic matter in sediments and sedimentary rocks. There are reports in the literature which describe the simple chromatographic separation of hydrocarbons from bulk samples. It is known, of course, that hydrocarbons can be quantitatively separated from *distillate fractions* under carefully controlled experimental conditions. For example, Fink *et al.* (1950) found that saturated hydrocarbons in catalytically cracked gasoline fractions can be separated from olefins and aromatic hydrocarbons on silica gel columns. Norris and O'Connor (1959) separated the saturated hydrocarbon fractions of naphtha distillates of petroleum into straight-chain, branched and cyclic groups using molecular sieves and silica gel columns with added organic components. Similar studies were also performed by Mair *et al.* (1956). Silica gel, aluminium oxide and "Fuller's earth" are some of the common chromatographic adsorbents used in these types of separations.

Heat during distillation may, however, decompose a part of the original compounds. It is, therefore, desirable to analyse unheated samples even if they are abundant in asphaltic matter. Kleinschmidt (1955) has shown that asphalt can be separated into, what appear to be, characteristic fractions without distillation if the asphaltenes are first removed by precipitation. Schwartz and Brasseaux (1958) separated the saturated hydrocarbons from crude oil residues by packing two grades of silica gel in the chromatographic columns; asphaltenes and resins were separated by the coarser silica gel layer. Analytical methods

* The terms "asphaltic" and "asphalt" are used to describe viscous, semi-solid petroleum.

which involve the removal of asphaltenes from the samples prior to analysis can account, of course, only for a partial composition. In geochemical studies it is often desirable to know the chemical composition of the entire, bulk sample.

There are reports in the geological literature which are based on the assumption that the *n*-heptane eluate fractions represent the total saturated hydrocarbon content of bulk, asphaltic samples. Such claims have been made even when the eluate fractions were not analysed. The assumption may be an acceptable approximation but it is not a rigorous analytical statement. The following experiment may indicate the separation efficiency of one saturated hydrocarbon, *n*-octadecane, from asphaltic matter.

Experimental Work

C^{14}-labelled *n*-octadecane, $CH_3(CH_2)_{16}C^{14}H_3$, was thoroughly mixed with the viscous McMurray (Athabasca) petroleum. The *n*-octadecane was obtained from the New England Nuclear Corp.; it had a specific activity of 2·04 millicuries/millimole. The manufacturers estimated that the *n*-octadecane sample contained approximately 3 per cent or less impurities.

The McMurray petroleum was quantitatively separated at room temperature with methylene chloride from a sample of a sandstone member of the McMurray formation. The rock sample was obtained from the Abasand Quarry, which is near McMurray, Alberta, Canada. After the evaporation of the solvent, the McMurray extract appeared as a semi-solid, glossy and brownish-black residue.

From 3 to 12 mg portions of the labelled *n*-octadecane, in *n*-heptane solutions, were mixed by swirling with 0·2–0·4 g portions of the asphaltic residue which was redissolved in CH_2Cl_2. Because methylene chloride fully and mutually dissolved both materials, a thorough mixing of the labelled hydrocarbon and the petroleum appeared to take place in solution. Consequently, the *n*-heptane and methylene chloride solvents were evaporated and the sample was redissolved in *n*-heptane (which only dissolves a part of the asphalt). The resultant slurry was transferred to the chromatographic columns.

Because each of the eluate fractions had to be dried before they were counted, the errors caused by the evaporation losses were first determined. Curves *A* and *D* in Fig. 1 show the evaporation losses of 0·155 mg portions of the *n*-octadecane (the weight was determined from aliquot volumes taken from a known concentration), dried in aluminium planchets at room temperature, and at 15 cm distance from a General Electric, Reflector, 250 W, infra-red lamp, respectively. Curves *B* and *C* illustrate the evaporation effects of *n*-octadecane–asphalt mixtures, 1 : 476 *n*-octadecane to asphalt weight ratios, dried at room temperatures and under the infra-red lamp, respectively. A glass thermometer placed under the infra-red lamp in place of the planchets registered a temperature of approximately 130°C. The four curves illustrate that the presence of the asphalt in the mixture reduced the loss of the *n*-octadecane by evaporation in both the air drying and the infra-red drying processes. Curves *A* and *B* show that drying the eluate fractions at room temperature yields the least error. The counting error due to the absorption of the β-radiation by the asphalt (when 1 unit weight of *n*-octadecane was mixed with 476 unit weights of asphalt) is significant, but it is believed not to be sufficiently

high to affect the usefulness of the tracer method in the elution experiment. This can be seen by comparing curves *A* and *B*. All counts are relative and geometric effects were not taken into account. A thin (1·4 mg/cm^2 mica), end-window, Geiger–Müller counter was used. The back-ground counts have been subtracted from all counts shown in Figs. 1 and 2. The accuracy of the counts in curves *A*, *B* and *D* (Fig. 1) was at least 10 per cent at 63 per cent confidence level; that of curve *C* was 3 to 4 per cent at the same confidence level. The accuracy of the

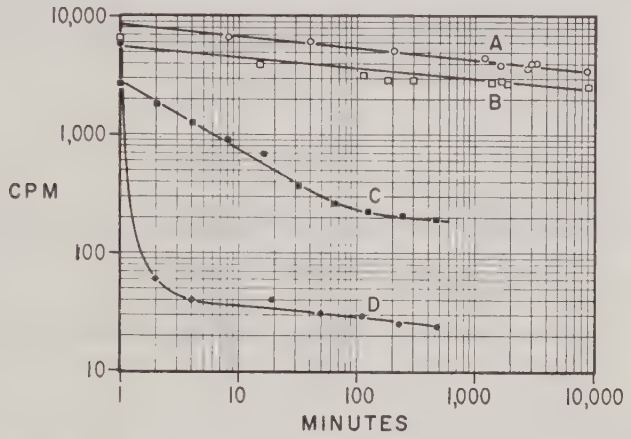

Fig. 1. Evaporation losses of *n*-octadecane-1-C^{14} and *n*-octadecane-1-C^{14}–asphalt mixtures. Curve *A*, *n*-octadecane-1-C^{14}, air dried; curve *B*, *n*-octadecane-1-C^{14}–asphalt mixture, air dried. Curve *C*, *n*-octadecane-1-C^{14}–asphalt mixture, infra-red lamp dried; curve *D*, *n*-octadecane-1-C^{14}, infra-red lamp dried.

n-heptane eluate counts in Fig. 2 was 1 per cent, that of the subsequent counts was 10 per cent, all at 63 per cent confidence level.

Three adsorbents were used for the chromatographic experiments. Silica gel, Davison Chemical Company, Baltimore, Maryland, grade 923, 100–200 mesh; aluminium oxide, "Woelm", non-alkaline (almost neutral), activity grade I, Alupharm Chemicals, Inc., New Orleans, Louisiana; and aluminium oxide, Fisher Scientific Company, Cat. No. A-540 (described to be alkaline but not so specified in the Fisher Chemical Index, no. 123). The adsorbents were used as received without additional activation.

The same series of eluents were used in all experiments in the following order: (1) *n*-heptane, (2) carbon disulphide, (3) carbon tetrachloride, (4) benzene, (5) methylene chloride, (6) chloroform, (7) diethyl ether, (8) pyridine, (9) ethyl acetate, (10) methyl alcohol and (11) ethyl alcohol. Eluents nos. 2-10 were C.P. grade, no. 11 U.S.P. grade, and no. 1 was technical grade. The adsorbent to sample ratios were always kept at 295: 1 or higher. The columns were prewet with 15 ml of *n*-heptane and at least 100 ml of each eluent were passed through each column. Approximately 120 of the 10 ml fractions were collected, evaporated and counted in each of the runs. Elution experiments were conducted at different rates of flow on Woelm alumina and silica gel columns.

First, the purity of the labelled hydrocarbon was checked. The C^{14}-labelled *n*-octadecane in *n*-heptane solution was passed through silica gel or alumina

columns. The columns were eluted with the specified series of eleven solvents. It was found that the majority of the radioactive material was recovered with *n*-heptane. Non-hydrocarbon impurities were present; however, they could be separated since they came off with benzene (from alumina) or with methylene chloride (from silica gel). It was also found that the recovery of the radioactive material did not increase upon the introduction of additional volumes of *n*-heptane into the columns during *n*-heptane elution.

The elution experiments with the asphaltic mixtures employed both purified and non-purified *n*-octadecane-1-C^{14}. The latter led to significantly higher amounts

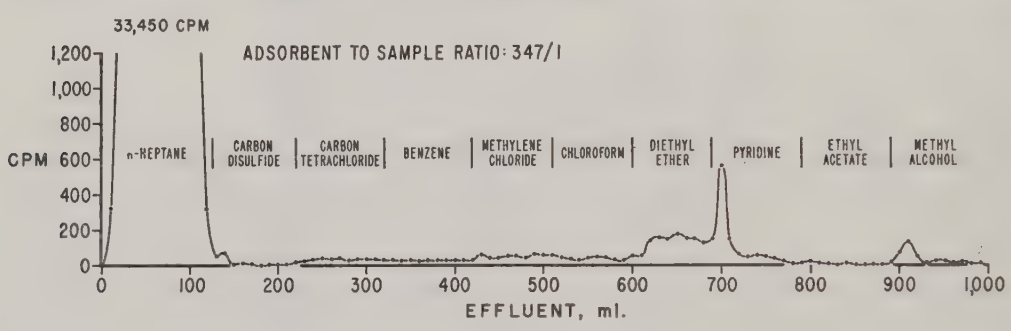

Fig. 2. Elution curve of *n*-octadecane-1-C^{14}–asphalt mixture.

of activity in the post-*n*-heptane fractions. The purified *n*-octadecane-1-C^{14} consisted of the *n*-heptane eluate fractions from alumina columns. The purification process is expected to have removed the non-hydrocarbon impurities. If it did not fully remove them, then the post-*n*-heptane counts may be caused by the impurities. However, because the purification of the C^{14}-labelled hydrocarbon was itself done by chromatography, failure to obtain a pure hydrocarbon would be evidence for the incomplete separation efficiency of the contaminant and *n*-octadecane mixture.

The next step was the elution of the *n*-octadecane-1-C^{14}-asphaltic mixtures. The *n*-heptane and carbon disulphide eluate fractions were colourless, oily and semi-solid residues after the evaporation of the solvents. The benzene fraction was yellow-brown and the ether fraction was dark brown. A heavy, almost black and glossy residue was eluted with pyridine. All eluents removed some material, but those named were found to be the most effective. Weight percentage recoveries were reproducible within acceptable limits of error and the total recovery of the samples was from 83 to 89 per cent. Radioactive material was always present in the *n*-heptane and in some of the subsequent fractions, such as in the pyridine fractions.

Fig. 2 illustrates one of the elution curves, one from Fisher alumina, of a *n*-octadecane–asphalt mixture. The adsorbent to sample ratio was 327 : 1 in this experiment. The counts were taken on air-dried fractions. The *n*-octadecane was purified immediately before mixing with the asphalt by elution with *n*-heptane on a Fisher alumina column at 8154 : 1 adsorbent to sample ratio. The radioactive counts of the pyridine fractions shown in Fig. 2 are somewhat lower than those

found in some of the other elution experiments. The sum of the counts appearing after the *n*-heptane eluate fractions was found to be equivalent to 2·32 per cent of the total *n*-heptane counts.

Discussion

The two most likely causes of the post-n-heptane counts are the following.

(1) Incorporation of a part of the *n*-octadecane-1-C^{14} into some "organized" matter which is eluted only by polar solvents.

(2) Failure to remove the non-hydrocarbon impurities by the chromatographic purification process from the *n*-octadecane-1-C^{14} sample.

The second cause appears to be unlikely. Nevertheless, either of the two causes may indicate the difficulties involved in the chromatographic separation of saturated hydrocarbons.

The work of Brenneman *et al.* (1958) suggests that the post-*n*-heptane counts are caused by the incorporation of a part of the *n*-octadecane-1-C^{14} into organized units of asphalt. These investigators identified *n*-paraffins by mass spectrometric analysis in the ultracentrifuge sediments of petroleum.

In view of these difficulties, it is suggested that eluate fractions be analysed by suitable means in routine geological studies.

Acknowledgements—This investigation formed a part of a study of the chromatographic type fluid-flow in the sedimentary strata, sponsored by the National Science Foundation. The authors would also like to acknowledge the assistance and advice of Sister Mary Simon Peter, O.P., Fordham University, and the constructive comments of Drs. W. G. Meinschein and E. G. Baker of the Esso Research and Engineering Company. Problems of the chromatography of petroleum were discussed with Dr. R. D. Schwartz of Shell Research and Development Company. The rock sample was obtained through the courtesy of Mr. M. A. Carrigy of the Research Council of Alberta.

References

Brenneman M. C., Wanless G. G. and Witherspoon P. A. (1958) *Effect of Ultracentrifugation on Crude Oil.* Paper presented before the Annual Meeting of the ACS Chicago, Illinois.

Fink D. F., Lewis R. W. and Weiss F. T. (1950) Separation of cracked gasolines by chromatographic adsorption. Adsorbent characteristics and regeneration techniques. Factors affecting efficiency of separation. *Analyt. Chem.* **22,** 850–863.

Kleinschmidt L. R. (1955) Chromatographic method for the fractionation of asphalt into distinctive groups of components. *J. Res. Nat. Bur. Stand,* **54,** 163–166.

Mair B. J., Montjar, J. J. and Rossini F. (1956) Fractionation of hydrocarbons by absorption with added components. *Analyt. Chem.* **26,** 56–61.

Norris M. S. and O'Connor J. G. (1959) Separation of paraffin-cyclo-paraffin portion of naphtha into normal, branched and cycloparaffins. *Analyt. Chem.* **31,** 275–279.

Schwartz R. D. and Brasseaux D. J. (1958) Separation of saturated hydrocarbons from petroleum residues. *Analyt. Chem.* **30,** 1999–2002.

Geochimica et Cosmochimica Acta, 1960, Vol. 21, pp. 156 to 158. Pergamon Press Ltd. Printed in Northern Ireland

LETTER TO THE EDITOR

Cosmic-ray produced manganese-53 in iron meteorites*

(*Received* 28 *March* 1960)

THE radioactivity of manganese in three iron meteorites has been measured. The activities found are ascribed to cosmogenic Mn^{53}.

During the last decade the existence of cosmic ray produced nuclides in meteorites has been established. So called cosmic-ray ages for some meteorites have been calculated from the relative amounts of H^3–He^3, (BEGEMANN and GEISS, 1957; FIREMAN and SCHWARTZER, 1957); Cl^{36}–Ar^{36}, (SPRENKEL, 1958); Ar^{38}–Ar^{39} (FIREMAN, 1958), etc. The data indicate cosmic-ray ages for iron and stone meteorites in the 10^8 to 10^9 year and 10^7 to 5×10^7 year ranges, respectively. Unfortunately there are only a few known cosmic ray produced nuclides in meteorites whose half lives are in these ranges, viz. $K^{40}(1{\cdot}25 \times 10^9$ years) and $Be^{10}(2{\cdot}5 \times 10^6$ years). Another possibility is Mn^{53} with a half life of $\geq 1{\cdot}3 \times 10^5$ years (HUIZENGA and WING, 1957). Since iron meteorites are reported to have cosmic-ray irradiations of $>10^8$ years, it might be expected that the Mn^{53} activity in a specimen of terrestrial age $<10^5$ years is nearly saturated.

Although there have been no direct experimental measurements of Mn^{53} production from iron, SHELINE and HOOPER (1957) have estimated the Mn^{53} activity in a newly fallen iron meteorite. Using the energy spectrum and intensity of the cosmic radiation (PETERS, 1952), and an assumed cross-section for the bombarding protons which varies as 1/E, they estimated the Mn^{53} activity in a small iron meteorite to be about 35 dis/min per kg meteorite.

The search for Mn^{53} was performed in connexion with a separation of other cosmogenically produced radioactive nuclides, viz. Be^{10}, Al^{26}, Cl^{36} and K^{40}, in the iron meteorites Odessa, Grant, and Williamstown (HONDA, 1959, and SHEDLOVSKY, 1960). The Odessa sample was obtained from Wards Scientific Establishment and those of Grant and Williamstown furnished through the courtesy of Dr. E. P. HENDERSON and Dr. B. MASON, respectively. The samples, whose weights were: Odessa, 3540 g; Grant, 459 g; and Williamstown, 170 g; were dissolved in aqua regia and a small portion of the solution set aside for chemical analysis. Manganese carrier was added to two of the samples (Grant and Williamstown) along with the other carriers. Iron and cobalt were removed by ether extraction and anion exchange of their chloro complexes.

Further purification was done by standard chemical methods involving hydroxide precipitation with ammonia, manganese dioxide precipitations from strong acid solutions, and scavenging of manganous solutions with strontium sulphate, copper sulphide, and ferric hydroxide. Details will be published in a forthcoming paper (HONDA, SHEDLOVSKY and ARNOLD, 1960).

A final purification was done by anion exchange, the manganese fraction collected and manganese dioxide precipitated with bromate. The sample was washed, dried and mounted for counting. The chemical yield was based on the amount of manganese recovered, as determined by EDTA titration after counting, from the carrier added and the natural content of the sample.

The recycle chemistry included a copper sulphide scavenge, manganese dioxide precipitation with bromate, oxidation to permanganate in acid solution which was then scavenged with ferric hydroxide, reduction to manganous, and a final manganese dioxide precipitation with bromate. Manganese dioxide was recovered from the ferric hydroxide scavenge and included in the second chemical recycle.

* This article is based upon a dissertation to be submitted by author in partial fulfillment of the requirements for the degree of Doctor of Philosophy at Princeton University.

The samples were counted as manganese dioxide in cylindrical geometry with a thin walled, 1 mg/cm^2 aluminized mylar, low level β-flow counter (MARTELL, 1957). The samples were first counted with argon which had been bubbled through ethanol at 0°C, and then with Q gas (98·7% He, 1·3% butane) both in the GM region. Since Mn^{53} is thought to exhibit a pure orbital electron capture decay, CrX-rays of 5·4 keV are emitted along with Auger electrons. As the range of these electrons is less then 0·1 mg/cm^2, none will be counted. The X-rays, however, will penetrate into the counter and produce pulses in the Ar–EtOH mixture, whose mass absorption coefficient for these X-rays is about 350 cm^2/g, COMPTON and ALLISON (1935). On the other hand, as the mass absorption coefficient in Q-gas for these X-rays is only about 0·8 cm^2/g, its X-ray counting efficiency is very low. A standard source of Fe^{55}, obtained from W. S. LYON of the Oak Ridge Laboratory, and whose specific activity was measured by M.

Table 1. Manganese-53 activity in iron meteorites

Sample name	Weight of manganese counted (mg)	Chemical yield (%)	Sample self absorption (%)	Net counting rate (counts/min)		Specific activity (dis/min per kg meteorite)
				Ar–EtOH	Q-gas	
Odessa	19·8	52·8	22·0	7·17 ± 0·36	0·06 ± 0·05	203 ± 11
recycle 1	10·0	26·7	13·5	4·03 ± 0·11	0·11 ± 0·05	199 ± 6
recycle 2	10·9	29·1	14·4	4·63 ± 0·16	0·06 ± 0·04	216 ± 8
					weighted av.	204 ± 5
Grant	24·9	88·4	26·0	3·05 ± 0·24	0·25 ± 0·07	390 ± 35
recycle 1	8·0	28·4	11·4	0·98 ± 0·11	0·10 ± 0·03	317 ± 41
recycle 2	17·4	61·7	20·0	1·79 ± 0·03	0·12 ± 0·04	307 ± 7
					weighted av.	310 ± 7
Williamstown	3·4	34·0	5·7	0·73 ± 0·06	0·34 ± 0·04	299 ± 55
recycle 1	1·2	12·0	0·5	0·155 ± 0·026	0·011 ± 0·025	293 ± 73
					weighted av.	296 ± 44
Carrier Blank	9·0			0·015 ± 0·029		

HONDA, was used to calibrate the counter for total efficiency. A value of 2·6 ± 0·3 per cent was obtained with the Ar–EtOH mixture. After suitable corrections for relative fluorescence yields and mass absorption coefficients, the Mn^{53} total counting efficiency in the Ar–EtOH mixture was 2·4 ± 0·3 per cent.

The samples were also counted for γ-activity to eliminate any effect of Mn^{54} contamination, which also decays by orbital electron capture. The detection apparatus in this case consisted of a NaI(Tl) well-type crystal, $1\frac{3}{4}$ in. × 2 in., connected to a 100-channel pulse height analyser. A standard source of Mn^{54} was used to calibrate the counter, the 840 keV photopeak being counted with an efficiency of 7·5 per cent.

The results are summarized in Table 1. The specific activity (in dis/min/per kg meteorite) was obtained in each case by taking the difference of the net counting rate for Ar–EtOH and Q-gas and making suitable corrections for:

(1) Counting efficiency.
(2) Chemical yield.
(3) Sample self absorption (CAMPION, 1957).

The net γ-activity of each sample over the 840 keV photopeak was negligible and applying a 3 σ confidence limit gave a Mn^{54} contamination of <8 per cent.

These results show considerably more Mn^{53} activity than predicted by SHELINE. The low-energy nucleon cross-section for Mn^{53} production will be much greater than for high-energy reactions and it seems quite likely that the low-energy secondary nucleon flux in meteorites is much larger than has heretofore been assumed. To account for the activities measured, one

might have to consider a low-energy secondary flux that is ten times the primary flux. Alternatively one might argue that the half-life of Mn^{53} is in the 5×10^7 year range and that 10^8 years ago the cosmic-ray flux was several times its present-day value. Since the stone meteorites have apparent cosmic-ray ages of between 10^7 and 5×10^7 years, measurement of the Mn^{53} activity in the metallic phase might settle this point.

It is of interest to note that these samples of cosmic-ray produced Mn^{53} are now free of Mn^{54} contamination, whereas all man-made samples contain enough Mn^{54} to completely mask the Mn^{53} activity.

Acknowledgement—The writer wishes to thank Professor J. R. Arnold for instruction and encouragement throughout this work and Dr. M. Honda for many helpful discussions. This research was supported by the Office of Ordnance Research, U.S. Army.

Gulf Research & Development Company J. P. Shedlovsky
Pittsburgh 30, *Pennsylvania*

References

Begeman F. and Geiss J. (1957) The radiation age of a meteorite from cosmic ray produced He^3 and H^3. *Phys. Rev.* **107**, 540–542.

Campion P. J. (1957) National Academy of Sciences—National Research Council Publication No. 573, 87–91.

Compton A. H. and Allison S. K. (1935). *X-rays in Theory and Experiment.* Van Nostrand, New York.

Fireman E. L. and Schwarzer D. (1957) Measurement of lithium-6, helium-3, and hydrogen-3 in meteorites and its relation to cosmic radiation. *Geochim. et Cosmochim. Acta* **11**, 252–262.

Fireman E. L. (1958) Argon-39 in the Sikhote-Alin meteorite fall. *Nature, Lond.* **181**, 1613–1614.

Honda M. (1959) Cosmogenic K^{40} in Fe Meteorites. *Geochim. et Cosmochim. Acta* **17**, 148–150.

Honda M., Shedlovsky J. and Arnold J. R. (1960) Radioactive species produced by cosmic rays in iron meteorites. *Geochim. et Cosmochim. Acta* (in press)

Huizenga J. R. and Wing J. (1957) *Half-life Limit on* Mn^{53}. U.S. Atomic Energy Commission Report ANL-5738.

Martell E. A. (1957) AECU Report No. 3297.

Peters B. (1952) Progress in cosmic ray physics. Chap. 4. North Holland Pub. Co., Amsterdam.

Sheline R. K. and Hooper J. E. (1957) Probable existence of Mn^{53} in iron meteorites. *Nature, Lond.* **179**, 85.

Shedlovsky J. (1960) Thesis, Princeton University.

Shedlovsky J., Honda M. and Arnold J. R. (1960) To be published.

Sprenkel E. L., Davis R. and Wüg E. O. (1958). Cosmic ray-produced Cl^{36} and Ar^{39} in iron meteorites. *Bull. Amer. Phys. Soc.* **4**, 223.

INFORMATION FOR CONTRIBUTORS

I. GENERAL

1. Papers on *geochemistry* should be submitted to the appropriate Executive Editor—Prof. L. R. WAGER for papers from the United Kingdom and British Commonwealth, and for papers in English from Europe; Prof. C. W. CORRENS for papers in German or French; Prof. E. INGERSON for papers from the American continents. Papers submitted for publication will naturally be judged from the standpoint of scientific originality and novelty. Technical details of apparatus used in scientific investigation can, however, be presented in brief notes. Critical comments or preliminary results requiring early publication should be submitted as letters to the editors. Where possible, letters should be confined to 500 words. The preparation of progress reports and review articles will be invited by the editors from time to time. The journal appears as independent and complete numbers, which are combined into volumes of about 300 pages.

2. Only papers which have not been previously published can be accepted. Authors must agree not to publish elsewhere a paper submitted to and accepted by *Geochimica et Cosmochimica Acta*.

3. Fifty reprints of each paper are provided free. Additional copies can be purchased if ordered at the time the first proofs are returned. A reprint order form will accompany first proofs.

II. SCRIPT REQUIREMENTS

1. Scripts must be written in one of the three official languages—English, French or German.

2. The script should be typed (not a carbon copy). The text must be ready for printing and should be carefully checked for errors. Authors will receive proofs for correction.

3. Illustrations should accompany the script, mounted on separate sheets. Line diagrams that require to be redrawn should include all relevant details. Half-tone illustrations should be restricted to the minimum necessary. Photographs should be enlarged sufficiently to permit their clear reproduction and if words or numbers appear on them, two copies should be sent, one clearly printed and the other without inscription. All illustrations should be provided with descriptive legends, which should be given on a separate sheet. Any lettering on diagrams—other than Greek letters, symbols, etc.—should be stencilled and should be sufficiently large and bold to permit reproduction when the diagram has been reduced to a size suitable for inclusion in the journal.

4. References in the text should be given by quoting the author's name and year of publication, i.e. AHRENS (1952). *Full references should be listed at the end of each paper, in alphabetical order, in the following manner*

AHRENS, L. H. (1952). The use of ionization potentials—I. Ionic radii of the elements. *Geochim. et Cosmochim. Acta* **2**, 155–169.

and should include the full title of the article, standard abbreviated title of the journal, year, volume number and inclusive page numbers.

5. The text of articles submitted should be concise and in a readily understandable style. The technical description of the methods used should only be given in detail when such methods are new. The essential contents of each paper should be briefly recapitulated in an abstract in English. Such an abstract, may, however, be submitted by the author in the language of the original typescript for translation into English by the editorial staff.

6. To conserve space, authors are requested to mark less important portions of the paper (such as description of methods, record of experimental results, etc.) for printing in smaller type.

7. Indices of refraction should be denoted by the symbols α, β, γ, ω, ε, n, and vibration directions by X, Y, Z, O and E.

Pergamon Press are also publishers of the following Journals:

JOURNAL OF NUCLEAR ENERGY (*including* THE SOVIET JOURNAL OF ATOMIC ENERGY*). PART A: REACTOR SCIENCE; PART B: REACTOR TECHNOLOGY; PART C: PLASMA PHYSICS—ACCELERATORS—THERMONUCLEAR REACTORS
HEALTH PHYSICS (*The Official Journal of the Health Physics Society*)
JOURNAL OF INORGANIC AND NUCLEAR CHEMISTRY
TETRAHEDRON (*The International Journal of Organic Chemistry*)
TALANTA (*An International Journal of Analytical Chemistry*)
INTERNATIONAL JOURNAL OF APPLIED RADIATION AND ISOTOPES
BIOCHEMICAL PHARMACOLOGY
ARCHIVES OF ORAL BIOLOGY
* BIOPHYSICS
* JOURNAL OF MICROBIOLOGY, EPIDEMOLOGY AND IMMUNOBIOLOGY
* PROBLEMS OF HEMATOLOGY AND BLOOD TRANSFUSION
* PROBLEMS OF VIROLOGY
* PROBLEMS OF ONCOLOGY
* SECHENOV PHYSIOLOGICAL JOURNAL OF THE U.S.S.R.
* PAVLOV JOURNAL OF HIGHER NERVOUS ACTIVITY
* ELECTRIC TECHNOLOGY, U.S.S.R.
* RADIO ENGINEERING
* RADIO ENGINEERING AND ELECTRONICS
* TELECOMMUNICATIONS
* PHYSICS OF METALS AND METALLOGRAPHY
* THE ABSTRACTS JOURNAL OF METALLURGY
* APPLIED MATHEMATICS AND MECHANICS
CHEMICAL ENGINEERING SCIENCE
JOURNAL OF ATMOSPHERIC AND TERRESTRIAL PHYSICS
PLANETARY AND SPACE SCIENCE
ANNALS OF THE INTERNATIONAL GEOPHYSICAL YEAR
SPECTROCHIMICA ACTA
JOURNAL OF THE MECHANICS AND PHYSICS OF SOLIDS
ACTA METALLURGICA
(*for the Board of Governors of Acta Metallurgica*)
INTERNATIONAL JOURNAL OF THE PHYSICS AND CHEMISTRY OF SOLIDS
DEEP-SEA RESEARCH
JOURNAL OF NEUROCHEMISTRY
JOURNAL OF PSYCHOSOMATIC RESEARCH
JOURNAL OF INSECT PHYSIOLOGY
INTERNATIONAL JOURNAL OF AIR POLLUTION
INTERNATIONAL ABSTRACTS OF BIOLOGICAL SCIENCES (*for Biological and Medical Abstracts Ltd.*)
RHEOLOGY ABSTRACTS
VACUUM
OPERATIONAL RESEARCH QUARTERLY
ANNALS OF OCCUPATIONAL HYGIENE
ELECTROCHIMICA ACTA
JOURNAL OF CHILD PYSCHOLOGY AND PSYCHIATRY
JOURNAL OF SMALL ANIMAL PRACTICE
SOLID-STATE ELECTRONICS
INTERNATIONAL JOURNAL OF MECHANICAL SCIENCES

* *Translations of Russian journals published on behalf of the Pergamon Institute, a division of Pergamon International Corporation*

Leaflets giving further details and subscription rates of each of these journals are available on request

27 Feb 61

THE GEOCHEMICAL SOCIETY

OFFICERS

TOM F. W. BARTH, President
HAROLD C. UREY, Vice-President
KONRAD B. KRAUSKOPF, Secretary
GEORGE T. FAUST, Treasurer

COUNCILLORS

E. F. OSBORN, 1958–1960
H. G. THODE, 1958–1960
ALBERT E. J. ENGEL, 1959–1961
FRIEDRICH G. HOUTERMANS, 1959–1961
RALPH CANNON, 1960–1962
TH. G. SAHAMA, 1960–1962

REGIONAL VICE-PRESIDENTS

LOUIS H. AHRENS
RUI RIBEIRO FRANCO
ING. GEORGES ORDOÑEZ
C. W. CORRENS
J. F. LOVERING
KEN SUGAWARA

COMMITTEES

Auditing Committee:
JOSEPH J. TREGONING, Chairman
WILLIAM L. HILL
C. R. NASSER

Constitution and By-Laws Committee:
MICHAEL FLEISCHER, Chairman
JULIAN R. GOLDSMITH
DENIS M. SHAW

Education Committee:
H. D. HOLLAND, Chairman
J. A. S. ADAMS
D. M. HENDERSON
KURT E. LOWE
G. D. NICHOLLS
HANS P. EUGSTER

Membership Committee:
R. M. GARRELS, Chairman
HARVEY C. DIEBL
CHESTER B. SLAWSON
JAMES E. SLOSSON
IRVING BREGER

Nominating Committee:
WM. T. PECORA, Chairman
T. G. SAHAMA
C. E. TILLEY
G. TUNELL

Programme Committee:
H. T. EVANS, Chairman
GORDON J. F. MACDONALD
H. E. LOWENSTAM

Publications Committee:
E. W. HEINRICH, Chairman
JULIAN R. GOLDSMITH
JOHN C. MAXWELL
N. W. RAKESTRAW
S. C. ROBINSON
L. R. WAGER
EARL INGERSON

Research Committee:
C. G. DODD, Chairman
W. F. BRADLEY
R. A. ROWLAND
T. G. THOMPSON

Russian Translations Committee:
EARL INGERSON

Standards Committee:
ALVIN VAN VALKENBERG, Chairman
MICHAEL FLEISCHER
LOREN STIEFF
GEORGE SWITZER
GEORGE TILTON

Tellers Committee:
CHARLES MEYER, Chairman
HENRY R. CORNWALL
COLIN O. HUTTON